THE UNIVERSITY OF
SYDNEY

The Epigenetics of Pluripotency in Embryonic Stem Cells

Andreas Ardhika Antoninus

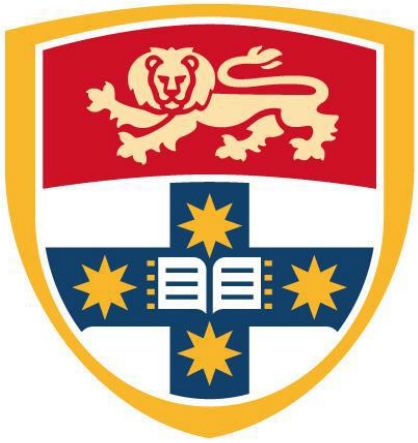

Northern Clinical School, Sydney School of Medicine,

Human Reproduction Unit,

Sydney Centre for Developmental and Regenerative Medicine,

Kolling Institute, Royal North Shore Hospital

The University of Sydney, 2065

Australia

Thesis submitted to the Sydney School of Medicine, University of Sydney, in fulfillment of the requirements for the degree of Master of Philosophy in Medicine.

2015

TABLE OF CONTENTS

DECLARATION

I hereby certify that the work embodied in this thesis is the result of original research and has not previously been submitted for a degree to any other university.

This thesis is of my own composition and to the best of my knowledge does not contain material that has been published or written by any other person except where acknowledgement is made in the text.

Andreas Ardhika Antoninus

ABSTRACT

The ability of pluripotent cells to differentiate into all cell types is a promising approach to regenerative medicine. This promise requires that pluripotent cells are faithfully maintained in a pluripotent state. One epigenetic feature associated with pluripotency in the embryo is the relative global hypomethylation of cytosine (at CpG dinucleotides, 5meC) that occurs within the nucleus of the inner cell mass and epiblast. It is surprising therefore that the global levels of 5meC in embryonic stem cells (ESCs) propagated under conventional methods are as high as many differentiated somatic cells. It was recently shown that changing media formulations to include pharmacological inhibitors of the ERK MAP Kinase and GSK signaling pathways (2i media) decreased global 5meC levels and increased the pluripotency of ESCs.

Conventional chemical methods of 5meC measurement require large numbers of cells and thus limit the strategies available for investigating the regulation of methylation in ESCs. Immunolocalization may be more useful for this purpose because it allows assessment of individual cells and also provides information on the localization of 5meC within each nucleus, information that can't be obtained by current chemical methods of 5meC measurement. It was shown, however, that conventional methods of immunolocalization underestimate the 5meC levels detected in cells. This is due to antigenic 5meC being present within two pools. One pool is detected after acid-induced denaturation of chromatin (and this is the pool detected by conventional immunolocalization). A further trypsin-sensitive pool has been discovered and the size of this pool is highly variable, depending upon the developmental state and growth disposition of cells. Using the newly developed antigen retrieval method that incorporates both acid and trypsin based epitope retrieval processes this project assessed the effects of culture conditions on global levels and localization of 5meC in ESCs.

In normal plate culture, 2i media caused a progressive loss of global methylation in ESC over 14 passages compared to conventional media (DMEM, serum plus LIF). Changing culture conditions to favour the formation of embryoid bodies (EBs) in suspension accelerated the loss of 5meC, and reduced the heterogeneity of staining levels between cells. 2i media also caused the pattern of 5meC staining within nuclei to change from a generalized staining across the nucleoplasm to being predominantly associated with heterochromatic foci. This was observed within both plated cells and suspended EBs. The reduction in the global 5meC level was accompanied by an increase in immunodetectable 5´-hydroxymethylcytosine (5hmC). These changes were associated with an increase in the pluripotency of cells, as assessed by alkaline phosphatase activity. The transfer of ESC from 2i to DMEM medium with serum but without LIF (a media that does not support pluripotency) caused an increase in the global levels of 5meC in the cells within 24 h. The increase of the global 5meC level occurred before morphological signs of differentiation or a reduction in alkaline phosphatase activity were detected.

Assessment of the methylation enzymes of ESCs in several culture conditions that affect the global methylation of ESCs showed that DNMT3A and DNMT3B, and not DNMT1, were found to be the major contributors to the changes in DNA methylation levels in ESCs. The static expression of TET1 suggested that the changes in 5hmC levels in ESCs were determined by other factors, including the levels of *de* novo methylation enzymes.

The study shows that the loss of global DNA methylation accompanied increased pluripotency achieved by ESC in 2i media or in suspension culture of EBs. It shows for the first time that this was accompanied by the recruitment of 5meC to heterochromatin. It also showed that global hypermethylation is an early response to conditions that favour the loss of pluripotency, and occurs before evidence of the loss pluripotency or morphological differentiation. This

finding provides a new framework for further investigation of the epigenetic requirements of the pluripotent state.

ACKNOWLEDGEMENTS

I would like to express my gratitude to my supervisor Professor Christopher O'Neill for giving me the opportunity to work on my Master of Philosophy in Medicine degree under his supervision at the Human Reproduction Unit and for giving me valuable advices regarding how to do a proper science, to my co-supervisor Dr. Yan Li for her endless supports and advices for doing experiments in the laboratory, to my post-graduate coordinator Dr. Carolyn Scott for helping me in the administration in Kolling Institute, to the University of Sydney for giving me the opportunity to do my Masters degree, to Australia Awards Scholarships for making it possible for me to study in Australia and get so much valuable experience, to the Australia Awards Manager Amy Wan and Australia Awards Officer Bojan Bozic for answering a lot of my questions and supporting me during my study in the University of Sydney, to my undergraduate supervisors Diah Iskandriati and Silmi Mariya (Primate Research Center) for inheriting their passion in research and initiating my interest in stem cell research. I would like to thank Dr. Gillian Begg for critically reading my thesis.

I am grateful to the members of the Human Reproduction Unit, Greg Mulhearn for managing the laboratory, Charlotte Rollo and Michelle Seah for inducting me to the laboratory, and Xing Jin for helping in retrieving the western blot results. I would like to thank the members of Kolling Institute: Sergey Kurdyukov for teaching me confocal microscopy, Sue Smith for her kind support in using the cryostat facility, and Carl Benson for organising and inviting me to the sports games with the other Kolling members.

I offer my sincerest gratitude to the members of the Bible Study Group for the endless supports and prayers. Special thanks to Tania Herman for being there all the time, to Roy Suwandi for his teaching in the words of God and his precious counseling, to Reinard Surya for his prayer during my low times, to Sandersan Onie for being the caring thesis buddy, to Maria Felicita

and Daniel Budiman for their support during my initial time in the group, and to Ryana Rachmat for her meaningful reminder that God will always bring us from glory to glory. I am thankful for my scholarships friends Yustina, Larasati, and Dozi for the wonderful time during our stay in Sydney.

I would like to thank my family, my father, Yana, and mother, Lydia, for their endless caring and prayers, to my brother, Adrio, and sister, Arantxa, for their visit during my time in Australia. Finally, all glory to God for all His plans that He has for me. I can do all things through Him who strengthens me.

LIST OF ABBREVIATIONS

°C	centigrade
µl	microlitre
5caC	5-carboxylcytosine
5fC	5-formylcytosine
5hmC	5-hydroxymethylcytosine
5meC	5-methylcytocine
A. U.	arbitrary units
ADD	ATRX-DNMT3-DNMT3L domain
AID	activation-induced cytosine deaminase protein
APOBEC1	apolipoprotein B mRNA editing enzyme, catalytic polypeptide 1
BAH	bromo-adjacent homology domain
BER	base excision repair
BS-Seq	bisulfite sequencing
BSA	bovine serum albumin
Ca^{2+}	calcium ion
CAB-Seq	chemical modification-assisted bisulfite sequencing
cm^2	square centimetre
CO_2	carbon dioxide
CpG	Cytosine-phosphate-Guanine
DAPI	4',6-diamidino-2-phenylindole
DMEM	Dulbecco's Modified Eagle Medium
DMRs	differentially methylated regions
DMSO	dimethyl sulfoxyde
DNA	deoxyribonucleic acid

DNMTs	DNA methyl transferases
DPBS	Dulbecco's phosphate buffer saline
DPBT	Dulbecco's phosphate buffer saline with Tween-20
EBs	embryoid bodies
EDC	1-ethyl-3-[3-dimethylaminopropyl]-carbodiimide hydrochloride
EDTA	ethylenediaminetetraacetic acid
ERK	extracellular-signal-regulated kinase proteins
ESCs	embryonic stem cells
FBS	fetal bovine serum
FITC	fluorescein isothiocyanate
GSK3	glycogen synthase kinase 3 protein
h	hour(s)
H3K9ac	Histone H3 Lysine-9 acetylation
HCl	hydrochloric acid
HDAC	histone deacethylase protein
HIF-1α	hypoxia-inducible transcription factor 1 alpha
ICM	inner cell mass
IgG	Immunoglobulin G
KO-DMEM	knockout Dulbecco's Modified Eagle Medium
LIF	mouse Leukemia Inhibitory Factor
LTR	long-terminal-repeat
M	molarity
MBD	methyl-binding domain
MBPs	methyl-binding proteins
MeCP2	methyl-CpG-binding protein

MEF	mouse embryonic fibroblasts
mg	milligram
Mg^{2+}	magnesium ion
min	minute(s)
miRNA	micro ribonucleic acid
ml	millilitre
mM	millimolar
mm	millimetre
MSCC	Methyl-Sensitive Cut Counting
MSP	methylation-specific PCR
mTOR	mammalian target of rapamycin
N	normality
O_2	oxygen
oxBS-Seq	oxidative bisulfite sequencing
p	probability (p value, level of significance)
Par	portioning defective
PBHD	polybromo-1 protein
PCNA	proliferating cell nuclear antigen
PFA	paraformaldehyde
PHD	plant homeodomain
PI	propidium iodide
PI3K	phosphoinositide-3-kinase protein
pO_2	partial pressure oxygen
PWWP	Proline-Tryptophan-Tryptophan-Proline domain
redBS-Seq	reduced bisulfite sequencing

rpm	revolutions per minute
RRBS	reduced representation bisulfite sequencing
RT	room temperature
SAM	S-adenosyl-L-methionine
sec	second(s)
SEM	standard error of the mean
SFES	serum free ES medium
Sox	SRY-related HMG box
SRA	SET and RING finger-associated
TBST	Tris-HCl, pH 7.4, 0.15 M NaCl, with Tween-20
TCL1	T-cell leukemia/lymphoma 1
TDG	thymine DNA glycosylase
TET	ten eleven translocation proteins
TR	Texas Red
TRD	target recognition domain
UNIANOVA	univariate analysis of variance
v/v	volume by volume
w/v	weight by volume

LIST OF FIGURES

LIST OF TABLES

1. CHAPTER 1: LITERATURE REVIEW

1.1. INTRODUCTION

The use of pluripotent cells has been an important development in the field of regenerative therapy. Due to their properties of self-renewal and pluripotency, pluripotent cells have the potential to be a source of all cell types. This makes them a promising solution for the scarcity of organs for transplant in medicine. These properties, however, could also lead to problems, as undifferentiated pluripotent cells could form a type of tumour called teratoma inside the host (Mitjavila-Garcia et al., 2005, Cheng, 1995a). Consequently, one of the biggest concerns in the use of pluripotent cells in practical therapy is finding a way to effectively direct the differentiation of pluripotent cells into a desirable cell lineage and prevent uncontrolled proliferation inside the host. Several techniques have been developed in the past few years to differentiate embryonic stem cells (ESCs) into specific cell types, including improved culture conditions (growth factors, substrate, and 3D scaffold) and molecular modification (genes activation and suppression) (Dawson et al., 2008, Dang and Tropepe, 2006). However, these techniques have proved inefficient, at least in terms of producing large numbers of transplant-grade cells (Dang and Tropepe, 2006, Hwang et al., 2008). Therefore, the development of reliable and efficient ways to differentiate pluripotent cells into clinical-grade cells is still a work in progress.

In recent years, epigenetics has been found to be one of the major contributors in determining the fate of cells in both normal development and disease conditions. Epigenetics is defined as the study of lineage-specific patterns of gene expression that arise during development. These are mitotically and/or meiotically heritable, and do not cause a change in DNA sequence (Russo et al., 1996). There are several types of epigenetic factors, including chromatin structure, micro RNA (miRNA) expression and DNA methylation. Among these epigenetic processes, DNA

methylation is the most intensively investigated epigenetic trait (Klose and Bird, 2006). This enzyme-mediated process catalyses the addition of methyl groups to DNA and this is mainly restricted to CpG dinucleotides in mammals, and plays essential roles in maintaining genomic stability (Altun et al., 2010, Bird, 2002). Cytosine methylation is also involved in a broad range of physiological processes such as embryogenesis and genome imprinting (Li, 2002). Several studies suggest that the inactivation of cytosine methylation in various mammalian cells results in growth defects, cell death, and genomic instability (Eden et al., 2003, Jackson-Grusby et al., 2001, Dodge et al., 2005). Generally, cytosine methylation acts as a repressive mark that inhibits DNA transcription, either by preventing transcription factors from binding to the DNA or by recruiting methyl-binding proteins (MBPs) that change the chromatin structure (Auclair and Weber, 2012). The repression of DNA transcription by cytosine methylation regulates gene activation during embryogenesis and in the somatic cells of mammals (Jaenisch and Bird, 2003). Methylation-deficient embryonic stem cells have a limited capacity for differentiation (Fouse et al., 2008). These results suggest that epigenetics plays an important role in defining the development and differentiation of stem cells, and an understanding of this mechanism is likely to be important in decoding the regulation of pluripotency and lineage specification in ESCs.

This study will focus on DNA methylation as one type of epigenetic modification that affects the development and differentiation of mouse ESCs. Embryonic stem cells are derived from the inner cell mass (ICM) of the embryo, and are cultured *in vitro* until a stable ES cell line is established (Tang et al., 2010). Evans and Kaufman (1981) reported the first derivation of murine ESCs from *in vitro* cultures of mouse blastocysts. In suspension culture, ESCs form spheroid aggregates called embryoid bodies (EBs) (Doetschman et al., 1985). It has been shown that differentiation of ESCs into EBs mimics the formation of post-implantation embryonic tissues (Desbaillets et al., 2000). The initial focus of the present study will be a

comparison of the methylation state of plated ESCs, EBs, and embryos. Another interesting question is whether there is a correlation between the methylation state of ESCs and their expression of pluripotency genes (*Oct4*, *Sox2*, *Nanog*, and *Utf1*), methylation enzymes (DNMT1, DNMT3A, and DNMT3B), and the putative demethylation enzymes (TET1, TET2, TET3). Furthermore, the effect of differentiation of ESCs on their methylation state is a promising topic that will be investigated. The aim of this study is to investigate the effects of various factors including growth conditions, culture media, and differentiation on the methylation status of mouse ESCs, and the effects of any changes in methylation status on the expression of several key genes. An understanding of all these mechanisms will provide better tools to control the differentiation of pluripotent cells in a robust, reliable, and stable manner.

1.2. METHYLATION AND DEMETHYLATION ENZYMES

The following sections will review the current knowledge of the enzymes responsible for methylation and will discuss current theories regarding mechanisms for demethylation.

1.2.1. Methylation enzymes

There are several methylation enzymes involved in establishing and maintaining global DNA methylation patterns in the mammalian genome. Methylation of the mammalian genome is catalysed by enzymes of the DNA methyltransferase (DNMT) family, which consists of three active members with a conserved catalytic domain: DNMT1, DNMT3A, and DNMT3B (Auclair and Weber, 2012). There are also several DNMT family members in mammals that do not exhibit DNA methyltransferase activity, such as DNMT2 and DNMT3L.

1.2.1.1. DNMT1

DNMT1 is generally considered to be responsible for DNA methylation maintenance during DNA replication. In mouse, DNMT1 is a 190 kD protein that is encoded by 39 exons regulated by 3 sex-specific promoters (Latham et al., 2008). The most upstream promoter encodes the DNMT1O protein, which is active in oocytes and responsible for maintaining maternal and paternal methylation imprints during early development in the embryo (Latham et al., 2008). The second promoter, 6kb downstream of the oocyte-specific promoter, encodes the DNMT1 protein, which is common to ESCs and all somatic cells (Latham et al., 2008). The last promoter downstream of the somatic promoter encodes a non-translated transcript found in pachytene spermatocytes.

The mouse DNMT1 protein consists of two domains, a large N-terminal domain that comprises approximately two thirds of the whole protein and a catalytic C-terminal domain (**Error! eference source not found.**). These two domains are connected by a sequence of alternating glycyl and lysyl residues. In mammals, the N-terminal domain serves as a regulatory domain and consists of sequences that bind with proteins such as proliferating cell nuclear antigen (PCNA) (Chuang et al., 1996), histone deacetylase HDAC1 (Fuks et al., 2000, Robertson et al., 2000) and HDAC2 (Rountree et al., 2000), DMAP1 (Rountree et al., 2000), the transcription factor E2F (Robertson et al., 2000), and the Rb tumour suppressor protein (Robertson et al., 2000). Furthermore, this domain contains a nuclear localisation sequence that binds DNMT1 to the DNA replication fork (Leonhardt et al., 1992), a zinc finger CXXC (Cys-X-X-Cys) domain that is essential for DNA binding and catalytic activity (Lee et al., 2001, Pradhan et al., 2008), and a bromo-adjacent homology (BAH) domain that acts as a protein-protein interaction module, specialised in gene silencing (Callebaut et al., 1999). Each of these components of the N-terminal domain may serve as a component of the DNA methylation

machinery that regulates the mammalian DNMT1 protein in its role as a maintenance DNA methylation enzyme. The C-terminal domain, which is known as the methyltransferase domain, is further divided into the catalytic core and the target recognition domain (TRD)/DNA binding domain (Song et al., 2012).

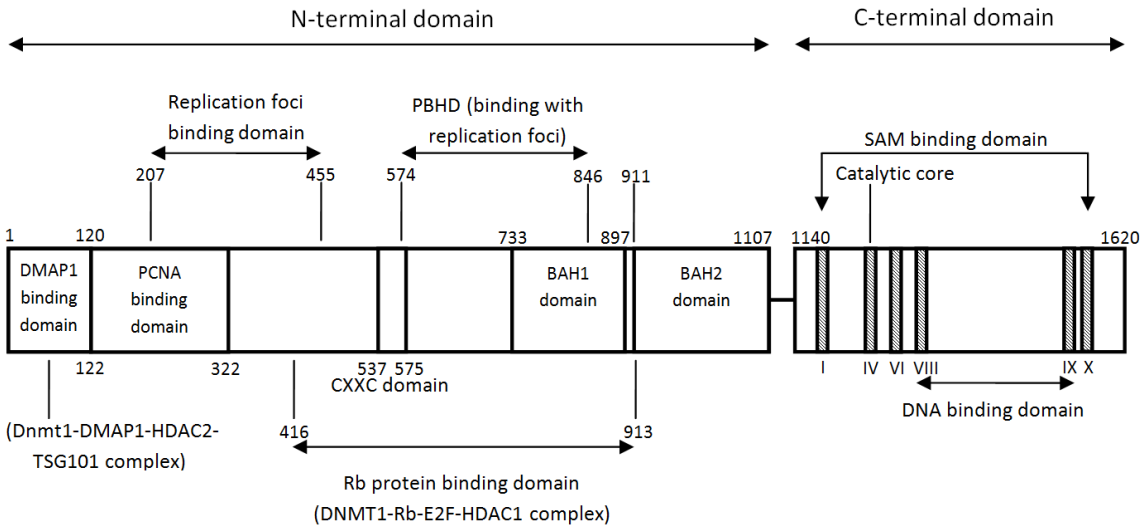

Figure 1-1 domain mapping of DNMT1 sequence.

The DNMT1 protein in humans binds with PCNA, an auxiliary factor for DNA replication and repair, through amino acids 122 to 322 in the N-terminal domain, specifically the amino acids Arg^{163}, Gln^{164}, Thr^{166}, Ile^{167}, His^{170}, and Phe^{171} (Chuang et al., 1996). The binding of mammalian DNMT1 to the PCNA domain is important for the recruitment of DNMT1 to the newly synthesised DNA and the specificity of DNMT1 to hemimethylated DNA, as part of the DNA maintenance process. By binding to PCNA, mouse DNMT1 is recruited to the newly synthesised DNA, which suggests the involvement of DNMT1 protein in the preservation of methylation in the newly replicated DNA (Iida et al., 2002). Furthermore, the specificity of mouse DNMT1 to hemimethylated DNA is regulated by its binding to PCNA, as the specificity to hemimethyated DNA is lost when the PCNA-binding site of DNMT1 is removed (Vilkaitis et al., 2005). A study in human cancer cells revealed that the lack of DNMT1 protein in cancer

cells induces cell arrest in the G2-phase due to excessive hemimethylated DNA, which in turn leads to abnormal mitotic entry as the hemimethylated DNA is recognised as damaged DNA, and finally cell death (Chen et al., 2007).

Besides DNA replication, PCNA is also essential in DNA repair mechanisms (Chuang et al., 1996). This suggests that mammalian DNMT1 is also involved in DNA repair. Intriguingly, tumour suppressor $P21^{WAF1}$, which is activated by P53 in response to DNA damage, has been found to inhibit the formation of DNMT1-PCNA complexes and prevents hypermethylation of damaged DNA (Chuang et al., 1996). This finding suggests that mammalian DNMT1 hampers the DNA repair process by hypermethylating the damaged DNA, and that $P21^{WAF1}$ prevents this by blocking the access of DNMT1 to PCNA (Chuang et al., 1996). This finding suggests that PCNA is required in both DNA replication and DNA repair, but that DNMT1 should be prevented from binding to PCNA in the DNA repair process. However, there is evidence that mouse DNMT1 is involved in mismatch repair as one of the mismatch repair components in mouse ESCs (Guo et al., 2004). This model is very plausible, because mismatch repair is part of the DNA replication process and mammalian DNMT1 is involved in maintaining the stability of newly replicated DNA by preserving its methylation status. This means that mammalian DNMT1 is involved in DNA repair when the repair process is associated with the DNA replication process, but not with PCNA-mediated DNA repair mechanisms. Despite the importance of PCNA in directing DNMT1 to the hemimethylated DNA, this protein is not the only determinant of DNMT1 preference towards hemimethylated DNA. UHRF1 (formerly known as NP95 in mouse and ICBP90 in human) guides mammalian DNMT1 towards hemimethylated DNA, as this protein forms a direct interaction with mammalian DNMT1 and has a SET and RING finger-associated (SRA) domain that binds to hemimethylated DNA (Bostick et al., 2007, Sharif et al., 2007). Together with PCNA, UHRF1 directs DNMT1 towards hemimethylated DNA. Moreover, the catalytic domain of DNMT1 itself has an

intrinsic affinity to hemimethylated DNA that can be amplified by the interaction with the Zn-binding domain (Fatemi et al., 2001).

Eukaryotic DNMT1 also binds with histone deacetylase protein complexes. These are multi-subunit complexes that consist of at least 7 subunits, including HDAC1 and HDAC2, SIN3, RbAp48, RbAp46, SAP30, and SAP18 (Zhang et al., 1998). The interaction between DNMT1 and histone deacetylase proteins may occur via the recruitment of methyl-CpG-binding protein (MeCP2) to DNA that is methylated by DNMT1, followed by binding of this protein with histone deacetylase protein complex, which triggers the removal of acetyl group from the histone (Ng and Bird, 2000). However, in mouse, one of the two transcription repression domains (CXXC domain) of DNMT1 also interacts directly with the HDAC1 protein (Fuks et al., 2000). Furthermore, the transcriptional repression activity of mouse DNMT1 is partly related to the nucleosome remodeling activity of HDAC1 (Fuks et al., 2000). The connection between these two mechanisms is still not clear; it may be that the interaction of DNMT1 and HDAC1 is the prerequisite for the recruitment of MeCP2 protein, or it may be that MeCP2 is the mediator of the DNMT1-HDAC1 interaction. Nevertheless, as DNA methylation and histone deacetylation are two important mechanisms of gene silencing, it is possible that they cooperate with each other in creating a stable silenced epigenetic state. The mechanism of transcriptional repression caused by histone deacetylation is possibly mediated by the recruitment of polyamines to the deacetylated DNA, which creates a higher chromatin structure preventing the recruitment of transcription factors to the DNA (Pollard et al., 1999), or by removing the acetyl signal itself that is required by bromodomain-containing transcriptional regulators to activate the transcription process (Winston and Allis, 1999).

In the context of the DNMT1-HDAC1 complex, the A/B pocket region of the Rb protein also interacts with mammalian DNMT1 between amino acids 416 and 913 (Robertson et al., 2000).

The A/B pocket regulates the cell cycle, differentiation, and apoptosis of the cell, and is a frequent target of mutations in human tumours (Grana et al., 1998). Therefore, the interaction between mammalian DNMT1 and Rb protein may be a mechanism for the tumour repression activity of DNMT1. The specificity of DNMT-Rb complex-mediated repression is linked to the interaction between Rb and E2F proteins. The Rb-E2F complex associated with HDAC1 represses transcription from promoters that have a E2F-binding site, and many of these loci are related to proliferation and cell cycle-related genes (Luo et al., 1998). The recruitment of HDAC1 by the Rb-E2F complex is dependent on the presence of DNMT1 (Robertson et al., 2000). Thus, DNMT1 is capable of forming a complex with Rb, E2F, and HDAC1 which determines the specificity of DNMT1 binding to promoters that have E2F-binding sites. The DNMT1/HDAC1 interaction creates a stable repression mechanism at those sequences. This mechanism may be a sufficient explanation for the involvement of mammalian DNMT1 in repressing tumour formation. In summary, there are multiple interactions between DNMT1 and HDAC1, as shown in Figure 1-2.

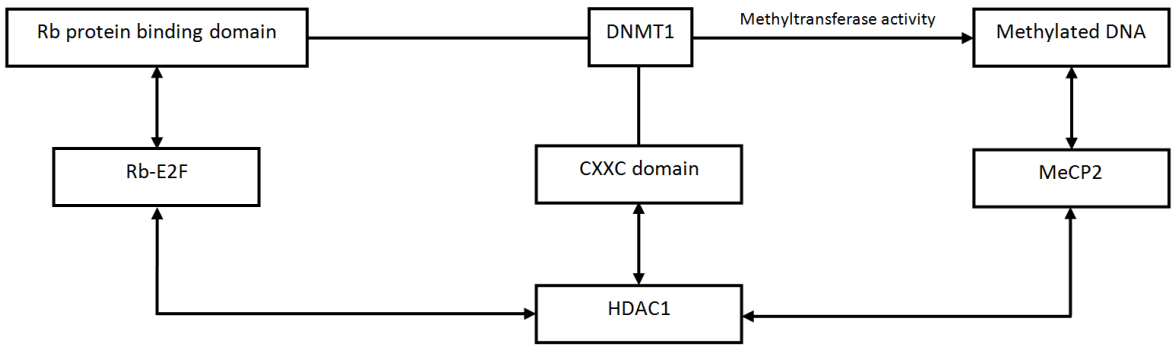

Figure 1-2 multiple interactions between mouse DNMT1 and HDAC1.

Another example of such interactions is the complex formed by the interactions of eukaryotic DNMT1 with HDAC2 and DMAP1. DMAP1 interacts with the first 120 amino acids of DNMT1 throughout the S phase of the cell-cycle, while the first 286 amino acids of HDAC2

interact directly with the first 1250 amino acids of DNMT1 protein during the late S phase (Rountree et al., 2000). The DNMT1-DMAP1 complex further interacts with TSG101, which has tumour suppressor activity (Watanabe et al., 1998). On the other hand, the interaction of DNMT1 and HDAC2 in the late S-phase is consistent with the maintenance of the deacetylated form of histones after DNA synthesis, to form a transcriptionally repressive heterochromatin (Grunstein, 1998). This example shows how the actions of DNMT1 can be coordinated with the cell cycle to allow timely regulation of gene expression (Figure 1-3).

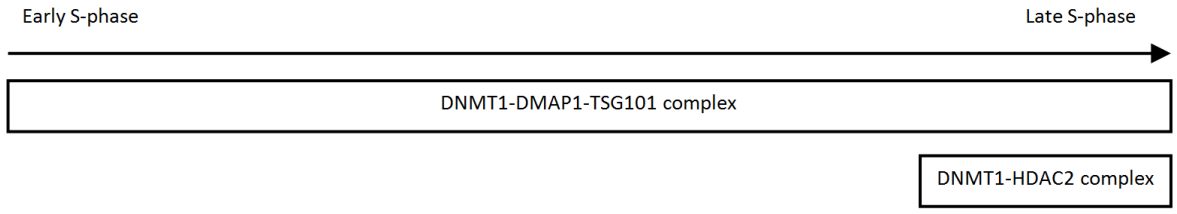

Figure 1-3 Interactions of DNMT1 with DMAP1 and HDAC2 during the cell cycle.

Another sequence in the N-terminal domain of DNMT1 that has a role in binding DNA is the replication foci binding domain. This domain is located between amino acids 207–455 of the N-terminal domain, and has been shown to direct mammalian DNMT1 to the replication foci during the S-phase of the cell cycle (Leonhardt et al., 1992). The removal of this sequence does not affect the enzymatic activity of mammalian DNMT1 (Bestor, 1992), suggesting that this sequence may function as a DNA targeting sequence that helps mammalian DNMT1 to localise to the newly replicated DNA. This role is consistent with the maintenance methylation property of DNMT1. However, this sequence is not the only one that targets DNMT1 to the replication foci. The mouse DNMT1 sequence of amino acids 574–846 has homology with Polybromo-1 protein (PBHD), and this also has the capacity to direct DNMT1 to replication foci, although it is not as effective as the replication foci binding domain (Liu et al., 1998, Song et al., 2011).

The large number of replication foci binding sites may increase the affinity of DNMT1 to replication foci.

The CXXC domain is a cysteine-rich region between amino acids 537–575 that has the ability to bind Zn. This domain has a role in discriminating between unmethylated and hemimethylated DNA, as the removal of this sequence results in the activation of mammalian DNMT1 *de novo* methylation activity (Bestor, 1992). The mechanism of this preference is explained in mouse by the ability of the CXXC domain to bind methylated DNA and increase the activity of DNMT1 towards hemimethylated DNA through direct binding of the CXXC domain with the catalytic domain (Fatemi et al., 2001). This means DNMT1 will methylate DNA only if the Zn binding protein has access to methylated DNA, leaving fully unmethylated DNA alone. However, a different scenario is proposed by the authors of another study, in which the zinc finger domain, in conjunction with BAH proteins, is able to prevent *de novo* methylation through two distinct mechanisms: 1) by forming a complex of CXXC-BAH1 between the unmethylated DNA and the catalytic domain of human and mouse DNMT1; and 2) by forming loop structures of BAH2-TRD proteins that prevent the interaction of TRD with the major groove of the unmethylated DNA (Song et al., 2011). Thus, these two models have different approaches to deciphering the CXXC domain mechanism in mouse: one model suggests that the CXXC domain increases the activity of the catalytic domain towards hemimethylated DNA, while the other model proposes that the preference for methylated DNA is due to the autoinhibition of the CXXC-BAH complex after binding unmethylated DNA. Despite the differences, these two models emphasis the function of CXXC domain as a component that directs DNMT1 to hemimethylated DNA. Perhaps the CXXC domain performs both mechanisms depending on the characteristics of the DNA that DNMT1 is attached to, by detecting the methylation state of the target DNA and switching between two mechanisms as necessary. However, this hypothesis remains to be tested.

Although a major function of the CXXC domain is to direct DNMT1 towards hemimethylated DNA, other evidence shows that DNMT1 retains a preference for the hemimethylated substrate in the absence of this zinc finger element. The hemimethylated CpG recognition mechanism of the TRD in the C-terminal domain of DNMT1 is able to compensate considerably for the absence of the autoinhibitory mechanism of the CXXC domain (Song et al., 2012). This is consistent with the previous finding that the catalytic domain of DNMT1 itself has a preference for hemimethylated DNA (Fatemi et al., 2001). These integrated hemimethylated DNA recognition mechanisms ensure the high specificity of DNMT1 towards hemimethylated CpG, supporting the role of DNMT1 as a maintenance methylation enzyme.

A different function of the BAH domain is proposed by another study, which shows that it acts as a protein-protein interaction module that is important in connecting DNA methylation, replication, and transcriptional regulation (Callebaut et al., 1999). This model is different to one described above which describes BAH domain as an inhibitor of *de novo* methylation by DNMT1. It is important to note that the evidence for the BAH domain promoting transcriptional regulation is an assumption based on the sequence homology of this protein with the Orc1p protein found in other species such as *Saccharomyces cerevisiae* (Callebaut et al., 1999). Therefore, there might be differences between the function of the Orc1p protein and that of the BAH domain in mammalian cells, including the function of directing DNMT1 to hemimethylated DNA. Nevertheless, it is possible that the BAH domain in mammalian cells functions as a connection between DNA methylation, replication, and transcriptional regulation, as mammalian DNMT1 is also correlated with those mechanisms. It is also possible that the BAH domain works in both scenarios within mammalian cells, supporting the full functions of DNMT1 in the cells.

The catalytic domain of DNMT1 contains 10 characteristic sequence motifs, of which 6 are highly conserved between species (Posfai et al., 1989, Wilson, 1992). The most conserved region of this domain contains motif IV, which is the catalytic core; motif I and X, which form the S-adenosyl-L-methionine-binding pocket; and some residues from motif II-V (Chen and Li, 2004). The more variable region between motif VIII and IX is responsible for target DNA recognition (Chen and Li, 2004). The catalytic core (motif IV) is responsible for adding methyl groups to DNA. Methyl group addition is mediated by a nucleophilic attack at carbon 6 of cytosine by the enzyme's cysteine, which forms a C^5-carbanion that attacks the methyl group of S-adenosyl-L-methionine (SAM), resulting in the formation of methylated cytosine and S-adenosyl-L-homocysteine (Cheng, 1995b, Bestor and Verdine, 1994). The target recognition domain (TRD) functions as a DNA recognition domain which interacts with the major groove of DNA and flips the cytosine in the minor groove of the catalytic core in order to allow methylation (Cheng, 1995a). Further investigation showed that the catalytic domain of mouse DNMT1 is bound specifically to hemimethylated CpGs (Fatemi et al., 2001). As it has been mentioned that the catalytic region interacts with the Zn binding domain which directs DNMT1 to hemimethylated DNA, the two regions putatively cooperate in determining the specificity of DNMT1 towards hemimethylated CpGs.

1.2.1.2. DNMT3A and DNMT3B

The other two members of the active DNA methyltransferase family are DNMT3A and DNMT3B. In contrast to DNMT1, which functions as a maintenance methylation enzyme, these two enzymes have been widely implicated in *de novo* DNA methylation. DNMT3A and DNMT3B are highly expressed during the blastocyst stage of development and germ cell development, which is considered to involve the establishment of new genome wide-DNA methylation (Li, 2002). DNMT3-deficient mice have their *de novo* methylation blocked and

develop several defects during development, which suggests that the presence of DNMT3 enzymes and *de novo* methylation are important in mouse embryo development (Okano et al., 1999, Ueda et al., 2006). Similar results are found in mouse ESCs, where the reintroduction of DNMT3 enzymes in double knockout ($DNMT3A^{-/-}$, $DNMT3B^{-/-}$) mouse ESCs results in the restoration of DNA methylation patterns (Chen et al., 2003). The introduction of the DNMT1 enzyme in those double knockout mouse ESCs could not restore the DNA methylation patterns (Chen et al., 2003). These findings suggest that DNMT3A and DNMT3B are essential in establishing *de novo* DNA methylation during mouse embryo development. Specifically, DNMT3B is essential in the early stages of embryo development (Borgel et al., 2010), while DNMT3A is required in establishing the DNA methylation pattern in maturing gametes (Kaneda et al., 2004). DNMT3A and DNMT3B have some overlapping activities, which explains why a deficiency of one of the two proteins in mouse embryonic development is more tolerated than a deficiency of both proteins (Latham et al., 2008). However, a deficiency of DNMT3B is more severe than a deficiency of DNMT3A, probably because DNMT3B is the first *de novo* methyltransferase expressed in the inner cell mass during mouse embryonic development (Watanabe et al., 2002). DNMT3A and DNMT3B also have an important role in mouse DNA methylation maintenance by filling the gap in methylation of hemimethylated DNA that is missed by the maintenance methyltransferase DNMT1 (Chen et al., 2003).

These two proteins share similar primary structures and domain organisation (Figure 1-4). Both proteins have a highly conserved N-terminal domain that consists of a variable N-terminal domain (Chedin, 2011) followed by a PWWP (Pro-Trp-Trp-Pro) domain (Maurer-Stroh et al., 2003), and a cysteine-rich zinc-finger binding domain (Chedin, 2011). The C-terminal domain of these enzymes has six highly conserved cytosine C5-DNA methyltransferase motifs, as previously described in studies of methyl transferases (Posfai et al., 1989), and a target recognition domain (Kumar et al., 1994).

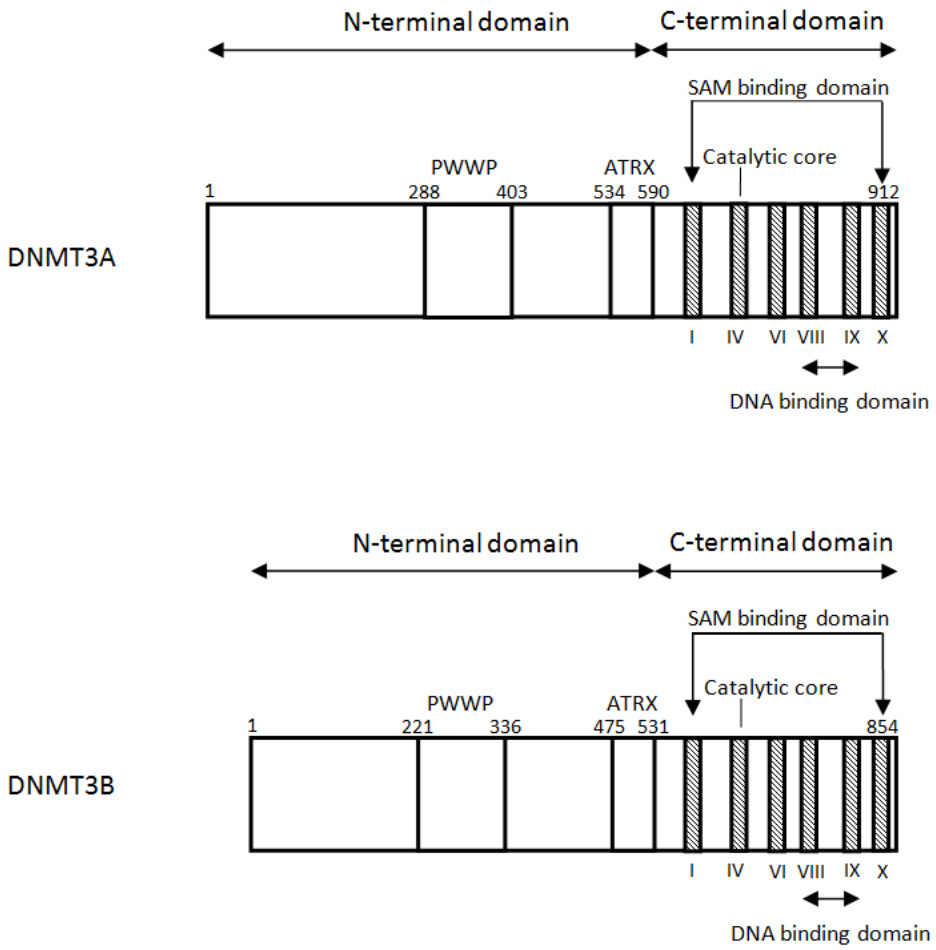

Figure 1-4 Domain mapping of DNMT3A and DNMT3B sequences.

Similar to DNMT1, the catalytic activity of DNMT3A and DNMT3B occurs in the C-terminal domains of the enzymes. The mechanisms of catalytic activity in the C-terminal domains of DNMT3A and DNMT3B are also similar to the mechanisms of catalytic activity in the C-terminal domain of DNMT1. The catalytic core (motif IV) in the domain mediates a nucleophilic attack on carbon 6 of the target cytosine followed by the flipping of the target cytosine to the enzyme active site pocket by a conserved glutamate residue (motif VI), leading to the formation of a covalent DNMT-cytosine intermediate (Klimasauskas et al., 1994). This intermediate triggers the second nucleophilic attack on the C5 position on the methyl group by SAM, producing methylated cytosine and S-adenosyl-L-homocysteine (Wu and Santi, 1987).

Beside their catalytic activity, the C-terminal domains of both DNMT3A and DNMT3B have also been found to interact with the DNMT3L protein. Upon binding, DNMT3L activates the DNA methyltransferase activity of DNMT3A and DNMT3B as well as protecting the DNA that is supposed to be unmethylated by binding histone tails of the unmethylated DNA (Jia et al., 2007). The catalytic domain of DNMT3A and DNMT3B also contain a putative target recognition domain (TRD) which spans between motif VIII and IX, and there is diversity in this region between the DNMT3A and DNMT3B protein sequences, possibly suggesting different target preferences (Kumar et al., 1994).

The high conservation of the catalytic domains of mammalian DNMT3A and DNMT3B does not occur with their N-termini (Chedin, 2011). The N-terminal domains are responsible for targeting the enzymes to chromatin (Latham et al., 2008); therefore, the diversity of N-termini among these enzymes may determine the specificity of the enzymes. The PWWP region in the N-terminal domain of DNMT3 is characterised by a structural motif of 100–150 amino acids containing a highly conserved proline-tryptophan-tryptophan-proline motif (Stec et al., 2000, Wu et al., 2011). The function of this domain in the DNMT3 enzymes is still poorly understood. The presence of this positively charged area and the ability of this domain in the mammalian DNMT3B to bind DNA *in vitro* have led to the hypothesis that this domain functions as a DNA-binding module (Qiu et al., 2002). However, most of the DNA-binding area of this domain is not conserved across species, leading to uncertainty as to whether this DNA binding property is a general function of the PWWP motif (Slater et al., 2003). In fact, several studies have found that the PWWP motif has homology to the Tudor domain and chromodomain, which both have the capacity to mediate protein-protein interactions (Maurer-Stroh et al., 2003, Nielsen et al., 2002, Selenko et al., 2001, Jacobs and Khorasanizadeh, 2002). Therefore, it is possible that protein-protein binding is the main function of the PWWP motif. Moreover, this

hypothesis is consistent with the function of the N-terminal region of DNMT3A and DNMT3B to localise the enzymes to the chromatin (Latham et al., 2008).

The cysteine-rich zinc-finger binding domain of human DNMT3 family is unrelated to the CXXC domain of DNMT1 (Xie et al., 1999). Instead it has sequence homology with a similar domain found in the X-linked *ATRX* gene of the SNF2/SW1 family (Picketts et al., 1996). This ATRX domain has a role in a gene repression mechanism which is connected to the function of DNMT3 proteins. This structure is also called plant homeodomain (PHD), a domain that has a cysteine-rich zinc finger region that can also be found in Rb-binding protein RBP2 (Aasland et al., 1995). The connection of this domain with Rb raises the possibility that DNMT3A and DNMT3B are also involved in chromatin-mediated transcriptional regulation and tumour repression mechanisms. Moreover, DNMT3A and DNMT3B have been found to interact with HDAC1 and RP58 through this region (Bachman et al., 2001, Fuks et al., 2001). Since HDAC1 and RP58 have a role in transcriptional regulation, these findings further affirm the involvement of DNMT3A and DNMT3B in transcriptional regulation processes. Taken together, the findings suggest that function of the cysteine-rich zinc-finger binding domain is to mediate the interaction between DNMT3 proteins and transcription repressor proteins in order to maintain the chromatin-mediated transcriptional regulation of the cells.

Several isoforms of DNMT3A and DNMT3B proteins have been discovered in mammalian cells. The murine *Dnmt3a* gene produces at least two products, DNMT3A and DNMT3A2, with lengths of 908 and 689 amino acids, respectively (Chen and Li, 2004). The DNMT3A2 isoform is derived from a transcript with different promoters, resulting in the lack of an N-terminal region in this isoform (Chen et al., 2003). In consequence, this isoform has a different localisation pattern from its longer counterpart, even though both of them have active *de novo* methylation activity. DNMT3A is localised in the heterochromatin, while DNMT3A2 is

localised in the euchromatin (Chen et al., 2002, Latham et al., 2008). This fact suggests that the N-terminal region of DNMT3A localises the enzyme to the heterochromatin. The difference in localisation of these enzymes also suggests different functions for these enzymes in embryo development. Primarily DNMT3A2 is found in co-expression with DNMT3L in the germ cells during *de novo* methylation, suggesting that DNMT3A2 functions to generate imprints in the mouse germ-line (Lees-Murdock et al., 2005, Sakai et al., 2004). This enzyme is also found in undifferentiated mouse ESCs, while DNMT3A is expressed at low levels in almost all somatic cells, where DNMT3A2 is not detected (Chen et al., 2002).

The only known active isoforms of DNMT3B in mammals are DNMT3B1 and DNMT3B2, while the other isoforms are known to be inactive due to the lack of some motifs in their domains (Chen et al., 2003). In contrast to the expression of DNMT3A isoforms, the formation of DNMT3B isoforms is mediated through an alternative splicing of its gene product (Chen et al., 2003). Mouse DNMT3B3 and DNMT3B6 lack parts of the conserved methyltransferase motif IX (Aoki et al., 2001, Chen et al., 2003), while mammalian DNMT3B4 and DNMT3B5 lack the conserved methyltransferase motifs IX and X (Robertson et al., 1999, Chen et al., 2003). These DNMT3B isoforms show patterns of expression depending on the cell type. Similar to DNMT3A, DNMT3B3 is expressed at low levels in most somatic cells, while DNMT3B6 is only expressed in mouse ESCs, and DNMT3B1 is highly expressed in mouse ESCs, germ cells, and early embryos along with DNMT3A2 (Chen et al., 2002). Human DNMT3B4 and DNMT3B5 are primarily expressed in testis (Robertson et al., 1999). Based on the expression time and location, DNMT3A2 and DNMT3B1 might be the major enzymes that establish the methylation pattern of the early embryo, while DNMT3A, in cooperation with DNMT1, has a role in maintaining the methylation pattern of the somatic cells (Chen et al., 2003). The role of the inactive DNMT3B isoforms, however, is still unclear. Nevertheless, the

localisation of those proteins in specific tissues suggests that they actually have functions in gene regulation.

1.2.1.3. The catalytically inactive DNMT members

There are several members of the DNMT family that appear to be inactive due to the lack of methyltransferase activity. There are at least two members of this inactive group, the DNMT2 and DNMT3L proteins. DNMT2 is a small protein with 415 amino acids, similar to the prokaryotic DNA methyltransferase domain and lacking a large N-terminal domain (Latham et al., 2008). Despite the appearance of the conserved catalytic domain of DNA methyltransferase, methylation activity of this protein in humans is difficult to find (Dong et al., 2001, Van den Wyngaert et al., 1998). Moreover, genetic analysis showed that disruption of the *Dnmt2* gene in mouse ESCs does not affect the genomic methylation pattern of the cells or the ability of the cells to methylate newly integrated retrovirus DNA (Okano et al., 1998). Therefore, the literature suggests that DNMT2 is not essential for either *de novo* or maintenance methylation in mouse ESCs. However, a study in mouse has revealed that DNMT2 may function as an RNA methyltransferase as it has specificity to aspartic acid tRNA (Goll et al., 2006). Furthermore, depletion of Dnmt2 in the zebrafish embryo triggers differentiation defects in several organs such as brain, retina, and liver (Rai et al., 2007). Based on these findings, DNMT2 may have a role in methylating RNA. However, the effect of the DNMT2-mediated RNA methylation on development of the embryo, specifically the mammalian embryo, is still a subject of investigation.

In contrast with DNMT2, DNMT3L has been found to have important roles in the genome methylation process. DNMT3L is a protein that consists of 421 amino acids in mouse (Chen and Li, 2004). The DNMT3L protein is co-expressed with DNMT3A2 in germ cells, offering the possibility that the function of DNMT3L is to establish genome imprinting in germ cells

(Lees-Murdock et al., 2005, Sakai et al., 2004, Kaneda et al., 2004). The N-terminal region of mammalian DNMT3L contains a domain called an ADD (ATRX-DNMT3-DNMT3L) domain, due to its homology with the domain in DNMT3 and the ATRX domain, which contains a C2C2-type and an imperfect PHD-type zinc finger domain where the histidine of the CH4C3 consensus is substituted with cysteine (C4C4) (Aapola et al., 2001, Aapola et al., 2000). The fact that PHD domains have been found to be involved in chromatin-mediated transcriptional modulation (Aasland et al., 1995) suggests the involvement of ADD in the same mechanism. Therefore, DNMT3L may also be involved in transcriptional regulation, just like its methyltransferase-active counterparts DNMT3A and DNMT3B. This hypothesis has been confirmed by the finding that the mammalian DNMT3L protein interacts with HDAC1 through this PHD-like domain to perform transcriptional repression activity in unmethylated H3K4 (Aapola et al., 2002, Ooi et al., 2007). However, the transcription repression activity of DNMT3L is not caused by the methyltransferase activity of the protein itself. Although the catalytic region of mouse DNMT3L shares similarity with the conserved motifs I, IV, and VI of DNMT3A and DNMT3B, the region lacks the critical amino acids for catalytic activity: FGG in motif I, PC in motif IV, and ENV in motif VI (Aapola et al., 2001). Nevertheless, DNMT3L is important in germ cell imprinting, which is confirmed by the finding that the progeny of DNMT3L-deficient female mice lack imprints in both the embryo and extra-embryonic tissues and die in mid-gestation (Arima et al., 2006, Bourc'his et al., 2001, Hata et al., 2002). Moreover, DNMT3L-deficient male mice exhibit impaired spermatogenesis due to hypomethylation of both long-terminal-repeat (LTR) and non-LTR retrotransposons, which causes meiotic catastrophe in the cells (Webster et al., 2005, Bourc'his and Bestor, 2004).

DNMT3L has a similar expression pattern to DNMT3A and DNMT3B during mouse development and also interacts with DNMT3A and DNMT3B in the nuclei of mammalian cells (Hata et al., 2002). This interaction stimulates the activities of the other DNMT3 proteins by

increasing the binding of DNMT3 with SAM and lowering the K_m of the enzymes (Gowher et al., 2005). DNMT3L acts as a transcriptional regulator through dual mechanisms: 1) the interaction with HDAC1 has chromatin-mediated transcriptional regulation activity by itself; and 2) the interaction of DNMT3L with the other DNMT3 proteins increases the methyltransferase activity of the proteins. The interaction with HDAC1 recruits the DNMT3L-DNMT3 complex to the unmethylated H3K4, inducing *de novo* methylation at the sites in germ-cell lines (Jia et al., 2007).

1.2.2. Demethylation enzymes

Logically, a mechanism for DNA demethylation would seem to be required, since several examples of acute loss of methylation have been reported, including the process of epigenetic reprogramming during embryo development (Chen and Riggs, 2011, Seisenberger et al., 2013). However, the mechanisms for DNA demethylation are still poorly understood. There are two types of DNA demethylation proposed: passive and active demethylation. Passive demethylation can be achieved simply by not methylating the DNA after each replication, for example by the inhibition of DNMT1 (Chen et al., 2007). The mechanisms of active demethylation require further investigation.

To date, unequivocal evidence of an active demethylase has only been found in plants, with the involvement of a specific 5meC-glycosylase that removes the base of methylated DNA and triggers a repair mechanism to replace the former methylated base with the unmethylated one (Zhu, 2009). The downstream repair mechanism is similar to the base excision repair (BER) mechanism found in mammals in the mismatch repair process, leading to the suggestion that BER may also be involved in mammalian active demethylation (Chen and Riggs, 2011). However, the upstream mechanism that initiates this process appears to be different from that in plants (Chen and Riggs, 2011). There are several candidates for the upstream demethylation

processes, including thymine DNA glycosylase (TDG) and methyl-CpG-binding domain protein 4 (MBD4) (Zhu et al., 2000a, Zhu et al., 2000b), activation-induced cytosine deaminase (AID) and apolipoprotein B mRNA editing enzyme, catalytic polypeptide 1 (APOBEC1) (Morgan et al., 2004), and ten eleven translocation (TET) proteins (Ito et al., 2010, Pastor et al., 2013).

1.2.2.1. TDG and MBD4

Although there is no homolog of plant glycosylases in mammals, there are several weak 5meC glycosylases found in humans, including TDG and MBD4 (Zhu et al., 2000a, Zhu et al., 2000b). MBD4 is reported to bind to both hemi-methylated and non-methylated DNA; however, the 5meC glycosylation activity of this protein is only found with hemi-methylated DNA and it is 30 times lower than the T-G mismatch glycosylation activity of this protein (Zhu et al., 2000a). Similar to MBD4, TDG also has affinity to hemi-methylated DNA, and the 5meC glycosylation activity is also 30 times lower compared to the T-G mismatch glycosylation activity of this protein (Zhu et al., 2000b). Therefore, the function of both MBD4 and TDG as 5meC DNA glycosylases that stimulate BER-mediated DNA demethylation is still unclear (Cortazar et al., 2007). Hormone-induced phosphorylation of MBD4 is reported to stimulate its 5meC glycosylase activity, leading to active demethylation of the *CYP27B1* gene promoter in mice (Kim et al., 2009). However, *Mbd4*-knockout mice are found to be viable and fertile, despite the enhanced CpG mutability and tumourigenesis (Millar et al., 2002). Because DNA demethylation is reported to be important for embryo development, the viability of MBD4-null embryos suggests that MBD4 is not the major component of DNA demethylation. These findings indicate that there may be other DNA demethylation mechanisms in mammals.

1.2.2.2. AID and APOBEC1

Another proposed mechanism for active DNA demethylation is the deamination of 5meC into thymine, followed by BER for mismatch repair. The candidate proteins for this mechanism are AID and APOBEC1. The deamination of DNA (preferably single stranded) by AID and APOBEC1 is found to cause T-G mutation in methylated DNA and triggers BER by T-G mismatch glycosylases such as MBD4 and TDG (Morgan et al., 2004). Furthermore, both enzymes are found to be expressed in mouse oocytes, and AID is expressed in primordial germ cells suggesting a possible role of these enzymes in active DNA demethylation (Morgan et al., 2004). This hypothesis is supported by a study that finds overexpression of AID and MBD4, but not either alone, causes demethylation of DNA in zebrafish (Rai et al., 2008). Evidence for AID involvement in DNA demethylation mechanism is also found in mammals: firstly, the role of AID in demethylation of *Oct4* and *Nanog* promoters in heterokaryons from mouse fibroblasts and ESCs (Bhutani et al., 2010); and secondly, the higher methylation level in the genome of AID-deficient mouse PGCs (Popp et al., 2010). However, the level of methylation in the PGCs of AID-deficient mice is still low, indicating that DNA demethylation still occurs in the absence of AID (Popp et al., 2010). Therefore, there must be other factors involved in DNA demethylation of mammals, and whether AID and APOBEC1 are essential for DNA demethylation is still not clear.

1.2.2.3. TET

Recent discoveries of 5-hydroxymethylcytosine (5hmC) in mammalian cells have raised new alternatives for DNA demethylation. The detection of 5hmC modification in mouse Purkinje neurons (Kriaucionis and Heintz, 2009) and mouse ESCs (Tahiliani et al., 2009) has lead to the realisation that 5meC is not the only DNA modification occurring in mammalian cells. Furthermore, the presence of 5hmC is particularly enriched in embryonic contexts and

correlates with the pluripotent state of the cells (Ruzov et al., 2011). The conversion of 5meC to 5hmC is mediated by members of the TET family of proteins, which consists of three active members: TET1, TET2, and TET3 (Figure 1-5) (Ito et al., 2010, Pastor et al., 2013). All the TET proteins have a broad expression pattern across tissues, with TET1 being expressed abundantly in ESCs, TET2 in hematopoietic cells, and TET3 in oocytes and zygotes (Auclair and Weber, 2012).

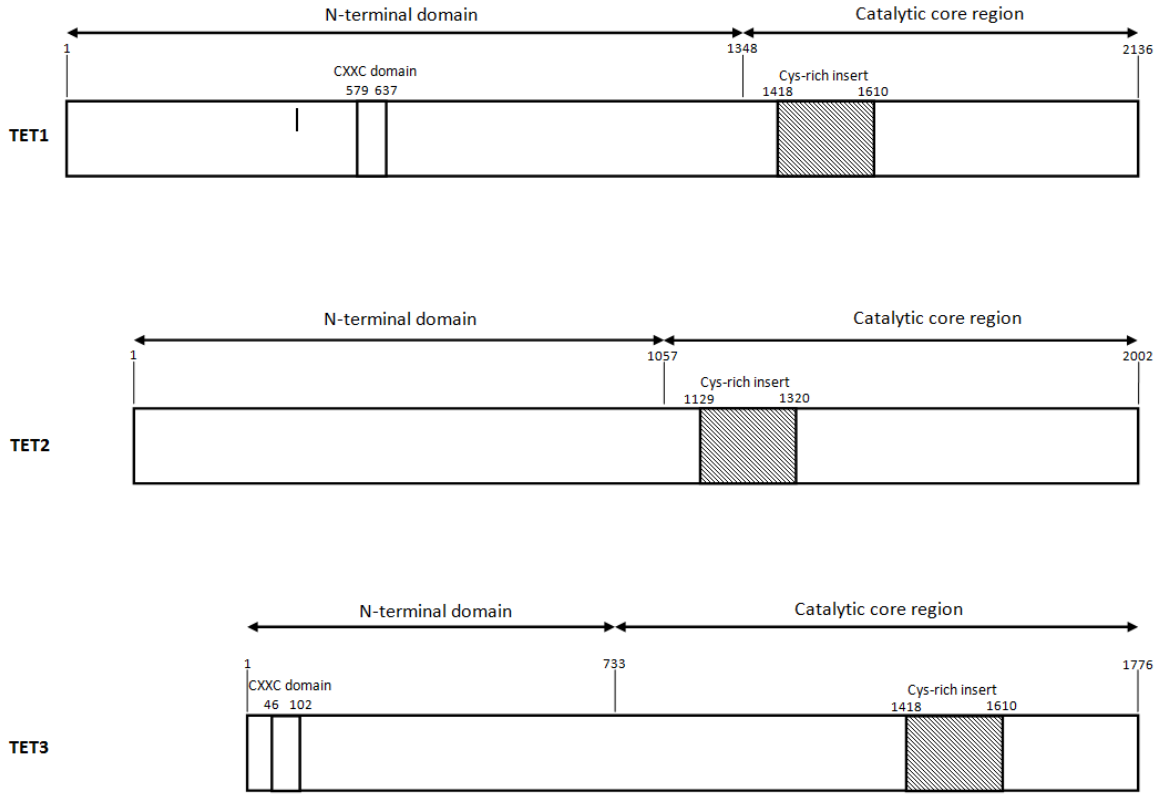

Figure 1-5 Domain mapping of TET proteins.

The proteins of the TET family each consist of a dioxygenase motif required for Fe(II) and α-ketoglutarate (α-KG) binding and a conserved cysteine-rich region that is thought to be involved in DNA binding (Ito et al., 2010, Iyer et al., 2009). The dioxygenase motif catalyses the conversion of 5meC to 5hmC by TET proteins in the presence of Fe(II)- and α-KG (Tahiliani et al., 2009). Additionally, TET1 and TET3 contain a CXXC zinc finger domain in

their N-terminus which is similar to other 5meC-related proteins (Iyer et al., 2009), but this domain in mouse TET1 binds to both unmethylated and methylated CpG-rich regions (Xu et al., 2011). This study proposed that the ability of TET1 to bind to unmethylated CpG may prevent access of DNMT proteins to methylate the CpG, primarily in euchromatin. This may suggest a role of TET in demethylation by preventing maintenance methylation of DNA. In contrast, mouse DNMT proteins can recruit MBD to the methylated CpG-dense DNA leading to the formation of a heterochromatic state and this may prevent TET proteins from binding to those regions, stabilising their hypermethylated state (Xu et al., 2011). These two mechanisms are promising models of epigenetic regulation requiring further investigation.

The knockdown of TET1 in ESCs reduces NANOG expression in the cells and is associated with increased methylation of the *Nanog* promoter. This caused a self-renewal defect and reduced growth of ESCs (Ito et al., 2010). Furthermore, downregulation of the TET1 protein in the mouse embryos prevents the embryonic cell specification towards ICM and directs differentiation of the embryonic cells towards the trophectoderm lineage (Ito et al., 2010). These results indicate that TET1 has an important role in maintaining pluripotency and cell fate in ESCs and embryos. The ability of TET1 to convert 5meC to 5hmC is most likely the key feature that determines the ability of this enzyme to maintain pluripotency, indicated by the high correlation between the expression of pluripotency markers and the amount of TET1 and 5hmC contained in the cells (Branco et al., 2012, Wu and Zhang, 2011). Another study has found that the expression of TET1 and TET2 is high in both ESCs and ICM and decreased in OCT4-negative cells present in the ICM outgrowth (Tang et al., 2010), which is consistent with the function of TET proteins in demethylating DNA and maintaining pluripotency.

A later study found that TET proteins can further oxidise 5hmC into 5-formylcytosine (5fC) and 5-carboxylcytosine (5caC), and both of these derivatives are found in mouse ESCs while

only 5fC has been found in mouse organs to date (Ito et al., 2011). This finding opens up another possible pathway of 5meC demethylation. It is observed that this TET-catalysed oxidation is similar to the conversion of thymine to uracil by conversion of thymine to iso-orotate followed by decarboxylation by the iso-orotate decarboxylase (Ito et al., 2011, Neidigh et al., 2009, Smiley et al., 2005). If this model is found in mammals, then the DNA demethylation processes could potentially occur without the need for BER. However, the enzyme that decarboxylates 5caC has not been found in mammals (Ito et al., 2011); therefore the possibility that BER is involved in DNA demethylation process still cannot be ruled out. Moreover, several lines of evidence have been found that implicate a two-step mechanism for active DNA demethylation in mammals, involving oxidation by TET followed by AID/APOBEC1-induced deamination, which finally triggers complete removal of the methyl group from the DNA by the TDG-mediated BER (Guo et al., 2011, Cortellino et al., 2011, He et al., 2011). This model is also supported by the finding that TDG can readily excise 5fC and 5caC, with a higher activity in 5fC removal compared to its T-G mismatch repair activity (Maiti and Drohat, 2011). With this finding, it is possible that TDG removes the formyl and carboxyl groups from the cytosine without the deamination process catalysed by AID/APOBEC1. With the discoveries of recent years, the mechanisms of active demethylation in mammals are being progressively revealed and the discovery of the complete model will not be too far away (Figure 1-6).

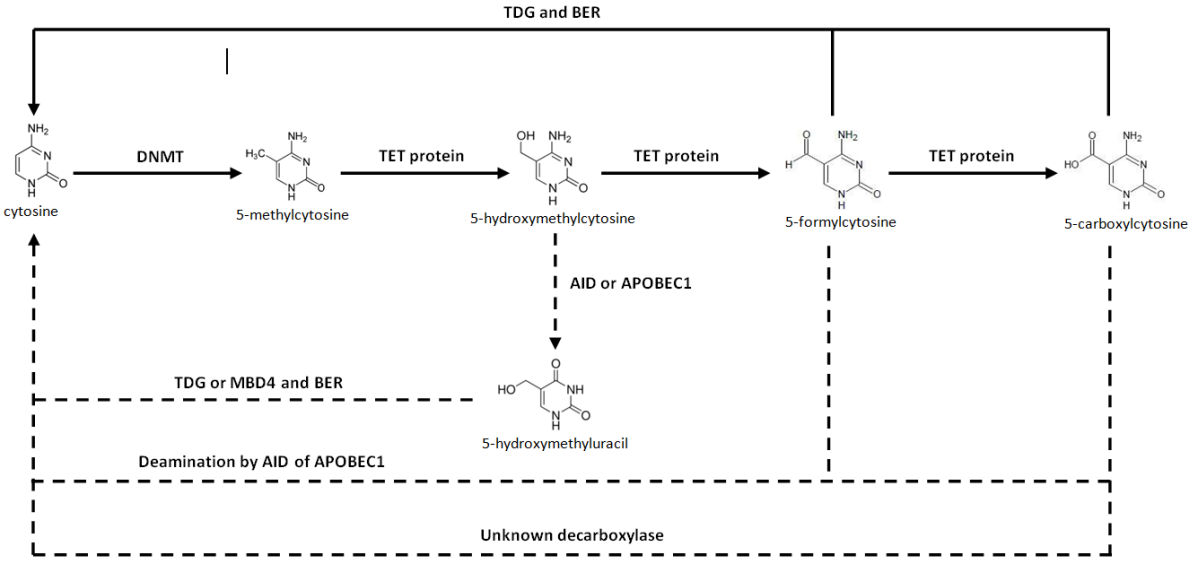

Figure 1-6 Known and putative mechanisms of DNA demethylation in mammals.

1.3. METHODS OF ANALYSIS

One important aspect of the analysis of cytosine methylation and demethylation is the method used for detecting DNA methylation. A robust and reliable method to detect the presence of DNA methylation is essential for generating reproducible high-throughput results. Moreover, a good method prevents systematic error that can lead to bias in interpreting the nature of methylation in mammalian genomes. Generally, methods for detecting DNA methylation are based on the following techniques: digestion with methylation-sensitive restriction enzymes, bisulfite conversion, and immunoassays (Altun et al., 2010).

1.3.1. DNA fragmentation by restriction enzymes

Detection of cytosine methylation by digestion with restriction enzymes is a conventional method that takes advantage of the methylation sensitivity of some restriction enzymes. For example, many restriction enzymes such as *Hpa*II, *Ava*I, *Hha*I, *Eco*RI, *Bam*HI, *Acc*I, *Cla*I and *Hae*II cleave only unmethylated DNA at their recognition sites and do not cleave the methylated counterparts (Bird and Southern, 1978, Okamoto et al., 2002, Tasseron-de Jong et

al., 1988, Nelson et al., 1993). In contrast, other restriction enzymes such as *Msp*I, which has similar recognition site with *Hpa*II, cleaves only methylated DNA (Butkus et al., 1987). In this method, sequences from different samples are put into reaction with the methylation-sensitive restriction enzymes. Next, the products are separated, run on a 2-dimensional gel, and assessed for the difference in methylation state of the sequences with restriction landmark genomic scanning map. One of the disadvantages of this method is that it is unable to provide single-nucleotide resolution (Altun et al., 2010). This problem can be resolved by combining this method with a next-generation sequencing approach called Methyl-Sensitive Cut Counting (MSCC) (Ball et al., 2009). In this method, the DNA sequence is digested with methylation-sensitive restriction enzyme such as *Hpa*II, and an adaptor containing *Mme*I (or another type-II restriction enzyme which cleaves several base pairs away from its recognition sequence) is ligated to the restricted sequence. Consequently, the sequence is restricted by *Mme*I. Next, the products are ligated to another adaptor to allow amplification of the sequences that contain unmethylated *Hpa*II restriction sites. Although this method is able to provide a single-nucleotide resolution, the observation is limited to the sequences that contain methylation-sensitive restriction enzymes recognition sites (Altun et al., 2010, Okamoto, 2009). Moreover, the restriction enzyme technique requires a large amount of genomic DNA (Okamoto, 2009), making it inefficient. Another major drawback of enzymatic methods in DNA methylation analysis is that the currently available enzymes do not distinguish between 5meC and 5hmC (Nestor et al., 2010), resulting in the overestimation of the amount of 5meC in the sequences.

1.3.2. Bisulfite conversion

Bisulfite conversion is currently one of the most widely used techniques for the analysis of DNA methylation. In this method, the DNA is denatured and treated with sodium bisulfate, which deaminates cytosine through formation of a 5,6-dihydrocytosine-6-sulfonate

intermediate at an acidic pH, followed by conversion to uracil at an alkaline pH, while leaving the methylcytosine largely unconverted (Okamoto, 2009, Frommer et al., 1992). Methylcytosine yields thymine when treated with sodium bisulfate, but with far slower conversion rates (Shapiro et al., 1970, Hayatsu et al., 1970b, Hayatsu et al., 1970a), therefore it is possible to optimise the conditions to distinguish between cytosine and 5-methylcytosine. With this method, it is possible to analyse the level of DNA methylation by comparing the converted and unconverted DNA. After replication, the unmethylated sites are read as thymine and the methylated sites stay as cytosine. This method also provides a high conversion rate of cytosine to uracil, usually ranging from 95–98% (Warnecke et al., 2002). The technique allows resolution of the methylation at the single base level.

For analytical purposes, bisulfite conversion is usually coupled with other techniques to improve its performance. One popular technique is methylation-specific PCR (MSP), a combination of bisulfite conversion and PCR to map the DNA methylation patterns in CpG islands (Okamoto, 2009). In this technique, DNA is treated with bisulfite to convert cytosine to uracil while leaving the 5-methylcytosine unconverted, followed by PCR with primers specific to methylated DNA (Herman et al., 1996, Clark et al., 1994, Frommer et al., 1992, Gonzalgo and Jones, 1997). Further modifications of this method may include quantitative PCR applied to the bisulfate-converted sequences to quantify the methylation level of the sequences (Eads et al., 2000). The addition of PCR to this method enables the analysis of the methylation level of small DNA samples with single-nucleotide resolution. To allow analysis of the whole genome, further modification is applied to the techniques, in which the amplified DNA is hybridised to an array containing probes for methylated and unmethylated DNA (Gitan et al., 2002). The drawback of this method is that the single-nucleotide resolution is sacrificed in order to cover the whole genome, due to the inability of the probes to distinguish a single base-pair difference.

Perhaps the most powerful bisulfite conversion variant is bisulfite sequencing (BS-Seq). Generally, bisulfite sequencing is the combination of bisulfite conversion with any sequencing technique. One example of the older methods is reduced representation bisulfite sequencing (RRBS), which involves digestion with a restriction enzyme followed by bisulfite conversion and sequencing (Meissner et al., 2005). Although this method also provides a single-nucleotide resolution, the range of the genome that can be analysed is limited due to the dependence on restriction enzymes. Another sequencing method that is used in conjunction with bisulfite conversion is the use of up to ~30,000 padlock probes to assess the methylation of selected regions in the genome through sequencing (Ball et al., 2009, Deng et al., 2009). Because this technique depends on detection by the probes, there are many disadvantages, such as low coverage area and the difficulty of analysing certain regions due to probe design considerations (Altun et al., 2010). Finally, it has been reported that whole-genome bisulfite sequencing has been widely used in plants and mammals due to the improvements in next-generation sequencing technology (Lister et al., 2008, Booth et al., 2013, Lister et al., 2009). With the ability to provide single-nucleotide resolution in whole-genome sequencing, bisulfite sequencing is claimed to be the most powerful tool in the field of DNA methylation analysis.

Although bisulfite sequencing is a powerful tool in DNA methylation analysis, this technique is not without flaws. One of the problems of this technique is degradation of DNA caused by the long reaction time with sodium bisulfite (Tanaka and Okamoto, 2007, Okamoto, 2009). The degradation of DNA can lead to reduced reliability of the assay. Another problem is that bisulfite conversion cannot differentiate between 5meC and 5hmC because the reaction of 5hmC with bisulfite results in 5-methylaenesulfonate, which is not readily converted to uracil (Jin et al., 2010, Nestor et al., 2010, Huang et al., 2010, Ko et al., 2010). This lack of specificity leads to overestimation of the overall amount of 5meC in the genome. With the interesting recent findings about the role of 5hmC and its derivates, it is important that the technique used

to detect such epigenetic modifications has the ability to distinguish between all of the different modifications.

A new method called oxidative bisulfite sequencing (oxBS-Seq) has been introduced to detect 5hmC through the oxidation of 5hmC into 5fC, followed by bisulfite conversion of 5fC into uracil; this method allows the detection of 5hmC in genomic DNA at single-base resolution (Booth et al., 2012). However, due to the reaction mechanism that converts 5hmC into 5fC, this technique still cannot differentiate between 5hmC, 5fC, and 5caC. Therefore, other techniques such as reduced bisulfite sequencing (redBS-Seq) and chemical modification-assisted bisulfite sequencing (CAB-Seq) have been developed to differentiate 5fC and 5caC from other DNA modifications (Booth et al., 2014, Lu et al., 2013). The redBS-Seq technique is performed using a specific chemical reaction that reduces 5fC to 5hmC prior to bisulfite treatment, such that all 5fC are read as C; then the output is compared with BS-Seq, which reads 5fC as T and 5hmC as C, to calculate 5fC at single-nucleotide resolution (Booth et al., 2014). The CAB-Seq technique uses chemical selective labeling of 5caC with an amide bond formation between the carboxyl group of 5caC and a primary amine group of 1-ethyl-3-[3-dimethylaminopropyl]-carbodiimide hydrochloride (EDC), which protects the 5caC from deamination through the bisulfite treatment (Lu et al., 2013). The same base-protection technique with hydroxylamine can also be used to protect 5fC from bisulfate deamination, to provide a single-base resolution of 5fC profiling in genomic DNA (Song et al., 2013). The combination of these bisulfite sequencing techniques has been used to generate a genome-wide profiling of 5meC, 5hmC, 5fC, and 5caC in mouse ESCs (Shen et al., 2013, Booth et al., 2014). Regardless of the limitations of the bisulfite conversion technique, it has been a mainstay of analysis and is considered the gold standard for DNA methylation analysis.

1.3.3. Immunoassay

Immunoassay is another major technique that is commonly used for detecting DNA methylation in cells. Basically, immunoassays are tests that measure or detect the presence of an antigen – in this case 5-methylcytosine or its derivatives – in the samples by using antibodies that specifically bind the antigens (Darwish et al., 2000, Reynaud et al., 1992). The antibody-labeled DNA is then assessed for DNA modification. Immunoassays can be performed directly in the cells or after retrieving the DNA. The most common technique to assess DNA methylation directly in the cells uses immunofluorescence-labeled antibodies. The immunofluorescence-labeled antibodies recognise and bind to the antibodies that bind to the DNA. Assessment by retrieving the DNA can be performed using several techniques, such as capillary electrophoresis (Wang et al., 2009), magnetic particles (Wang et al., 2010), microspheres (Ge et al., 2012), nitrocellulose membrane (Deobagkar et al., 2012), microarray (Kelkar and Deobagkar, 2009) and sequencing (Down et al., 2008).

In contrast to the bisulfite conversion method, immunoassay methods offer a specific distinction between 5meC and 5hmC (Jin et al., 2010). When used in conjunction with sequence analysis, this technique can provide whole genome coverage, as proved by a study on a plant genome (Zhang et al., 2006). However, the drawback of utilising a conventional immunoassay is that it does not provide single-nucleotide resolution. Reasonable resolution of the whole genome with the microarray method can be costly, and even next-generation sequencing cannot provide single-nucleotide resolution due to the utilisation of affinity purification with antibodies (Altun et al., 2010). However, a recent finding has made single-nucleotide resolution possible with the immunoassay technique. In this new method, the DNA target is treated with bulge-inducing DNA such that only the 5-methylcytosine located in the

bulge is detected by the antibody, due to the rotation caused by the bulge (Kurita and Niwa, 2012). With this method, analysis at the single-nucleotide level is possible. Currently, this method is able to provide whole-genome DNA methylation analysis with good sensitivity and specificity at single-nucleotide resolution. With a wide variety of antibodies available, this method has overcome the coverage limitation of the enzyme restriction digest method, which depends on a limited variety of enzymes. With the bulge technology, immunoassay is on par with bisulfite conversion in terms of resolution.

The selection of an appropriate analysis method is an essential factor in elucidating the enigmatic epigenetic process in mammalian cells, and both bisulfite conversion and immunoassay have their advantages and limitations. The main advantage of the immunoassay method is that it can provide single cell resolution and is more cost effective and less labour intensive than bisulfite conversion techniques (Table 1-1 Current major techniques of methylation analysis).

Table 1-1 Current major techniques of methylation analysis

Methods	**Single-nucleotide resolution**	**Genome coverage**	**Sample required**	**5meC derivatives recognition**	**Others**
Restriction enzymes	Limited (MSCC)	Limited	Large	No	
Bisulfite conversion	Yes	Whole genome (next generation sequencing)	Small	Yes	Issue with degraded DNA
Immunoassay	Yes (bulge-inducing DNA)	Whole genome (next generation sequencing)	Small	Yes	

1.3.4. The limitations associated with antigen retrieval in immunoassay

Immunolocalisation studies initially indicated that a global active demethylation occurs within the paternally-inherited genome of the zygote soon after fertilisation, relative to the maternally-inherited genome (Oswald et al., 2000, Morgan et al., 2005, Wossidlo et al., 2010). However, recent chemical analyses showed little difference in methylation levels between the paternally and the maternally-inherited genomes during the process of embryo development (Smith et al., 2012). The recent chemical analyses are also supported by recent immunofluorescence analyses that show little asymmetry in the levels of methylation between the paternal and the maternal genome (Salvaing et al., 2012, Li and O'Neill, 2012). These contradicting results were apparently due to change in the immunolocalisation protocol used.

Technically, a valid immunolocalisation procedure requires the antigen to be fully solvent-exposed, which means the preparation should not significantly degrade or mask the epitope and the antigen-antibody interaction should approach thermodynamic equilibrium (saturated) (Salvaing et al., 2014). Comprehensive analyses of the immunoassay methodology used in the zygote showed that the reports of active demethylation from the paternal genome were caused by masking of the 5meC antigen rather than its loss (Li and O'Neill, 2012, Li and O'Neill, 2013a, Salvaing et al., 2014). The 5meC modification is located on the major groove of DNA, so it should be readily solvent-exposed in a linear DNA. However, native DNA is often compacted, which leaves little of the DNA accessible to the antibody. Therefore, an additional treatment is needed to denature the DNA and make it accessible to the antibody. The exposure of fixed cells to a brief process of acidification in 2–4M HCl is widely used as a standard approach to denature the DNA (Salvaing et al., 2014, Iqbal et al., 2011, Wossidlo et al., 2011). However, studies have found a dynamic acid-resistant antigen masking that requires additional treatments to remove (Li and O'Neill, 2012, Li and O'Neill, 2013a). The acid-resistant masking

is caused by a range of chromatin and non-chromatin proteins that are attached to the 5meC; for example, the proteins from MBD1 which are found to be present in both paternal and maternal pro-nuclei (Li and O'Neill, 2012). The study found that a short exposure of the fixed zygote to trypsin following the acid treatment was sufficient to remove the proteins, and this was accompanied by an increase in detectable 5meC.

The changes in chromatin structure during zygotic maturation are the suggested cause of the dynamic levels and proportions of the two pools of antigen-masking during embryo development. Another study in mouse embryonic fibroblasts has confirmed that the antigen-masking of 5meC is not unique to the zygote, but also occurs in a culture of mouse embryonic fibroblasts (Çelik et al., 2014). The relative proportion of the two types of 5meC masking in cells also depends on their stage in the cell cycle and the age of the cells. Acid-induced denaturation of chromatin followed by epitope retrieval using trypsin digestion has improved antigen retrieval during immunoassay detection of 5meC, and revealed a more dynamic response of 5meC levels and expression patterns to the changes over the cell growth cycle (Çelik et al., 2014).

Recent studies have shown that the long-accepted conventional methods of immunolocalisation overlook the presence of antigen masking of 5meC in the cells; this causes underestimation of 5meC levels by conventional methods of immunostaining. This fact challenges the popular beliefs that have been held for a long time regarding the levels and patterns of 5meC expression in cells. Therefore, the newly designed antigen retrieval methods for detecting 5meC and 5hmC levels and distribution patterns will be used in this study. These methods will be optimised for the immunolocalisation procedures for detecting 5meC and 5hmeC in mouse ESCs. By optimising these methods, detection of DNA modifications will be improved, allowing a more

reliable assessment of DNA modification in the ESCs in association with the changing culture conditions.

1.4. PLURIPOTENCY, DIFFERENTIATION, AND DNA METHYLATION

Many studies have described DNA methylation as a major epigenetic phenomenon in mammalian cells. It has been widely shown that epigenetic processes control the expression of genes in the cells necessary for normal cell growth and development. Therefore, the connection between epigenetic processes, specifically DNA methylation, and pluripotency and differentiation of the cells is an important area of investigation in embryology and stem cell research. Even though several questions regarding this connection have been answered, there are still many factors that remain to be elucidated in order to understand the nature of embryo and stem cell biology.

1.4.1. Pluripotency and differentiation

During embryogenesis, cells in mammalian embryo undergo several stages of division and differentiation. The process starts after fertilisation with cell division (cleavage) from 1 cell to 2 cells, then 4 cells, and so on, until the embryo forms a body of 16–32 cells called a morula. When there are around 64 cells in the formation, the first cell fate decision occurs, where two types of cells are formed, and at this stage the embryo is called a blastocyst. The outer layer of this structure is called trophectoderm, and it surrounds the inner cell mass and a cavity called the blastocoel. The trophectoderm will form the extraembryonic structures and provide embryo implantation into the uterus, while the inner cell mass will undergo a second cell fate decision that gives rise to the epiblast and hypoblast. These two layers create a sandwich formation, and gastrulation will then occur in the epiblast to form three layers: the ectoderm, mesoderm, and endoderm. The hypoblast will only form extraembryonic structures.

To identify the differentiation stages of the cells in the embryo, several markers are used. There are several categories of molecular markers, such as pluripotent markers (*Oct4*, *Sox2*, *Nanog*, *Dppa4*, *Dppa5*, *Sall4*, *Utf1*, *Rex2*, and *Rif1*) that are expressed in ICM as well as ESCs, and early differentiation markers, which are further divided into ectoderm markers (*Pax6*, *Otx1*, *Neurod1*, *Nes*, *Lhx5*, and *Hoxb1*), mesoderm markers (*Tbx2*, *T*, *Nkx2-5*, *Myod1*, *Myf5*, *Mesdc1*, *Mesdc2*, *Kdr*, *Isl1*, *Hand1*, and *Eomes*), endoderm markers (*Onecut1*, *Gata4*, *Gata5*, and *Gata6*) and extraembryonic markers (*Cdx2* and *Tpbpa*) (Tang et al., 2010, Ito et al., 2010, Sakaue et al., 2010).

Pluripotency is maintained through a network of several transcription factors, which can be divided into two categories: upstream pluripotent transcription factors and downstream effectors. Upstream pluripotent transcription factors include OCT4, STAT3, SOX2, and NANOG; downstream effectors include ERAS, TCL1, UTF1, SALL4, B-MYB, and C-MYC (Niwa, 2007).

1.4.1.1. Upstream pluripotent transcription factors

The transcription factor POU5F1, also known as OCT4, is one of the major regulators of mouse ESC pluripotency; it is the gatekeeper that prevents mouse ESC differentiation (Nichols et al., 1998). OCT4 is known to prevent differentiation of mouse ESCs to trophectoderm through the repression of CDX2, a transcription factor for trophectoderm differentiation (Niwa et al., 2005). Another transcription factor essential for maintaining mouse ESC pluripotency is STAT3; the activation of this transcription factor prevents the differentiation of ESCs to primitive endoderm-like cells through the repression of GATA6 (Niwa et al., 1998). Interestingly, the overexpression of OCT4 in ESCs has similar effects to the inhibition of STAT3, which is differentiation towards primitive endoderm-like cells (Niwa et al., 2000). It has been found that STAT3 activates an unidentified co-factor that forms a complex with OCT4

and a general transcription unit (Niwa, 2001). This complex activates target genes that prevent differentiation of mouse ESCs into primitive endoderm (Niwa, 2007). The overexpression of OCT4 causes disruption to the formation of the complex due to protein saturation (Niwa, 2001). Therefore, the correct amount of OCT4 expression is key to maintaining pluripotency in the mouse embryo and ESCs. In mouse ESCs, the activation of STAT3 via the JAK/STAT pathway can be initiated through the binding of LIF to a heterodimeric receptor consisting of the LIF-receptor β and gp130 (Niwa, 2007). This is considered the mechanism by which LIF prevents mouse ESC differentiation *in vitro*.

A third transcription factor that can maintain cell pluripotency is NANOG. NANOG has been found to direct mouse ESC self-renewal and also acts independently of the JAK/STAT pathway in promoting pluripotency (Chambers et al., 2003, Mitsui et al., 2003). Moreover, the overexpression of NANOG can bypass the JAK/STAT pathway in maintaining mouse ESC pluripotency in the absence of LIF, suggesting that it may be a GATA6 repressor (Mitsui et al., 2003). While there is no direct evidence that NANOG inhibits the expression of GATA6, NANOG can block the differentiation of mouse ESCs towards primitive endoderm-like cells when LIF is removed (Chambers et al., 2003).

Another major transcription factor that determines the pluripotency of mouse ESCs and embryo is SOX2. SOX2 is a member of the *Sox* (SRY-related HMG box) family, which contain DNA binding HMG domains and are thus involved in transcriptional regulation (Kuroda et al., 2005). The NANOG promoter is one of the target genes mediated by the binding of SOX2 and OCT4. The SOX2/OCT4 complex activates the expression of NANOG by binding with the Octamer/SOX element in the NANOG promoter region (Rodda et al., 2005, Kuroda et al., 2005). These core transcription factors are essential in maintaining the pluripotency of the ICM

and mouse ESCs, and work in concert through a transcription factor network to prevent differentiation.

1.4.1.2. Downstream effectors of pluripotency

Besides the transcription factors that prevent differentiation, there are several transcription factors that maintain pluripotency via other mechanisms. One mechanism is through regulation of the cell cycle. ESCs divide symmetrically approximately every 12 hours. During the cell-cycle, most ESCs are in S-phase and only a small proportion are in G1 (Burdon et al., 2002). The maintenance of this cell cycle is driven by the phosphoinositide-3-kinase (PI3K)/AKT signalling pathway (Niwa, 2007). There are some effectors that play a pivotal role in modulation of this pathway, including ERAS, TCL1, B-MYB, C-MYC, UTF1, and SALL4. These transcription factors are located downstream of the pluripotency transcription factors network, as most of them are known to be activated by the core transcription factors, such as OCT4, STAT3, NANOG, and SOX2 (Niwa, 2007).

ERAS is an active form of a RAS-family GTPase that activates the PI3K/AKT pathway, and is specifically expressed in mouse ESCs (Takahashi et al., 2005). The activated PI3K/AKT pathway further utilises several downstream effectors such as mammalian target of rapamycin (mTOR) to stimulate ESC proliferation (Takahashi et al., 2003, Takahashi et al., 2005). It is reported that null-ERAS mouse ESCs still retain pluripotency, but their proliferative capacity is reduced (Takahashi et al., 2003).

T-cell leukaemia/lymphoma 1 (TCL1) is known to augment AKT signal transduction in the PI3K/AKT pathway, and enhances cell proliferation and survival (Teitell, 2005). Furthermore, the knockdown of TCL1 in mouse ESCs is found to have several effects on pluripotency, including impaired self-renewal, induced differentiation, and repressed proliferation (Ivanova

et al., 2006, Matoba et al., 2006). It is also reported that the expression of this transcription factor is regulated by OCT4 (Matoba et al., 2006). Because TCL1 is regulated by OCT4, which is one of the major pluripotency transcription factors in ESCs, it is possible that TCL1 acts as one of the effectors of cell-cycle progression in order to maintain the pluripotency of ESCs.

Another transcription factor, B-MYB, promotes mouse ESC cell cycle progression (Niwa, 2007). This function is proved by the G1-S cell-cycle arrest that occurs in ESCs following the induction of a dominant-negative form of B-MYB (Iwai et al., 2001). This transcription factor is expressed during the G1 phase of the ESC cell cycle, and its function is to promote the transition from G1 to S-phase by maintaining the levels of cyclin E/CDK2 (and possibly cyclin A/CDK2) that are needed for cell progression into S-phase (Joaquin and Watson, 2003). There is another cell-cycle accelerator called C-MYC that also works in the G1-S transition through the activation of cyclin E expression (Hooker and Hurlin, 2006). It is reported that the overexpression of a dominant-positive form of C-MYC can support the self-renewal ability of ESCs in the absence of LIF via binding with STAT3, whereas the overexpression of a dominant-negative form promotes differentiation of ESCs (Cartwright et al., 2005). This finding supports the model of C-MYC as a downstream effector of the LIF/STAT3 pathway in the regulation of ESC cell-renewal ability. Moreover, this model is consistent with the finding that the majority of ESCs are in S phase (Burdon et al., 2002) when cell self-renewal is maintained through cell proliferation.

UTF1 and SALL4 are two transcription factors that also promote proliferation in ESCs, as the reduced expression of these transcription factors leads to reduced proliferation (Nishimoto et al., 2005, Sakaki-Yumoto et al., 2006). UTF1 is activated by the synergistic action of OCT4 and SOX2 (Nishimoto et al., 1999), while SALL4 is known to interact with NANOG in maintaining the proliferation of ESCs (Wu et al., 2006). The connection between these

transcription factors suggests the existence of a transcription factor network in maintaining the pluripotency of ESCs and the embryo.

The role of UTF1 in maintaining the pluripotency of ESCs is connected with a chromatin-based mechanism for maintaining pluripotency of ESCs. The maintenance of a specific modification pattern of chromatin, called a bivalent domain, on key developmental genes is proposed to silence these developmental genes in ESCs while keeping them poised for activation (Bernstein et al., 2006). A bivalent domain consists of large regions of H3 lysine-27 methylation harbouring smaller regions of H3 lysine-4 methylation. UTF1 is found to maintain this chromatin bivalency by limiting PRC2 loading and histone 3 lysine-27 trimethylation, which sets activation thresholds for these bivalent genes (Jia et al., 2012). UTF1 also promotes nuclear tagging of messenger RNAs, which has two functions: 1) it tags messenger mRNAs transcribed from insufficiently silenced bivalent genes for cytoplasmic degradation; and 2) ensures cell proliferation by blocking the MYC-ARF feedback control (Jia et al., 2012). These functions of UTF1 promote the pluripotency and proliferation of ESCs.

SALL4 regulates the proliferation and pluripotency of stem cells through multiple putative mechanisms (Zhang et al., 2015). First, SALL4 regulates the activation of several important signalling pathways in stem cells including the Wnt/β-catenin pathway (Sato et al., 2004, Ma et al., 2006), STAT3 pathway (Niwa et al., 1998), Hedgehog signalling pathway (Choudhry et al., 2014), and Akt pathway (Watanabe et al., 2006). Second, SALL4 modulates the transcription of key stemness factors including OCT4, NANOG, SOX2, and C-MYC (Yang et al., 2008, Yang et al., 2010, Wu et al., 2006, Tanimura et al., 2013). Third, SALL4 may regulate the expression of key genes of stem cell self-renewal and differentiation through the modulation of Histone 3 Lysine-4 trimethylation and Histone 3 Lysine-79 dimethylation at the promoter region (Yang et al., 2007, Li et al., 2013). In summary, SALL4 promotes the

pluripotency and proliferation of stem cells through its interaction with several signalling pathway, transcription factors, and epigenetic modulators (Zhang et al., 2015).

1.4.1.3. Pluripotent transcription factor networks

Pluripotency is maintained through a network of upstream and downstream transcription factors that work in concert to promote self-renewal and prevent differentiation. The upstream transcription factors maintain pluripotency by preventing differentiation, while the downstream regulators maintain pluripotency through regulation of the cell cycle and proliferation (Figure 1-7). Moreover, the upstream regulators also activate the downstream regulators to execute their role in maintaining pluripotency. OCT4 and SOX2 have a crucial role in this network, as both of them regulate the expression of other transcription factors such as NANOG (Kuroda et al., 2005, Rodda et al., 2005) and UTF1 (Nishimoto et al., 1999), while OCT4 itself inhibits CDX2 expression, thus preventing differentiation into trophectoderm (Niwa et al., 2005). Interestingly, OCT4 and NANOG themselves are activated through a positive feedback loop via the complex of OCT4/SOX2 in pluripotent cells (Chew et al., 2005). This finding confirms that OCT4 and SOX2 are upstream mediators of the pluripotency network. As discussed above, it is possible that NANOG has an inhibitory activity towards GATA6 (Mitsui et al., 2003), similar to the activity of STAT3 (Niwa et al., 1998), which prevents cell differentiation towards primitive endoderm-like cells. NANOG also activates SALL4 and receives a positive feedback loop from this downstream transcription factor (Wu et al., 2006). STAT3 activates the downstream transcription factor C-MYC (Cartwright et al., 2005). All of these activated downstream regulators manipulate the cell cycle and proliferation of ESCs to promote pluripotency and self-renewal of the cells.

Important evidence for a regulatory network involving the pluripotency genes in ESCs was generated by chromatin immunoprecipitation analysis. This showed that OCT4, SOX2, and

NANOG share at least 353 target genes, besides the thousands of target genes that are associated with each gene separately (Boyer et al., 2005, Loh et al., 2006). The large number of target genes for these three transcription factors supports the importance of these transcription factors as the core pluripotency guardians. SALL4 is also known to interact with OCT4 and NANOG, adding one more connecting transcription factor to the regulatory network of ESCs (Wu et al., 2006, Yang et al., 2008).

One utilisation of the pluripotency transcription factor networks in cell reprogramming is in the induction of somatic cells into pluripotent cells. It has been demonstrated that the introduction of a few defined factors such as OCT3/4, SOX2, C-MYC, and KLF4 to mouse embryonic or adult fibroblasts, as well as adult human fibroblasts, leads to the generation of induced pluripotent stem cells (iPS cells) (Takahashi and Yamanaka, 2006, Takahashi et al., 2007). The studies showed that the generated iPS cells are similar to ESCs in morphology, proliferation, surface antigens, gene expression, epigenetic status of pluripotent-cell specific genes, and telomerase activity. These observable changes in the cell pluripotency by the introduction of just a few defined factors shows that the cell pluripotency is maintained by transcription factor networks that response to the changes in the balance of the factors involved in them. One question that remains is what regulates the expression of these major transcription factors in the maintenance of pluripotency in normal development embryos and ESCs. The answer to this question lies in the difference in epigenetic status between pluripotent cells and differentiated cells.

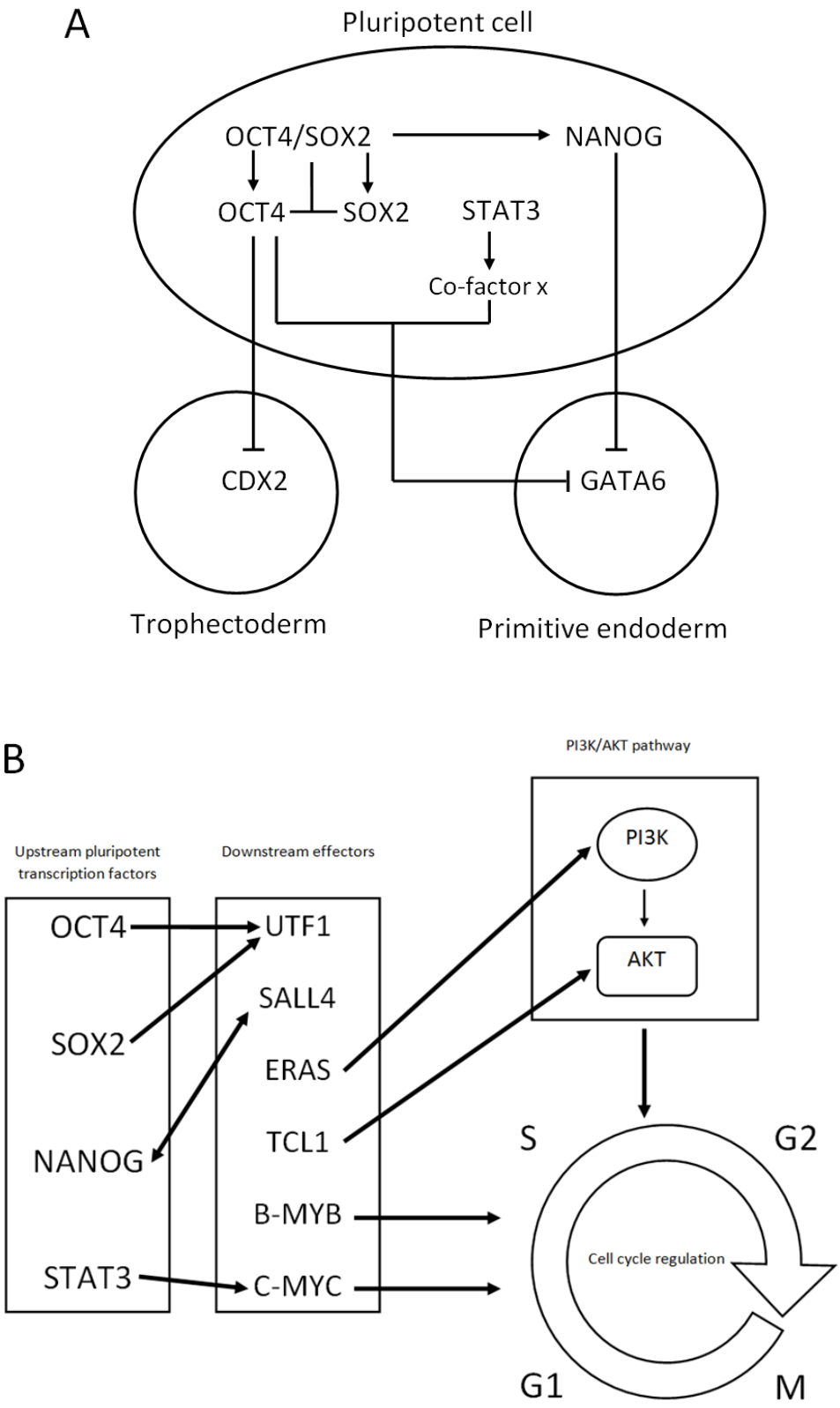

Figure 1-7 Transcription factor network in mouse ESCs to A) prevent differentiation and B) regulate cell cycle. Images are adapted from (Niwa, 2007).

1.4.1.4. Cell fate decisions in embryo development

There are several processes that are suggested affecting the cell fate decision, including positional information, cell polarity, and transcription factors. In the first fate decision, the cells in the inner cell mass (ICM), which is located inside the blastocyst, retain pluripotency, while the cells located outside differentiate into extraembryonic lineages (Zernicka-Goetz et al., 2009, Johnson and McConnell, 2004). Recent studies also show that the methylation level of the cells can depend on the position of the cells (Salvaing et al., 2012). Specifically, after the morulae stage, where the cells are exposed to different positional information for the first time, it is found that the cells exposed to the outside environment are generally more methylated than the cells located inside (Li and O'Neill, 2013b). Interestingly, despite the different positional information received between these two types of cells, there is no developmental commitment to certain cell lineages at this stage (Johnson and McConnell, 2004). This indicates that the methylation status of the cells occurs before the cells differentiate into certain lineages, and at this stage the cells can still change their differentiation fate. The evidence suggests that positional information may be the determinant of the methylation state of the cells, which later determines the commitment of the cells into specific cell lineages by altering the genetic expression of the cells. This hypothesis is also supported by the finding that a knockdown of TET1 in pre-implantation embryos resulted in a tendency of the cells to differentiate towards a trophectoderm lineage, caused by hypermethylation of DNA that decreased the expression of NANOG (Ito et al., 2010).

Blastomeres are polarised along their apical-basal axis before the formation of ICM, generating two types of cells in the blastocyst (Johnson and Ziomek, 1981). Cell fate decision is caused by the polarity of the cell surface, which leads to asymmetric cell divisions. The polarity of the cells is regulated by the conserved portioning defective (Par) gene family (Plusa et al., 2005).

Consequently, the polar cells form trophectoderm and the non-polar cells are located inside and become the ICM (Fleming et al., 2001). It has also been found that the expression of pluripotency genes is downregulated by the presence of CDX2, which differentiates the cells into the trophectoderm lineage (Niwa et al., 2005). The relationship between these mechanisms and changes in DNA methylation level is yet to be established. One hypothesis is that all these factors work in concert to regulate the cell fate decision in embryonic development (Zernicka-Goetz et al., 2009). Asymmetric cell division and positional information taken by the cells could lead to a difference in CDX2 expression between cells. Similarly, the differences in expression of CDX2 also give signals to the cells, forming a positive feedback loop.

The second cell fate decision involves differentiation of cells in the ICM into two different lineages, the epiblast and hypoblast. There are several positional information cues received by the ICM: the cells exposed to trophectoderm develop into epiblast while the cells exposed to blastocoel develop into hypoblast. Several transcription factors such as GATA4 and GATA6 are upregulated during the differentiation of ICM into hypoblast, and the expression of pluripotency genes such as NANOG are downregulated (Chazaud et al., 2006). Evidence of polarity is shown in the two subsequent rounds of asymmetric division, during the 8-to-16-cell stage and 16-to-32-cell stage, which form the ICM (Johnson and McConnell, 2004). It is likely that all these factors work in concert to drive the differentiation of ICM into epiblast and hypoblast lineages. In summary, several factors work in concert during the first and second cell fate decisions in embryo development, including positional information, cell polarity, and the expression of transcription factors. Each factor induces and receives signals from the other factors, creating a positive feedback loop.

1.4.2. Epigenetics of embryo development

The connection between epigenetics, in this case DNA methylation, and the pluripotent state of cells during embryo development has become an interesting topic in embryology and the stem cell field. It is generally considered that the hypermethylated DNA state is associated with inactivation of genes. In terms of pluripotency, the pluripotent transcription factors such as OCT4 and NANOG are inactivated by hypermethylation of DNA in association with the differentiation of ESCs and embryo (Latham et al., 2008). A recent study has found that although most of the CpG islands in the human genome (70-80%) are stably methylated, the differentially methylated regions (DMRs) between cell lineages are usually at lineage-specific gene regulatory elements, and these DMRs often contain single nucleotide polymorphisms specific for cell-type diseases (Ziller et al., 2013). This indicates that DMRs may be the regulator of cell fate decisions in normal development and disease. Moreover, DMRs can even be used to classify the lineage of unknown samples: DMRs specific for cell lineages have been used to identify unknown samples based on those signature regions (Ziller et al., 2013). The results showed that the clustering of the samples based on these signature DMRs was in high agreement with genome-wide 1-kb tiling-based clustering of the same samples. The signature DMRs can even differentiate cells in a mixed cell population based on the proportions of the signature DMRs in the population. This indicates that DNA methylation is highly related to the lineage specification of the cells, and may be a primary determinant of cell fate decisions and differentiation in the embryo. DNA methylation also has a critical role in maintaining genomic stability (Bird, 2002, Ooi et al., 2009).

There is still limited information regarding the regulation of this epigenetic status in embryo development. Despite many extensive investigations performed to date regarding the connection between DNA methylation and pluripotency, the mechanisms that determine the

methylation status in embryo are still not understood completely. In recent decades, developmental epigenetics in mammals has been dominated by a classic model of genetic reprogramming of methyl-CpG within the genome during embryo development. It is believed that both the paternally and maternally-inherited genomes undergo global demethylation after fertilisation (Chen et al., 2003). The paternal genome is actively demethylated through the oxidation of 5meC into 5hmC, 5caC, and 5fC by TET3 (Gu et al., 2011, Oswald et al., 2000, He et al., 2011, Inoue et al., 2011, Inoue and Zhang, 2011, Wu and Zhang, 2014). It is suggested that the oxidised forms of 5meC are further diluted by passive DNA replication series or by the BER process (Inoue et al., 2011, Inoue and Zhang, 2011, Wu and Zhang, 2014, He et al., 2011). On the other hand, the maternal genome is passively demethylated upon subsequent mitoses (Wu and Zhang, 2014, Seisenberger et al., 2013). Finally, after implantation, the embryo genome is overwritten by the new epigenetic information (Auclair and Weber, 2012, Morgan et al., 2005). A genome-scale DNA methylation map in the pre-specified embryo supports the global DNA demethylation model in mammals by showing that the parental genomes are gradually unmethylated from zygote to blastocyst stage, and regain the methylation after the blastocyst stage (Smith et al., 2012). The model is further refined by a finding that both the paternal and maternal genomes are both actively demethylated during embryo development, because the oxidised forms of 5meC are also found in the maternal genome (Wang et al., 2014). Also, the conversion of the 5meC derivatives to unmodified cytosines is independent of the passive dilution (Wang et al., 2014). However, the model of rapid demethylation in the paternal genome is challenged by a immunofluorescence study which showed that the loss of 5meC is caused by antigen masking in mouse preimplantation embryos rather than demethylation below the level observed in the female pronuclei (Li and O'Neill, 2012).

1.4.3. DNA methylation in the embryo

The occurrence of active DNA demethyation in the zygote was first proposed based on the asymmetric reduction of 5meC levels in the paternally-inherited genome relative to the maternally-inherited genome observed by immunostaining (Rougier et al., 1998, Mayer et al., 2000). The demethylation is considered active because it occurs within hours of fertilisation, before the onset of DNA replication (Santos et al., 2002). Further, it was proposed that the active demethylation process is followed by a passive demethylation process by failure of methylation maintenance, based mainly on the asymmetric staining of the sister chromatids of metaphase chromosomes (Rougier et al., 1998). These subsequent demethylation processes have been accepted as the model of 5meC remodeling during embryo development, which lets the embryo achieve a 'clean state' and enables the embryo to undergo further reprogramming (Salvaing et al., 2014). However, studies in other mammalian species have shown contradictory results, including no loss of 5meC in the early development embryo of sheep (Beaujean et al., 2004), and a limited loss of 5meC in the paternal genome of rabbit and bovine embryos (Lepikhov et al., 2008) followed by increased staining at the end of the 1-cell stage (Park et al., 2007, Reis Silva et al., 2011). The most recent report showed that the 5meC levels in the mouse embryo do not decrease during the first few cell cycles (Li and O'Neill, 2012).

Molecular analyses of post-fertilisation embryos also revealed that the sperm genome was hypermethylated relative to the oocyte genome, but had lost a significant proportion of the methylation by the time of the late zygote stage, resulting in the similar levels of methylation between sperm and oocyte (Guo et al., 2013, Smith et al., 2012). After fertilisation, there is only a modest decline in methylation over subsequent cell cycles, followed by a further loss of 5meC in the ICM (Smith et al., 2012, Guo et al., 2013, Smallwood et al., 2011). Thus, the immunolocalisation results, which indicated that active demethylation occurred after

fertilisation, are not confirmed by the molecular analysis. However, the molecular analyses used in these studies have several limitations, including the limited CpG islands analysed with the technique used, and the inability of the molecular analyses to distinguish between 5meC and its derivates such as 5hmC, 5fC, and 5caC (Salvaing et al., 2014, Huang et al., 2010). Therefore, the immunolocalisation technique remains an important tool for obtaining information regarding the level and distribution of 5meC during embryo development, despite its limitation of being a semi-quantitative measurement. It provides the advantage of being able to distinguish 5meC and its derivates, as well as providing genome-wide data that is not restricted to CGI.

Despite the advantages of immunolocalisation, there is still some confusion in the literature on the interpretation of the results. Some earlier studies found a marked asymmetry of methylation between the paternal and the maternal genome of the zygote, and an active demethylation followed by a passive demethylation during subsequent cell cycles, resulting in a 'clean state' of the embryo ready to be reprogrammed. However, more recent studies showed little asymmetry between the paternal and the maternal genome (Li and O'Neill, 2012, Salvaing et al., 2012). The later results are more in agreement with recent molecular analyses. These contradictory findings may be the result of protocol differences. As discussed in the methods of analysis (Section 1.3.4), valid use of immunolocalisation analysis requires that the antigen be fully solvent exposed. Therefore, the epitope should not be degraded or masked significantly and the antigen-antibody reaction should be approaching thermodynamic equilibrium (saturated) (Salvaing et al., 2014). There are two types of antigen-masking that hinder the access of the antibody to the DNA: acid-sensitive masking and trypsin-sensitive masking (Çelik et al., 2014, Li and O'Neill, 2012). The changes in chromatin structure during the zygotic maturation are the suggested cause of the dynamic levels and proportions of these two types of antigen-masking during embryo development. One study found that a short exposure of the

fixed zygote to trypsin following the acid treatment was sufficient to remove the proteins, and it was accompanied by an increase in the detectable 5meC (Li and O'Neill, 2012). This model provides a new basis for understanding epigenetics during embryo development.

1.4.4. DNA methylation in embryonic stem cells

The correlation between the changes in the DNA methylation status and the pluripotent status of the cells during embryo development has been extensively studied in recent years. The same correlations are also an important topic to study in ESCs. ESCs are derived from ICM that is isolated from the embryo and then cultured *in vitro* until a stable ES line is established (Tang et al., 2010). Evans and Kaufman (1981) reported the first derivation of murine ESCs from *in vitro* cultures of mouse blastocysts. Because ESCs are derived from a part of the embryo, there is an assumption that these two cell types share similar characteristics. Both share a similar pluripotency status, which is determined by several pluripotent transcription factors (OCT4, STAT3, NANOG, and SOX2). The expression of these transcription factors are controlled in part by epigenetic factors such as DNA methylation and histone modification (Niwa, 2007). However, there is a fundamental difference in terms of growth and development between these cell types. While the embryo development directs the embryo towards differentiation, which causes the embryo to lose the capacity for self-renewal, the ESCs undergo a significant molecular transition that switches the cells from the normal developmental program into unrestricted self-renewal, while retaining the capacity to differentiate into diverse cell types (Tang et al., 2010). There are also major changes in the epigenetic status of the cells along with the shift from normal development into unrestricted self-renewal, which leads to the suggestion that the epigenetic status of the cells helps to stabilise these changes in ESCs (Tang et al., 2010). The self-renewal capacity of ESCs may be attained because of different epigenetic controls in ESCs that alter the expression of several pluripotent genes, leading to an

acceleration of the cell cycle (Tang et al., 2010, Niwa, 2007). The study of these differences between embryos and ESCs is important in understanding the role of epigenetic modifications in embryos and ESCs.

Several studies show DNA methylation is not essential in ESCs. It was recently observed that the knockdown of all three active members of the DNMT enzymes does not affect the self-renewal property of ESCs in the undifferentiated state (Tsumura et al., 2006). The study also confirmed that chromosome condensation and segregation during mitosis occurs normally in ESCs in the absence of CpG methylation by these DNMT enzymes. The unique cell-cycle regulation and metabolic gene expression of ESCs may explain the robust growth of ESCs without CpG methylation (Hong and Stambrook, 2004). Furthermore, triple DNMT-deficient ESCs transferred into the ICM of embryo could commit to the epiblastic lineage (Sakaue et al., 2010). However, the same study also indicated that the survival of the epiblastic lineage is dependent on DNA methylation, shown by the increasing number of apoptotic cells in the periphery of triple knockout embryoid bodies as well as the failure of these triple knockout embryoid bodies to mature into cystic embryoid bodies. This finding is consistent with a previous study which reported that methylation-deficient ESCs have limited differentiation potential (Fouse et al., 2008). Another study found that severely hypomethylated ESCs fail to differentiate upon removal of LIF, but they do remain viable (Latham et al., 2008). Collectively, these results indicate that DNMT enzymes are required for differentiation rather than for maintenance of the undifferentiated state (Altun et al., 2010).

The pluripotency of mouse ESCs is plausibly correlated with the capacity of the cells to protect the genome from *de novo* methylation, possibly via PRDM14 which represses the expression of DNMT3A and DNMT3B (Leitch et al., 2013). Although some studies found that mouse ESCs can tolerate DNA methylation deficiencies better than the mouse embryo, in fact the cells

of the early preimplantation epiblast also have their *de novo* methylation enzymes downregulated, similar to ESCs (Hirasawa et al., 2008, Hirasawa and Sasaki, 2009). Also, a knockdown of TET1 in ESCs, which can oxidise 5meC into 5hmC, causes hypermethylation of the *Nanog* promoter and decreases the expression of NANOG, leading to decreased pluripotency (Ito et al., 2010). Hence, demethylation can preserve the pluripotency of mouse ESCs. Moreover, the global methylation state of mouse ESCs is also directly responsive to the culture environment, and the methylation state can be completely reversed by changing the culture conditions (Leitch et al., 2013). Similar results were shown in a genome-scale DNA methylation mapping for ESCs, in which the methylation of CpGs are dynamic and undergo extensive changes during cellular differentiation (Meissner et al., 2008). These changes may have a similar basis to the role of positional information in defining lineage specification in the development of the embryo. These similarities and differences between embryos and ESCs have given rise to many questions regarding their DNA methylation status.

The differences of methylation between embryos and ESCs also raise concerns regarding the quality of ESCs compared to the embryos. A prolonged culture of ESCs *in vitro* showed aberrant hypermethylation of CpG islands associated with a specific set of developmentally regulated genes, in a similar pattern with some primary tumours (Meissner et al., 2008). DNA methylation mapping of iPS cells also shows increased deviation from the ESCs references in small number of genes, including the hypermethylation of several genes similar to the condition in several fibroblast cell lines (Bock et al., 2011). The potential of tumour development in ESCs and the incomplete reprogramming in iPS cells are among many others possible consequences of utilising pluripotent cells for regenerative therapy. These findings escalates the importance of a better understanding of the epigenetic mechanisms in pluripotent cells to ensure the safe applications of the cells in regenerative therapy.

1.4.5. 2i media, pluripotency, and DNA methylation in embryonic stem cells

Despite evidence that DNMT is not required for maintaining the proliferative and pluripotent state of ESCs, and the fact that the ICM is hypomethylated, it is surprising that many studies have found that ESCs have global methylation levels similar to the ones found in somatic cells. An alternative formulation of ESC media called '2i' (for two inhibitors) is used to improve the pluripotency of ESCs by implementing small molecules to block specific kinases (Nichols and Smith, 2011, Silva et al., 2008). The signal inhibition promotes the reprogramming of ESCs to ground state pluripotency, marked by up-regulation of OCT4 and NANOG, reactivation of the X chromosome, transgene silencing, and competence for somatic and germline chimaerism (Silva et al., 2008). This increase in pluripotency is associated with a marked reduction in global 5meC (Leitch et al., 2013). The two inhibitors in 2i, CHIR99021 and PD0325901, inhibit extracellular-signal-regulated kinases (ERK) and glycogen synthase kinase 3 (GSK3), respectively (Ying et al., 2008). The inhibition of the ERK signalling pathway prevents the differentiation promoted by autoinductive stimulation of the mitogen-activated protein kinase (ERK1/2) pathway, which occurs in the normal embryo development (Ying et al., 2008, Nichols et al., 2009). On the other hand, a clear mechanism for the effect of GSK3 inhibition in maintaining the pluripotency of the cells has not been elucidated. It is only found that the propagation of ESCs under the inhibition of ERK pathway is inefficient unless the GSK3 pathway is inhibited, which suggests that the inhibition of GSK3 pathway is crucial for balancing the loss of ERK pathway in maintaining metabolic activity, biosynthetic capacity, and overall viability (Ying et al., 2008). Another study proposed that GSK3 inhibition specifically promotes translation in the context of ESC culture in 2i (Wray et al., 2010). Culturing ESCs in 2i improves the pluripotency of the cells, as marked by the stable upregulation of OCT4 and NANOG, reactivation of the X chromosome, transgene silencing, and competence for somatic and germline chimaerism (Silva et al., 2008).

The reduction in 5meC observed in 2i media (Leitch et al., 2013) is also accompanied by several changes in expression related to DNA methylation, including a reduction in DNMT3A and DNMT3B while the maintenance DNMT1 remains unchanged, and a change in expression of the genes affected by the triple-knockout of DNMT1, DNMT3A, and DNMT3B. It is suggested that the transcriptional differences between the conventional media and 2i may be due to altered DNA methylation (Leitch et al., 2013). However, the study also found that the ESCs in 2i have reduced 5hmC, which argues against 5hmC having a role as the intermediate of DNA demethylation. The immunolocalisation methods used in this study only include acid treatment for the antigen retrieval procedure. As reviewed earlier, there are two types of antigen-masking present in the embryo and mouse embryonic fibroblast that can hinder the antigen-antibody reaction: the acid-sensitive pool and the trypsin-sensitive pool (Li and O'Neill, 2012, Çelik et al., 2014). Therefore, there may still be antigen-masking present during the immunolocalisations in this study, especially from the trypsin-sensitive pool. It cannot be verified whether the reduction of 5meC and 5hmeC observed is caused by the authentic reduction of the modifications or caused by the antigen-masking that was not removed by the methods. The study described in this thesis will utilise the newly designed antigen retrieval methods to assess DNA methylation regulation in the ESCs for the first time, ensuring an optimal antigen-antibody interaction. The results will be important in revealing the DNA methylation regulation in the ESCs relative to the DNA methylation in the embryo.

1.5. THE AIM OF THE STUDY

Recent studies have suggested that the classic model of active demethylation during embryo development may be incorrect, and that in fact the DNA methylation in embryos is determined by a combination of positional information and cell polarity, which forms a positive feedback loop with a network of transcription factors. Recent findings on the presence of antigenic

masking, which give the appearance of DNA demethylation, raise a question regarding the validity of the immunolocalisation studies performed to date investigating DNA methylation in embryo development. The aim of this study is to assess the level of epitope masking of 5meC in ESCs, assess the effects of various culture conditions on the total level of 5meC and its level of masking, and to assess the relationship between pluripotency and the level and localisation of 5meC in ESCs.

2. CHAPTER 2: GENERAL MATERIALS AND METHODS

Materials and methods common to a number of chapters are described here. Specific materials and methods are given in the relevant chapters.

2.1. CELL CULTURE

2.1.1. Cell strain

Cells used for all experiments were ES-D3 (ATCC®, Cat. No. CRL-1934™), embryonic pluripotent stem cells derived from *Mus musculus* (mouse) embryo, strain 129S2/SvPas. All cells were passage 10–30.

2.1.2. Culture media

Cells were cultured in one of two growth media: (1) knockout Dulbecco's Modified Eagle Medium (KO-DMEM) (Invitrogen Life Technologies, Cat. No. 10829-018) supplemented with 2 mM L-glutamine (Invitrogen, Cat. No. 25030-081), 100 µM MEM Non-Essential Amino Acids Solution (Invitrogen, Cat. No. 11140-050), 25 U/ml penicillin, 25 µg/ml streptomycin (Invitrogen, Cat. No. 15140-148), 100 µM 2-mercaptoethanol (Sigma-Aldrich Co, Cat. No. M-3148), heat inactivated ES-cells Qualified Fetal Bovine Serum (FBS) (AusGeneX, Cat. No. FBS500-S) used at 10% (v/v), and mouse Leukemia Inhibitory Factor (LIF) (Merck Millipore, ESG1107) added at 1000 U/ml; (2) 2i media, composed of serum free ES medium (SFES) supplemented with 1 µM GSK3 inhibitor PD03259010 (Sigma, Cat. No. PZ0162-5MG), 3 µM ERK inhibitor CHIR99021 (Bio Scientific, Cat. No. 4423/10), 2 mM L-glutamine (Invitrogen, Cat. No. 25030-081), $1.5x10^{-4}$ M monothioglycerol (Sigma, Cat. No. M61425), and 1000 U/ml mouse Leukemia Inhibitory Factor (LIF) (Merck Millipore, ESG1107). SFES is composed of neurobasal medium (Gibco, Cat. No. 21103-049) and DMEM/F12 (Gibco, Cat. No. 11320-033) (1:1) supplemented with N2 supplement (Gibco, Cat. No. 17502-048) added at 0.5% (v/v),

B27 supplement + retinoic acid (Gibco, Cat. No. 17504-044) added at 1% (v/v), 50 mg/ml bovine serum albumin (Sigma, Cat. No. A1470), and 50 U/ml penicillin, 50 µg/ml streptomycin (Invitrogen, Cat. No. 15140-148). These two media will be abbreviated as DMEM and 2i throughout this thesis.

Differentiation media replaced growth media in the differentiation study. Differentiation media had the same composition with DMEM minus mLIF.

2.1.3. Surface coating of culture vessels

Cell growth surfaces were coated with 0.1% (w/v) gelatin from porcine skin type A (Sigma, Cat. No. G1890) in Dulbecco's Phosphate Buffered Saline (DPBS) (Sigma, Cat. No. D5773). Coating was performed for 30 min, then the coating solution was removed. For a short period of culture in 2i (24 h), cell growth surfaces were coated with 100 µg/ml laminin from Engelbroth-Holm-Swarm murine sarcoma basement membrane (Sigma, Cat. No. L2020) in DPBS. Coating with laminin was performed for 1 h, then the coating solution was removed.

2.1.4. Cryopreservation and cell thawing

The freezing medium used was 2X freezing medium containing 40% (v/v) DMEM, 40% (v/v) heat inactivated FBS (AusGeneX, Cat. No. FBS500-S), and 20% (v/v) dimethyl sulfoxide (DMSO) (Sigma, Cat. No. D-2650). Cells were detached with 1 ml 0.25% trypsin-EDTA (Invitrogen, Cat. No. 25200-56). Trypsin was inactivated with 2 ml DMEM and removed by 1000–1200 rpm centrifugation for 3 min. Supernatant was removed and the cells were resuspended in 0.5–1.0 ml DMEM. Cells were counted using haemocytometer and cell concentration was adjusted to $2x10^6$ cells/ml using DMEM. The cell suspension was mixed with 2X freezing medium with the ratio 1:1. 1 ml cell suspension was transferred to each

cryotube. Cryotubes were transferred to −20 °C overnight, then to −80 °C overnight, and to −196 °C.

Frozen vials were thawed at 37 °C. Cells were suspended in 9 ml DMEM and centrifuged for 3 min at 1000–1200 rpm. Supernatant was removed, and the cells were resuspended in 0.5–1.0ml DMEM. A small volume of cells (10 µl) was mixed with (1:1) Trypan Blue solution (0.4%) (Gibco, Cat. No. 15250-061), and counted using haemocytometer (Hirchmann EM Techcolor, 0.100 mm depth) to determine the number of viable (not stained) and dead (blue stained) cells. All cells were seeded into 0.1% (w/v) gelatin (Sigma, Cat. No. G1890)-coated T25 flask (Thermo Scientific, Cat. No. 156340) containing 5 ml growth media.

2.1.5. Cell passage

Cells were washed with DPBS (Gibco, Cat. No. 14190-144) (Ca^{2+}, Mg^{2+} free) and detached with 1 ml 0.25% trypsin-EDTA (Invitrogen, Cat. No. 25200-56). Trypsin was inactivated with 2 ml DMEM and removed by 1000–1200 rpm centrifugation for 3 min. Supernatant was removed and the cells were resuspended in 0.5–1.0 ml DMEM. Cells were counted using haemocytometer. Cells were seeded in gelatin coated T25 flasks (1200 cells/cm^2).

2.1.6. Plated cells and embryoid body culture preparation

For plated cell culture the cell concentration was adjusted to 10000 cells/ml. The cell suspension was seeded into 4-well dish containing autoclaved cover slips (12 mm round) (Livingstone International Pty. Ltd., Cat. No. CS12RD) coated with gelatin or laminin (0.5 ml cell suspension/well). For embryoid body culture, cell concentration was adjusted to $1x10^6$ cells/ml for DMEM and $4x10^6$ cells/ml for 2i. 1 µl of cell suspension was placed onto each of the 20 µl drops of media on the lid of a 100 mm cell culture dish (Thermo Scientific, Cat. No. 150350) and then the lid was inverted and placed on the base of the cell culture dish containing

3 ml DPBS (Gibco, Cat. No. 14190-144) (Ca^{2+}, Mg^{2+} free) to maintain humidity. Cells were cultured for 24-48 h prior to the fixation.

2.2. IMMUNOFLUORESCENCE

Cells were washed with DPBS (Sigma, Cat. No. D5773) and fixed with 4% (w/v) paraformaldehyde (PFA) (Sigma, Cat. No. P6148) for 30 min at RT. Cells were permeabilised with DPBS containing 0.5% (v/v) Tween-20 (Sigma, Cat. No. P7949) and 0.5% (v/v) Triton X-100 (Bio-Rad Laboratories In., CA, USA, Cat. No. 161-0407) for 40 min at RT. For immunolocalisation of 5meC, chromatin was denaturated with HCl (4N) (Ajax Finechem Pty Ltd., Cat. No. A256) containing 0.1% Triton X-100 for 10 min at RT. Acid was removed with extensive washing in DPBS containing 0.05% (v/v) Tween-20 (DPBT). Cells were then exposed to 0.25% trypsin-EDTA for 10–15 s (embryoid body sections) or 20-30 s (plated cells). Trypsin was inactivated with 10% (v/v) sheep serum (Sigma, Cat. No. S3772) or goat serum (Sigma, Cat. No. G9023) in DPBS depending on the secondary antibody used. This was followed by extensive washing in 2% bovine serum albumin (BSA) (Sigma, Cat. No. A1470) in DPBT. Blocking in 30% (v/v) sheep serum or goat serum in DPBT was performed, depending on the secondary antibody used, at 4 °C overnight. Cells were stained using indirect immunofluorescence. Cells were incubated with the primary antibody (Table 2-1) or non-immune IgG with the same concentration in DPBT containing 5% sheep serum or goat serum at 4 °C overnight. Cells were washed extensively with 2% BSA in DPBT. Cells were incubated in a fluorescein-conjugated secondary antibody (Table 2-2) in 2% BSA in DPBT for 1 h at RT. Cells were washed with 2% BSA in DPBT, and then DPBS. Cells were mounted in ProLong® Gold Antifade Mountant with DAPI (Life Technologies, Cat. No. P36935).

Table 2-1 List of the primary antibodies used in this thesis

Antigen	Manufacturer	Developed in	Stock concentration	Usage dilution
5hmC	Active Motif, Cat. No. 39769	Rabbit	1.0 mg/ml	1:300
5meC	Serotec Ltd., Cat. No. MCA2201	Mouse	1.0 mg/ml	1:100
DNMT1	Abcam, Cat. No. ab19905	Rabbit	0.8 mg/ml	1:100
DNMT3A	Imgenex, Cat. No. IMG-268A	Mouse	0.5 mg/ml	1:100
DNMT3B	Imgenex, Cat. No. IMG-184A	Mouse	0.5 mg/ml	1:100
H3K9ac	Abcam, Cat. No. ab4441	Rabbit	1.0 mg/ml	1:100
OCT4	Abcam, Cat. No. ab19857	Rabbit	1.0 mg/ml	1:200
TET1	Millipore, Cat. No. 09-872	Rabbit	1.0 mg/ml	1:100

Table 2-2 List of the secondary antibodies used in this thesis

Antigen	Manufacturer	Developed in	Conjugate	Stock concentration	Usage dilution
Mouse IgG	Sigma, Cat. No. F6257	Sheep	Fluorescein Isothiocyanate (FITC)	1.1 mg/ml	1:300
Mouse IgG	Abcam, Cat. No. ab6787	Goat	Texas Red (TR)	2.0 mg/ml	1:300
Rabbit IgG	Sigma, Cat. No. F1262	Goat	Fluorescein Isothiocyanate (FITC)	1.1 mg/ml	1:300

2.3. MICROSCOPY AND IMAGE ANALYSIS

Global levels of staining in the cells were analysed by the epifluorescence microscope Eclipse 80i (Nikon Instruments Inc., USA). Images were captured using DS-Ri1 camera (Nikon Instruments Inc., USA), and analysed by ImageJ (National Institutes of Health, USA). Images were captured using the same setting of UV power, gain, and exposure time for all treatments in the same experiment and antibody. Analysis was performed with the original images without any adjustment. Measurement of staining level was performed on at least 50 nuclei per treatment per replicate in plated cells and 100 nuclei were analysed per treatment per replicate in EBs by selecting random nuclei using a drawing tool. Experiments were performed for at three independent replicates. All representative images shown are for staining in comparison to non-immune control antibody (data not shown).

Alkaline phosphatase activity and morphology of the cells were analysed by the inverted microscope Eclipse Ti-U (Nikon Instruments Inc., USA). Images were captured using DS-Fi1c camera (Nikon Instruments Inc., USA), and analysed by ImageJ (National Institutes of Health, USA). Alkaline phosphatase analysis was performed with the original images without any adjustment. Measurement of staining level was performed on at least 20 plated clumps and 5 EBs per treatment per replicate. Experiments were performed for three independent replicates.

Immunolocalisation was done using a Leica TCS SP5 Confocal Microscope (Leica Mycrosystems). Images were captured using the Leica Application Suite Advanced Fluorescent (LAS AF) software (Leica Microsystems). Images were captured using the adjusted laser power, gain, and offset specific to every sample to generate good localisations. Images were analysed by ImageJ (National Institutes of Health, USA). Experiments were performed for three independent replicates. All representative images shown are for staining in comparison to non-immune control antibody (data not shown).

2.4. Graphs and error bars

The measurement was represented using bar graphs representing the optical intensity (arbitrary units) mean ± standard error of the mean (SEM) of three independent replicates. Graphs were made using SigmaPlot (Systat Software Inc., USA).

2.5. Statistical analysis

Statistical analysis was performed in SPSS program, version 21. Analysis used was univariate analysis of variance (UNIANOVA). The difference between results was considered by significance levels of p values (probability): $p<0.05$ = *, $p<0.01$ = **, $p<0.001$ = ***.

3. CHAPTER 3: OPTIMISATION AND VALIDATION OF THE METHODS OF 5meC ANALYSIS

3.1. INTRODUCTION

A growing body of evidence implicates global levels of CpG methylation in the pluripotent state of ESCs. The cost and relative insensitivity of biochemical methods of detection of 5meC limit its uses for high throughput analysis of the factors that govern methylation status. Immunolocalisation may be more useful for this purpose because it allows assessment of individual cells and also provides information on the localisation of 5meC within each nucleus. It was shown, however, that conventional methods of immunolocalisation underestimate the 5meC levels detected in cells (Li and O'Neill, 2012). This is due to antigenic 5meC being present within two pools (Çelik et al., 2014). One pool is detected after acid-induced denaturation of chromatin; this is the pool detected by conventional immunolocalisation. A further trypsin-sensitive pool has been discovered, and the size of this pool is highly variable, depending upon the developmental state and growth disposition of cells. A new antigen retrieval method combining the acid and trypsin treatment was proved to increase the amount of 5meC in embryo and mouse embryonic fibroblasts (Li and O'Neill, 2012, Çelik et al., 2014).

In this chapter, the extent of trypsin sensitive masking of 5meC in ESCs was assessed and the methods for immunolocalisation were developed and validated in the assessment of 5meC in ESCs. This included validation of permeabilisation. The antigen retrieval methods that have been validated for the immunoassay in embryos were also optimised and validated for use in ESCs. The effect of culture conditions on ESCs were assessed, including the oxygen concentration and the culture time.

3.2. MATERIAL AND METHODS

3.2.1. Cell Culture

D3-ESCs were cultured in DMEM and 2i media prepared in the Human Reproduction Unit. See chapter 2.1.2 for DMEM and 2i media details. Cells were cultured at 37 °C with 5% CO_2, and either 21% O_2 or 5% O_2 in air. See Section 2.1.6 for details of plated cells and embryoid body culture preparation. Plated cells were cultured for 24h and 48h prior to the fixation. Embryoid bodies were cultured for 48h prior to the fixation.

3.2.2. Permeabilisation optimisation on EBs

Permeabilisation of the whole EBs was done by incubating the EBs in 1X DPBS containing 0.5% (v/v) Tween-20 (Sigma, Cat. No. P7949) and 0.5% (v/v) Triton X-100 (Bio-Rad Laboratories In., CA, USA, Cat. No. 161-0407) for 40 min at RT. The optimisation of the permeabilisation process was performed by incubating the EBs in 1X DPBS containing 1.0% (v/v) Tween-20 (Sigma, Cat. No. P7949) and 1.0% (v/v) Triton X-100 (Bio-Rad Laboratories In., CA, USA, Cat. No. 161-0407) for 80 min at 37 °C with agitation.

3.2.3. Immunolocalisation of 5meC in mouse embryonic fibroblasts (MEF)

Cells were washed with DPBS (Sigma, Cat. No. D5773) and fixed with 4% (w/v) paraformaldehyde (PFA) (Sigma, Cat. No. P6148) for 30 min at RT. Cells were permeabilised with DPBS containing 0.75% (v/v) Tween-20 (Sigma, Cat. No. P7949) and 0.75% (v/v) Triton X-100 (Bio-Rad Laboratories In., CA, USA, Cat. No. 161-0407) for 60 min at RT. Chromatin was denaturated with HCl (4N) (Ajax Finechem Pty Ltd., Cat. No. A256) containing 0.1% Triton X-100 for 10 min at RT. Acid was removed with extensive washing in DPBS containing 0.05% (v/v) Tween-20 (DPBT). Cells were then exposed to 0.25% trypsin-EDTA for 1 min. Trypsin was inactivated with 10% (v/v) sheep serum (Sigma, Cat. No. S3772) in DPBS. This

was followed by extensive washing in 2% bovine serum albumin (BSA) (Sigma, Cat. No. A1470) in DPBT. Blocking in 30% (v/v) sheep serum in DPBT was performed at 4 °C overnight. Cells were stained using indirect immunofluorescence. Cells were incubated with mouse anti-5-methylcytidine (1:100) (Serotec Ltd., Cat. No. MCA2201) or mouse non-immune IgG (Sigma, M7894) with the same concentration in DPBT containing 5% sheep serum at 4 °C overnight. Cells were washed extensively with 2% BSA in DPBT. Cells were incubated in sheep anti-mouse IgG conjugated with fluorescein isothiocyanate (FITC) (Sigma, Cat. No. F6257) in 2% BSA in DPBT for 1 h at RT. Cells were washed with 2% BSA in DPBT, and then DPBS. Cells were mounted in ProLong® Gold Antifade Mountant with DAPI (Life Technologies, Cat. No. P36935).

3.2.4. Cryosectioning

EBs were washed with 1X DPBS following fixation, then EBs were dyed with 0.04% (v/v) Trypan Blue in 1X DPBS for 30 min at RT to add colour to the EBs. EBs were rinsed with 1X DBPS until the Trypan Blue solution was removed, then transferred into tissue freezing medium (Leica Mycrosystems, Cat. No. 14020108926) in the Tissue-Tek® Biopsy Cryomold® Molds 15 mm x 15 mm x 10 mm (Sakura® Finetek USA Inc., Cat. No. 4565). Molds were frozen at -15 °C and cut into sections with a Leica CM1900 UV Cryostat (Leica Mycrosystems). Section thickness was 5 µm. Sections were fixed on Platinum PRO slides (Matsunami, Cat. No. PRO-11). Slides were treated for immunoassay as per section 2.2 using slide mailers (ProSciTech, Cat. No. H161) for incubation processes up to trypsin treatment and inactivation. Sections were marked with Dako Pen (Dako, Cat. No. S2002) prior to blocking to create liquid barrier around the sections.

3.2.5. Antibodies

Primary antibodies used were: (i) mouse anti-5-methylcytidine (Serotec Ltd., Cat. No. MCA2201); (ii) rabbit anti-OCT4 (Abcam, Cat. No. ab19857); and (iii) rabbit anti-histone 3 (acetyl K9) (Abcam, Cat. No. ab4441). Non-immune control antibodies were mouse IgG (Sigma, M7894) and rabbit IgG (Sigma, I5006). The secondary antibodies used to detect the binding of the primary antibodies were: (i) sheep anti-mouse IgG conjugated with fluorescein isothiocyanate (FITC) (Sigma, Cat. No. F6257); and (ii) goat anti-rabbit IgG conjugated with FITC (Sigma, Cat. No. F1262).

3.2.6. Antigenic Retrieval

For 5meC and OCT4 staining, cells were treated with HCl for 10 min, followed by trypsin (0.4%) either for 10–15 s (EB sections) or 20–30 s (plated cells and whole EBs). Acid and trypsin treatment were not done for H3K9ac staining.

3.3. RESULTS

3.3.1. Validation of 5meC staining on ESCs

The protocol for immunofluorescence was based on the immunofluorescence method for embryos and mouse embryonic fibroblasts (MEF) that was previously optimised in our laboratory (Li and O'Neill, 2012, Çelik et al., 2014). Further modifications were performed to make it suitable for ESCs. To validate the protocol, 5meC staining was performed on MEF and ESCs with no epitope retrieval, epitope retrieval by acid denaturation, and epitope retrieval by acid denaturation followed by trypsin digestion.

Immunostaining of MEF showed that a short exposure of the cells to trypsin for 1 min after acid treatment increased the intensity of the 5meC signal compared to the acid treatment alone and the untreated cells (Figure 3-1). The same protocol was used for the immunostaining of ESCs, with some modifications. The permeabilisation reagent concentration was reduced from 0.75% (v/v) Tween-20 and 0.75% (v/v) Triton X-100 in DPBS to 0.5% (v/v) Tween-20 and 0.5% (v/v) Triton X-100 in DPBS. The permeabilisation time was also reduced from 60 min to 40 min. The time of tryptic digestion was reduced from 1 min to 20–30 s. Immunofluorescence microscopy of ESCs showed similar results with the MEF. A short exposure of the cells to trypsin for 20–30 s after acid treatment increased the intensity of the 5meC signal compared to the acid treatment alone and the untreated cells (Figure 3-2).

3.3.2. Permeabilisation validation and optimisation

With the protocol for 5meC staining in ESCs confirmed, the next question was whether the same protocol could be used for 5meC staining on embryoid bodies (EBs). A first observation on the 5meC staining pattern on a whole embryoid body showed that the 5meC was expressed on the outermost layer of the cells, marked by full staining on most of the cells on the top

section (Figure 3-3-C) and the bottom section (Figure 3-3-O), and a ring formation staining on the sections closer to the equatorial (Figure 3-3-F-I-L).

To further investigate the implication of the pattern showed by the 5meC staining on the EBs, a staining of the pluripotent marker OCT4 was performed. A similar pattern was observed on the staining of a whole EB with the antibody to OCT4 (**Error! Reference source not found.**). This attern raised the question of whether adequate permeabilisation for EBs occurred with the methods used. Histone H3 Lysine-9 acetylation (H3K9ac) staining on embryoid body also showed the staining of only the outer cells of the structure, marked by full staining on the entire cells only on the top and the bottom part of the structure (Figure 3-5-C-O). On the middle part of the structure, the staining appeared as a ring with no staining in the middle (Figure 3-5-I).

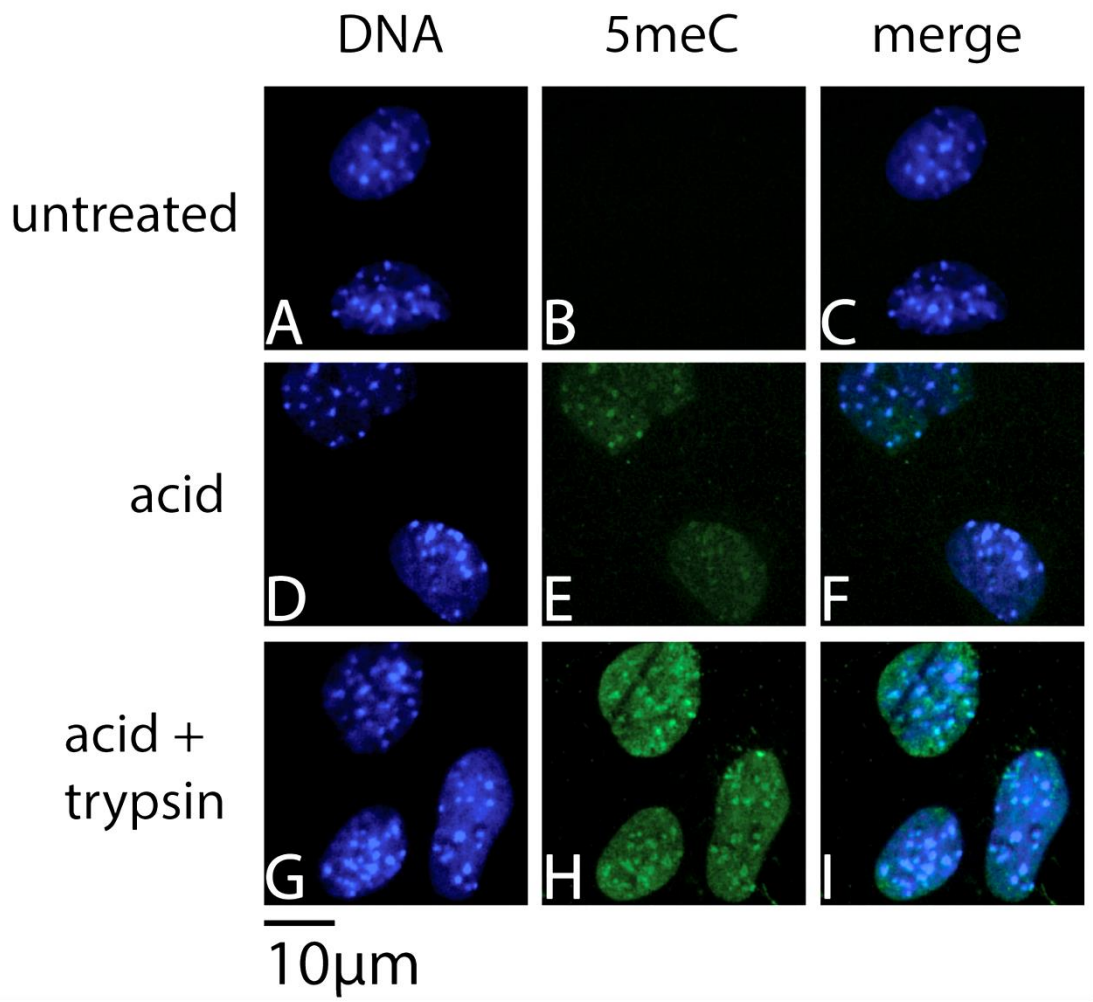

Figure 3-1 Validation of the immunostaining protocol for MEF.

MEF were fixed and permeabilised. They were then either untreated, treated with 4N HCl (acid), or treated with trypsin (0.25%) for 1 min after acid (acid + trypsin). The cells were stained with anti-5meC and counterstained with DAPI. Immunofluorescence microscopy showed that trypsin treatment increased staining of 5meC compared to acidic treatment alone. Scale bar = 10 µm.

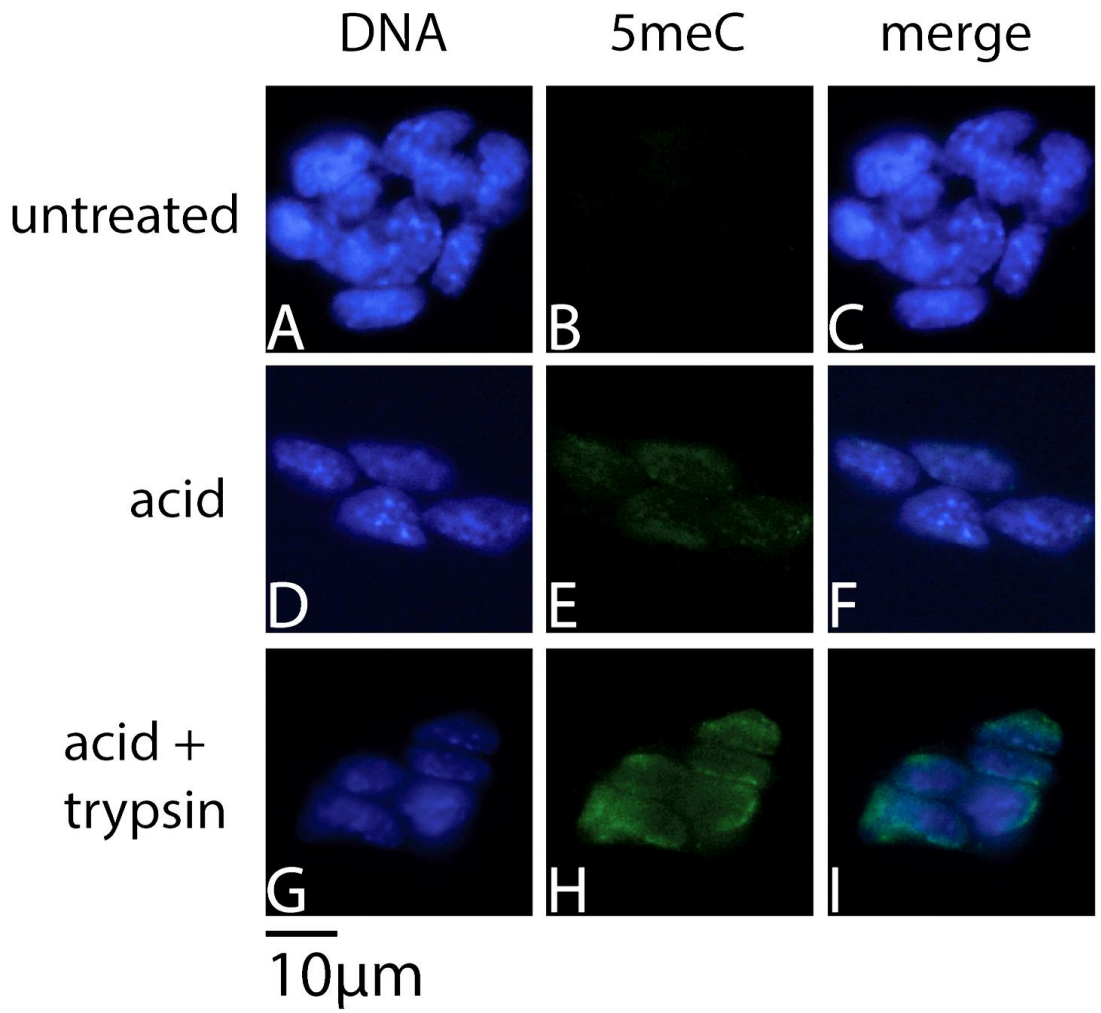

Figure 3-2 Validation of the immunostaining protocol for ESCs.

ESCs were fixed and permeabilised. They were then either untreated, treated with 4N HCl (acid), or treated with trypsin (0.25%) for 20–30 s after acid (acid + trypsin). The cells were stained with anti-5meC and counterstained with DAPI. Immunofluorescence microscopy showed that trypsin treatment increased staining of 5meC compared to acidic treatment alone. Scale bar = 10 µm.

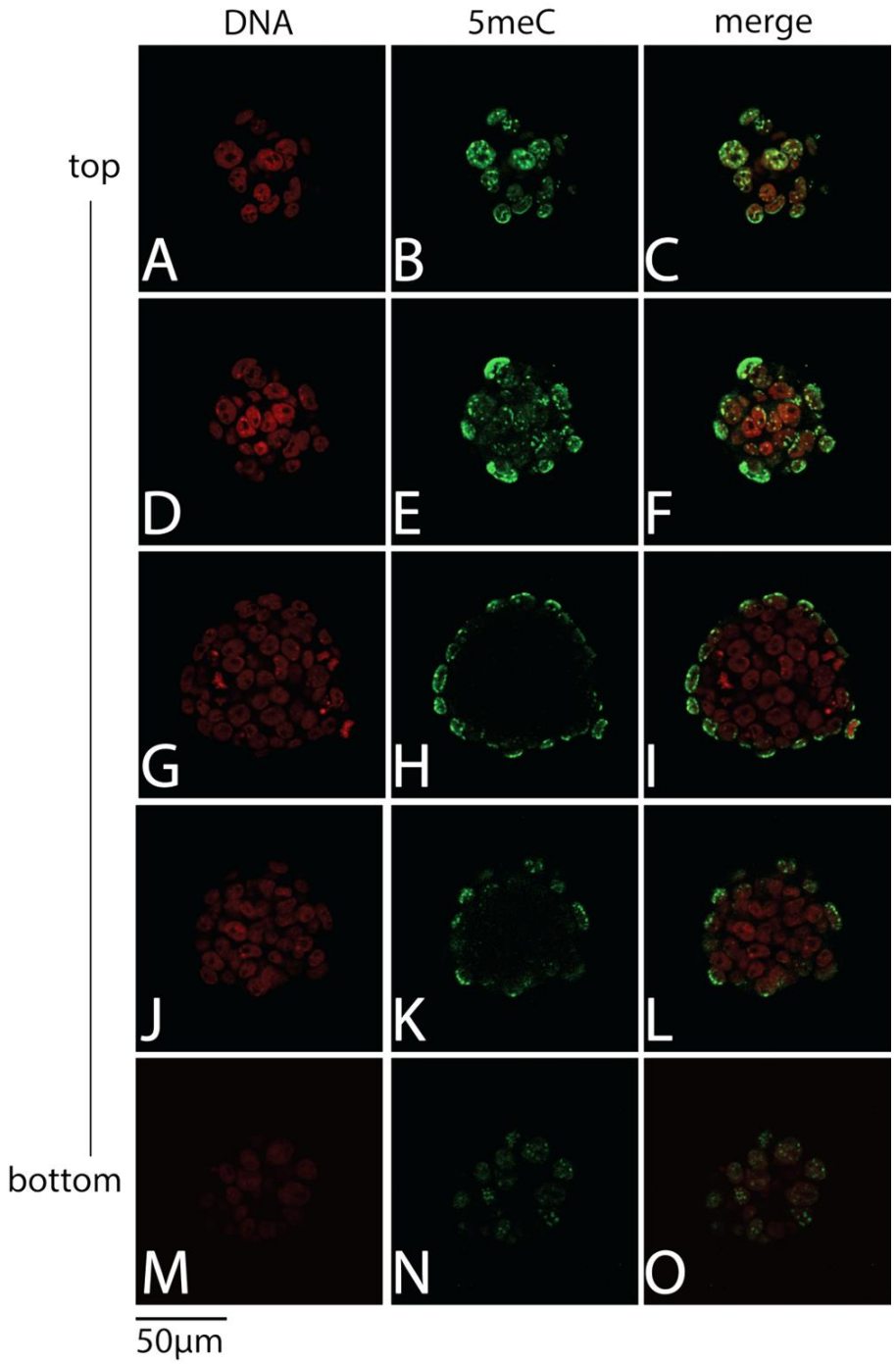

Figure 3-3 Analysis of 5meC staining on the whole EB.

Embryoid bodies were stained with the antibody to 5meC and counterstained with PI. Permeabilisation was performed according to the protocol optimised for plated cells. Images were taken using optical sectioning showing (A-F) the upper parts, (G-I) the equatorial section, and (J-O) the bottom parts of the embryoid body. The sectioning showed the 5meC staining on the outermost layer of the cells. Images are representative of three independent replicates. Scale bar = 50 µm.

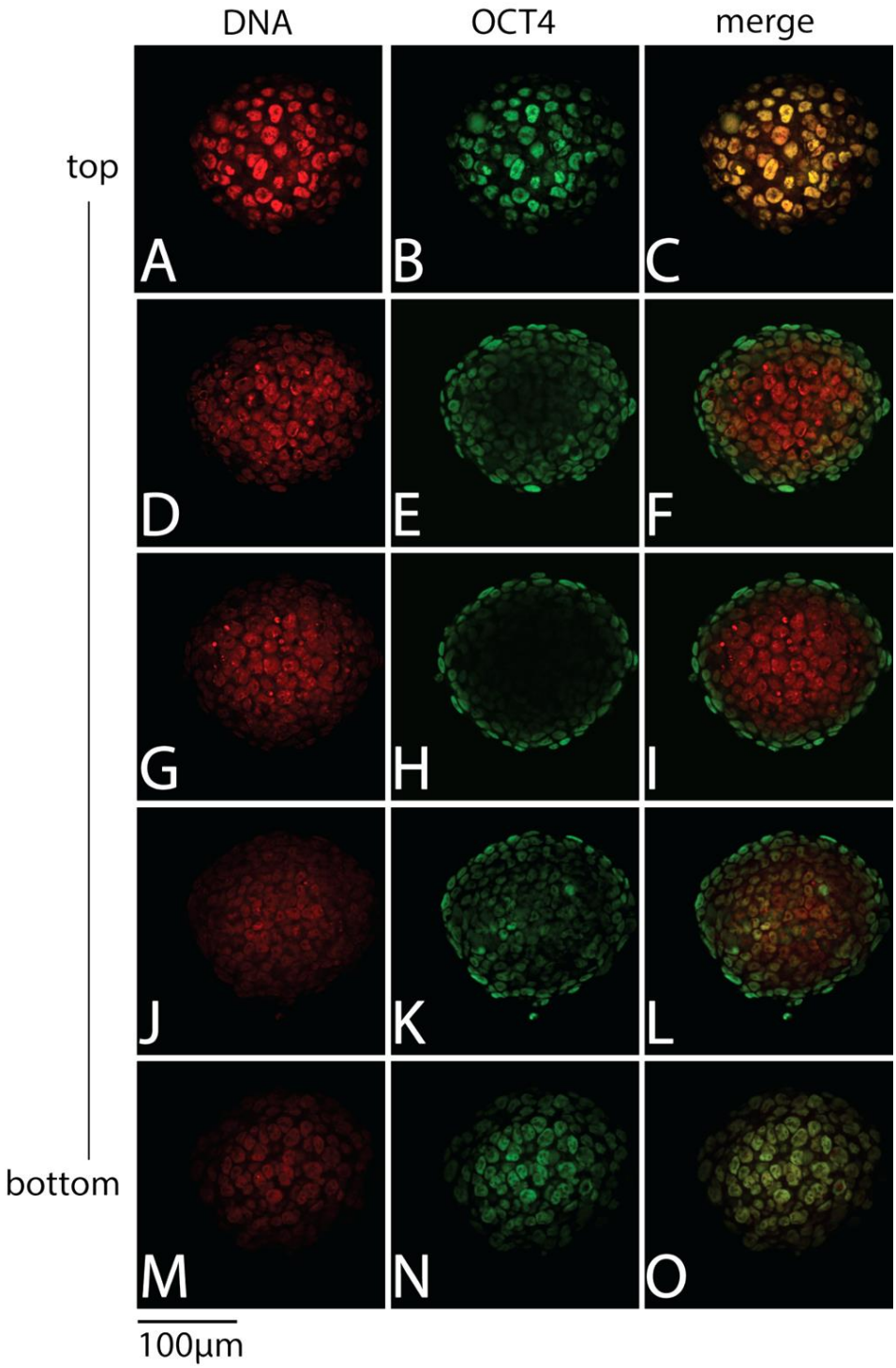

Figure 3-4 Analysis of OCT4 staining on the whole EB.

ESCs embryoid bodies were stained with the antibody to OCT4 and counterstained with PI. Permeabilisation was done according to the protocol optimized for plated cells. Images were taken using optical sectioning showing (A-F) the upper parts, (G-I) the equatorial section, and (J-O) the bottom parts of the embryoid body. OCT4 staining showed a similar pattern to the 5meC staining on the whole EBs. Images are representative of three independent replicates. Scale bar = 100 µm.

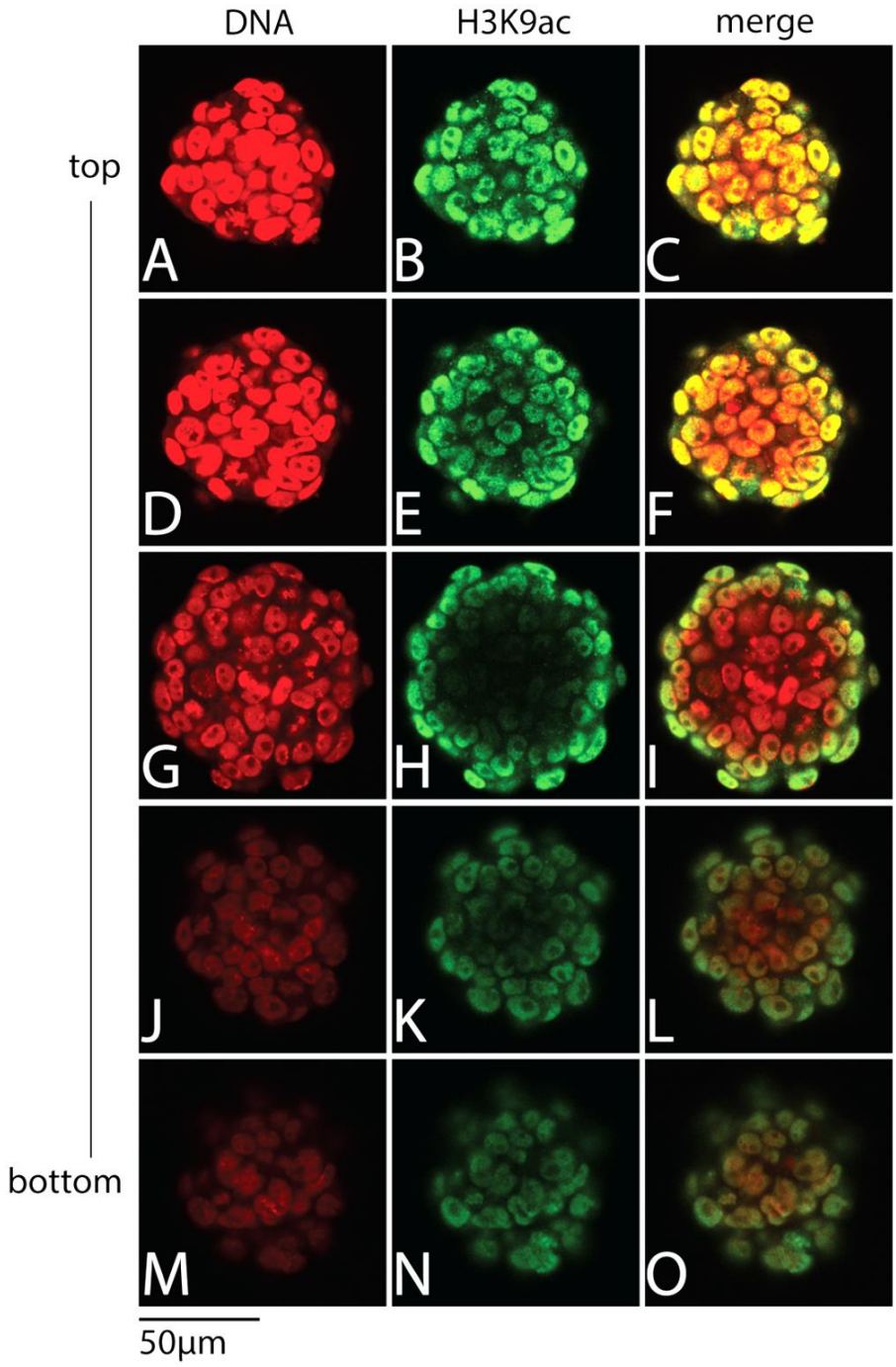

Figure 3-5 Analysis of H3K9ac staining on the whole EB.

Embryoid bodies were stained with the antibody to H3K9ac and counterstained with PI. Permeabilisation was performed according to the protocol optimised for plated cells. Images were taken using optical sectioning showing (A-F) the upper parts, (G-I) the equatorial section, and (J-O) the bottom parts of the embryoid body. H3K9ac staining showed a similar pattern to the 5meC and OCT4 staining on the whole EBs, indicating inadequate permeabilisation for the whole-EB staining protocol. Images are representative of three independent replicates. Scale bar = 50 µm.

Improvement of the permeabilisation methods was attempted by increasing the concentration of the permeabilisation reagent (DPBS + 0.5% Tween-20 + 0.5% Triton X-100 to DPBS + 1% Tween-20 + 1% Triton X-100), increasing the incubation temperature (room temperature to 37 °C), increasing the incubation time (40 min to 80 min), and adding agitation during the incubation. The increased treatments improved the embryoid body permeabilisation, shown by H3K9ac staining up to the second cell layer below the outermost cell layer (Figure 3-6-F). This treatment compromised the embryoid body structure, marked by the reduction of DNA staining quality (Figure 3-6-A-D-G). However, the structure was only partially permeabilised, shown by the absence of H3K9ac staining on the nuclei of the cells in the middle of the EB structure (Figure 3-6-F). This indicates that this permeabilisation procedure is not effective for the embryoid body.

To address the problem, embryoid bodies were cut into thin sections using a cryosectioning procedure after the fixation process. The staining for H3K9ac in the cut sections showed that the antibody could bind to all cells in the section (Figure 3-7). The observed H3K9ac staining in the middle of the structure also confirms that the non-stained cells in the whole embryoid body were artifacts. The 5meC staining on EBs using this newly validated protocol showed a different staining pattern compared to the 5meC staining with the previous methods. 5meC staining was observed on the cells across the section (Figure 3-8). All further immunostaining on EBs was performed using this method.

The problem of permeabilisation was less severe in plated cells as the antibody could penetrate to the structures and bind the cells in the middle of the structure (Figure 3-9). There was still variability in the staining of the middle part of colonies, as the colonies got bigger. This was especially the case when the plated cells were cultured for 48 h (Figure 3-9-I). Thus, all further experiments were performed on plated cells cultured for 24 h or less.

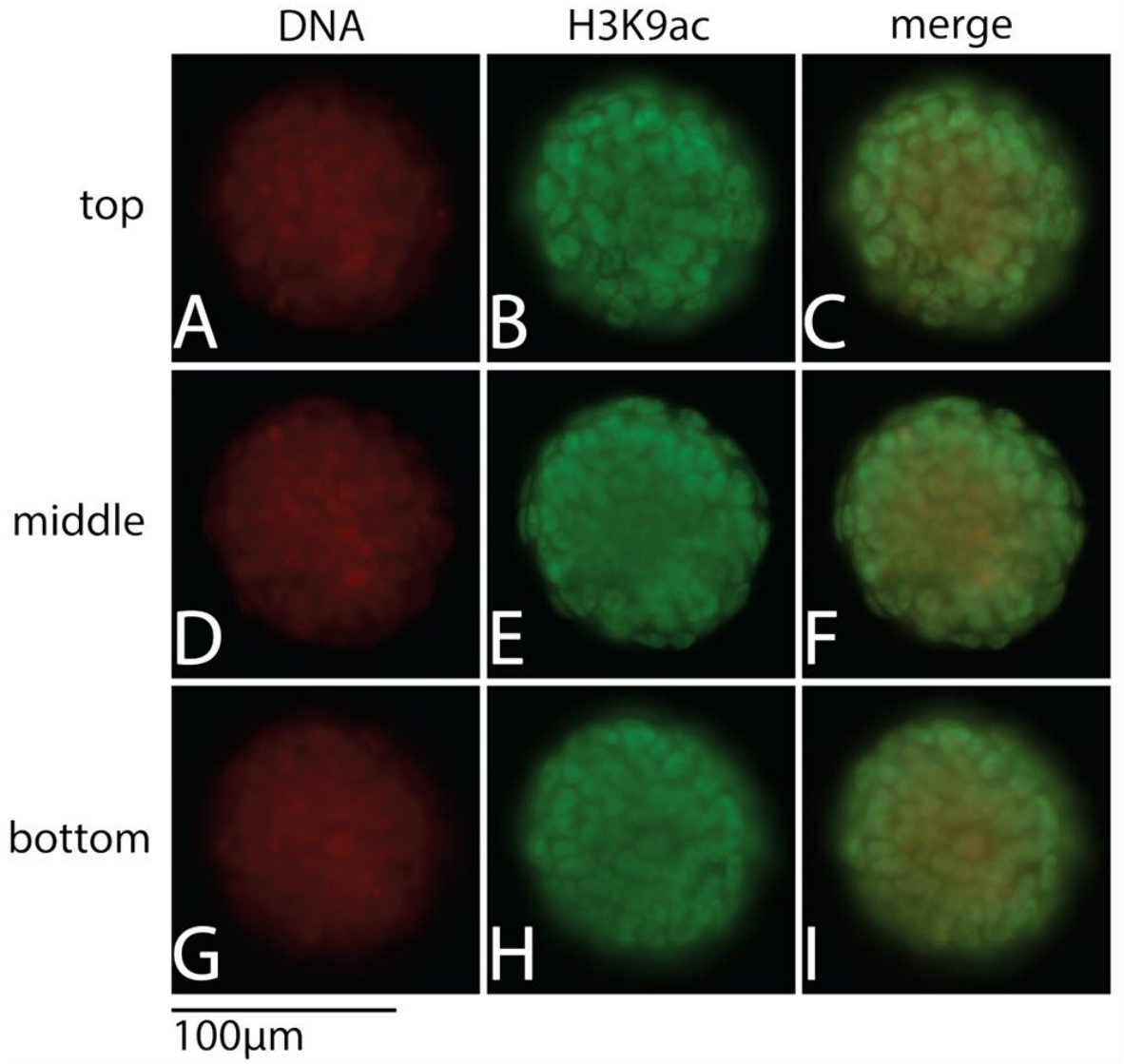

Figure 3-6 The effects of permeabilisation optimisation on the whole EB staining.

Embryoid bodies were permeabilised using the optimised permeabilisation protocol. Optimisation was done by increasing the concentration of the permeabilisation reagent (DPBS + 0.5% Tween-20 + 0.5% Triton X-100 to DPBS + 1% Tween-20 + 1% Triton X-100), increasing the incubation temperature (room temperature to 37 °C), increasing the incubation time (40 min to 80 min), and adding agitation during the incubation. The embryoid body was stained with the antibody to H3K9ac and counterstained with PI showing (A-C) the top section, (D-F) the equatorial section, and (G-I) the bottom section of the embryoid body. Immunofluorescence microscopy showed partial permeabilisation of the whole EB after the optimisation, indicated by increased but not complete staining of H3K9ac across the whole EB. DNA counterstaining showed reduced integrity of the whole EB, marked by the reduced effectiveness of the PI staining on the nuclei of the EB. Images are representative of three independent replicates. Scale bar = 100 µm.

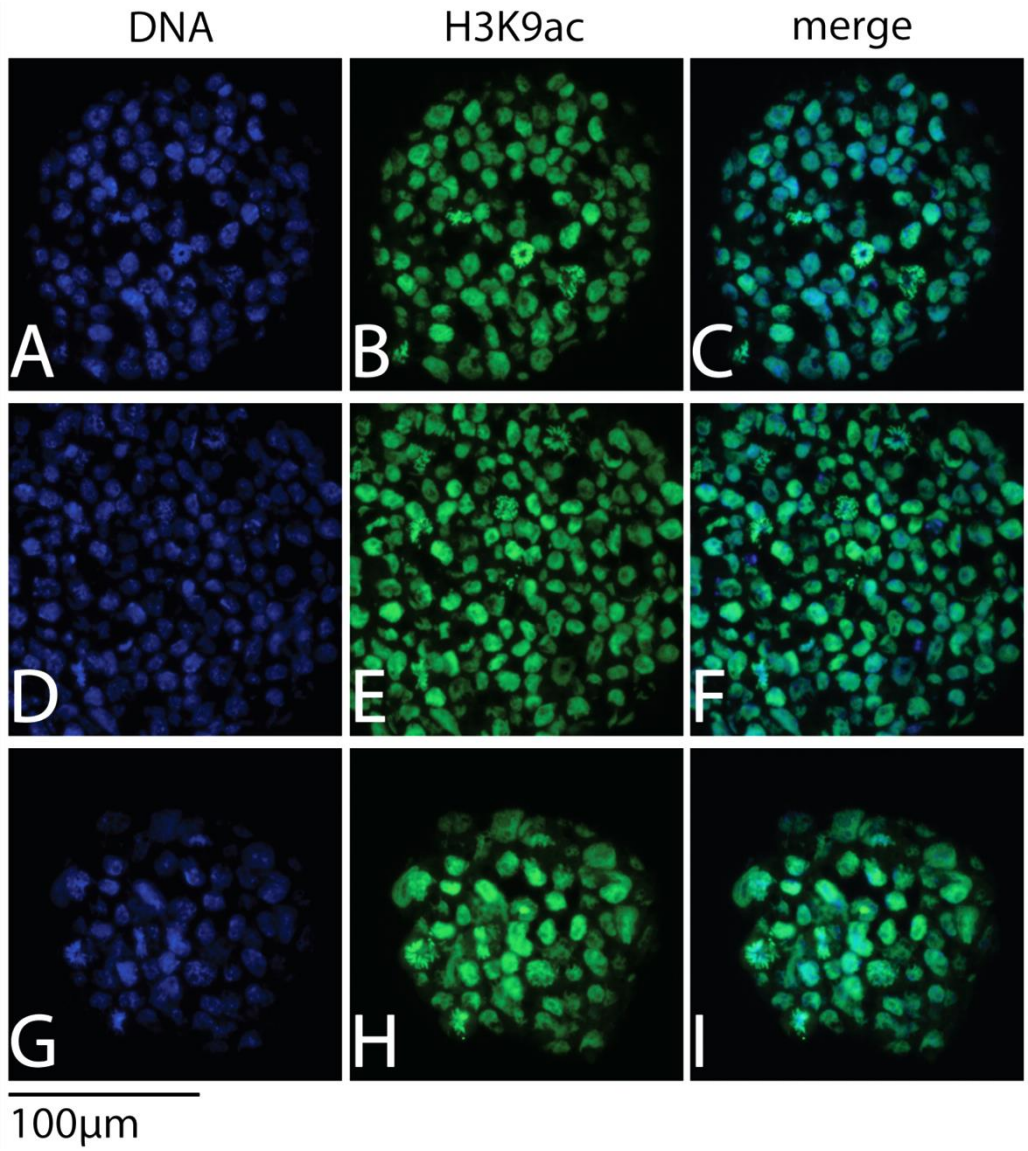

Figure 3-7 Analysis of H3K9ac staining on the ESC embryoid body sections.

EBs were cut into thin sections using the cryosectioning method prior to the immunostaining protocols. EB sections were stained with the antibody to H3K9ac and counterstained with DAPI. Images were taken using optical sectioning showing three embryoid body sections (A-C, D-F, G-I). Immunofluorescence showed H3K9ac staining across the sections. Images are representative of three independent replicates. Scale bar = 100 µm.

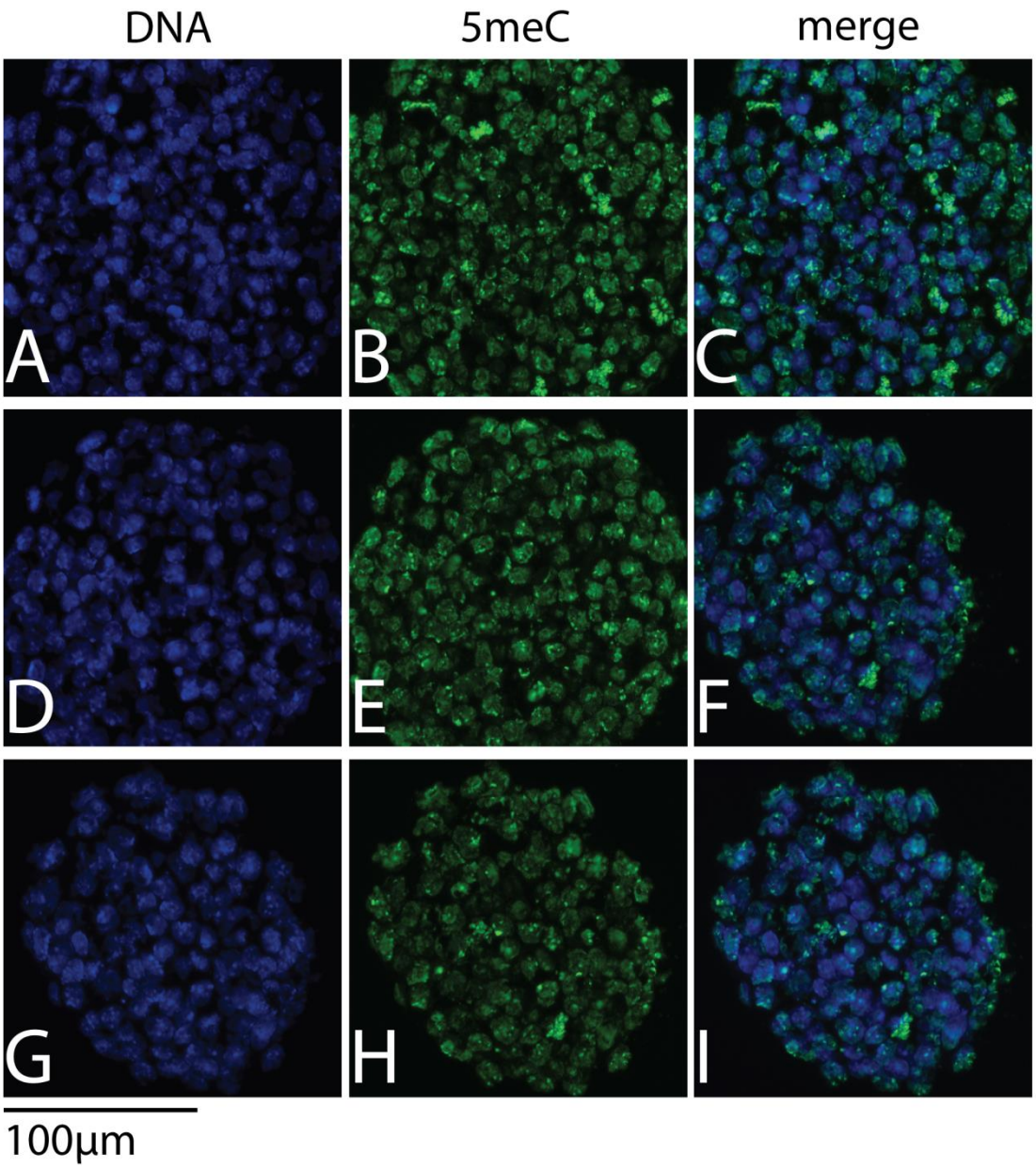

Figure 3-8 Analysis of 5meC staining on the ESC embryoid body sections.

EBs were cut into thin sections using the cryosectioning method prior to the immunostaining protocols. EB sections were stained with the antibody to 5meC and counterstained with DAPI. Images were taken using optical sectioning showing three embryoid body sections (A-C, D-F, G-I). Immunofluorescence showed 5meC staining across the sections similar to H3K9ac staining on EB sections. Images are representative of three independent replicates. Scale bar = 100 µm.

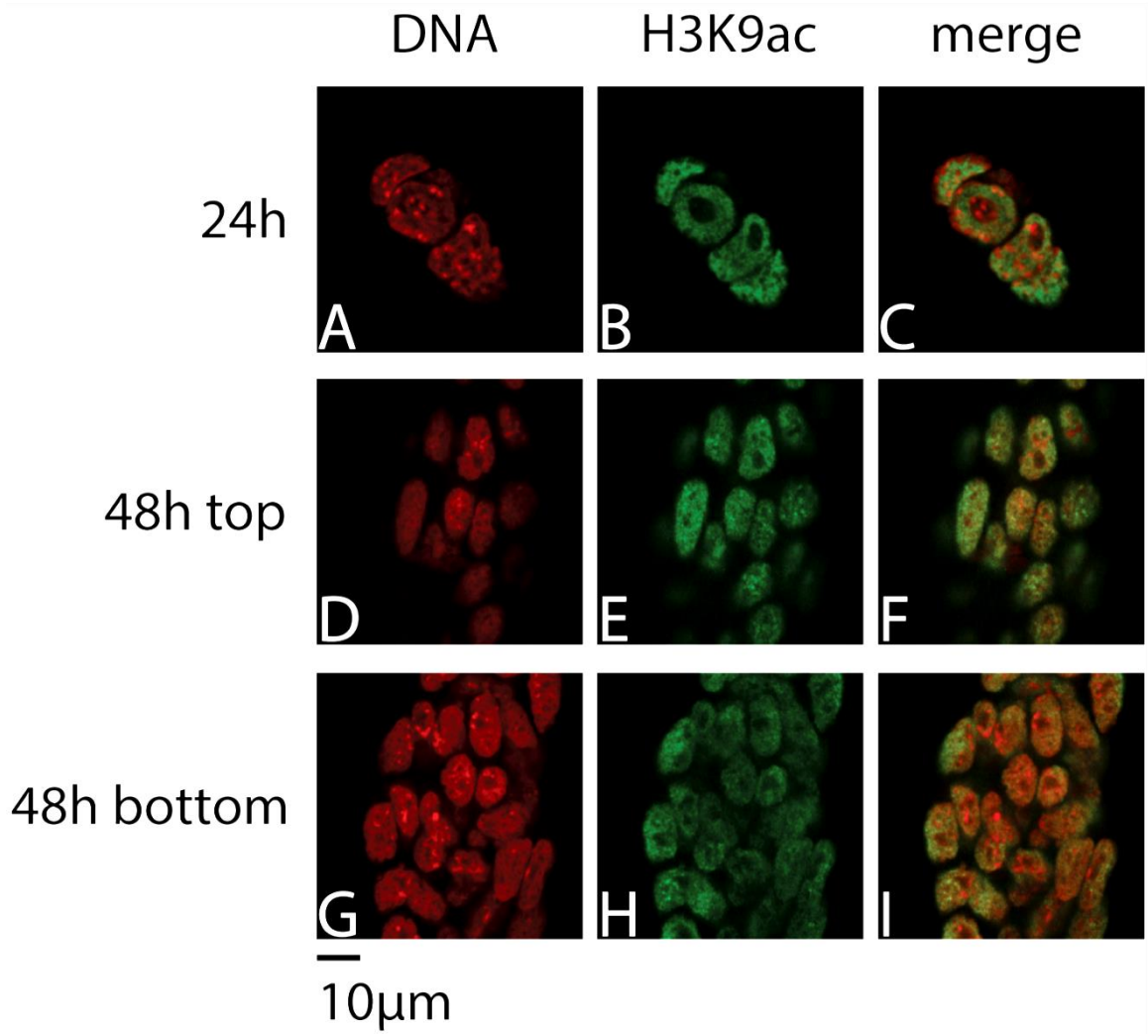

Figure 3-9 Analysis of H3K9ac staining on the plated ESCs.

Plated ESCs were stained with the antibody to H3K9ac and counterstained with PI. Permeabilisation was performed according to the protocol optimised for ESCs. Images were taken using optical sectioning showing (A-C) the colony after 24 h incubation, (D-F) the upper section of 48 h colony, and (G-I) the bottom section of the 48 h colony. Immunofluorescence showed adequate permeabilisation on the 24h plated ESCs, but the effectiveness was reduced on the larger 48 h plated ESCs. Images are representative of three independent replicates. Scale bar = 10 µm.

3.3.3. Validation of the antigen retrieval methods for the detection of 5meC and 5hmC in ESCs

To detect 5meC and 5hmeC levels in the ESCs, an antigen retrieval method must be performed to remove the protein masking which prevents the antibody attachment to the target. Antigen retrieval methods are performed by treating the cells with acid and trypsin to remove the antigenic masking (Section 3.3.1). In this section, the timing for the acid-induced denaturation and tryptic digestion processes was validated for antigen retrieval in ESCs.

ESCs were treated with HCl following the permeabilisation. The incubation time for the acid treatment in this experiment was based on the protocol optimised in MEF, which is 10 min for both plated cells and EB sections. A short period of tryptic digestion was performed after the acid treatment. In general, plated cells are more resistant to the trypsin treatment compared to the thin EB sections. Therefore, plated cells require longer trypsin treatment compared to the EB sections. The trypsin time used for plated cells was 20–30 s. The trypsin time used for embryoid body sections was 10–15 s.

The staining of the ESCs treated with acid and acid followed by trypsin showed that the improved antigen retrieval procedure is important for detection of 5meC levels (Figure 3-10 and Figure 3-11). The plated cells and embryoid body sections with the acid treatment showed a lower level of staining (Figure 3-10-B and Figure 3-11-B) compared to their counterparts treated with acid followed by trypsin (Figure 3-10-E and Figure 3-11-E). This indicates the incomplete antigen retrieval for the immunolocalisation of 5meC and 5hmC in ESCs, which could lead to underestimation of the 5meC levels in the cells.

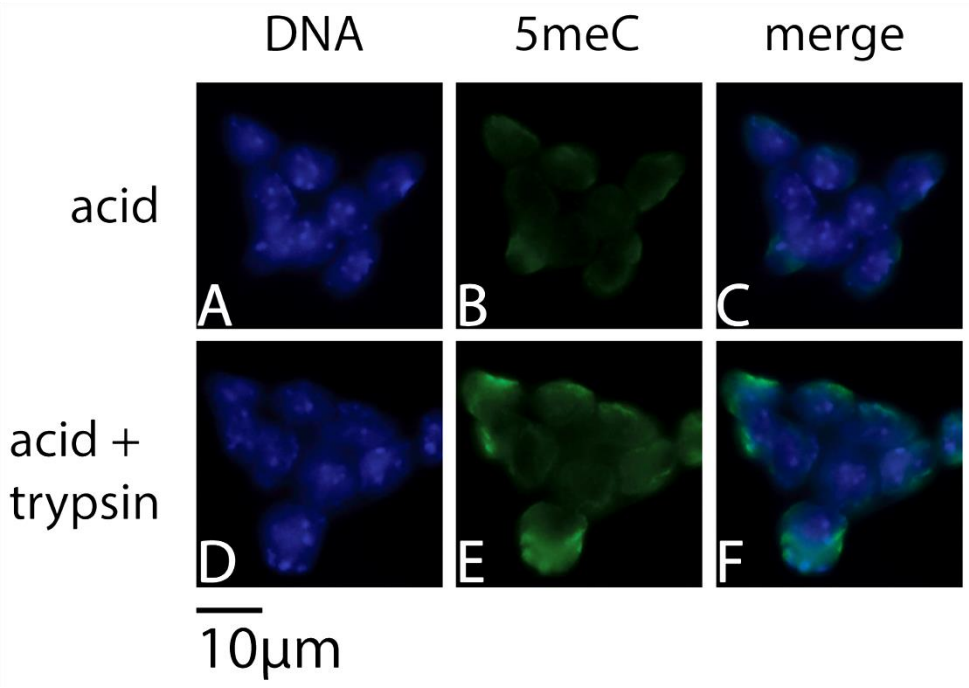

Figure 3-10 The effect of trypsin digestion on the retrieval of 5meC antigen in plated ESCs.

Plated ESCs were fixed and permeabilised. They were then either treated with 4N HCl (acid) or treated with trypsin (0.25%) for 20–30 s after acid (acid + trypsin), then stained with anti-5meC and counterstained with DAPI. Immunofluorescence microscopy showed that trypsin treatment increased staining of 5meC compared to acidic treatment alone. Images are representative of three independent replicates. Scale bar = 10 µm.

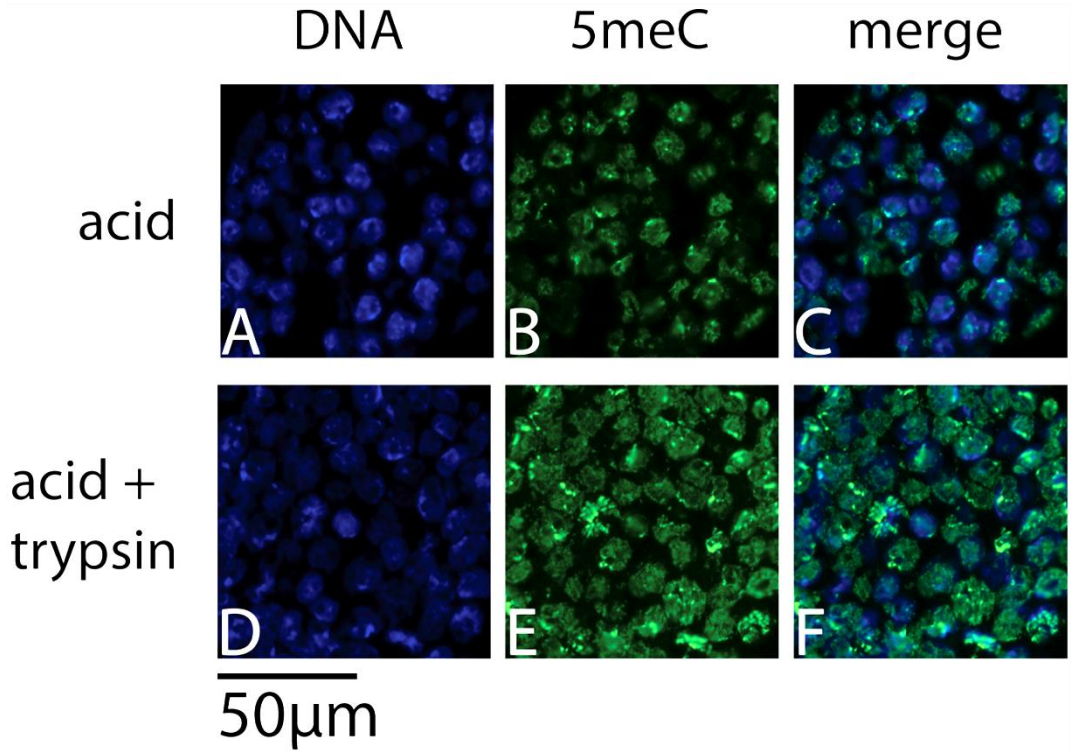

Figure 3-11 The effect of trypsin digestion on the retrieval of 5meC antigen in ESC EB section.

ESC EBs were fixed, sectioned, and permeabilised. They were then either treated with 4N HCl (acid) or treated with trypsin (0.25%) for 20–30 s after acid (acid + trypsin), then stained with anti-5meC and counterstained with DAPI. Immunofluorescence microscopy showed that trypsin treatment increased staining of 5meC compared to acidic treatment alone. Images are representative of three independent replicates. Scale bar = 50 µm.

3.3.4. The effect of oxygen concentration on DNA methylation

In this section, the effect of oxygen concentration on the methylation levels of ESCs was assessed. D3-ESCs were cultured in either 5% or 21% oxygen in air for 24 h, and stained for 5meC levels to observe any difference between the two culture conditions (Figure 3-12). The 5meC staining intensity measurement on plated ESCs showed higher 5meC levels in the ESCs cultured in 21% oxygen compared to the ESCs cultured in 5% oxygen ($p<0.001$) (Figure 3-13).

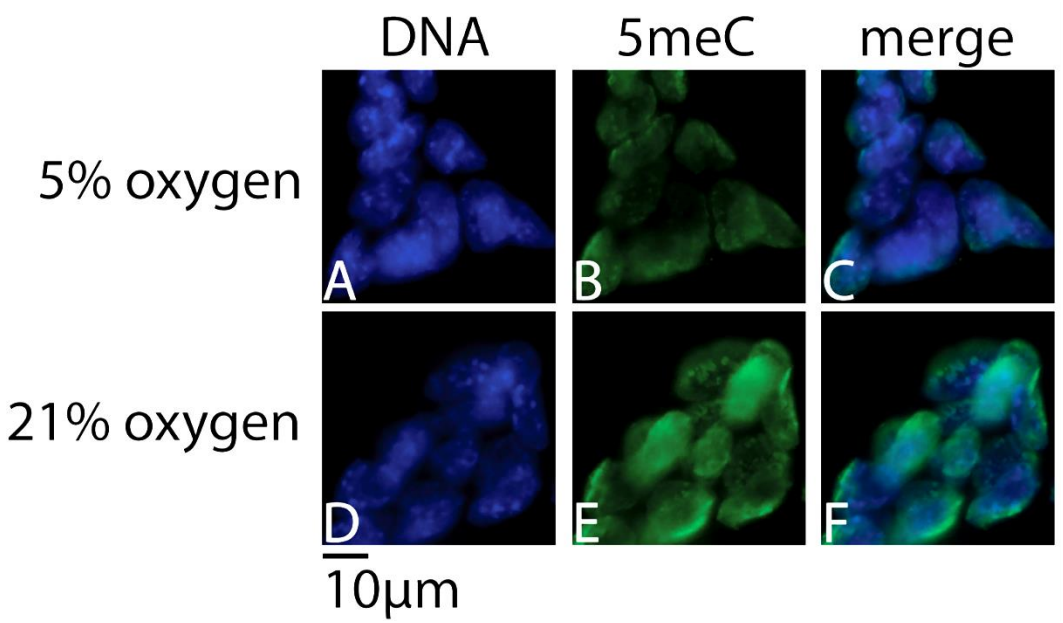

Figure 3-12 The effect of oxygen concentration on 5meC levels in plated ESCs.

Plated ESCs were cultured in either 5% or 21% oxygen in air for 24 h and stained with anti-5meC and counterstained with DAPI. Immunofluorescence microscopy staining on the ESCs plated cells cultured in 5% and 21% oxygen for 24 h showed higher 5meC levels in plated ESCs cultured in 21% oxygen. Images are representative of three independent replicates. Scale bar = 10 µm.

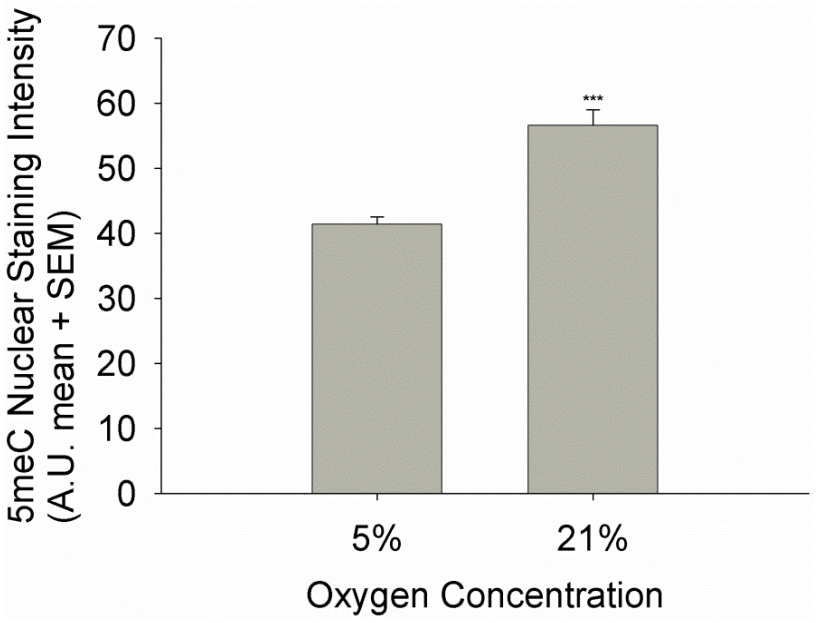

Figure 3-13 5meC nuclear staining intensity in ESCs cultured in 5% and 21% oxygen.

Staining intensity was measured in arbitrary units; mean ± SEM of three independent replicates are shown. At least 50 nuclei were analysed per treatment per replicate. Statistically significant differences are indicated by asterisks: $p<0.001$ = ***.

3.4. DISCUSSION

This chapter showed that 5meC antigen was detected in plated ESCs with the methods previously used for 5meC immunolocalisation in murine embryos and MEF, with minor modifications (Çelik et al., 2014, Li and O'Neill, 2012). A valid immunolocalisation procedure requires the antigen to be fully solvent-exposed, the preparation should not significantly degrade or mask the epitope and the antigen-antibody interaction should approach thermodynamic equilibrium (saturated) (Salvaing et al., 2014). Generally, ESCs form a larger clump of cells both in the plated cells and the embryoid body culture. The larger structures lead to an incomplete permeabilisation of the structures, thus preventing the antibodies getting to the innermost part of the structures.

To validate the permeabilisation of ESCs, H3K9ac staining was performed. Because it is reported to have high levels in all ESCs (Qiao et al., 2015), a thorough permeabilisation should allow exposure of the H3K9ac inside the structure to the antibody, thus showing a uniform staining across the whole structure. The permeabilisation process for plated cells was more reliable than the permeabilisation of EBs. The cells within small colonies in the plated cells were readily permeabilised by the standard procedures, marked by uniform H3K9ac staining across the small plated ESCs structures. However, non-stained cells were observed in the H3K9ac staining of larger colonies due to incomplete permeabilisation of the larger clumps. Therefore, solving the permeabilisation problem in the plated ESCs required that the immunolocalisation be performed before large clumps of cells formed, which is within 24h in this study. However, the incomplete permeabilisation in the whole EBs immunolocalisation persisted.

The permeabilisation process for EBs was modified by increasing the concentration of the permeabilisation reagent, increasing the incubation time, increasing the incubation

temperature, and adding agitation. No condition was found that allowed uniform staining across the EB and the increased permeabilisation parameters compromised the integrity of the EB structure to the point that the nuclei staining efficiency was reduced. The reduced integrity of the EB structure allowed the antibody to bind to the more inner layers of cells within the structure. However, the EBs were still not completely permeabilised, thus leaving the most center part of the structure unstained. In conclusion, the maximum permeabilisation parameters that still allowed the EB to retain its structure were not enough to permeabilise the whole EB.

Cryosectioning of EBs into thin sections allowed exposure of all the cells within the section to the solvent. The increased exposure also increased the sensitivity of the cells to the trypsin-based epitope retrieval process. Therefore, the trypsin treatment time was reduced from 20–30 s to 10–15 s in order to not degrade the nuclei. The H3K9ac staining of the EB sections showed a thorough staining across the sections, confirming that the non-stained cells in the middle part of the whole EBs during the EB staining were falsely negative staining caused by incomplete permeabilisation of the whole EB. Similar patterns were shown in the 5meC staining of EB sections. The 5meC staining was observed in the cells throughout the EB section. It was concluded that the cryosectioning method was suitable for the immunoassay in EBs.

The antigen retrieval methods used in this project incorporate both acid and trypsin-based epitope retrieval processes. Most reported immune-based analyses of 5meC have used acid treatment on fixed cells to denature the chromatin and expose the antigen (Ciccarone et al., 2012, Salvaing et al., 2012). The brief exposure of the fixed cells to acid was proved to increase the amount of detectable 5meC in the cells. However, recent analysis in the embryo showed that some percentage of 5meC remains masked even after acid treatment, and that the remaining masked 5meC can be detected after a brief exposure to trypsin (Li and O'Neill, 2012). The same results are shown in the 5meC staining in ESCs. A short tryptic digestion

increased the amount of detectable 5meC in both plated cells and EB sections. This confirms that antigenic 5meC in ESCs is present, both within the pool that is detectable after acid-induced denaturation and the pool that is detectable after trypsin digestion, similar to the CpG methylation found in mouse embryos and MEFs. Due to the variability of the relative proportions of these two pools of 5meC, reliable and reproducible antigenic retrieval methods become crucial in order to produce valid results in 5meC immunoassays.

To further optimise the cell culture conditions, the effect of changing the balance of complex signals in the ESC microenvironment was investigated. It has been known for some time that cell culture at low oxygen tension (hypoxia) promotes an undifferentiated state in several stem cell populations (Mohyeldin et al., 2010). In vivo, stem cells are located within a highly specific microenvironment provided by cells, blood vessels, matrix glycoproteins, and the three-dimensional space formed by this architecture (Scadden, 2006). Oxygen tension is one of the unique microenvironments that stem cells are exposed to. The oxygen tension of inspired air, measured by the partial pressure oxygen (pO_2), decreases as it reaches organs and tissues, from the ambient level of 21% to 2–9% (Brahimi-Horn and Pouyssegur, 2007). Therefore, stem cells *in vivo* are located in a hypoxic condition. Similarly, mammalian embryogenesis occurs in a relatively poor-oxygen environment because the delivery of oxygen before the establishment of circulatory systems is limited to oxygen diffusion, which only occurs to a distance of 150 µm (Folkman et al., 2000, Mohyeldin et al., 2010). It is found that culturing human embryonic stem cells (hESCs) under a similar oxygen tension (3–5%) is necessary to maintain full pluripotency, as it reduces the rate of differentiation without compromising the proliferation rate of hESCs (Ezashi et al., 2005). The suggested cause of this improvement in pluripotency is the activation of hypoxia signaling pathways by hypoxia-inducible transcription factor 1alpha (HIF-1α) for the response to the hypoxic condition in the microenvironment of hESCs (Ji et al., 2009). To assess the CpGs methylation in ESCs in comparison with CpGs methylation

in embryos, it is essential to create a growth environment for ESCs similar to its natural source, which is the ICM. Therefore, an assessment of the effect of oxygen tension on the global levels of 5meC in ESCs was performed. The results show that the ESCs grown under the ambient oxygen tension (21%) and the ESCs grown under the hypoxic condition (5%) exhibit similar staining patterns. However, the ESCs cultured in 21% oxygen exhibited higher global levels of 5meC compared to the ESCs cultured in 5% oxygen. Due to the more controlled growth of D3-ESCs, lower global 5meC levels, and passage-to-passage stability in low oxygen concentrations, all the D3-ESCs used in this project were cultured in 5% oxygen.

Several validation and optimisation procedures were performed in this project. They include the permeabilisation procedures, antigenic retrieval procedures, and the culture microenvironment conditions. All these validations and optimisations were done to produce valid results in investigating the epigenetic regulation of ESCs under different culture conditions by immunoassay.

4. CHAPTER 4: THE EFFECTS OF CULTURE CONDITIONS ON THE DNA METHYLATION OF ESCs

4.1. INTRODUCTION

One epigenetic feature associated with pluripotency in the embryo is the relative global hypomethylation of cytosine (at CpG dinucleotides, 5meC) that occurs within the nucleus of the inner cell mass. It is surprising, therefore, that the global levels of 5meC in ESCs propagated under conventional methods are comparable to the global levels of 5meC in MEF, as shown in the previous chapter. This leads to the question of whether global hypomethylation is a hallmark of pluripotency, or whether the hypomethylation of ESCs is an artifact of their culture conditions.

An alternative formulation of ESC media called '2i media' (for two inhibitors) was used to improve the pluripotency of ESCs by introducing small molecules to block specific kinases (Nichols and Smith, 2011). An immunolocalisation study showed that culture in 2i media caused reduced global DNA hypomethylation compared to cells in conventional media (Leitch et al., 2013). The reduction in 5meC observed in 2i media was accompanied by several changes in the expression of proteins related to DNA methylation, including a reduction in DNMT3A and DNMT3B while the maintenance protein DNMT1 remained unchanged, and a change in expression of the genes affected by the triple-knockout of DNMT1, DNMT3A, and DNMT3B (Leitch et al., 2013).

The immunolocalisation methods used by (Leitch et al., 2013) only included acid treatment as the antigen retrieval procedure. The antigenic 5meC is found within two pools, one detected after acid-induced denaturation of chromatin (the pool detected by conventional immunolocalisation); and a trypsin-sensitive pool. The trypsin-sensitive pool is variable in size,

depending upon the developmental state and growth disposition of cells (Çelik et al., 2014, Li and O'Neill, 2012). This finding raises the question of whether the observed reduction in 5meC in ESCs cultured in 2i media using the conventional immunoassay procedures was a true reduction in methylation or a change in size of the acid-sensitive pool of 5meC antigen. It was shown in the previous chapter that acid-induced denaturation was not sufficient to retrieve the majority of 5meC in ESCs in DMEM + LIF. The addition of a short period of trypsin digestion improved the amount of 5meC detected by the immunofluorescence assay, similar to the results in MEF (Çelik et al., 2014). The reduction in 5meC levels in 2i ESCs observed in the studies using the conventional immunolocalisation may be caused by an increase in trypsin-sensitive antigenic masking rather than a loss of 5meC.

The aim of this chapter is to assess the effects of culture in 2i media compared to conventional media on global methylation levels using using an antigen retrieval process that incorporates both acid- and trypsin-based epitope retrieval processes. The effect of these media change on pluripotency will be assessed by measuring alkaline phosphate activity. The effect of loss of pluripotency by LIF removal will also be assessed. These investigations are aimed to provide greater insight into the association between global 5meC levels and the pluripotent state in ESCs.

4.2. MATERIAL AND METHODS

4.2.1. Cell Culture

D3-ESCs were cultured in DMEM (DMEM, serum plus LIF) and 2i media prepared in Human Reproduction Unit. See Section 2.1.2 for DMEM and H2i media details. Cells were cultured at 37 °C with 5% CO_2 and 5% O_2 in air. Starting on passage 4, cells were prepared as plated cells or embryoid bodies in both media after every 2 passages. See Section 2.1.6 for details of plated cells and embryoid body culture preparation. Cells were cultured for 24h and 48h prior to the fixation.

4.2.2. Removal of LIF

D3-ESCs were cultured for 10 passages in the presence of LIF prior to the transfer to DMEM minus LIF. Cells were cultured as plated cells or embryoid bodies in DMEM minus LIF at 37 °C with 5% CO_2 and 5% O_2 in air. Cells were fixed at 24 h or 48 h upon the removal of LIF, and assessed for alkaline phosphatase, 5meC, and 5hmC. ESCs in DMEM and 2i media were used as controls.

4.2.3. Antibodies

Primary antibodies used were: (i) mouse anti-5-methylcytidine (Serotec Ltd., Cat. No. MCA2201); and (ii) rabbit anti-5hmC (Active Motif, Cat. No. 39769). Non-immune control antibodies were mouse IgG (Sigma, M7894) and rabbit IgG (Sigma, I5006). The secondary antibodies used to detect the binding of the primary antibodies were: (i) sheep anti-mouse IgG conjugated with Fluorescein Isothiocyanate (FITC) (Sigma, Cat. No. F6257); (ii) goat anti-rabbit IgG conjugated with FITC (Sigma, Cat. No. F1262); and (iii) goat anti-mouse IgG conjugated with Texas Red (TR) (Abcam, Cat. No. ab6787).

4.2.4. Antigenic Retrieval

For 5meC and 5hmC staining, cells were treated with HCl for 10 min, followed by trypsin (0.4%) either for 10–15 s (EB sections) or 20–30 s (plated cells).

4.2.5. Alkaline phosphatase assay

ESCs were assessed for alkaline phosphatase activity using the Alkaline Phosphatase Detection Kit (Millipore, Cat. No. SCR004). Culture media was removed, and cells were rinsed with 1X DPBS. Cells were fixed with 4% (w/v) paraformaldehyde (PFA) (Sigma, Cat. No. P6148) for 1 min at RT. Fixative was aspirated and wells were rinsed with Tris-HCl, pH 7.4, 0.15 M NaCl, 0.05% Tween-20 (TBST). Reagents for alkaline phosphatase staining were prepared by mixing Fast Red Violet solution (0.8 g/L stock) (Part No. 90239) with Naphthol AS-BI phosphate solution (4 mg/ml) in AMPD buffer (2 mol/L), pH 9.5 (Part No. 90234) and water in a 2:1:1 ratio (Fast Red Violet:Naphthol:water). Stain solution was added enough to cover each well. Cells were incubated in dark at RT for 15 min. Staining solution was aspirated and wells were rinsed with TBST. Cells were covered with 1X DPBS to prevent drying. Cells were observed using a conventional microscope.

4.3. RESULTS

4.3.1. Culture in 2i media reduces the levels of DNA methylation in ESCs

ESCs were cultured in either DMEM or 2i media. After 3 passages, cells were prepared as plated cells or embryoid bodies (EBs) in both media and stained for global 5meC and 5hmC levels. 5meC levels were measured every 2 passages and 5hmC levels were measured at passage 4, 10, and 14.

ESCs cultured in DMEM showed consistently high levels of 5meC at each passage in plated cells. Culture in 2i media resulted in a progressive reduction in the levels of global 5meC in both plated cells and EBs (Figure 4-1). The progressive loss of 5meC in plated cells was observable after 6 passages and reached a plateau after 10 passages. EB formation reduced 5meC levels in both DMEM and 2i media. The reduction in 5meC in the EB culture was observed as early as passage 4 and remained stable throughout subsequent passages. The differences in 5meC levels between ESCs in DMEM and 2i media were confirmed by measuring the staining intensity of the cells propagated under both conditions (Figure 4-2).

At passage 4, the 5hmC levels in both media were similar for the plated cells. The 5hmC levels in ESCs cultured in 2i media started to increase at passage 10, and was higher at passage 14 compared to 5hmC levels in ESCs cultured in DMEM (Figure 4-3 and Figure 4-4). In embryoid body formation, the increase of 5hmC in ESCs cultured in 2i media started from passage 4 and reached a plateau at passage 10.

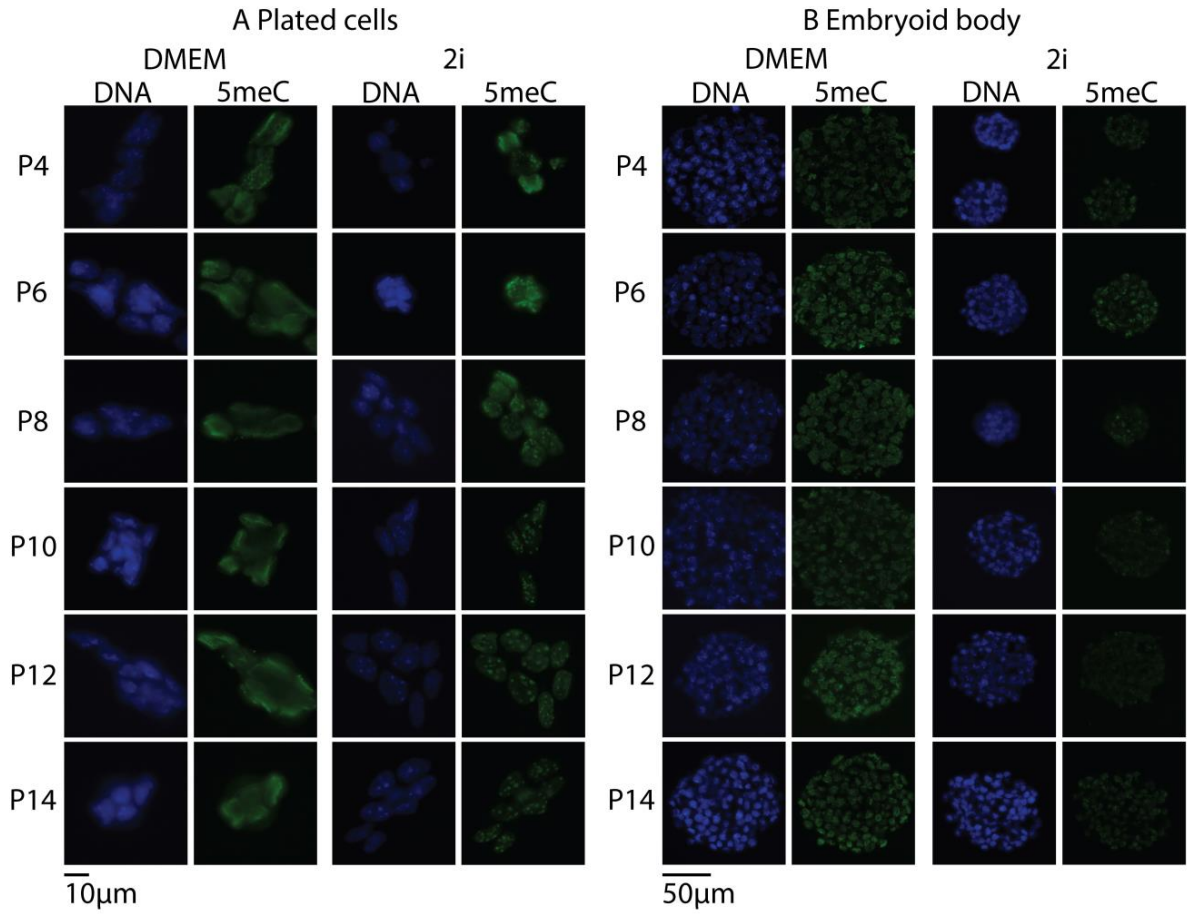

Figure 4-1 Progressive loss of global 5meC levels in ESCs cultured in DMEM and 2i media.

ESCs were grown in either DMEM or 2i media and were cultured in the form of either plated cells or EBs. They were stained with anti-5meC and counterstained with DAPI. (A) Immunofluorescence microscopy showed a progressive loss of 5meC in plated ESCs cultured in 2i media starting from passage 6 and reached plateau after 10 passages. Images are representative of three independent replicates. Scale bar = 10µm. (B) The loss of 5meC in ESCs EBs in 2i media occurred as early as passage 4 and was stable until passage 14. Images are representative of three independent replicates. Scale bar = 50 µm.

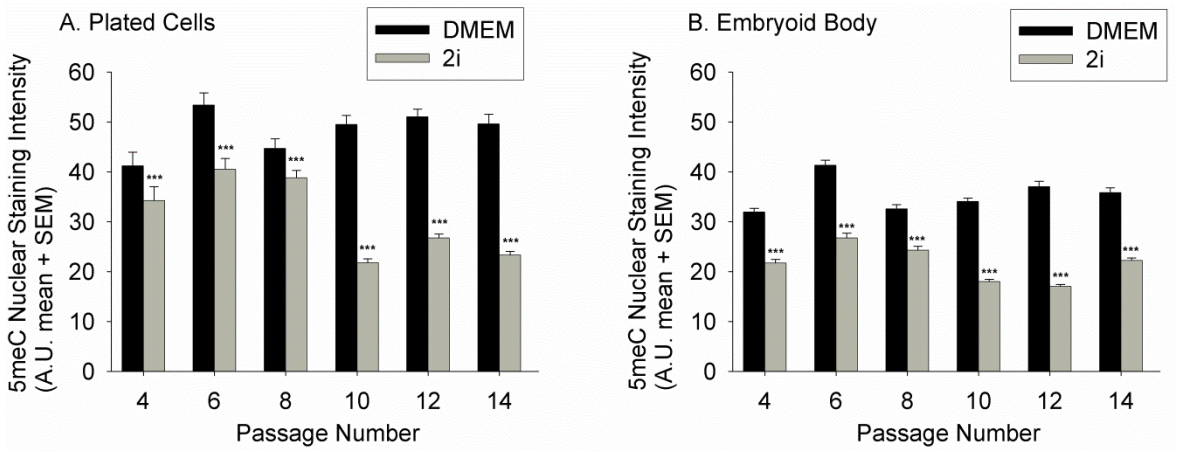

Figure 4-2 5meC nuclear staining intensity in ESCs cultured in DMEM and 2i media.

The 5meC nuclear staining intensity in ESCs cultured in DMEM and 2i media: (A) plated cells and (B) EBs. Staining intensity was measured in arbitrary units; mean ± SEM of three independent replicates are shown. At least 50 nuclei were analysed per treatment per replicate in plated cells and 100 nuclei were analysed per treatment per replicate in EBs. Statistically significant differences are indicated by asterisks: $p<0.001$ = ***.

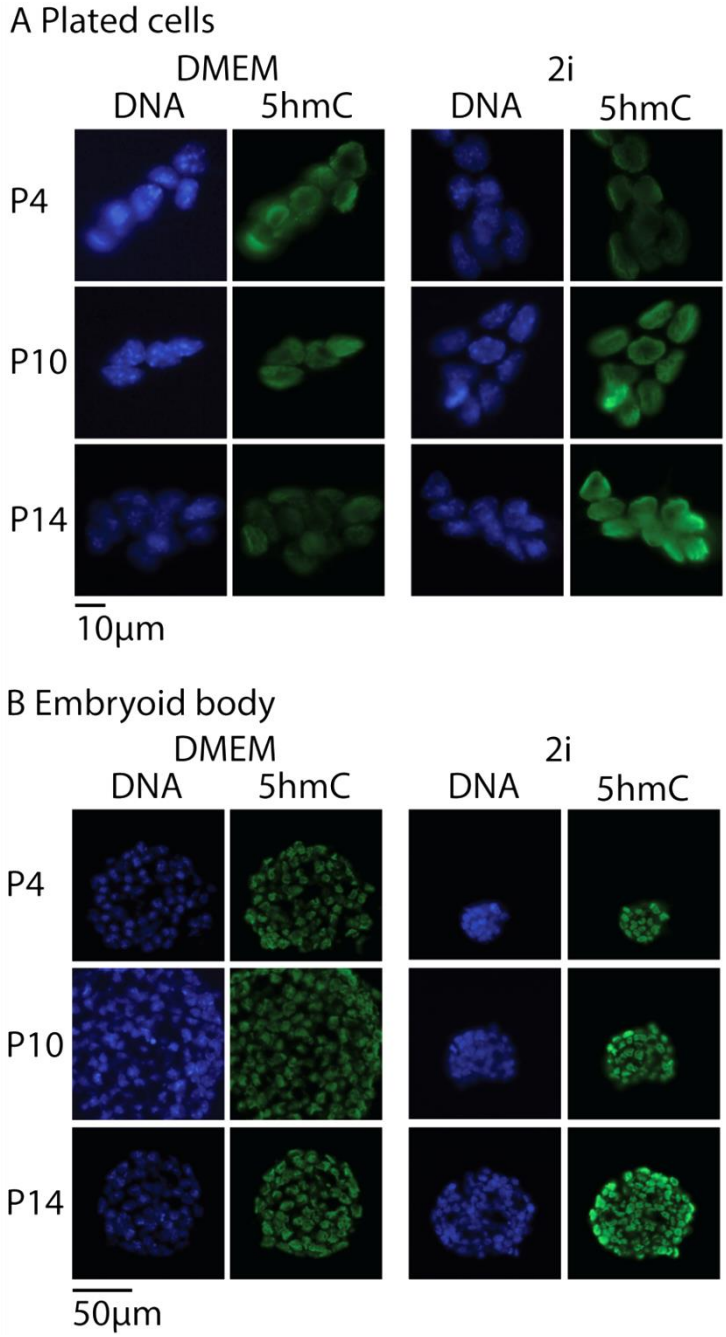

Figure 4-3 Progressive increase of global 5hmC levels in ESCs cultured in DMEM and 2i media.

ESCs were grown in either DMEM or 2i media and were cultured in the form of either plated cells or EBs. They were stained with anti-5hmC and counterstained with DAPI. (A) Immunofluorescence microscopy showed a progressive increase of 5hmC in plated ESCs cultured in 2i media starting from passage 10. Images are representative of three independent replicates. Scale bar = 10 µm. (B) The increase of 5hmC in ESCs EBs in 2i media occurred as early as passage 4 and reached a plateau at passage 10. Images are representative of three independent replicates. Scale bar = 50 µm.

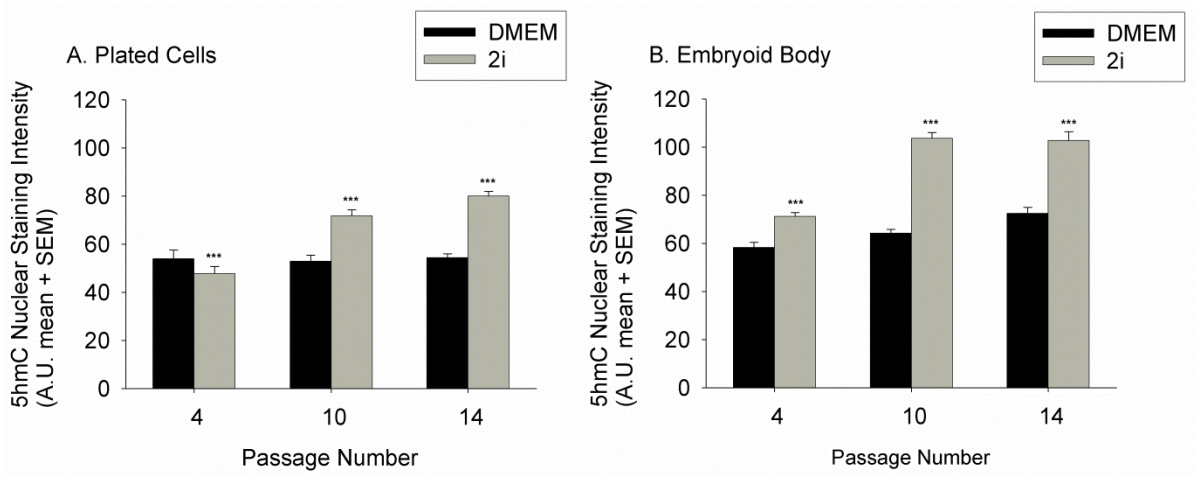

Figure 4-4 5hmC nuclear staining intensity in ESCs cultured in DMEM and 2i media.

The 5hmC nuclear staining intensity in ESCs cultured in DMEM and 2i media: (A) plated cells and (B) EBs. Staining intensity was measured in arbitrary units; mean ± SEM of three independent replicates are shown. At least 50 nuclei were analysed per treatment per replicate in plated cells and 100 nuclei were analysed per treatment per replicate in EBs. Statistically significant differences are indicated by asterisks: $p<0.001$ = ***.

4.3.2. Culture in 2i media increases the alkaline phosphatase expression in ESCs

To investigate whether the loss of 5meC and the increase in 5hmC coincided with an increase in pluripotency status of the ESCs cultured in 2i media, an alkaline phosphatase assay was performed in parallel with the measurement of global 5meC and 5hmC. Plated and EB ESCs were assayed for alkaline phosphatase every 2 passages from passage 4 to passage 14. Alkaline phosphatase assays showed an increase in activity for plated and EB ESCs cultured in 2i media from passage 6 (Figure 4-5 and Figure 4-6). The higher levels of alkaline phosphatase activity in 2i media were stable throughout the passages.

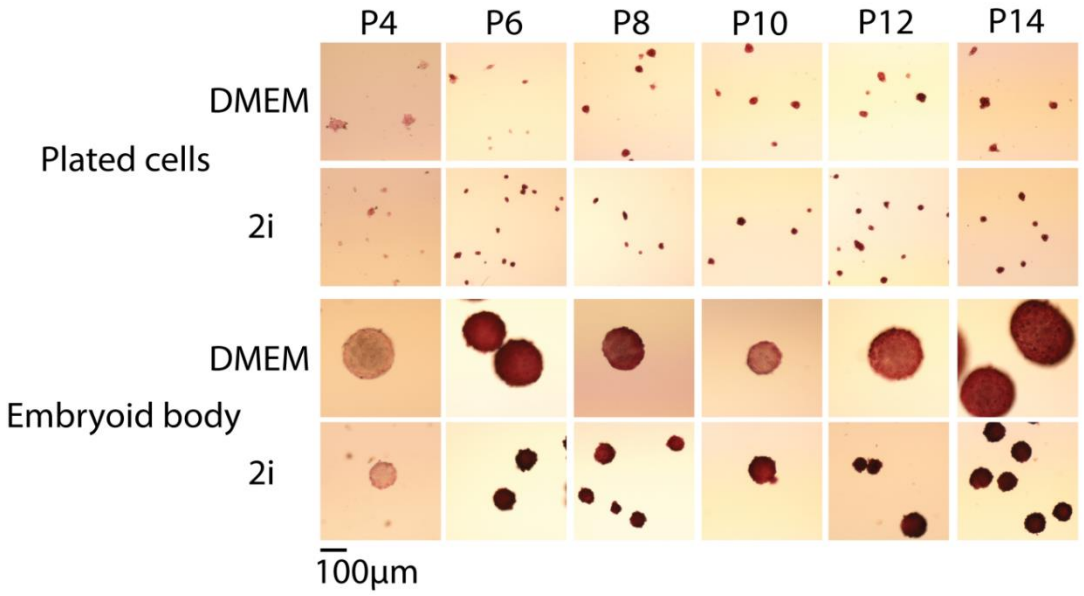

Figure 4-5 Alkaline phosphatase activity in ESCs cultured in DMEM and 2i media.

ESCs were grown in either DMEM or 2i media and were cultured in the form of either plated cells or EBs. They were assayed for alkaline phosphatase activity every 2 passages from passage 4 to passage 14. The bright-field images show a stable increase in alkaline phosphatase activity in 2i media. Images are representative of three independent replicates. Scale bar = 100 µm.

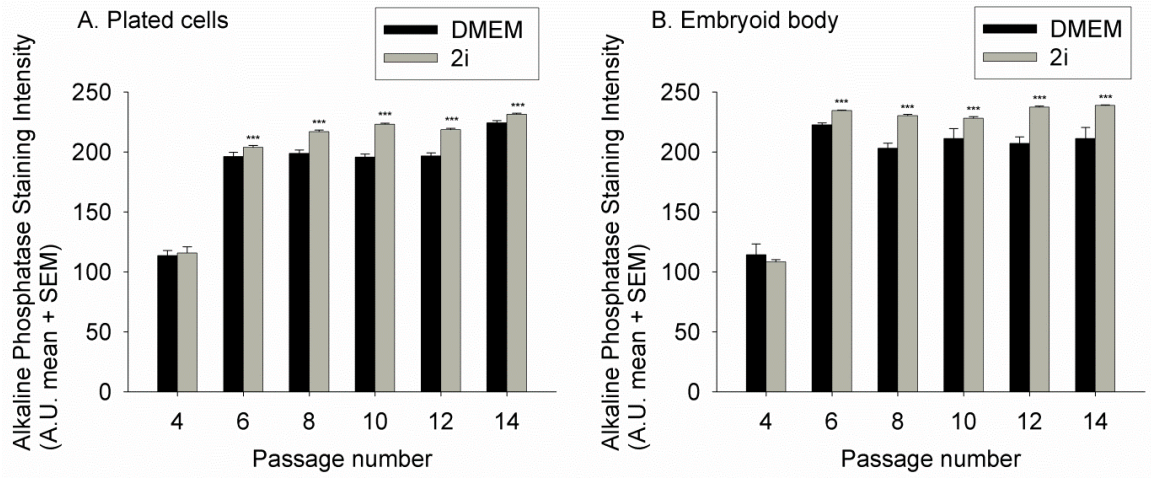

Figure 4-6 Alkaline phosphatase staining intensity in ESCs cultured in DMEM and 2i media.

The alkaline phosphatase staining intensity in ESCs cultured in DMEM and 2i media: (A) plated cells and (B) EBs. Staining intensity was measured in arbitrary units; mean ± SEM of three independent replicates are shown. At least 20 plated clumps and 5 EBs were analysed per treatment per replicate. Statistically significant differences are indicated by asterisks: $p<0.001$ = ***.

4.3.3. Culture in 2i media reduces the heterogeneity of 5meC levels in ESCs

Scatter plots of the intensity measurements of 5meC and 5hmC staining was performed to assess the level of heterogeneity of staining between ESCs cultured in DMEM and 2i media. ESCs cultured in DMEM showed a high level of heterogeneity of DNA methylation between cells (Figure 4-7 and Figure 4-9). The plated cell culture in DMEM showed that the cells surrounded by other cells were generally more hypomethylated than the peripheral cells. Culture in 2i media reduced the heterogeneity of 5meC between cells observed from passage 10 ($p<0.001$).

High magnification images of ESC nuclei in plated cells and EBs were taken with the confocal microscope to assess the effects of culture media formulation on the intranuclear localisation of 5meC and 5hmC staining. 5meC staining in 2i media tended to have a greater level of focal staining pattern while those cells in DMEM had a more generalised pattern of staining throughout the nucleoplasm (Figure 4-9 and Figure 4-10). The 5meC focal pattern in 2i plated cell culture was less observable at passage 4, and a high heterogeneity in the 5meC staining intensity measurement was detected. The focal pattern methylation became noticeable and stable after 10 passages, lowering the 5meC intensity heterogeneity. Embryoid body formation reduced the level of methylation and heterogeneity between cells in DMEM and 2i media ($p<0.001$) (Figure 4-7 and Figure 4-10). The 5meC focal pattern in the embryoid bodies cultured in 2i media occurred as early as passage 4 and remained stable throughout the passages. The 5hmC expression patterns in both ESCs cultured in DMEM and ESCs cultured in 2i media were heterogeneous (Figure 4-8). The increase in 5hmC levels in ESCs cultured in 2i media was associated with an increase in 5hmC heterogeneity. The expression of 5hmC under both conditions in plated cells occurred within the outer layer of cells, similar to the

5meC localisation in ESCs cultured in DMEM (Figure 4-9). The 5hmC localisation in embryoid bodies was generalised in the entire nucleus in both culture conditions (Figure 4-11).

The number of DAPI foci in plated and EB ESCs cultured in DMEM and 2i media were counted to observe the effect of culture conditions on the chromatin structure of ESCs. The counting of DAPI foci per nucleus in ESCs showed there was no significant difference in the average number of DAPI foci (Figure 4-12). However, changing culture conditions that favour the formation of EBs reduced the number of DAPI foci in both DMEM and 2i media. To further investigate the connection between the chromatin structure and the localisation of 5meC, the average proportion of DAPI foci co-stained with anti-5meC per nuclei of ESCs was counted. The counting showed that culture in 2i media increased the number of DAPI foci co-stained with anti-5meC (Figure 4-13). There was no significant difference of co-stained foci between plated cells and EBs.

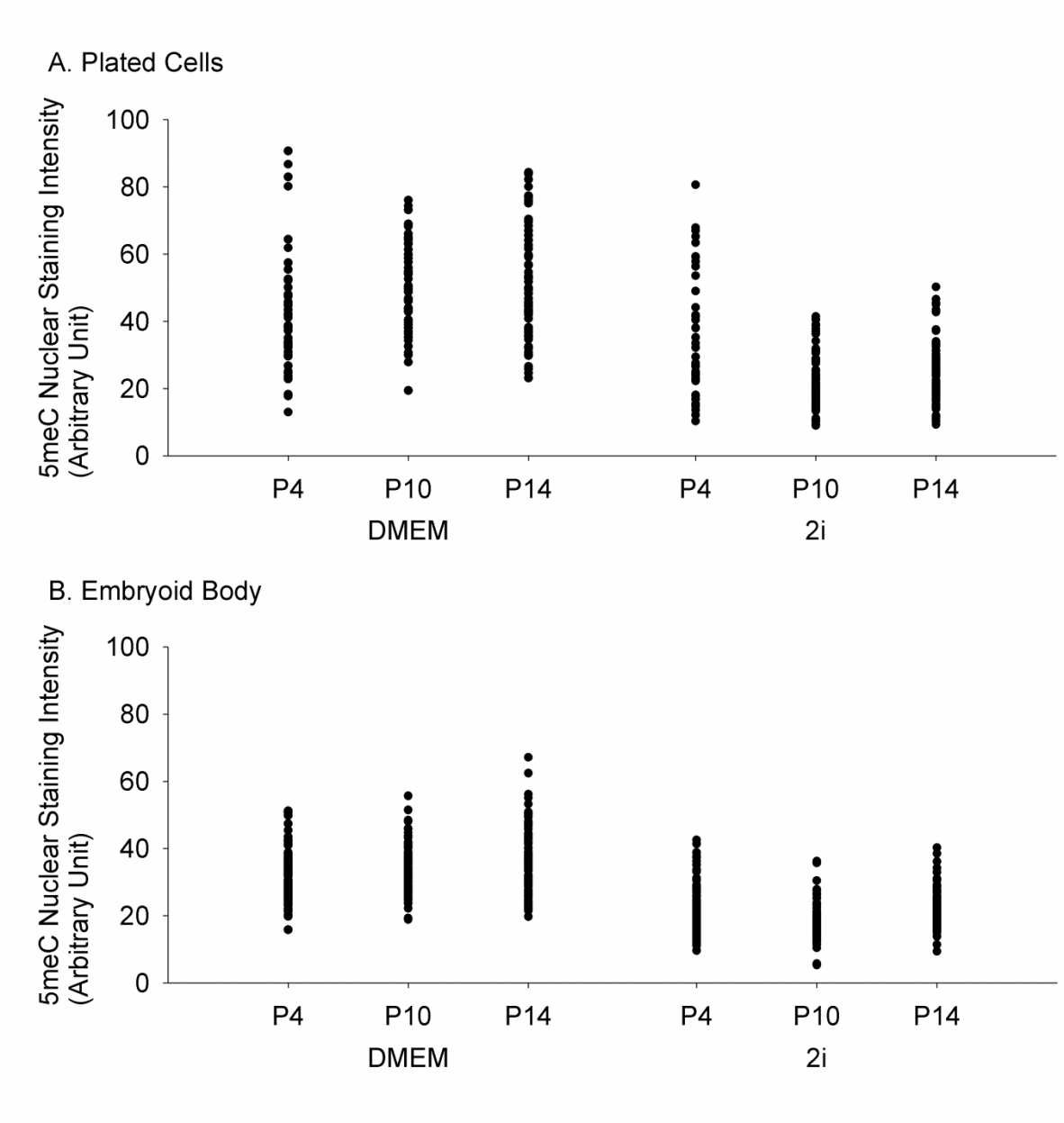

Figure 4-7 Scatter plots of 5meC nuclear staining intensity in ESCs cultured in DMEM and 2i media.

The 5meC nuclear staining intensity in ESCs cultured in DMEM and 2i media: (A) plated cells and (B) EBs. Staining intensity was measured in arbitrary units for three independent replicates. At least 50 nuclei were analysed per treatment per replicate in plated cells and 100 nuclei were analysed per treatment per replicate in EBs.

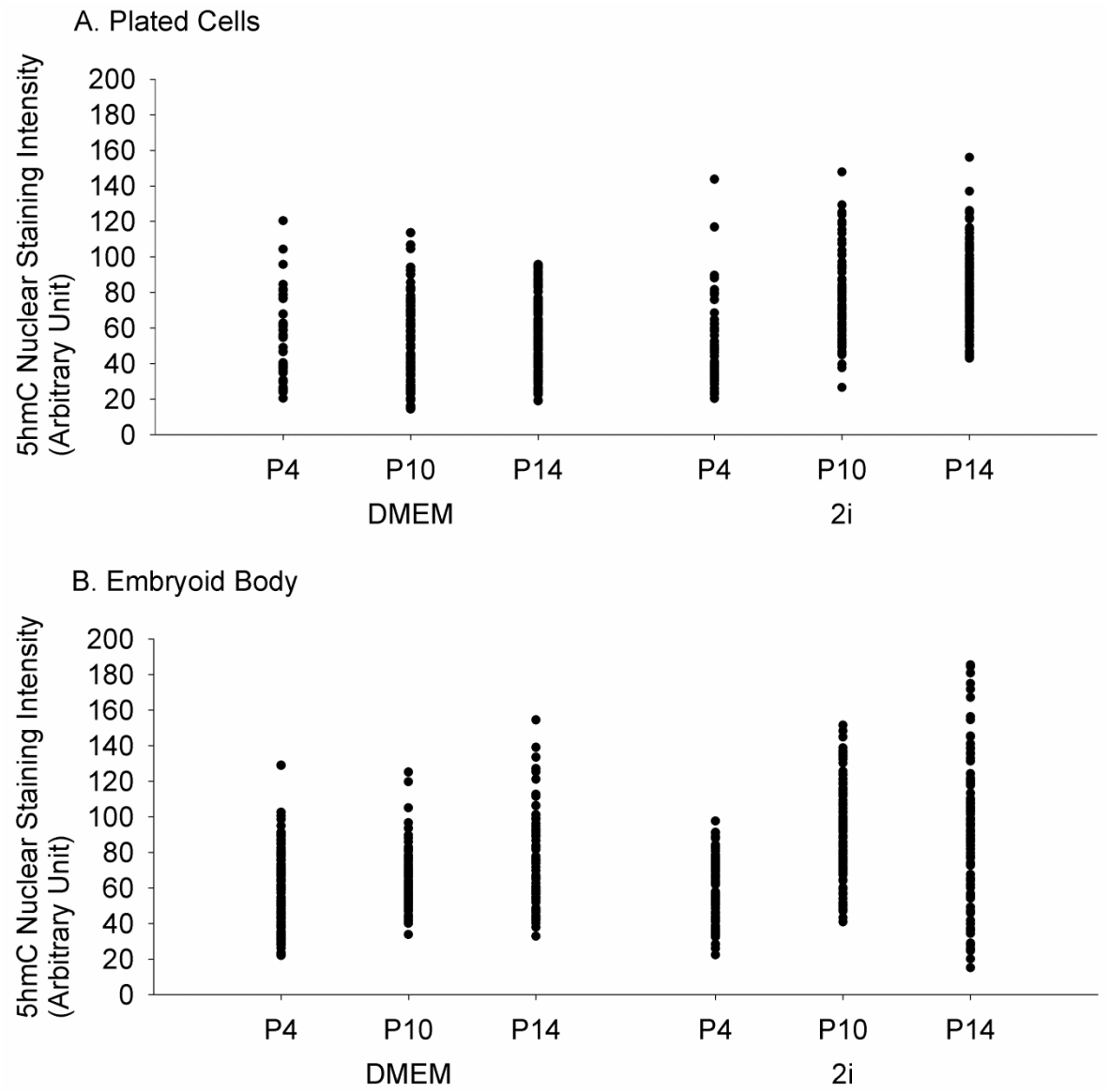

Figure 4-8 Scatter plots of 5hmC nuclear staining intensity in ESCs cultured in DMEM and 2i media.

The 5hmC nuclear staining intensity in ESCs cultured in DMEM and 2i media: (A) plated cells and (B) EBs. Staining intensity was measured in arbitrary units for three independent replicates. At least 50 nuclei were analysed per treatment per replicate in plated cells and 100 nuclei were analysed per treatment per replicate in EBs.

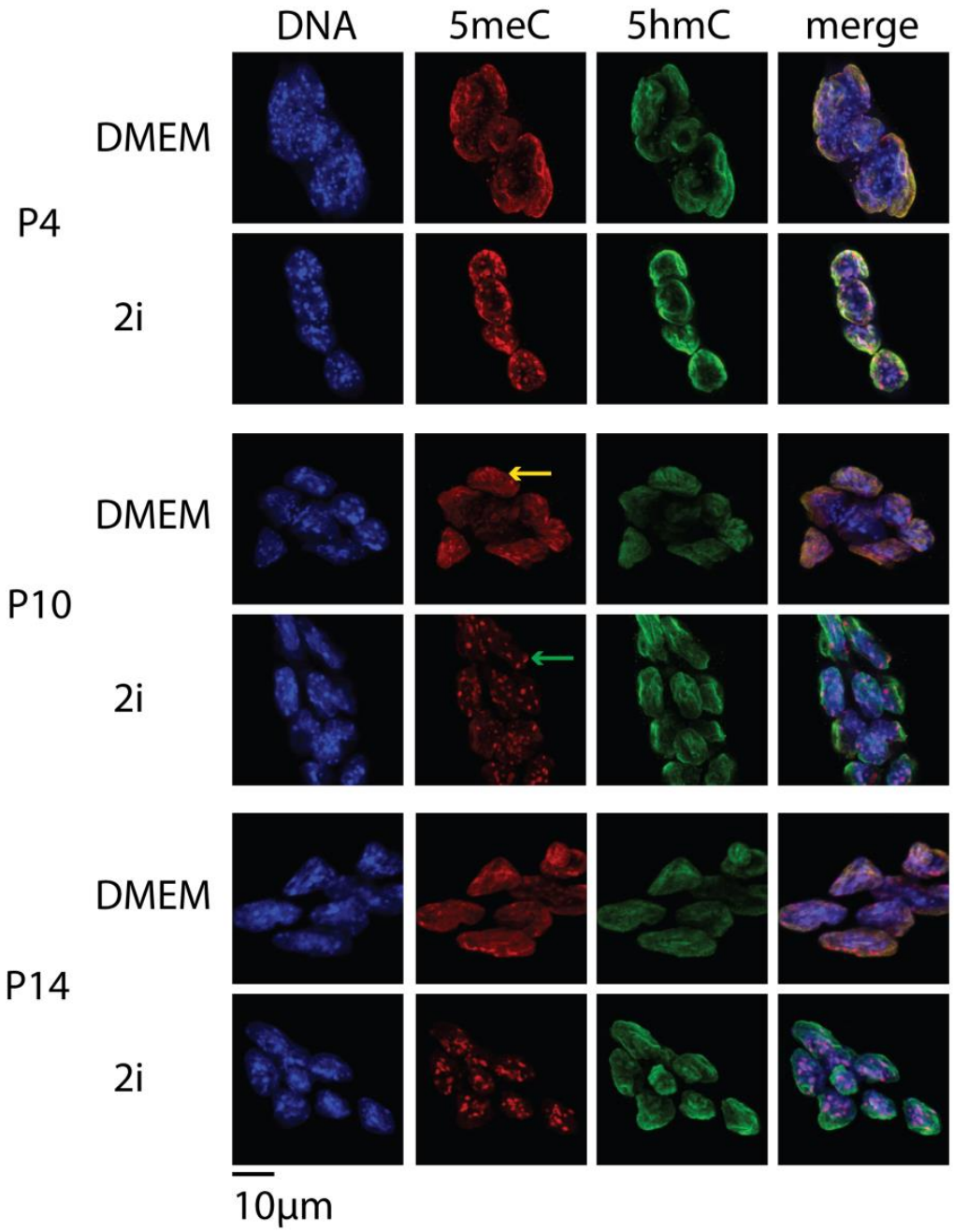

Figure 4-9 Immunolocalisation of 5meC and 5hmC in plated ESCs cultured in DMEM and 2i media.

Plated ESCs grown in either DMEM or 2i media were co-stained with anti-5meC and anti-5hmC and counterstained with DAPI. High resolution images were taken using the confocal microscope at passages 4, 10, and 14. Confocal microscopy showed generalised 5meC staining across the nucleoplasm in the ESCs cultured in DMEM as indicated with yellow arrow. The 5meC staining in the ESCs cultured in 2i media tended to occur within the heterochromatic foci starting from passage 10 as indicated with green arrow. The 5hmC localisation was similar in all culture conditions. Images are representative of three independent replicates. Scale bar = 10 µm.

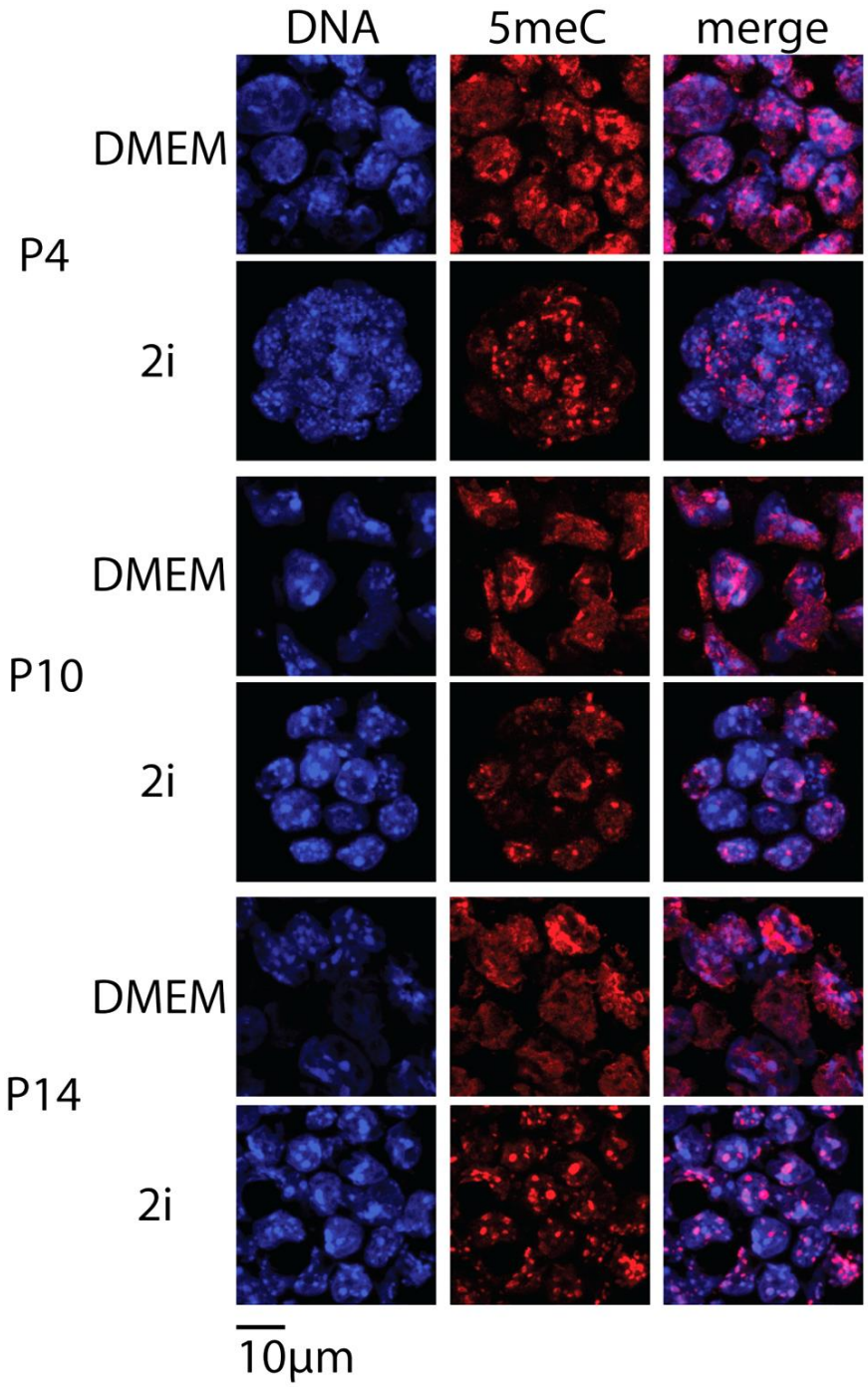

Figure 4-10 Immunolocalisation of 5meC in EB ESCs cultured in DMEM and 2i media.

ESCs were grown in either DMEM or 2i media and were formed into EBs. The EBs were processed into EB sections and were stained with anti-5meC and counterstained with DAPI. High resolution images were taken using the confocal microscope at passages 4, 10, and 14. Confocal microscopy showed generalised 5meC staining across the nucleoplasm in the ESCs cultured in DMEM. The 5meC staining in the ESCs cultured in 2i media tended to occur within the heterochromatic foci starting from passage 4. Images are representative of three independent replicates. Scale bar = 10 µm.

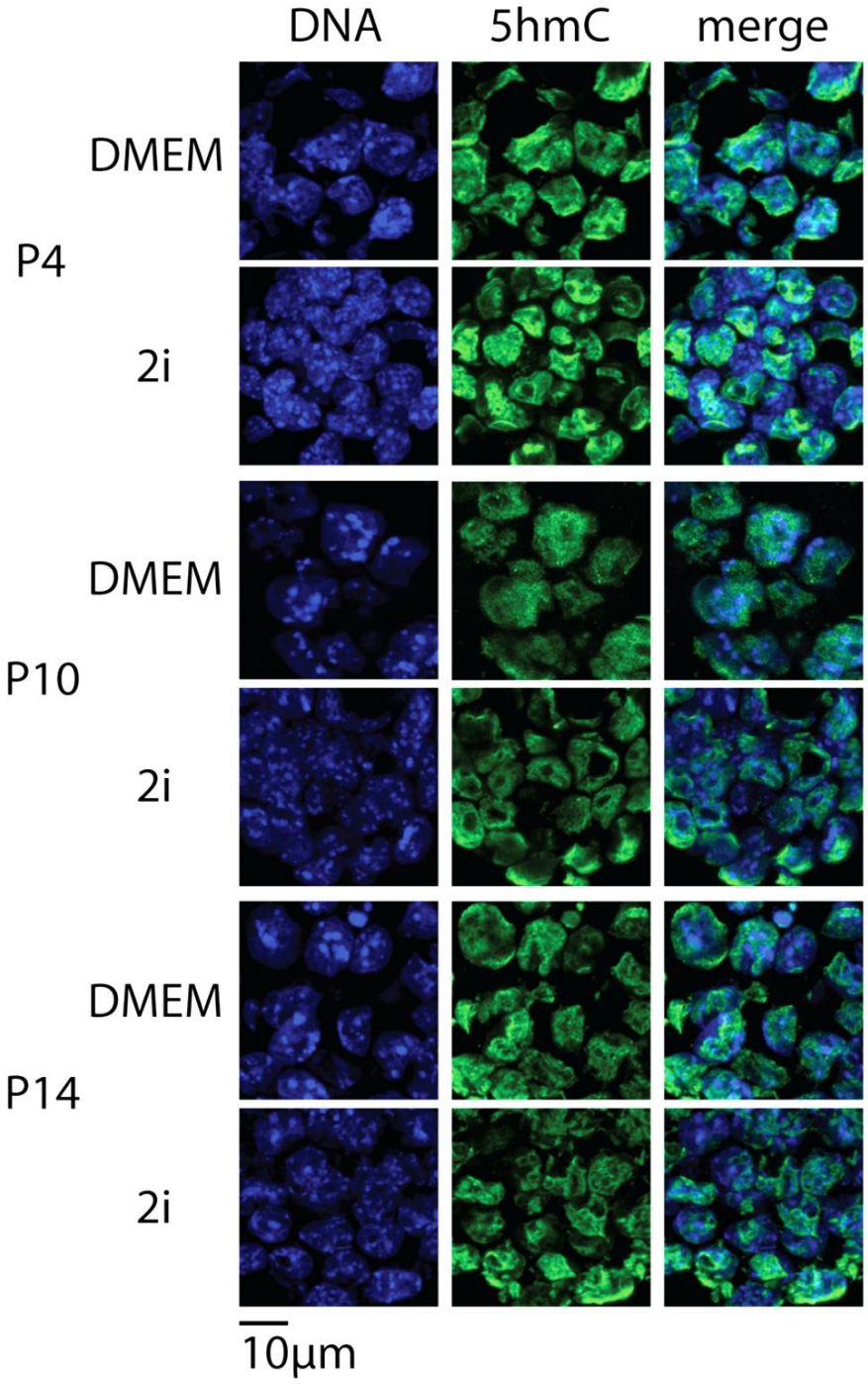

Figure 4-11 Immunolocalisation of 5hmC in EB ESCs cultured in DMEM and 2i media.

ESCs were grown in either DMEM or 2i media and were formed into EBs. The EBs were processed into EB sections and were stained with anti-5hmC and counterstained with DAPI. High resolution images were taken using the confocal microscope at passages 4, 10, and 14. Confocal microscopy showed generalised 5hmC staining across the nucleoplasm in all culture conditions. Images are representative of three independent replicates. Scale bar = 10 µm.

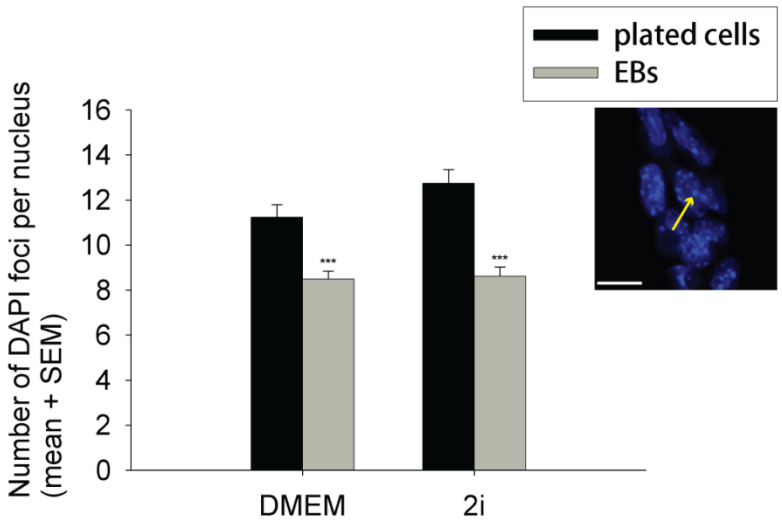

Figure 4-12 Average number of DAPI foci per nucleus of ESCs.

The average number of DAPI foci per nucleus of plated ESCs and EB ESCs cultured in DMEM and 2i media. Number of DAPI foci are shown as mean ± SEM of three independent replicates. At least 20 nuclei were analysed per treatment per replicate. Statistically significant differences are indicated by asterisks: $p<0.001$ = ***. DAPI foci are indicated with yellow arrow. Scale bar = 10 µm.

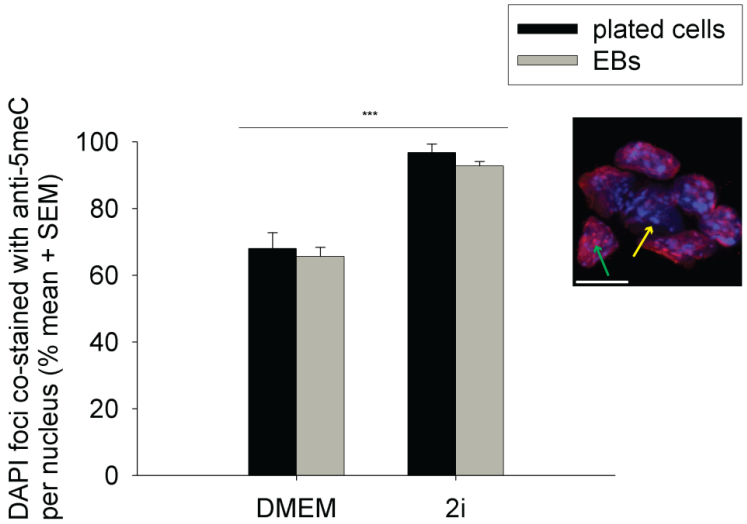

Figure 4-13 Proportion of DAPI foci co-stained with anti-5meC per nucleus of ESCs.

The average proportion of DAPI foci co-stained with anti-5meC per nucleus of plated ESCs and EB ESCs cultured in DMEM and 2i media. Data is shown as % mean ± SEM of three independent replicates. At least 20 nuclei were analysed per treatment per replicate. Statistically significant differences are indicated by asterisks: $p<0.001$ = ***.

DAPI foci that were 5meC negative or positive are indicated with yellow and green arrows, respectively. Scale bar = 10 μm.

4.3.4. Change of DNA methylation levels upon the removal of LIF

Removal of LIF was performed to assess the changes in 5meC and 5hmC levels in ESCs upon the loss of pluripotency. The loss of pluripotency was induced by culturing the ESCs in DMEM minus LIF. ESCs were cultured in DMEM and 2i media for over 10 passages before transferred to DMEM minus LIF. The ESCs were cultured in normal plated cells or EBs. 5meC staining showed increased levels of global 5meC in plated cells and EBs as early as 24 h after LIF removal (Figure 4-14, Figure 4-15, and Figure 4-16). The 5meC levels at 48 h after LIF removal were similar with the 5meC levels at 24 h. Staining intensity measurement on the 5meC levels showed a smaller increase in 5meC in the ESC culture that favours EB formation.

5hmC staining showed reduced global levels of 5hmC in plated cells upon LIF removal, compared to the ESC cultures with LIF, as early as 24 h after LIF removal (Figure 4-17). At 48 h after LIF removal, the 5hmC levels in plated ESCs previously cultured in 2i media were reduced to the same levels as plated ESCs previously cultured in DMEM at 48 h after LIF removal (Figure 4-19). The 5hmC levels in the EBs without LIF was similar to the 5hmC levels in the EBs cultured in DMEM, and those were less than the 5hmC levels in the EBs cultured in 2i (Figure 4-18 and Figure 4-19). The 5hmC levels in EB ESCs from both media at 48 h after LIF removal showed small decreases compared to the 5hmC levels of EB ESCs at 24 h after LIF removal.

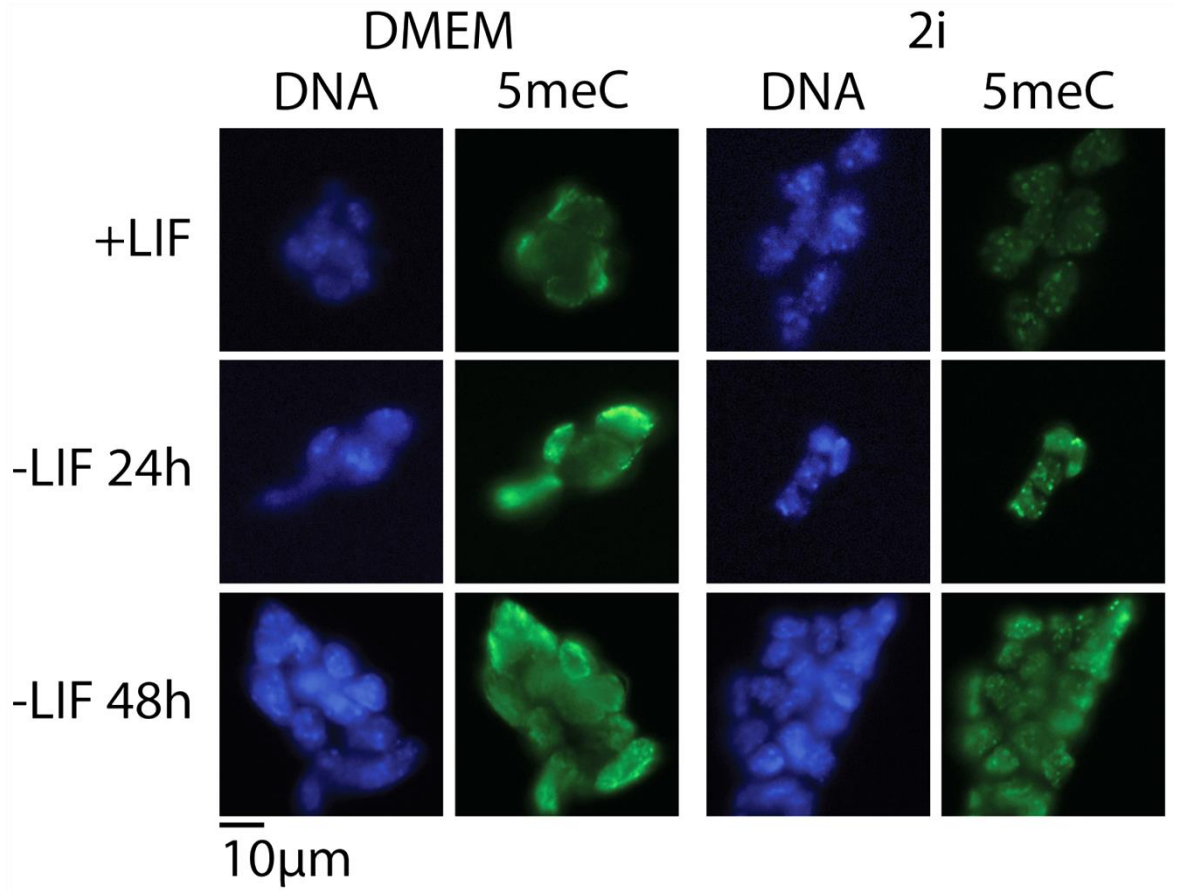

Figure 4-14 Increase in global 5meC levels in plated ESCs upon LIF removal.

ESCs were grown in either DMEM or 2i media for over 10 passages prior to transfer to DMEM minus LIF. Plated cells were stained with anti-5meC and counterstained with DAPI. Plated ESCs in DMEM and 2i were used as controls. Immunofluorescence microscopy showed an increase in 5meC in plated ESCs after being exposed to DMEM minus LIF for 24 h and 48 h. Images are representative of three independent replicates. Scale bar = 10 µm.

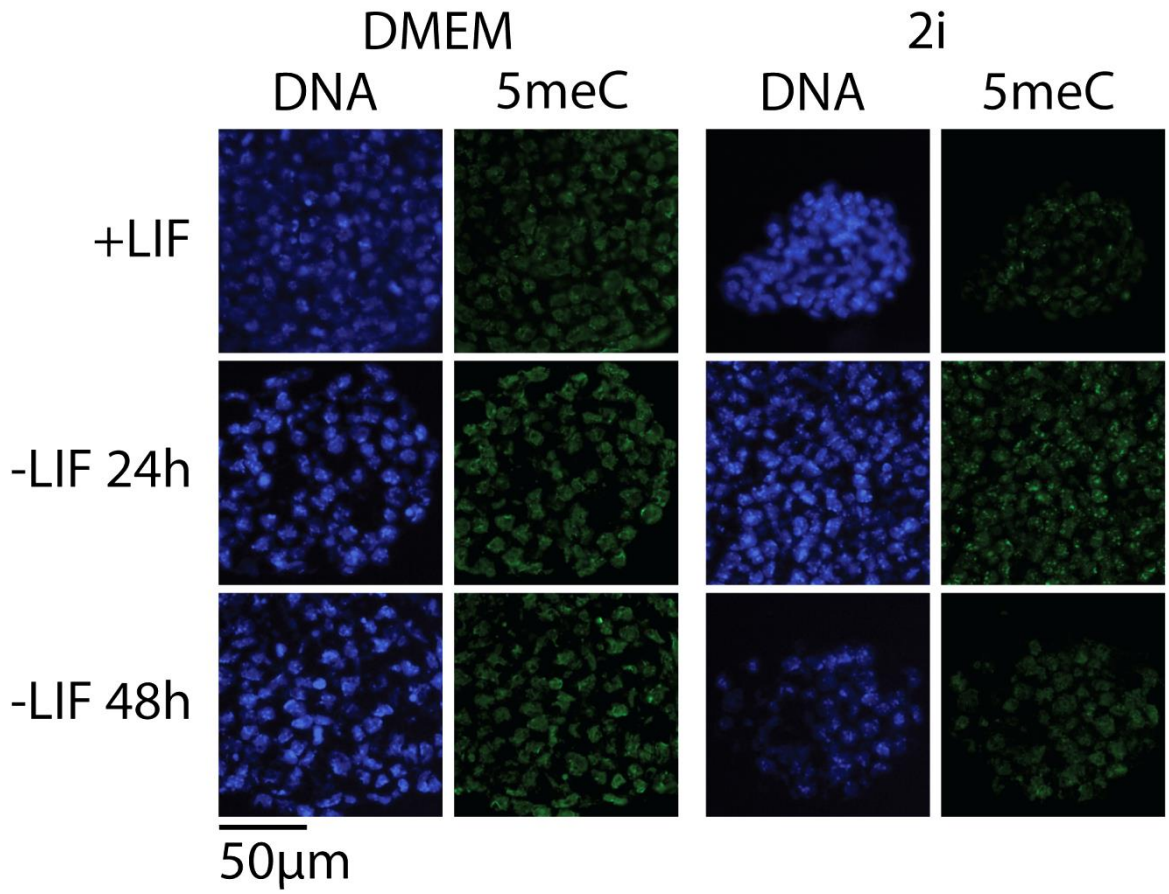

Figure 4-15 Increase in global 5meC levels in EB ESCs upon LIF removal.

ESCs were grown in either DMEM or 2i media for over 10 passages prior to transfer to DMEM minus LIF with growth conditions that support the formation of EBs. EB sections were stained with anti-5meC and counterstained with DAPI. EB ESCs in DMEM and 2i were used as controls. Immunofluorescence microscopy showed an increase in 5meC in EB ESCs after being exposed to DMEM minus LIF for 24 h and 48 h. Images are representative of three independent replicates. Scale bar = 50 µm.

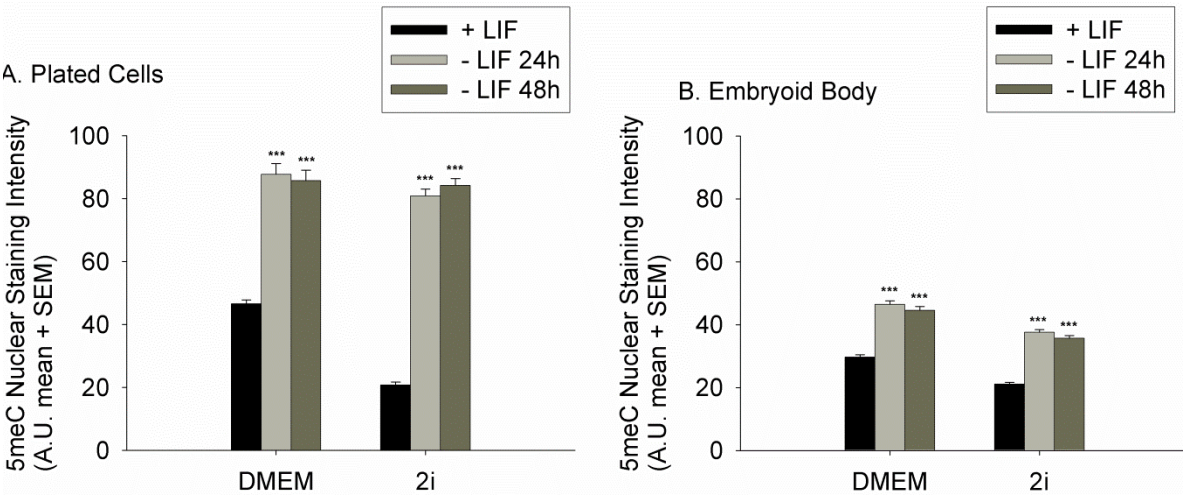

Figure 4-16 5meC nuclear staining intensity in ESCs upon LIF removal.

The 5meC nuclear staining intensity was measured in ESCs previously cultured in DMEM and 2i for over 10 passages prior to exposure to DMEM minus LIF for 24 h and 48 h: (A) plated cells and (B) EBs. Plated and EB ESCs in DMEM and 2i were used as controls. Staining intensity was measured in arbitrary units and is shown as mean ± SEM of three independent replicates. At least 50 nuclei were analysed per treatment per replicate in plated cells and 100 nuclei were analysed per treatment per replicate in EBs. Statistically significant differences are indicated by asterisks: $p<0.001$ = ***.

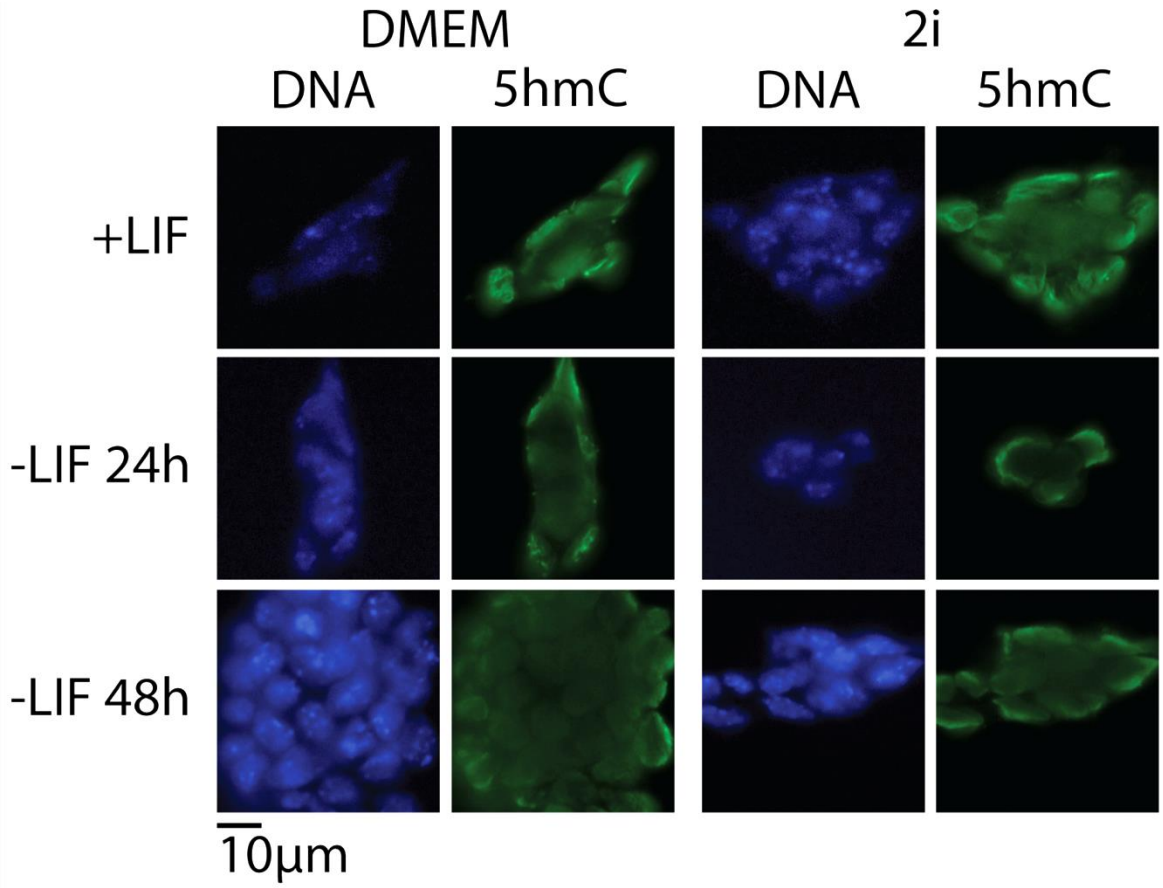

Figure 4-17 Loss of global 5hmC levels in EB ESCs upon LIF removal.

ESCs were grown in either DMEM or 2i media for over 10 passages prior to transfer to DMEM minus LIF. Plated cells were stained with anti-5hmC and counterstained with DAPI. Plated ESCs in DMEM and 2i were used as controls. Immunofluorescence microscopy showed a loss of 5hmC in plated ESCs after being exposed to DMEM minus LIF for 24 h and 48 h. Images are representative of three independent replicates. Scale bar = 10 µm.

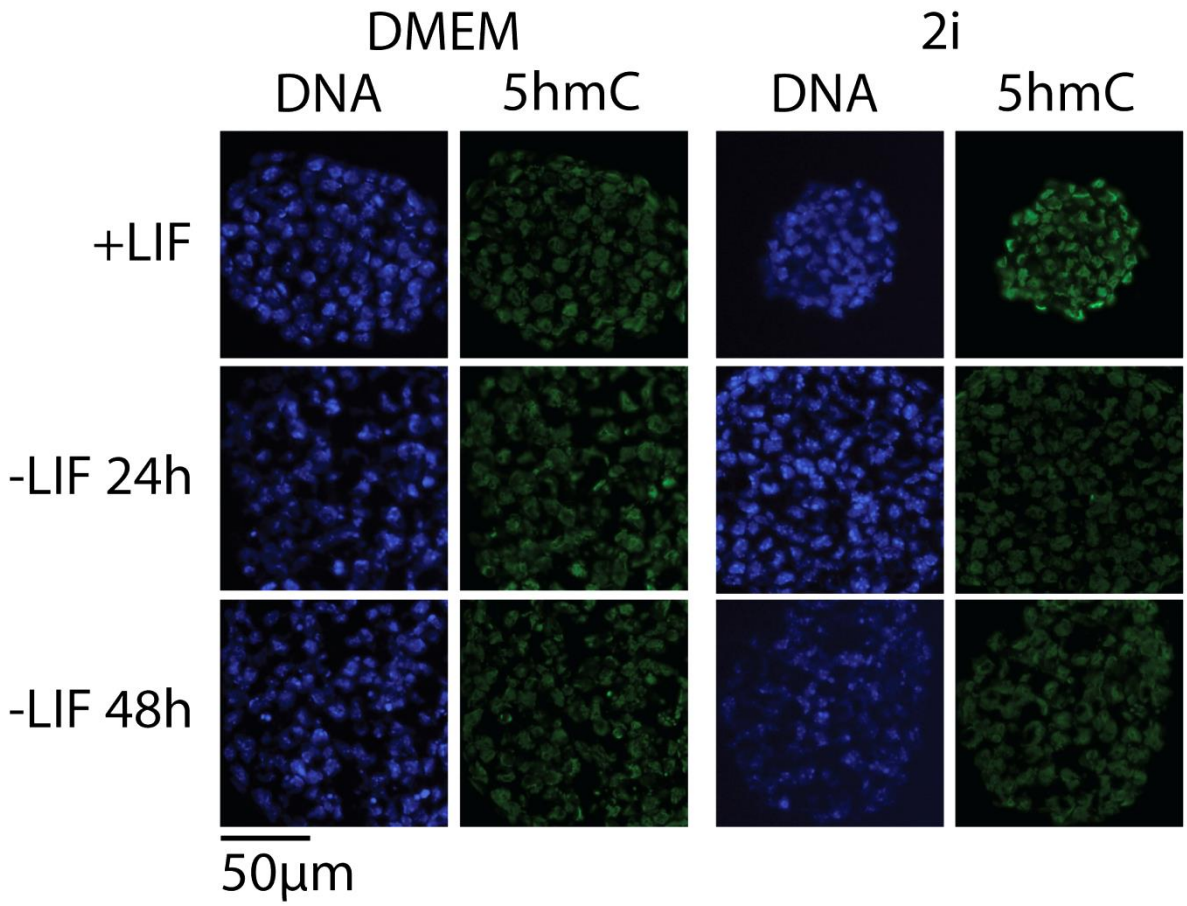

Figure 4-18 Loss of global 5hmC levels in EB ESCs previously cultured in 2i media upon LIF removal.

ESCs were grown in either DMEM or 2i media for over 10 passages prior to transfer to DMEM minus LIF with growth conditions that support the formation of EBs. EB sections were stained with anti-5hmC and counterstained with DAPI. EB ESCs in DMEM and 2i were used as controls. Immunofluorescence microscopy showed a loss of 5hmC in EB ESCs previously cultured in 2i after being exposed to DMEM minus LIF for 24 h. The 5hmC levels were reduced to a level similar to EBs in DMEM. The 5hmC levels in EB ESCs previously cultured in DMEM remained unchanged upon 24 h exposure to DMEM minus LIF. The 5hmC levels in EB ESCs from both media were reduced 48 h after LIF removal. Images are representative of three independent replicates. Scale bar = 50 µm.

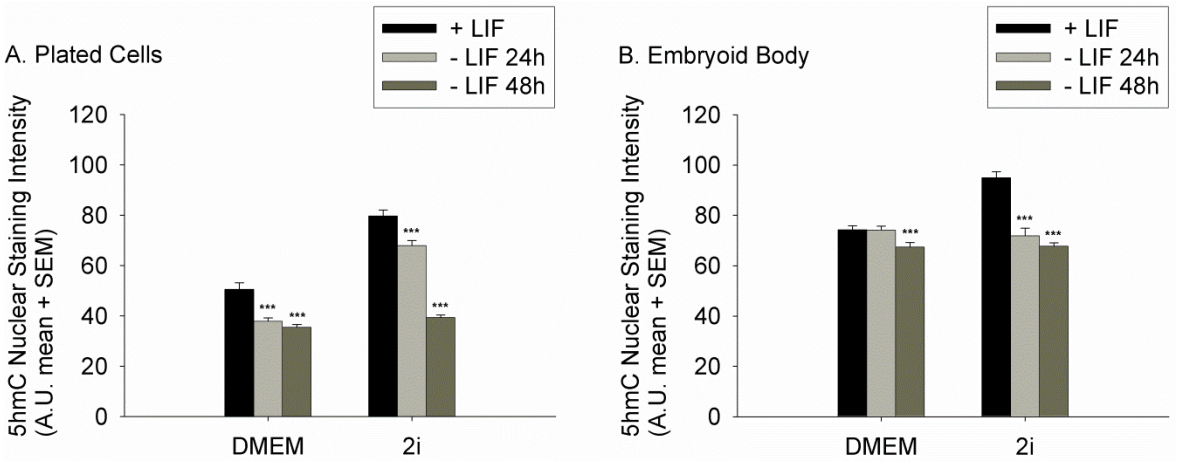

Figure 4-19 5hmC nuclear staining intensity in ESCs upon LIF removal.

The 5hmC nuclear staining intensity was measured in ESCs previously cultured in DMEM or 2i for over 10 passages prior to the exposure to DMEM minus LIF for 24 h and 48 h: (A) plated cells and (B) EBs. Plated and EB ESCs in DMEM and 2i were used as controls. Staining intensity was measured in arbitrary units and is shown as mean ± SEM of three independent replicates. At least 50 nuclei were analysed per treatment per replicate in plated cells and 100 nuclei were analysed per treatment per replicate in EBs. Statistically significant differences are indicated by asterisks: $p<0.001$ = ***.

4.3.5. Morphology and alkaline phosphatase activity in ESCs upon LIF removal

ESCs were assessed for changes in morphology and alkaline phosphatase activity upon LIF removal. Phase contrast images of plated ESCs showed no observable sign of morphological changes within 24 h of LIF removal (Figure 4-20). Plated ESCs maintained their small round colonies with only a small portion of colonies that started to show a spreading morphology. The signs of morphological changes appeared 48 h after LIF removal, when the cells from both media showed a flattened and outgrowth pattern. The EBs without LIF previously cultured in DMEM showed a similar shape and size to the EBs in DMEM. The EBs without LIF previously cultured in 2i showed a similar morphology to the EBs cultured in DMEM. Generally there was only one EB per drop, and the size was larger compared to the EBs in 2i media. EBs from both media were larger at 48 h after LIF removal.

Alkaline phosphatase assays on the ESCs showed similar activity in the plated and EB ESCs within 24 h of LIF removal compared to their respective controls containing LIF (Figure 4-21 and Figure 4-22). The level of alkaline phosphatase activity was higher in 2i media compared to DMEM, both in the ESCs with LIF and without LIF. The alkaline phosphatase activities were reduced 48 h after LIF removal.

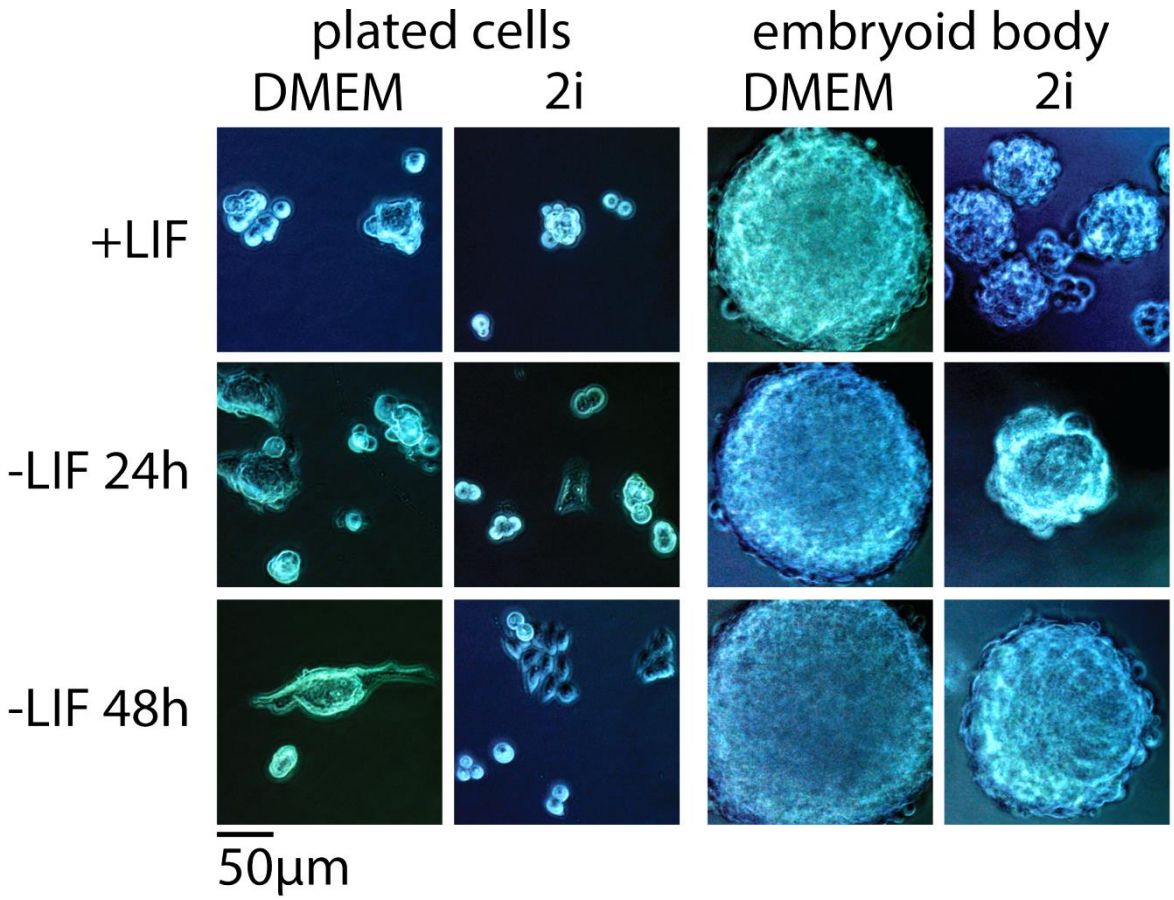

Figure 4-20 Morphology of ESCs upon LIF removal.

Plated and EB ESCs previously cultured in 2i or DMEM for over 10 passages were transferred to DMEM minus LIF for 24 h or 48 h. Plated and EBs ESCs cultured in DMEM and 2i were used as controls. Phase-contrast images taken using a conventional microscope showed no observable growth change in the plated cells within 24 h of LIF removal. Morphological changes in plated cells were observed at 48 h after LIF removal. The EBs without LIF previously cultured in 2i showed similar growth to the EBs cultured in DMEM. EBs from both media were larger 48 h after LIF removal. Images are representative of three independent replicates. Scale bar = 50 µm.

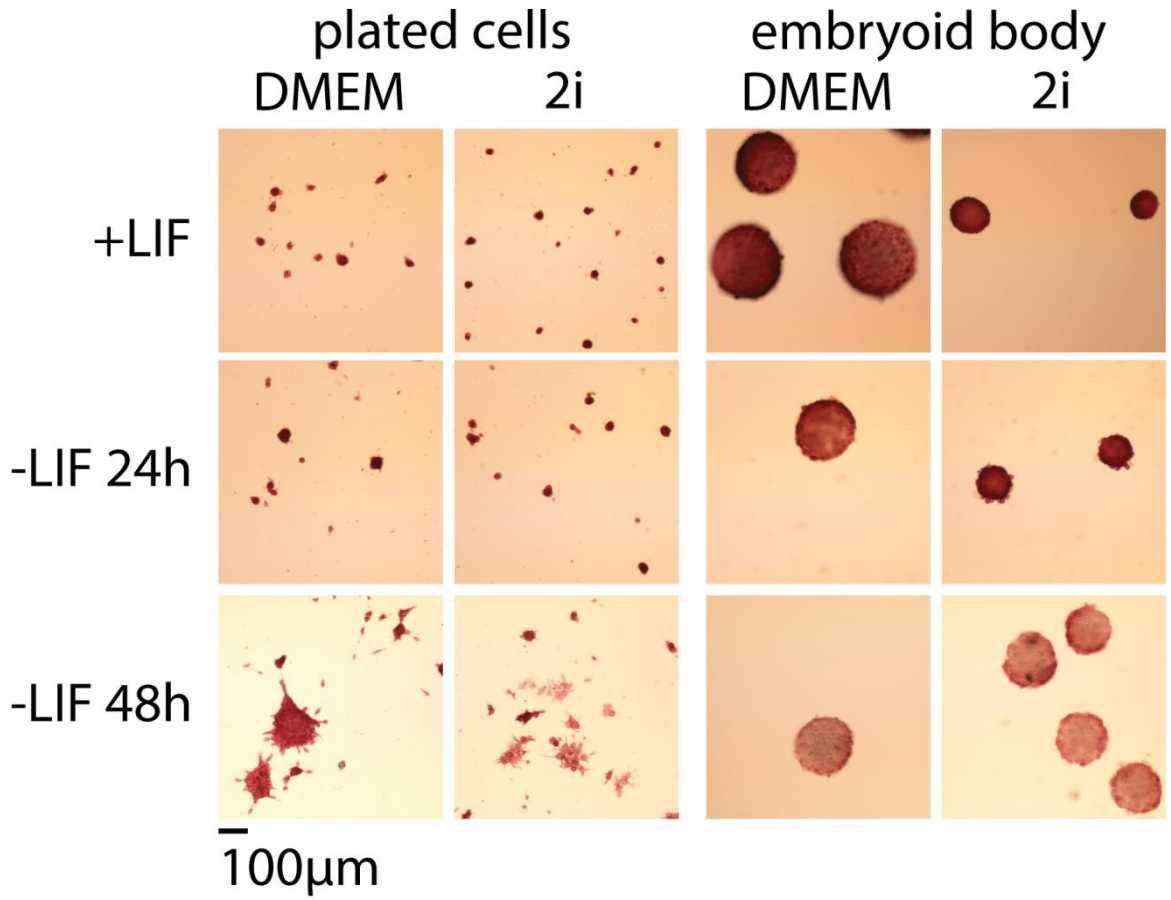

Figure 4-21 Alkaline phosphatase activity in ESCs upon LIF removal.

ESCs were previously cultured in 2i and DMEM for over 10 passages prior to exposure to DMEM minus LIF and were cultured in the form of either plated cells or EBs. They were assayed for alkaline phosphatase activity 24 h or 48 h after LIF removal. Plated and EBs ESCs cultured in DMEM and 2i were used as controls. The bright-field images 24 h after LIF removal showed similar alkaline phosphatase activities between the cells with LIF and without LIF, with higher activities in 2i media. The differences were more profound in EBs compared to plated cells. The alkaline phosphatase activities were reduced 48 h after LIF removal. Images are representative of three independent replicates. Scale bar = 100 µm.

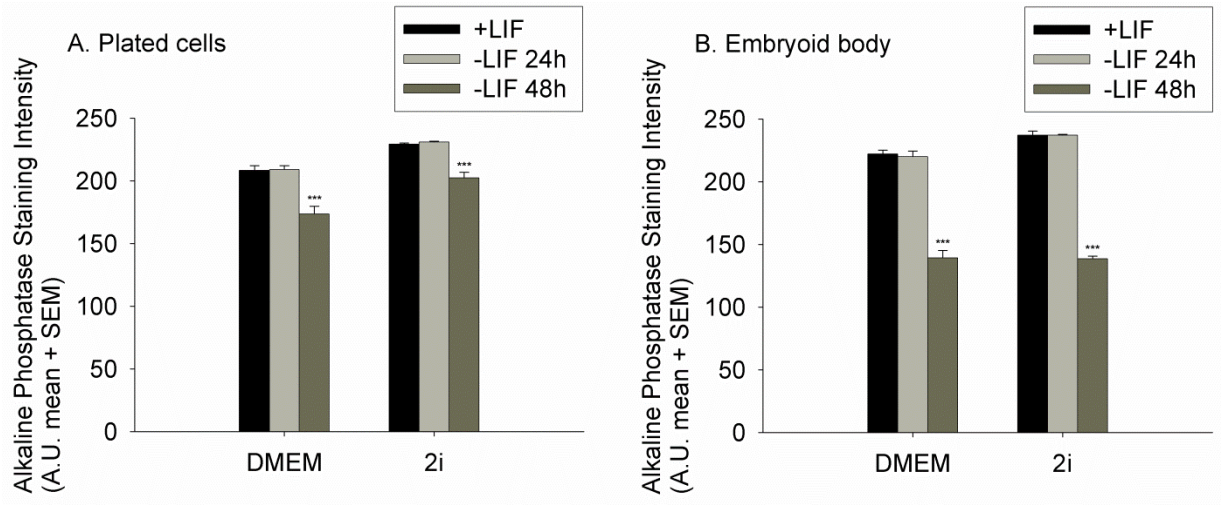

Figure 4-22 Alkaline phosphatase staining intensity in ESCs upon LIF removal.

The alkaline phosphatase staining intensity was measured in ESCs previously cultured in DMEM or 2i for over 10 passages prior to the exposure to DMEM minus LIF for 24 h and 48 h: (A) plated cells and (B) EBs. Plated and EB ESCs in DMEM and 2i were used as controls. Staining intensity was measured in arbitrary units and is shown as mean ± SEM of three independent replicates. At least 30 plated clumps and 5 EBs were analysed per treatment per replicate. Statistically significant differences are indicated by asterisks: $p<0.001$ = ***.

4.3.6. The increase in heterogeneity of 5meC levels in ESCs upon LIF removal

Scatter plots of the intensity measurements 5meC and 5hmC in ESCs (Figure 4-23 and Figure 4-24 showed that the removal of LIF for 24 h increased the heterogeneity of 5meC levels in plated ESCs, and the effect was more profound in ESCs previously cultured in DMEM ($p<0.001$). LIF removal in EB formation had less effect on the heterogeneity of 5meC levels in ESC, and the effect was even less in EB ESCs previously cultured in 2i media. LIF removal had little effect on the heterogeneity of 5hmC in either plated or EB ESCs, especially in ESCs previously cultured in DMEM. ESCs previously cultured in 2i had reduced 5hmC levels and this was associated with reduced 5hmC heterogeneity ($p<0.001$).

Immunolocalisation was performed to investigate the change in 5meC and 5hmC localisation in ESCs 24 h after LIF removal. ESCs were cultured in either DMEM or 2i for over 10 passages and transferred to DMEM minus LIF in culture media that supports the formation of plated cells or EBs. After 24 h exposure to DMEM minus LIF, the cells were stained for 5meC and 5hmC and images were taken with the confocal microscope. Confocal microscopy of plated ESCs showed that more 5meC was localised in the nuclei located in the middle of cell clumps on ESCs previously cultured in DMEM (Figure 4-25). 5meC in plated ESCs previously cultured in 2i media changed from being localised within foci to a generalised localisation across the nucleoplasm. There was no observable change in the localisation of 5hmC in all conditions. Localisation of 5meC in EB ESCs showed that EBs in DMEM showed a similar localisation pattern 24 h after LIF removal (Figure 4-26). A shift in 5meC localisation pattern after 24 h LIF removal was shown in EBs previously cultured in 2i, from being localised within foci to a generalised staining across the nucleoplasm. The 5hmC expression patterns were similar between EBs after 24 h LIF removal and their controls in both DMEM and 2i (Figure 4-27).

The number of DAPI-intense staining foci in the ESCs without LIF was counted to observe the effect of LIF removal on the chromatin structure of ESCs. The results showed a similar pattern to the control ESCs, in which changing culture conditions to those favour the formation of EBs reduced the number of DAPI foci per nucleus of ESCs both in DMEM and 2i media (Figure 4-28). Statistical analysis showed that the ESCs without LIF had a reduced number DAPI foci per nucleus compared to the control ESCs ($p<0.001$). To observe the correlation between the DAPI foci and 5meC, the proportion of DAPI foci co-stained with anti-5meC was counted per nucleus of ESCs. Results showed the ESCs without LIF had similar proportion of DAPI foci co-stained with anti-5meC to the control ESCs ($p > 0.05$), in which the ESCs in 2i had a higher proportion of DAPI foci co-stained with anti-5meC per nucleus compared to the ESCs in DMEM (Figure 4-29). Similar to the control ESCs, changing to EB culture did not change the proportion of DAPI foci co-stained with anti-5meC per nucleus of ESCs.

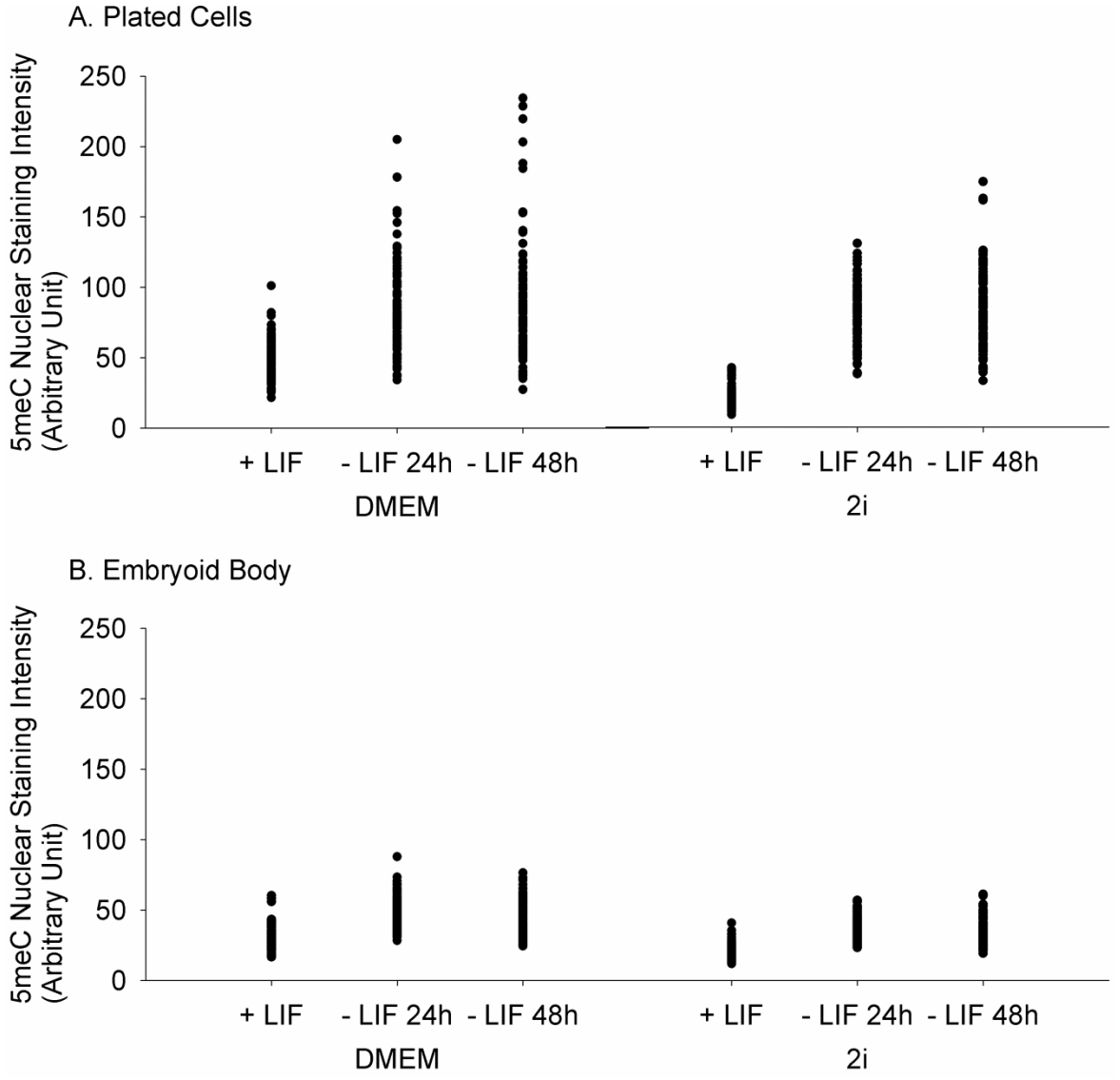

Figure 4-23 Scatter plots of 5meC nuclear staining intensity in ESCs cultured in DMEM and 2i media upon LIF removal.

The 5meC nuclear staining intensity was measured in ESCs previously cultured in DMEM or 2i for over 10 passages prior to exposure to DMEM minus LIF for 24 h and 48 h: (A) plated cells and (B) EBs. Plated and EB ESCs in DMEM and 2i were used as controls. Staining intensity was measured in arbitrary units for three independent replicates. At least 50 nuclei were analysed per treatment per replicate in plated cells and 100 nuclei were analysed per treatment per replicate in EBs.

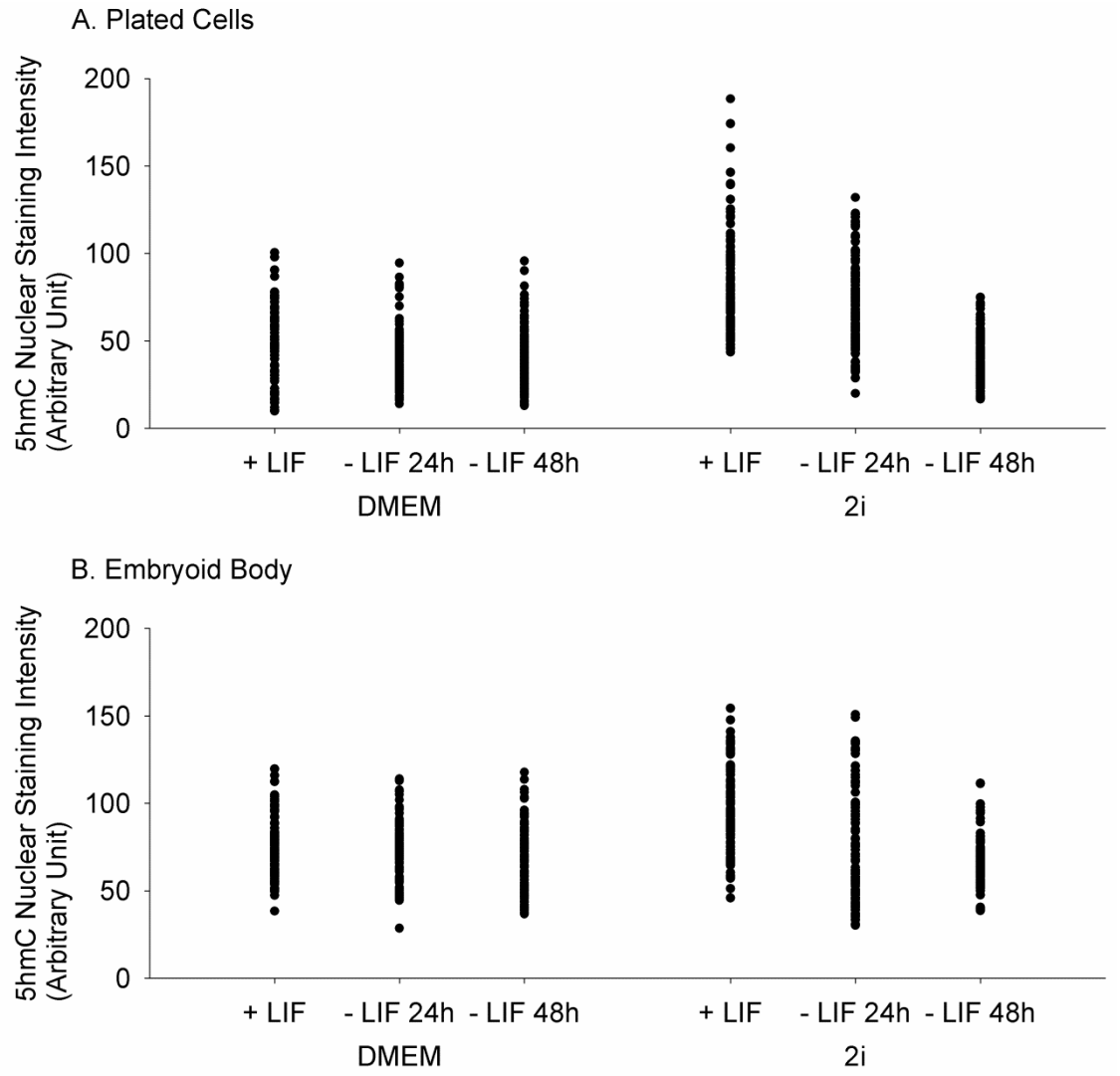

Figure 4-24 Scatter plots of 5hmC nuclear staining intensity in ESCs cultured in DMEM and 2i media upon LIF removal.

The 5hmC nuclear staining intensity was measured in ESCs previously cultured in DMEM or 2i for over 10 passages prior to exposure to DMEM minus LIF for 24 h and 48 h: (A) plated cells and (B) EBs. Plated and EB ESCs in DMEM and 2i were used as controls. Staining intensity was measured in arbitrary units for three independent replicates. At least 50 nuclei were analysed per treatment per replicate in plated cells and 100 nuclei were analysed per treatment per replicate in EBs.

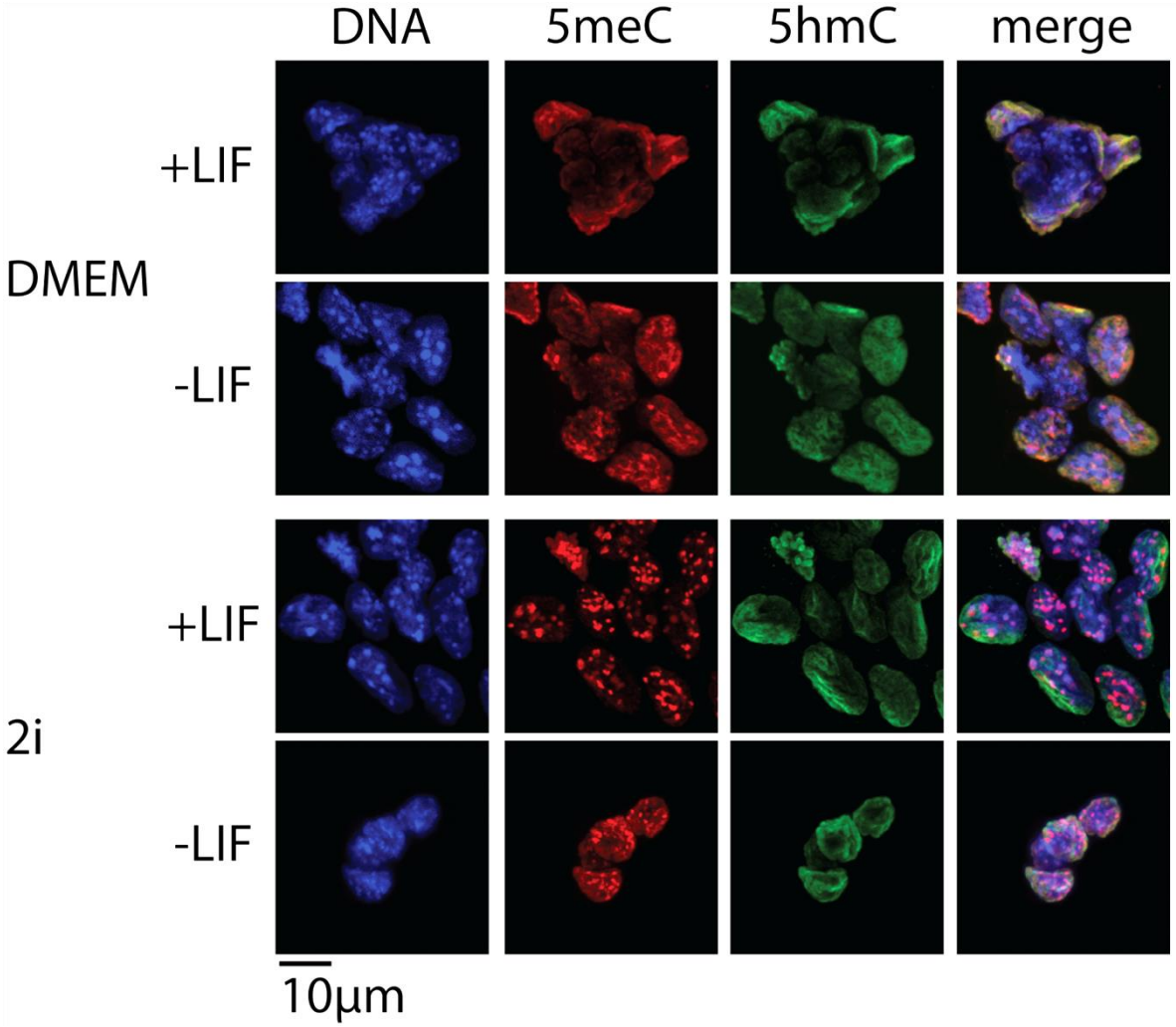

Figure 4-25 Immunolocalisation of 5meC and 5hmC expression in plated ESCs upon LIF removal.

Plated ESCs were grown in either DMEM or 2i media for over 10 passages prior to exposure to DMEM minus LIF. After 24 h in DMEM minus LIF, they were co-stained with anti-5meC and anti-5hmC and counterstained with DAPI. Plated ESCs cultured in DMEM and 2i media were used as controls. High resolution images were taken using a confocal microscope. Confocal microscopy on ESCs without LIF in DMEM showed more 5meC localised in the nuclei located in the middle of the clumps. Differentiated ESCs in 2i media showed a shift in localisation of 5meC, from a predominant association with heterochromatic foci to a generalised staining across the nucleoplasm. The 5hmC localisation was similar in all culture conditions. Images are representative of three independent replicates. Scale bar = 10 µm.

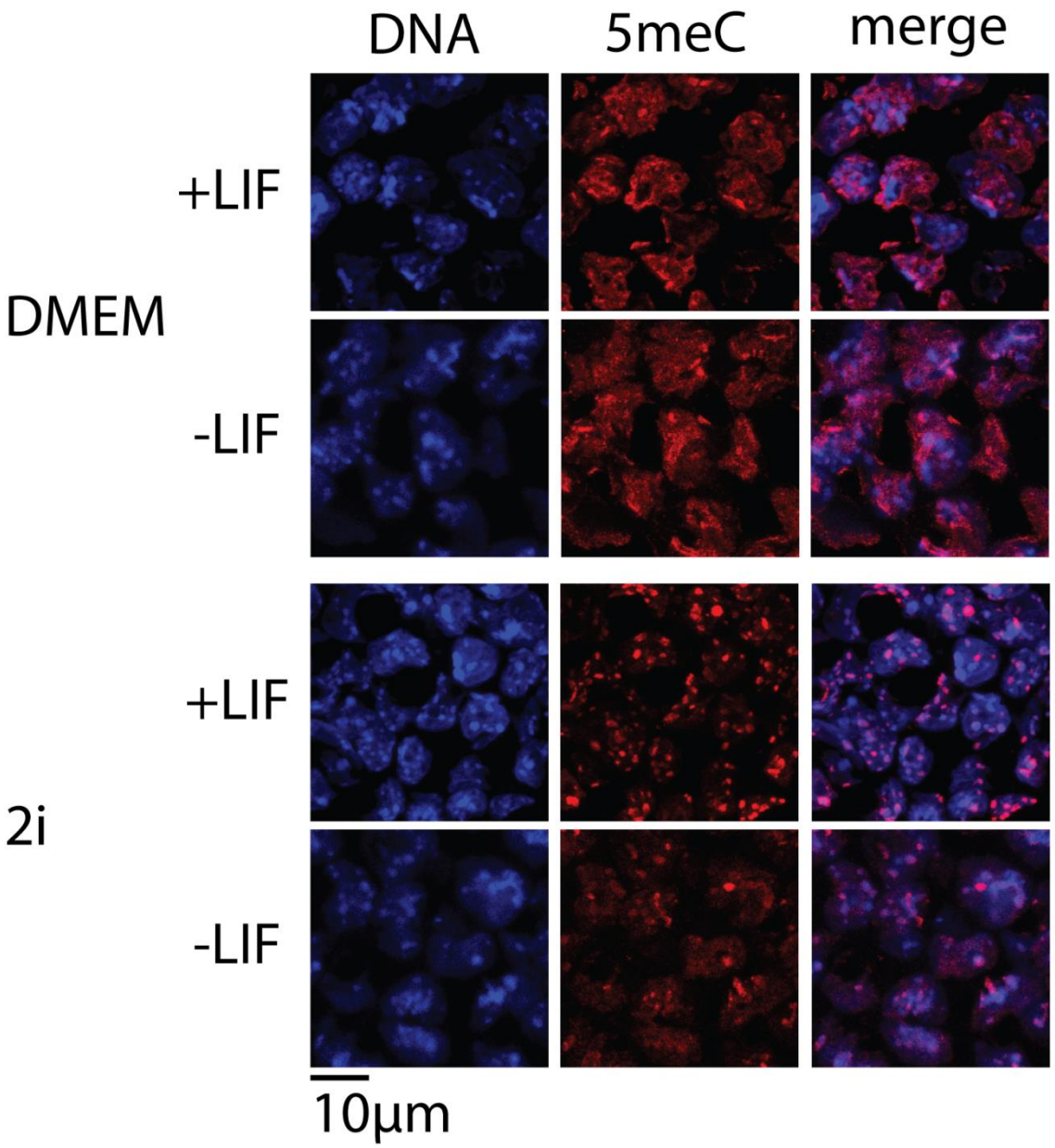

Figure 4-26 Immunolocalisation of 5meC expression in EB ESCs upon LIF removal.

ESCs were grown in either DMEM or 2i media for over 10 passages prior to exposure to DMEM minus LIF with growth conditions that support the formation of EBs. After 24 h in DMEM minus LIF, they were processed into EB sections and stained with anti-5meC and counterstained with DAPI. EB ESCs cultured in DMEM and 2i media were used as controls. High resolution images were taken using a confocal microscope. Confocal microscopy showed similar 5meC localisation in ESCs cultured in DMEM before and after LIF removal. Differentiated EB ESCs in 2i media showed a shift in localisation of 5meC, from a predominant association with heterochromatic foci to a generalised staining across the nucleoplasm. Images are representative of three independent replicates. Scale bar = 10 µm.

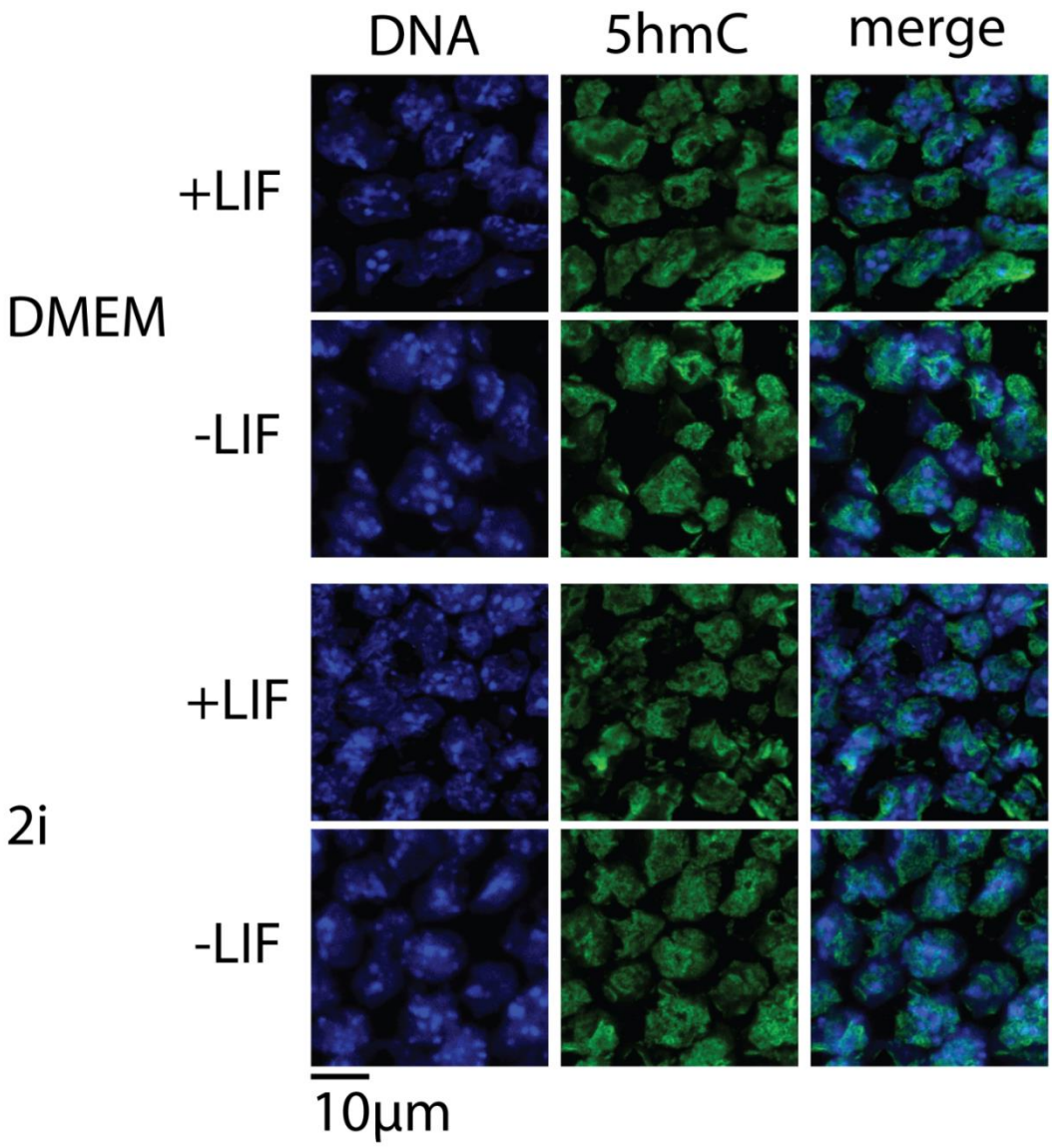

Figure 4-27 Immunolocalisation of 5hmC expression in EB ESCs upon LIF removal.

ESCs were grown in either DMEM or 2i media for over 10 passages prior to exposure to DMEM minus LIF with growth conditions that support the formation of EBs. After 24 h in DMEM minus LIF, they were processed into EB sections and stained with anti-5hmC and counterstained with DAPI. EB ESCs cultured in DMEM and 2i media were used as controls. High resolution images were taken using a confocal microscope. Confocal microscopy showed similar 5hmC localisation in ESCs in all conditions. Images are representative of three independent replicates. Scale bar = 10 µm.

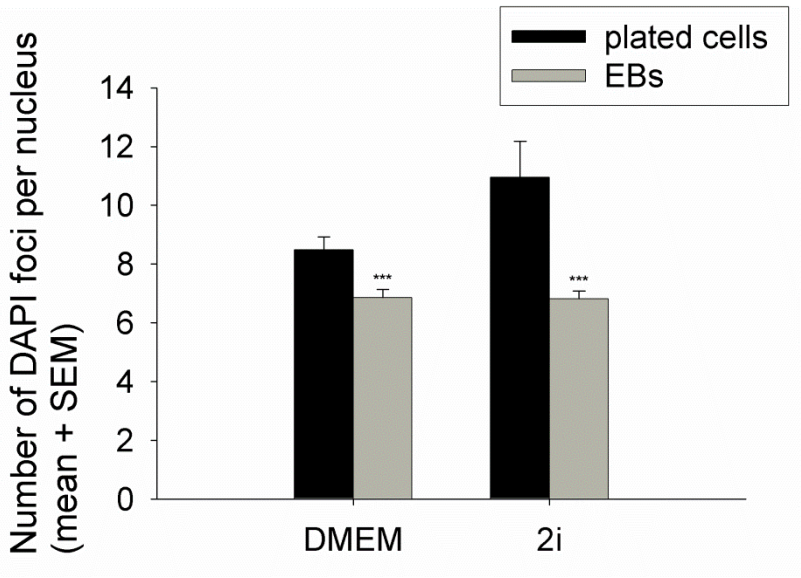

Figure 4-28 Average number of DAPI foci per nucleus of ESCs upon LIF removal.

The average number of DAPI foci per nucleus of plated ESCs and EB ESCs previously cultured in DMEM or 2i media for over 10 passages prior to exposure to DMEM minus LIF for 24 h. Number of DAPI foci are shown as mean ± SEM of three independent replicates. At least 20 nuclei were analysed per treatment per replicate. Statistically significant differences are indicated by asterisks: $p<0.001$ = ***.

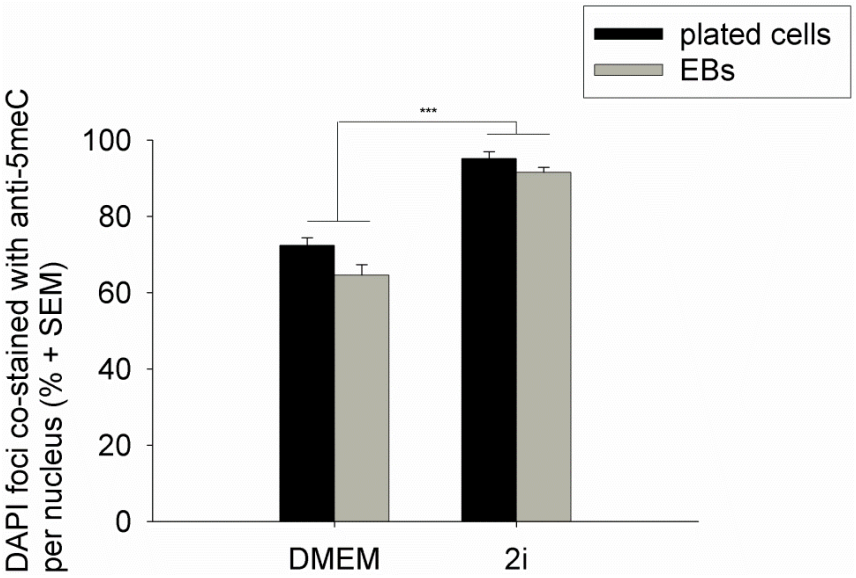

Figure 4-29 Proportion of DAPI foci co-stained with anti-5meC per nucleus of ESCs upon LIF removal.

The average proportion of DAPI foci co-stained with anti-5meC per nucleus of plated ESCs and EB ESCs previously cultured in DMEM and 2i media prior to exposure to DMEM minus LIF for 24 h. Proportion of co-stained foci are shown as % mean ± SEM of three independent replicates. At least 20 nuclei were analysed per treatment per replicate. Statistically significant differences are indicated by asterisks: $p<0.001$ = ***.

4.4. DISCUSSION

This chapter showed the first analysis of 5meC and 5hmC levels using antigen retrieval methods that incorporate both acid-induced denaturation of chromatin and trypsin digestion. These methods were used to investigate the effect of several conditions on the levels and localisation of 5meC and 5hmC in ESCs, as well as on the pluripotency status of the cells. The antigen retrieval processes that were incorporated into this study confirmed that the loss of methylation in ESCs cultured in 2i media in (Leitch et al., 2013) was not due to an increase in antigen masking.

The 5meC levels in ESCs were dynamic and associated with the pluripotency of the cells. Alkaline phosphatase is a known marker for pluripotent ESCs (Pease et al., 1990), and the increase in alkaline phosphatase activity in ESCs cultured in 2i media accompanied by reduced 5meC levels in ESCs indicating an association between methylation levels and pluripotency of ESCs. Removing support for the pluripotency of ESCs by removing LIF from the media increased the 5meC levels in ESCs, further confirming the association of methylation levels with pluripotency. However, the increase in methylation levels occurred prior to the change in morphology or the reduction in alkaline phosphatase activity, indicating that changes in global methylation is a very early changing in the cells ontological state. The observed low alkaline phosphatase activities at passage 4 for both plated cells and EBs cultured in both media were possibly due to the cells still adapting to the culture conditions. These changes in alkaline phosphatase activities were not correlated with the cell numbers nor the methylation status of the cells. Different cell strains might produce different results.

An increase in 5hmC accompanied the loss of 5meC in 2i media culture, and a loss of 5hmC accompanied the increase in 5meC in LIF removal. The negative correlation between 5meC and 5hmC may be consistent with conversion between these two forms of DNA modification

as to the pluripotency of ESCs changes. 5hmC has been known to be enriched in embryonic contexts and correlates with the pluripotent state of cells (Ruzov et al., 2011). It is expected that 5hmC levels associate with the pluripotency of ESCs, and negatively correlate with the 5meC levels of ESCs.

5meC and 5hmC staining localisation in plated ESCs were found to be heterogeneous due to interactions with neighbouring cells. A general pattern of increased cell interactions with lower levels of methylation appear in both media, and this may account for the lower levels and reduced heterogeneity in EBs. The 5hmC localisation in plated ESCs followed a similar pattern to 5meC localisation in plated ESCs. One study claimed that ESCs display heterogeneity at the molecular level due to a combination of intrinsic noise, coherent cellular states, and epigenetic regulation (Singer et al., 2014). Along with the heterogeneity at the molecular level, embryonic stem cells also display a dynamic DNA methylation pattern during culture (Tsai et al., 2012). Studies have found that the heterogeneous cell subpopulations can be determined by the 5meC/5hmC state of the subpopulations (Tajbakhsh et al., 2015, Shao et al., 2014). Taken together, the heterogeneity of DNA methylation in plated ESCs is correlated with the heterogeneity of the cell populations at the molecular level. It was further explained that DNA methylation determines the stochastic switching between cell states, and thus contributes to the heterogeneity of ESCs (Singer et al., 2014).

The reduced levels of staining in 2i media was associated with increased pattern of localised staining in a number of discrete foci. These generally corresponded with DAPI intense foci. Such DAPI foci are normally associated with the heterochromatin in the nucleus (Çelik et al., 2014) and the results may indicate an increased level recruitment of the 5meC marked genomic fraction to heterochromatin in conditions that showed reduced 5meC. The increased proportion of the DAPI foci that were co-stained with anti-5meC in ESCs cultured in 2i media suggested

that 2i media changes the localisation of 5meC to being predominantly associated with the heterochromatic foci. The same number of DAPI foci per nucleus in DMEM and 2i suggested that culture in 2i media does not change the chromatin structure of the cells, but changes the levels of 5meC modification within the chromatin of ESCs. The lower number of DAPI foci co-stained with anti-5meC in DMEM may be caused by the lower 5meC localisation in the chromatin of ESCs cultured in DMEM, or by the higher 5meC levels across the nucleoplasm which reduces the visibility of 5meC in the chromatin of ESCs.

It was found that 2i reduces the heterogeneity of ESCs at the molecular level through the inhibition of MEK and GSK3β (Marks et al., 2012, Wray et al., 2010). Further, 2i media was found to reduce the gene variability in ESCs either by eliminating the bimodality of cell states or increasing the expression of the genes, and a relatively hypomethylated DNA is needed to maintain this state (Singer et al., 2014, Marks et al., 2012, Leitch et al., 2013, Habibi et al., 2013, Ficz et al., 2013). Taken together, 2i media reduces the methylation levels and heterogeneity in ESCs leading to less heterogeneity of ESCs at the molecular level.

The progressive shifts of 5meC pattern in ESCs previously cultured in 2i media, from the focal pattern to the diffused staining across nucleoplasm within 24 h of LIF removal, suggested that the 5meC staining within the euchromatin is associated with the loss of pluripotency in ESCs. The 5meC localisation pattern in 2i media is closer to the 5meC localisation in the inner cell mass (ICM) of embryos, which is located in a few heterochromatic foci (Li and O'Neill, 2013b). This might also explain the reduced 5meC heterogeneity found in EB ESCs, and that the 5meC in EBs were less heterogeneous upon LIF removal. During the morulae stage of embryo development, where the cells are exposed to different positional information for the first time, it was found that the cells exposed to the outside environment are generally more methylated than the cells located inside (Li and O'Neill, 2013b). Changing the culture to EB formation also

provides similar positional information, where some cells are exposed to the environment while some cells are surrounded by other cells. Taken together, positional information is possibly one of the determinants of the methylation state of the cells.

Heterochromatic foci formation in 2i media is possibly caused by the interactions between the maintenance methylation enzyme DNMT1 with histone deacethylase (HDAC) protein complexes. The deacetylation of DNA by HDAC1 creates a higher structure chromatin, preventing the recruitment of transcription factors to the DNA (Pollard et al., 1999). DNMT1 also interacts with HDAC2 in the late S-phase to form a transcriptionally repressive heterochromatin after DNA synthesis (Grunstein, 1998). The complex formed between DNMT1, HDAC2, DMAP1, and TSG101 is also known to possess tumour suppressor activity (Watanabe et al., 1998). Taken together, the interactions between DNMT1, HDAC1, HDAC2, and other associated proteins form a stable repression mechanism in the heterochromatin which prevents the formation of tumours in the cells. Therefore, the observed 5meC pattern that is associated with the heterochromatic foci in 2i media suggests mechanisms by which ESCs maintain stable gene expression to prevent tumour formation while keeping the pluripotency genes active.

LIF removal reduced the number of DAPI foci per nucleus of ESCs without changing the proportion of the DAPI foci co-stained with anti-5meC. This means that LIF removal induces the changes in the chromatin structures of ESCs, which may explain the gradual changes in 5meC localisation in ESCs cultured in 2i media upon LIF removal. As discussed earlier, the function of the formation of higher chromatin structures in ESCs is to create a stable suppression mechanism that prevents tumour formation. The reduced number of this chromatin structure in differentiated cells might indicate that this repression mechanism is no longer needed as the cells start to undergo LIF removal and become more genetically stable.

Therefore, the fact that the 5meC localisation to the heterochromatic foci is less observable in ESCs cultured in DMEM might also indicate that the cells are already losing pluripotency, and thus do not require the tumour suppressor activity that the ESCs in 2i media possess.

Using the newly validated antigen retrieval methods, the experiments showed that 5meC and 5hmC levels in ESCs are dynamic and highly responsive to the culture conditions and positional information received by the cells. This chapter also shows that the loss of 5meC in 2i media was accompanied by increased association of the 5meC to the presumptive heterochromatic fraction of chromatin. The unexpectedly rapid change in 5meC and 5hmC upon the removal of LIF indicate that these changes are very early responses to changes in the cells pluripotency state. These results lead to questions regarding the expression of several proteins that play important roles in maintaining CpG methylation and hydroxymethylation in ESCs.

5. CHAPTER 5: ANALYSIS OF METHYLATION AND PLURIPOTENCY PROTEIN EXPRESSION IN ESCs

5.1. INTRODUCTION

The previous chapter showed that the changes in DNA methylation upon LIF removal occurred prior to observable morphological signs of loss of pluripotency or a change in alkaline phosphatase activity. This suggests that the changes in the methylation state of ESCs are a very early change preceding the loss of pluripotency in ESC. There are several methylation enzymes involved in establishing and maintaining the global DNA methylation pattern in the mammalian genome. These enzymes arer members of the DNA methyltransferase (DNMT) family, which consists of three active members with a conserved catalytic domain: DNMT1, DNMT3A, and DNMT3B (Auclair and Weber, 2012). Besides the methylation enzymes, there is a demethylation enzyme class of which TET1 is the most prominent, which is involved in the function of 5hmC and its derivates, which may form intermediates in a demethylation pathway (Auclair and Weber, 2012, Ito et al., 2010). 2i media is reported to cause changes of expression of DNA methylation related proteins, including the reduction of DNMT3A and DNMT3B, while the maintenance DNMT1 remains unchanged (Leitch et al., 2013).

In this chapter, the methylation enzymes of ESCs were assessed in several culture conditions that affect the global methylation of ESCs. This included the global hypomethylation of ESCs induced by culture in 2i media and the removal of LIF for 24 h. Proteins assessed included DNMT1, DNMT3A, DNMT3B, and TET1, as the enzymes that are involved in the methylation and demethylation of the mammalian genome. The expression of OCT4 in ESCs was measured to assess the pluripotency of ESCs in all culture conditions, as OCT4 is one of the major regulators of ESC pluripotency (Nichols et al., 1998). EB ESCs were the focus of these assessments due to their lower and less heterogeneous global 5meC levels. The effects of the

removal of LIF were assessed at 24 h after LIF removal, as the changes in DNA methylation occurred within this time frame. The results will confirm the connection between the DNA methylation of ESCs and the regulators of ESC pluripotency.

5.2. MATERIAL AND METHODS

5.2.1. Cell Culture

D3-ESCs were cultured in DMEM (DMEM, serum plus LIF) and 2i media in the Human Reproduction Unit. See Section 2.1.2 for DMEM and H2i media details. Cells were cultured at 37 °C with 5% CO_2 and 5% O_2 in air. After 10 passages, cells were prepared as embryoid bodies in both media. See Section 2.1.6 for details of embryoid body culture preparation. Cells were cultured for 24h prior to the fixation.

5.2.2. Removal of LIF

D3-ESCs were cultured for 10 passages in the presence of LIF prior to the transfer to DMEM minus LIF. Cells were cultured as embryoid bodies in DMEM minus LIF at 37 °C with 5% CO_2 and 5% O_2 in air. Cells were fixed at 24 h upon culture in DMEM minus LIF, and assessed for OCT4, TET1, DNMT1, DNMT3A, and DNMT3B. ESCs in DMEM and 2i media were used as controls.

5.2.3. Antibodies

Primary antibodies used were: (i) rabbit anti-OCT4 (1:200) (Abcam, Cat. No. ab19857); (ii) rabbit anti-TET1 (1:100) (Millipore, Cat. No. 09-872); (iii) rabbit anti-DNMT1 (1:100) (Abcam, Cat. No. ab19905); (iv) mouse anti-DNMT3A (1:100) (Imgenex, Cat. No. IMG-268A); and (v) mouse anti-DNMT3B (1:100) (Imgenex, Cat. No. IMG-184A). Non-immune control antibodies were mouse IgG (Sigma, M7894) and rabbit IgG (Sigma, I5006). The secondary antibodies used to detect the binding of the primary antibodies were: (i) sheep anti-mouse IgG conjugated with Fluorescein Isothiocyanate (FITC) (Sigma, Cat. No. F6257); and (ii) goat anti-rabbit IgG conjugated with FITC (Sigma, Cat. No. F1262).

5.2.4. Antigenic Retrieval

For OCT4 staining EBs were treated with HCl for 10 min, followed by trypsin (0.4%) for 10–15 s. For TET1 staining EBs were treated with HCl for 10 min. DNMT1, DNMT3A, and DNMT3B staining were performed without acid denaturation and trypsin treatment.

5.2.5. Western blot analysis

Western blot analyses were performed by Xing Jin from the Human Reproduction Unit. The D3-ESCs were harvested ($2x10^6$ cells/ml) and the proteins were extracted. The protein concentration was measured by BioPhotometer (Eppendof) and was calculated with the "A280 and Warburg-Christian Methods". 20 μg of protein was tested for each treatment. Proteins were denatured for 5 min at 95 °C in a water bath. Proteins were separated on 12.5% BioRad Pre-stack gel (15 wells) and transferred onto Trans-Blot Turbo PVDF (BioRad). Blocking was performed in 2% skim milk in 0.1% DPBT for 1 h at RT. Cells were incubated with the primary antibody overnight at 4 °C. Primary antibodies used were mouse anti-DNMT3B IgG (1:500) (2ug/mL) (Imgenex, Cat. No. IMG-184A); mouse anti-DNMT3A IgG (1:500) (Imgenex, Cat. No. IMG-268A); rabbit anti-DNMT1 IgG (1:500) (Abcam, Cat. No. ab19905); and rabbit anti-OCT4 IgG (1:500) (Abcam,Cat. No. ab19857). Detection of the housekeeping gene was performed with rabbit anti β-tubulin HRP-conjugated IgG (Abcam, Cat. No. ab21058) for 1 h at RT. Secondary antibodies were goat anti-mouse HRP conjugated IgG (1:5000) (Sigma, Cat. No. A2304) and goat anti-rabbit IgG conjugated with HRP (1:5000) (Sigma, Cat. No. A0545). Chemiluminescence was performed with the Laser4000 system.

5.3. RESULTS

5.3.1. The effect of culture conditions on OCT4 expression in ESC cells

Validation of the pluripotency of ESCs was performed by immunostaining for OCT4, in addition to the alkaline phosphatase assay. ESCs were cultured in DMEM and 2i for more than 10 passages before being transferred to DMEM minus LIF for 24 h. ESCs cultured in DMEM and 2i were used as controls. ESCs in all culture conditions were stained for OCT4 to observe any changes in the levels of OCT4 in accordance with the culture conditions. Co-staining of OCT4 and 5meC from our lab showed that acid and trypsin treatment did not reduce the OCT4 signal in immunofluorescence (data not shown). Therefore, OCT4 staining in this study was performed using acid and trypsin treatment for consistency of the protocols. Fluorescence microscopy showed similar OCT4 staining intensity in all culture conditions (Figure 5-1). The alkaline phosphatase assay showed higher alkaline phosphatase activity in EB ESCs cultured in 2i media compared to EB ESCs in DMEM, and there was no reduction in alkaline phosphatase activity within 24 h of LIF removal (Figure 5-2). The results were confirmed by the staining intensity measurement of OCT4 in EB ESCs (Figure 5-3) and the western blot analysis performed by Xing Jin from the Human Reproduction Unit (Figure 5-4).

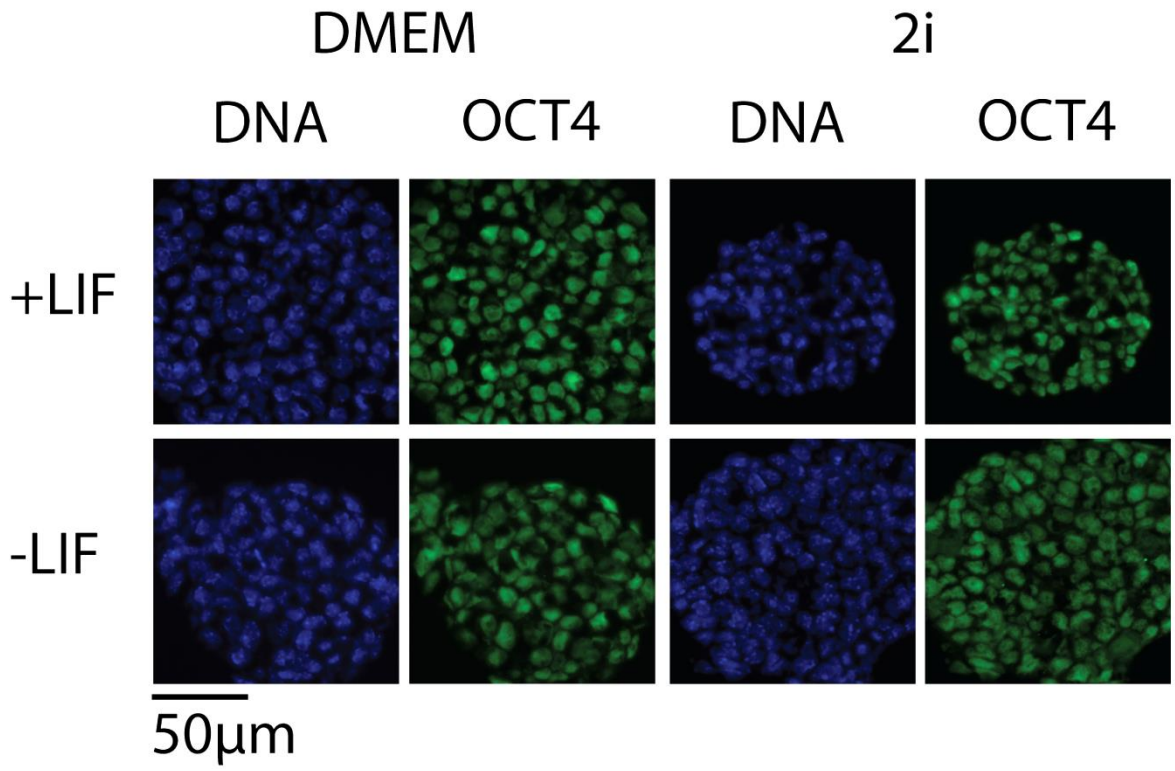

Figure 5-1 Immunostaining of OCT4 in EB ESCs.

ESCs were grown in either DMEM or 2i media for over 10 passages prior to transfer to DMEM minus LIF with growth condition that support the formation of EBs. EB sections were stained with anti-OCT4 and counterstained with DAPI. EB ESCs in DMEM and 2i were used as controls. Immunofluorescence microscopy showed similar levels of OCT4 in EB ESCs in all culture conditions. Images are representative of three independent replicates. Scale bar = 50 µm.

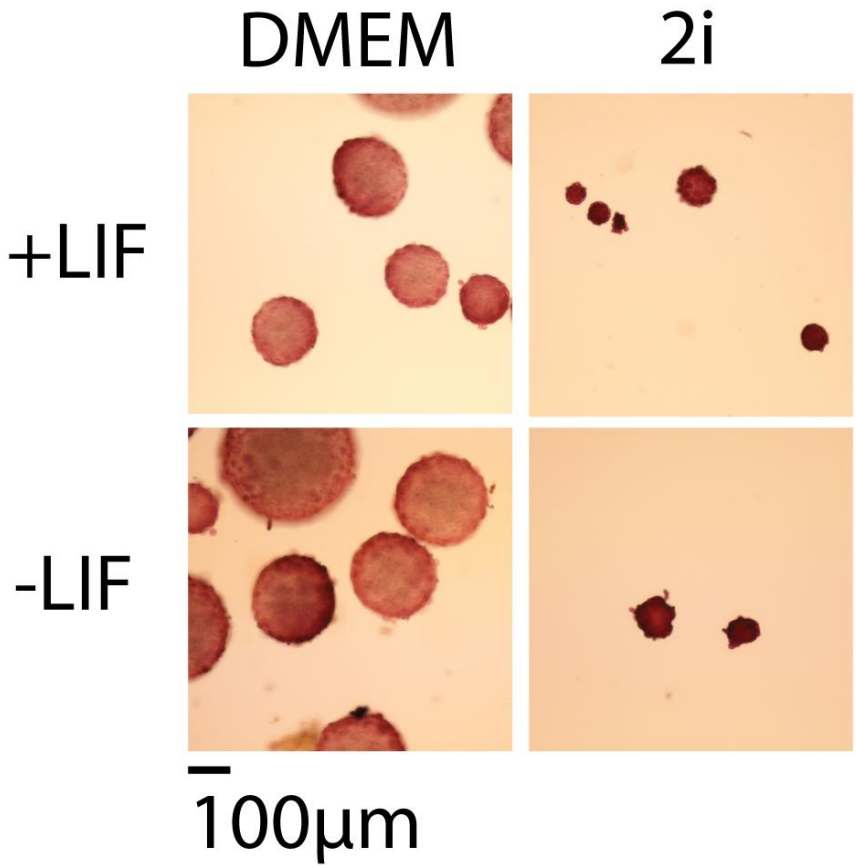

Figure 5-2 Alkaline phosphatase activity in ESCs upon LIF removal.

ESCs were previously cultured in 2i or DMEM for over 10 passages prior to exposure to DMEM minus LIF and were cultured in the form of EBs. They were assayed for alkaline phosphatase activity 24 h after LIF removal. EBs ESCs cultured in DMEM and 2i were used as controls. The bright-field images at 24 h after LIF removal showed similar alkaline phosphatase activities between the cells with LIF and without LIF,with higher activities in 2i media. Images are representative of three independent replicates. Scale bar = 100 µm.

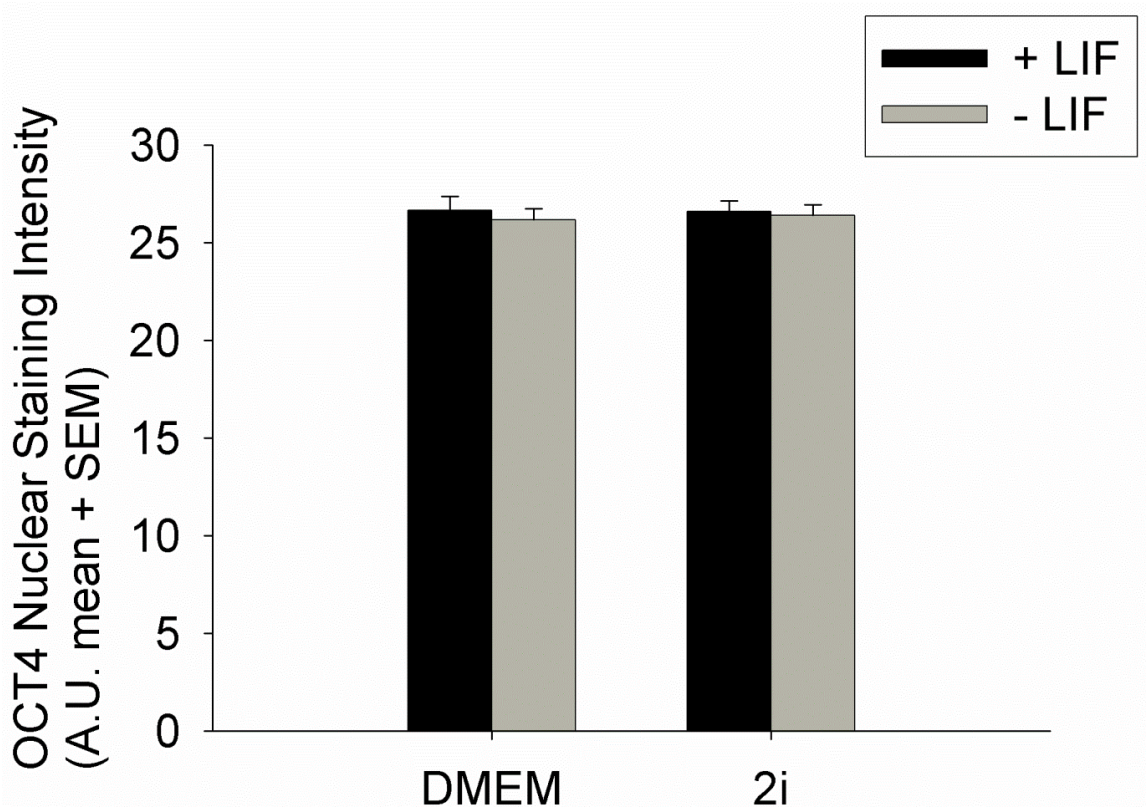

Figure 5-3 OCT4 nuclear staining intensity in ESCs.

OCT4 nuclear staining intensity was measured in ESC EBs previously cultured in DMEM or 2i for over 10 passages prior to exposure to DMEM minus LIF for 24 h. EB ESCs cultured in DMEM and 2i were used as controls. Staining intensity was measured in arbitrary units and is shown as mean ± SEM of three independent replicates. At least 100 nuclei were analysed per treatment per replicate.

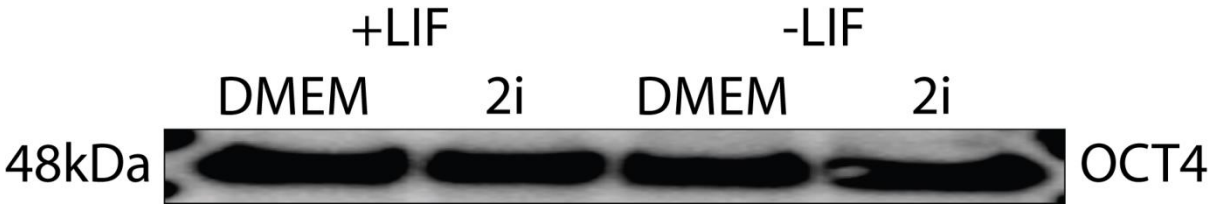

Figure 5-4 The western blot analysis of OCT4 in ESCs.

ESCs were grown in either DMEM of 2i media for over 10 passages prior to transfer to DMEM minus LIF. Cell proteins were collected and western blot analysis for DNMT1 was performed. ESCs in DMEM and 2i were used as controls. Western blot analysis showed the expected 48 kDa band for OCT4. There were similar OCT4 levels in all culture conditions. Images are representative of three independent replicates. Western blot analysis was performed by Xing Jin from Human Reproduction Unit.

5.3.2. The effect of culture conditions on DNMT expression

Immunostaining for DNMT1, DNMT3A, and DNMT3B were performed to investigate whether changes in global 5meC levels in ESCs were accompanied by changes in the expression level of the enzymes responsible for CpG methylation. Fluorescence microscopy of DNMT1 showed similar expression of DNMT1 in ESCs across all culture conditions (Figure 5-5), and this was confirmed by the DNMT1 staining intensity measurement (Figure 5-6). Western blot analysis showed multiple bands for DNMT1 including the expected 183 kDa band and the major 75kDa band; DNMT1 levels were similar in all culture conditions (Figure 5-7).

The DNMT3A immunostaining microscopy and intensity measurement showed it was lower in ESCs cultured in 2i media compared to those in DMEM (Figure 5-8 and Figure 5-9). LIF removal increased DNMT3A expression in ESCs, and the level was higher in ESCs previously cultured in DMEM. Western blot analysis showed a 75kDa band instead of the expected 120kDa band for DNMT3A (Figure 5-10). Moreover, this band was not observed in 2i media. The western blot results indicate that LIF removal increased DNMT3A expression, but the levels were similar between ESCs previously cultured in DMEM and 2i.

DNMT3B was lower in ESCs cultured in 2i media compared to those in DMEM (Figure 5-11 and Figure 5-12). LIF removal increased DNMT3B levels in ESCs previously cultured in either media. Western blot analysis showed the expected 116kDa band for DNMT3B (Figure 5-13). However, the DNMT3B band was not observed in 2i media. LIF removal increased the DNMT3B expression more than it increased DNMT3A, but the levels were similar between ESCs previously cultured in DMEM and 2i.

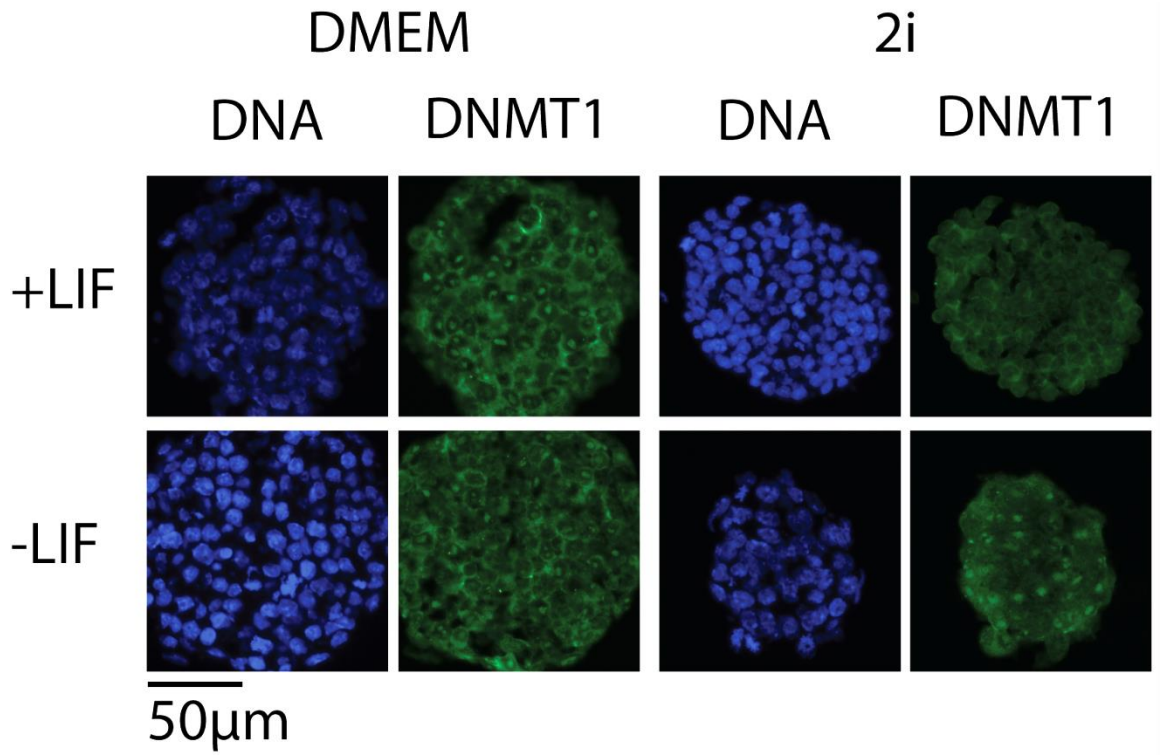

Figure 5-5 Immunostaining of DNMT1 in EB ESCs.

ESCs were grown in either DMEM or 2i media for over 10 passages prior to transfer to DMEM minus LIF with growth conditions that support the formation of EBs. EB sections were stained with anti-DNMT1 and counterstained with DAPI. EB ESCs in DMEM and 2i were used as controls. Immunofluorescence microscopy showed similar levels of DNMT1 in EB ESCs in all culture conditions. Images are representative of three independent replicates. Scale bar = 50 µm.

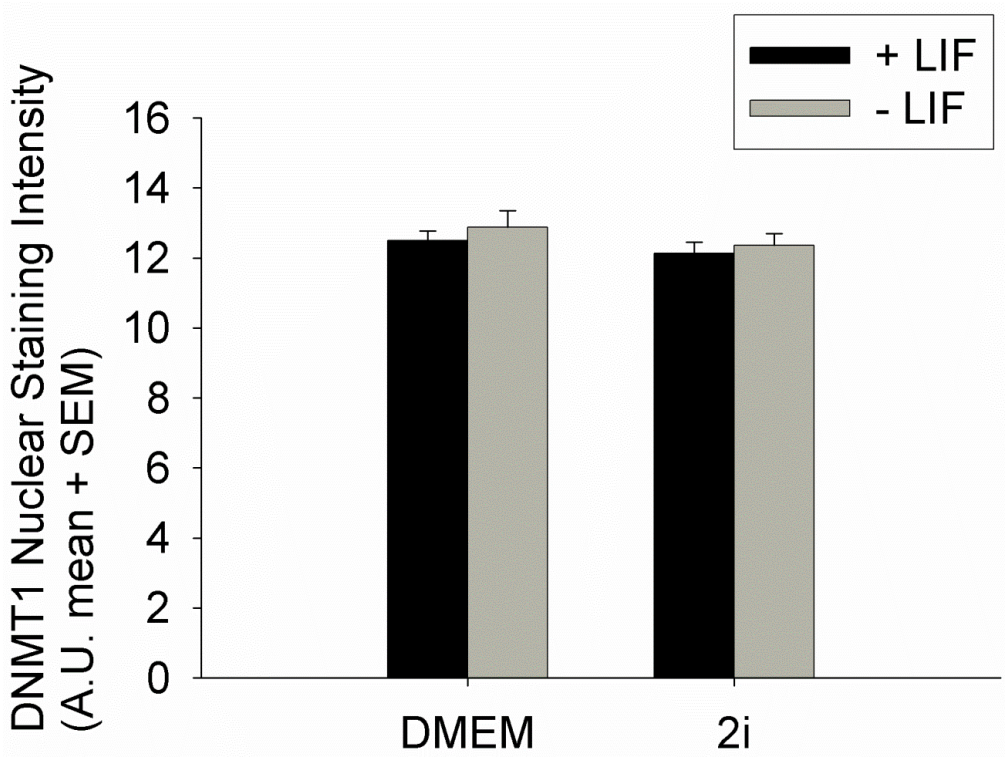

Figure 5-6 DNMT1 nuclear staining intensity in ESCs.

The DNMT1 nuclear staining intensity was measured in the ESC EBs previously cultured in DMEM or 2i for over 10 passages prior to exposure to DMEM minus LIF for 24 h. EB ESCs cultured in DMEM and 2i were used as controls. Staining intensity was measured in arbitrary units and is shown as mean ± SEM of three independent replicates. At least 100 nuclei were analysed per treatment per replicate.

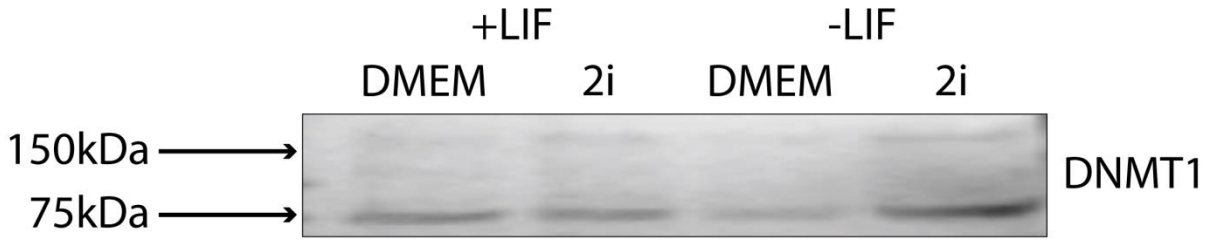

Figure 5-7 Western blot analysis of DNMT1 in ESCs.

ESCs were grown in either DMEM or 2i media for over 10 passages prior to transfer to DMEM minus LIF. Cell proteins were collected and western blot analysis for DNMT1 was performed. ESCs in DMEM and 2i were used as controls. Western blot analysis showed multiple bands for DNMT1 including the expected 183 kDa band and the major 75k Da band. There were similar DNMT1 levels in all culture conditions. Images are representative of three independent replicates. Western blot analysis was performed by Xing Jin from the Human Reproduction Unit.

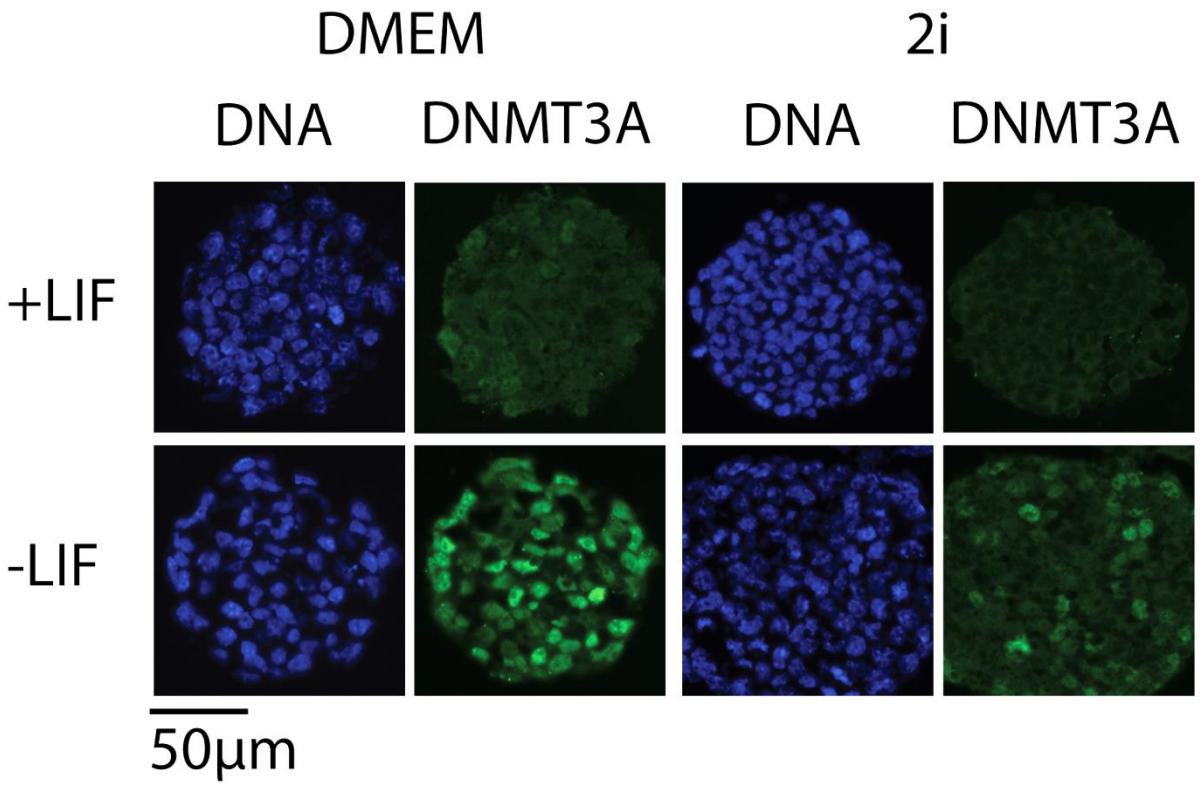

Figure 5-8 Immunostaining of DNMT3A in EB ESCs.

ESCs were grown in either DMEM or 2i media for over 10 passages prior to transfer to DMEM minus LIF with growth conditions that support the formation of EBs. EB sections were stained with anti-DNMT3A and counterstained with DAPI. EB ESCs in DMEM and 2i were used as controls. Immunofluorescence microscopy showed a low DNMT3A expression in EB ESCs cultured in 2i media. Induced differentiation increased the DNMT3A expression in ESCs in both media. Images are representative of three independent replicates. Scale bar = 50 µm.

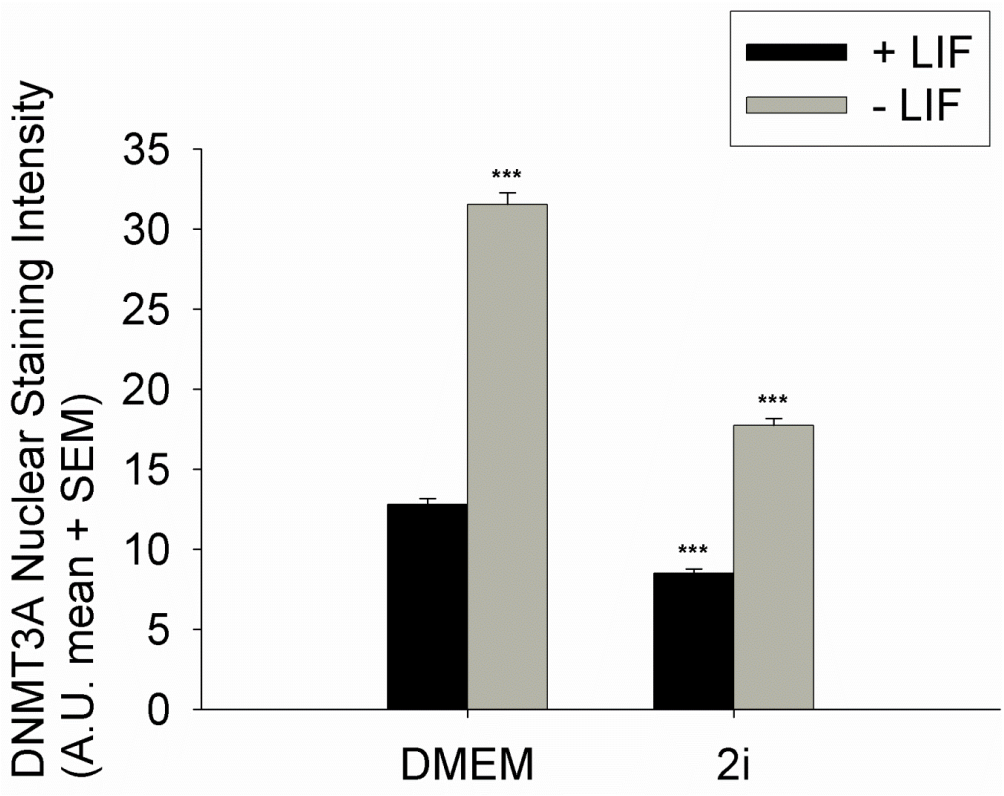

Figure 5-9 DNMT3A nuclear staining intensity in ESCs.

DNMT3A nuclear staining intensity was measured in ESC EBs previously cultured in DMEM or 2i for over 10 passages prior to exposure to DMEM minus LIF for 24 h. EB ESCs cultured in DMEM and 2i were used as controls. Staining intensity was measured in arbitrary units and is shown as mean ± SEM of three independent replicates. At least 100 nuclei were analysed per treatment per replicate. Statistically significant differences are indicated by asterisks: $p<0.001$ = ***.

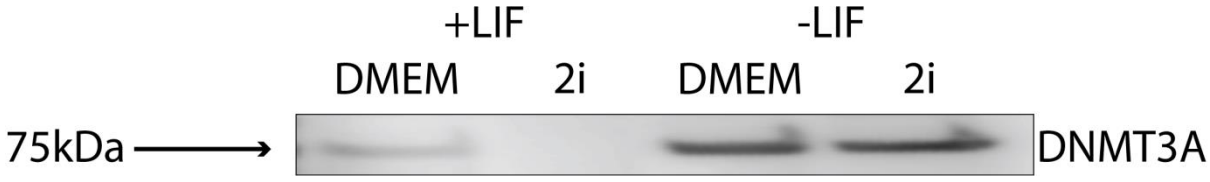

Figure 5-10 Western blot analysis of DNMT3A in ESCs.

ESCs were grown in either DMEM or 2i media for over 10 passages prior to transfer to DMEM minus LIF. Cell proteins were collected and western blot analysis for DNMT3A was performed. ESCs in DMEM and 2i were used as controls. Western blot analysis showed a 75 kDa band instead the expected 120 kDa band for DNMT3A. Culture in 2i media inhibited DNMT3A expression, and LIF removal increased DNMT3A expression. Images are representative of three independent replicates. Western blot analysis was performed by Xing Jin from the Human Reproduction Unit.

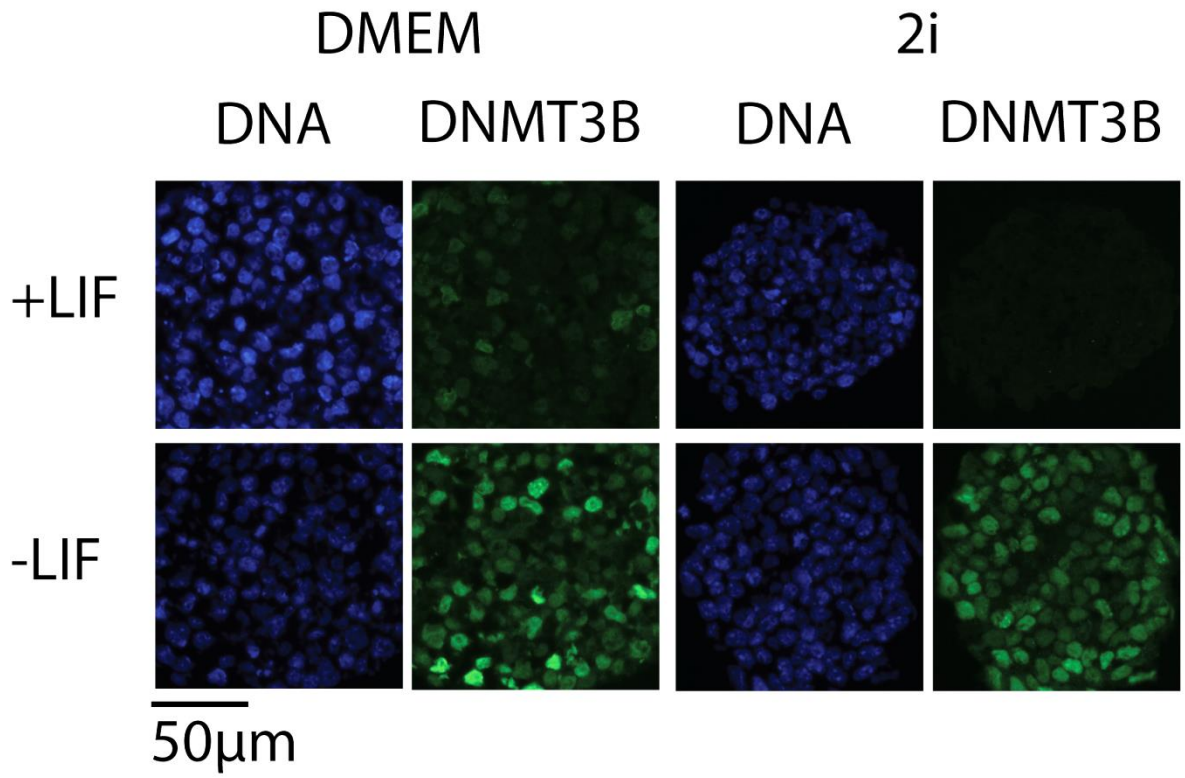

Figure 5-11 Immunostaining of DNMT3B in EB ESCs.

ESCs were grown in either DMEM or 2i media for over 10 passages prior to transfer to DMEM minus LIF with growth conditions that support the formation of EBs. EB sections were stained with anti-DNMT3B and counterstained with DAPI. EB ESCs in DMEM and 2i were used as controls. Immunofluorescence microscopy showed a low DNMT3B expression in EB ESCs cultured in 2i media. Induced differentiation increased the DNMT3B expression in ESCs in both media. Images are representative of three independent replicates. Scale bar = 50 µm.

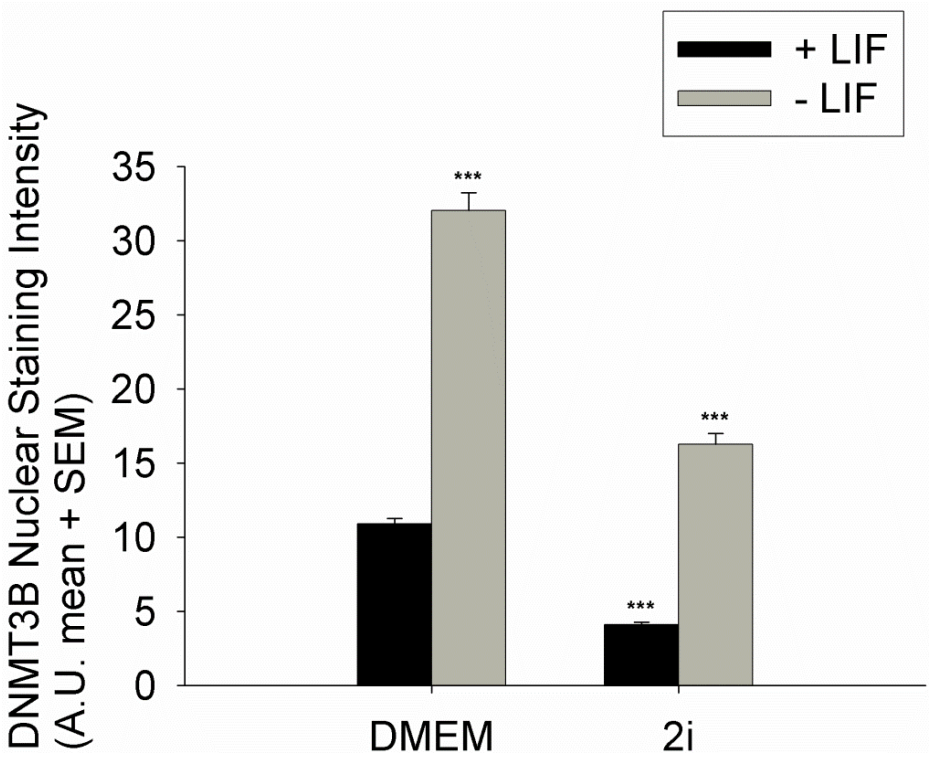

Figure 5-12 DNMT3B nuclear staining intensity in ESCs.

DNMT3B staining nuclear intensity was measured in ESC EBs previously cultured in DMEM or 2i for over 10 passages prior to exposure to DMEM minus LIF for 24 h. EB ESCs cultured in DMEM and 2i were used as controls. Staining intensity was measured in arbitrary units and is shown as mean ± SEM of three independent replicates. At least 100 nuclei were analysed per treatment per replicate. Statistically significant differences are indicated by asterisks: $p<0.001$ = ***.

Figure 5-13 Western blot analysis of DNMT3B in ESCs.

ESCs were grown in either DMEM or 2i media for over 10 passages prior to transfer to DMEM minus LIF. Cell proteins were collected and western blot analysis for DNMT3B was performed. ESCs in DMEM and 2i were used as controls. Western blot analysis showed the expected 116 kDa band for DNMT3B. Culture in 2i media inhibited DNMT3B expression, and LIF removal increased DNMT3B expression. Images are representative of three independent replicates. Western blot analysis was performed by Xing Jin from the Human Reproduction Unit.

5.3.3. The effect of culture conditions on TET1 expression in ESCs

Immunostaining for TET1 in EB ESCs was performed to investigate whether changes in global 5hmC levels in ESCs were accompanied by changes in the expression level of the the putative demethylation enzyme TET1. First, the immunostaining protocol was validated. Fluorescence microscopy showed increased localisation of anti-TET1 to the nuclei in the acid-treated EB ESCs compared to the untreated group (Figure 5-14). Therefore, epitope-retrieval by acid treatment was used to compare TET1 expression in ESCs. Similar levels of staining for TET1 were observed in all culture conditions (Figure 5-15). The intensity measurement confirmed there were no significant differences in the TET1 staining intensity between all culture conditions (Figure 5-16).

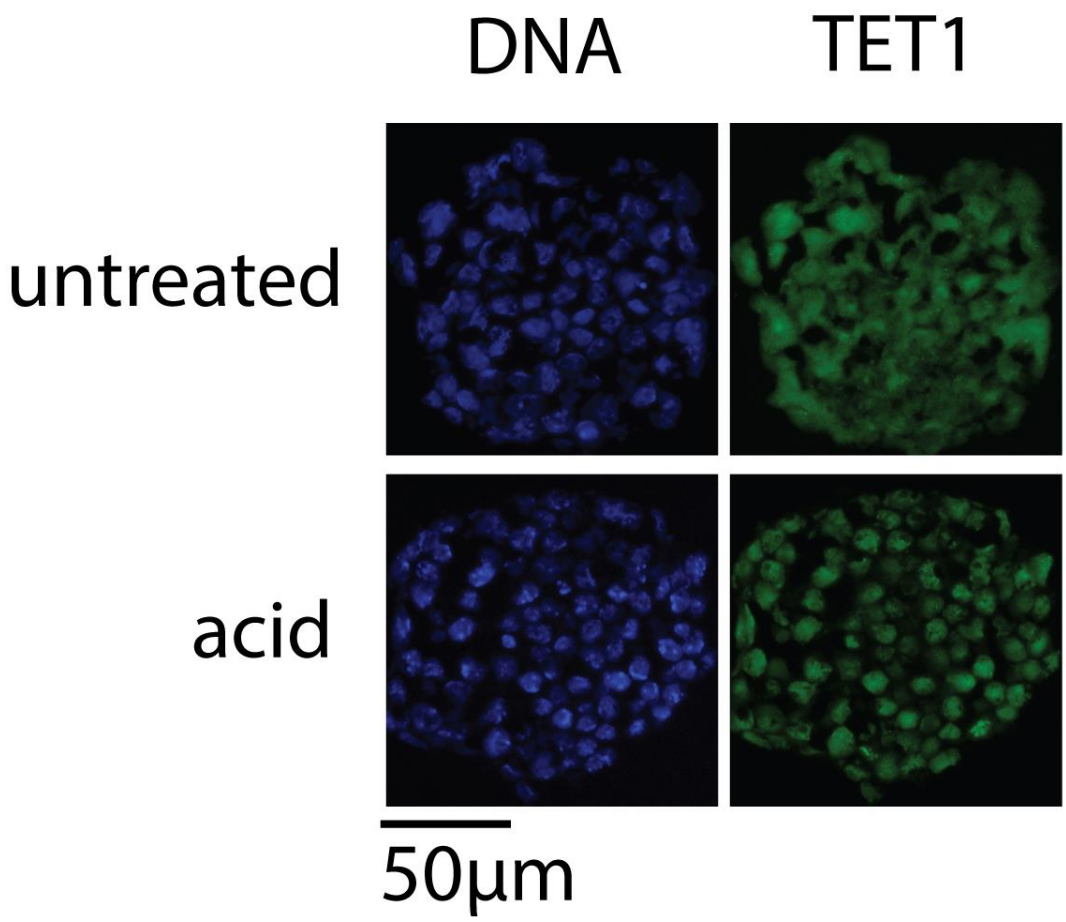

Figure 5-14 Validation of the immunostaining protocol for TET1.

EB ESCs were fixed and permeabilised. They were then either untreated or treated with 4N HCl (acid). The cells were stained with anti-TET1 and counterstained with DAPI. Immunofluorescence microscopy showed that acid treatment increased the localisation of anti-TET1 to the nuclei compared to the untreated group. Images are representative of three independent replicates. Scale bar = 50 µm.

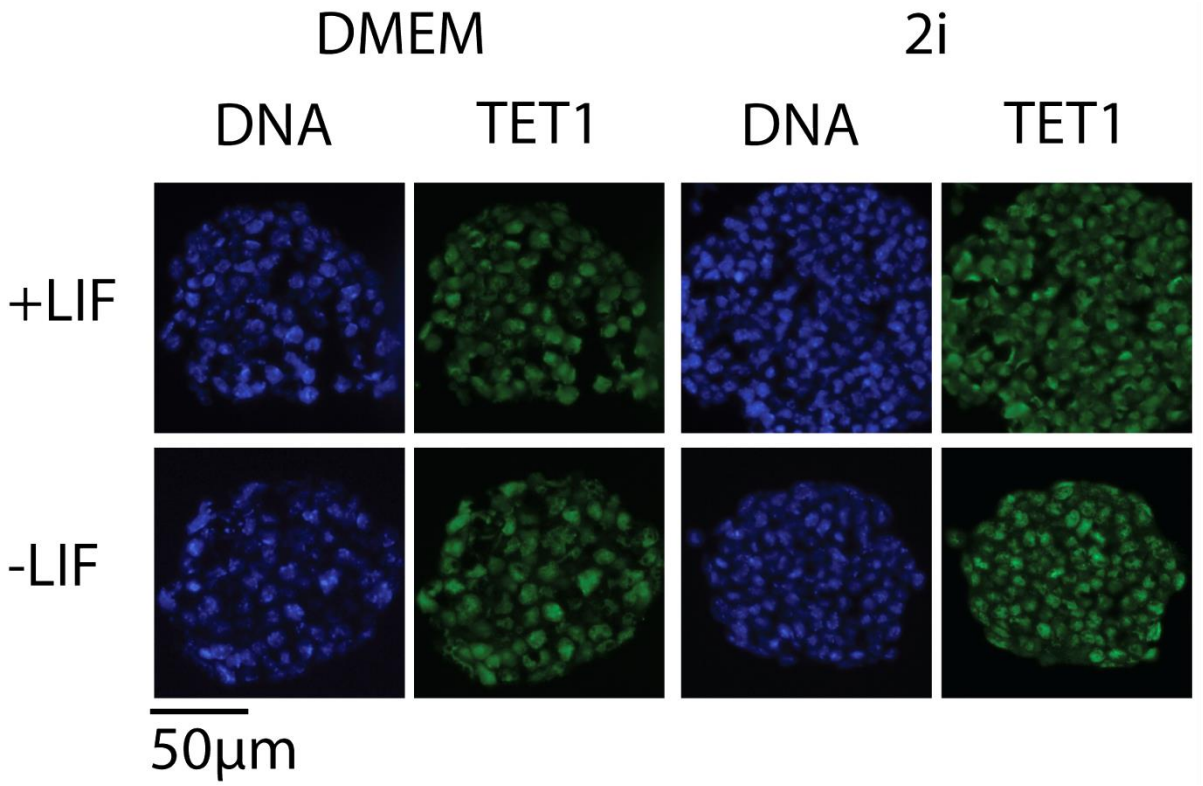

Figure 5-15 Immunostaining of TET1 in EB ESCs.

ESCs were grown in either DMEM or 2i media for over 10 passages prior to transfer to DMEM minus LIF with growth conditions that support the formation of EBs. EB sections were stained with anti-TET1 and counterstained with DAPI. EB ESCs in DMEM and 2i were used as controls. Immunofluorescence microscopy showed similar TET1 expression in all culture conditions. Images are representative of three independent replicates. Scale bar = 50 µm.

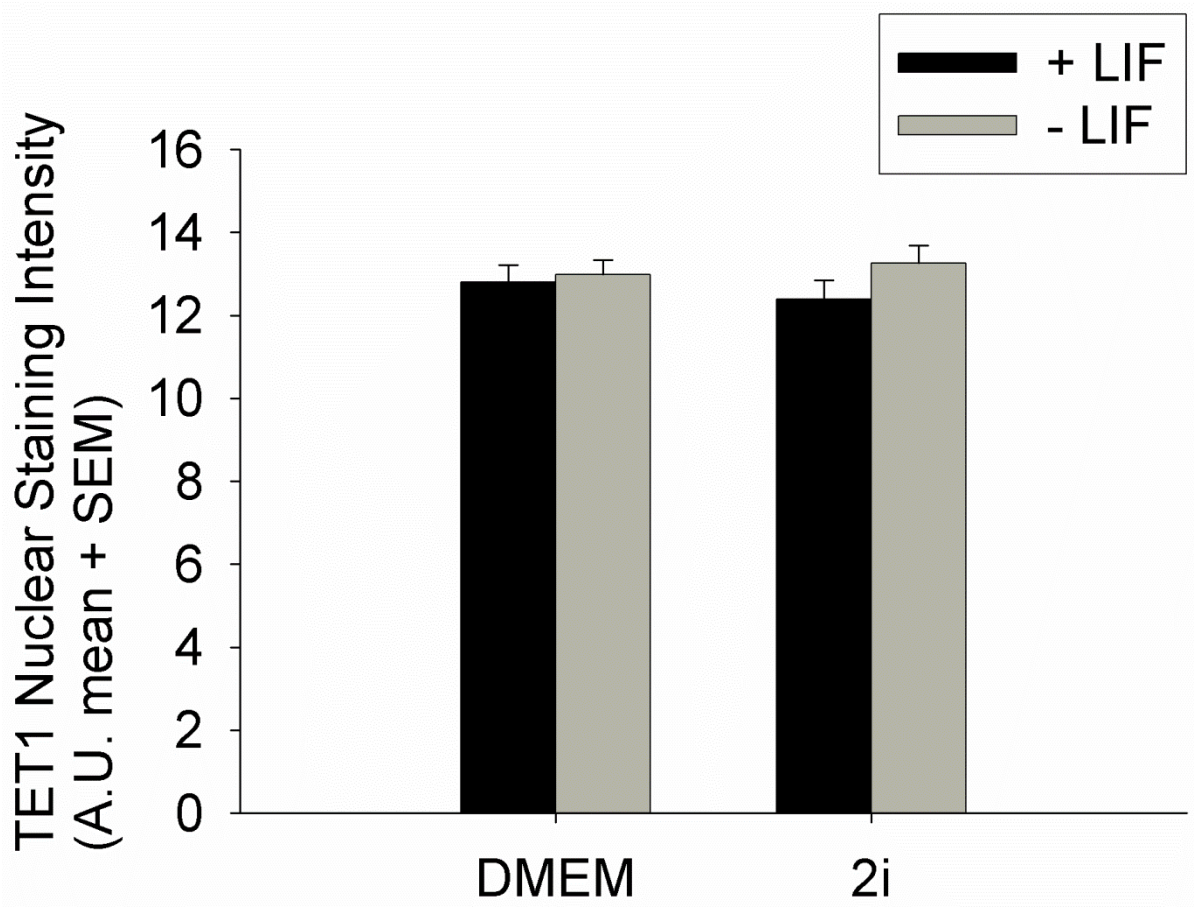

Figure 5-16 TET1 nuclear staining intensity in ESCs.

TET1 nuclear staining intensity was measured in ESC EBs previously cultured in DMEM or 2i for over 10 passages prior to exposure to DMEM minus LIF for 24 h. EB ESCs cultured in DMEM and 2i were used as controls. Staining intensity was measured in arbitrary units and is shown as mean ± SEM of three independent replicates. At least 100 nuclei were analysed per treatment per replicate.

5.4. DISCUSSION

The changes in 5meC and 5hmC levels in DMEM and 2i media after LIF removal were not accompanied by detectable changes in OCT4 levels. Although a reduction in alkaline phosphatase activity was not observed within 24 h of LIF removal, the alkaline phosphatase assay showed a notable increase in activity in EB ESCs cultured in 2i media. This indicates that in this model the alkaline phosphatase activity was a more sensitive indicator than OCT4 for detecting a change in the pluripotency of ESCs. The unchanged OCT4 level upon LIF removal shows that a loss of 5meC precedes a loss of OCT4. As OCT4 is one of the upstream pluripotency factors that regulate many transcription factor networks, the change in OCT4 level possibly occurs late during the loss of pluripotency. A study in retinoic acid-induced neural differentiation of human NT2 cells found the methylation of *Oct4* promoter occurred after 2 days following the retinoic acid treatment (Deb-Rinker et al., 2005). Another study in mouse embryonic carcinoma cells found that the *Oct-3/4* promoter harbors a *cis*-specific demodification element that protects the local regions from *de novo* methylation in post implantation embryos (Gidekel and Bergman, 2002). Through this mechanism, the *Oct4* promoter is protected from methylation in the early stages of embryogenesis. Therefore, it is expected that the methylation of *Oct4* promoter and a loss of OCT4 expression occur late during the loss of pluripotency.

The expression of *de novo* methylation enzymes changed in response to the culture environment, whether it was culture in 2i media or the removal of LIF. The previous chapter showed that the changes in 5meC levels preceded the changes in morphology and pluripotency of ESCs. Here it was shown that changes in the expression of the enzymes responsible for those changes in methylation also occurred early in response to the culture conditions. The DNA hypomethylation in ESCs induced by 2i media was accompanied by a loss of DNMT3A and

DNMT3B expression, which confirmed that 2i media protects ESCs from *de novo* methylation through the repression of *de novo* methylation enzymes (Leitch et al., 2013, Grabole et al., 2013, Ma et al., 2011, Yamaji et al., 2013). The increase in DNMT3A and DNMT3B expression in ESCs upon LIF removal further confirmed that the increase in 5meC during the loss of pluripotency was caused by *de novo* methylation. 2i media protects the ESCs from *de novo* methylation through the activation of PRDM14 which represses DNMT3A and DNMT3B expression (Leitch et al., 2013, Grabole et al., 2013, Ma et al., 2011, Yamaji et al., 2013). The immediate increase of DNMT3A and DNMT3B upon LIF removal in ESCs previously cultured in 2i media showed that the effect of MEK and GSK3β was independent of the actions of LIF. The smaller than expected DNMT3A bands observed in this study were most likely caused by proteolytic cleavage of the intact DNMT3A during the western blot analysis.

The persistence of DNMT1 in ESCs in all culture conditions confirmed that the DNA hypomethylation in response to culture in 2i media and the DNA hypermethylation after LIF removal were not associated with DNMT1. This enzyme works as the maintenance methylation enzyme in the replication foci during the S-phase of DNA replication and is involved in propagating the methylation pattern of DNA to daughter DNA (Grunstein, 1998, Rountree et al., 2000). The actions of DNMT1 during the S-phase of the cell cycle allow the timely regulation of gene expression and prevent tumour formation (Watanabe et al., 1998). These results suggest that the levels of methylation required for maintenance of ESCs are constant, independent of the pluripotency of ESCs.

The change in 5hmC levels in ESCs was not accompanied by a change in the expression of TET1, the putative hydroxymethylation enzyme. This suggests that differences in the levels of 5meC and 5hmC are determined by the levels of the methylation enzymes DNMT3A and DNMT3B rather than the levels of TET1. Koh *et al.* (2011) found that the expression of TET1

was regulated by OCT4, and the expressions of OCT4 and TET1 were not reduced until 3 days after LIF removal. This finding is in agreement with the similar levels of OCT4 and TET1 in ESCs in all culture conditions found in the present study.

Collectively, OCT4 immunostaining was found to be less sensitive to the changes in pluripotency of ESCs than the alkaline phosphatase assay, as the levels of OCT4 expression were similar in all culture conditions. DNMT3A and DNMT3B, and not DNMT1, were found to be the major contributors to the changes in DNA methylation levels in ESCs. The static expression of TET1 suggested that the changes in 5hmC levels in ESCs were determined by other factors, including the levels of *de novo* methylation enzymes. These studies provide a basis for further investigations into the epigenetic regulation in ESCs.

6. CHAPTER 6: GENERAL DISCUSSION

This thesis shows that the conventional immunofluorescence methods for assessing 5meC levels within cells can underestimate the levels of the antigen within ES cells. It shows that antigenic 5meC is present within two pools. One pool is detected after acid-induced denaturation of chromatin, and this is the pool detected by conventional immunolocalisation (Ciccarone et al., 2012, Salvaing et al., 2012). A further trypsin-sensitive pool has been discovered, and the size of this pool is highly variable, depending upon the developmental state and growth disposition of the cells. These observations extend recent findings regarding the requirement for a brief trypsin exposure to detect the 5meC present in the trypsin-sensitive pool within murine embryos and MEF (Li and O'Neill, 2012, Çelik et al., 2014). Since the percentages of 5meC antigen present in these two pools are variable and depend on many factors including cell-cycle and age in culture (Çelik et al., 2014), reliable and reproducible antigenic retrieval methods are required to produce valid results in 5meC immunoassays.

Besides the presence of antigenic masking and its removal by acid and trypsin treatment, other optimisations have to be performed to produce valid results in the immunostaining of ESCs. Generally, ESCs in culture form larger clumps, and these larger formations hinder access of antibodies to the target antigens. Therefore, the immunostaining of plated ESCs in this thesis was performed within 24 h or culture to prevent the formation of large clumps, and an additional cryosectioning protocol was performed on EBs to turn the large EB structures into thin sections that allow optimum exposure of the 5meC antigen to the antibody. Another optimization is to control the oxygen tension when culturing ESCs *in vitro*. It was found that culturing human ESCs under low oxygen tension is necessary to maintain full pluripotency, as it reduces the rate of differentiation without compromising the proliferation rate (Ezashi et al., 2005). The present study found that culturing ESCs with 5% oxygen in air reduced the global

5meC level of ESCs, and provided more controlled and stable morphology. Therefore, all cultures in this study used 5% oxygen in air.

Reduced global levels of 5meC were found to be associated with pluripotency in ESCs. The 5meC levels in ESCs in conventional media were comparable to the 5meC levels in MEF. Acid and trypsin treatments confirmed that the global demethylation observed in ESCs cultured in 2i media was not due to an increase in antigenic masking. The global demethylation, accompanied by the increase in alkaline phosphatase activity, confirmed the association between methylation and pluripotency of ESCs. The similar levels of OCT4 in ESCs cultured in 2i media suggested that the alkaline phosphatase assay is more sensitive than the OCT4 immunoassay in detecting changes in pluripotency in ESCs.

The unexpected rapid change in DNA methylation that precedes the loss of alkaline phosphatase activity and OCT4 expression after LIF removal indicates that DNA methylation is an early response to changes in the cell's pluripotency state. Along with the changes in DNA methylation, *de novo* methylation enzymes DNMT3A and DNMT3B, which are responsible for creating new sites of methylation in the mammalian genome, also underwent changes in response to the culture environment. The expression of maintenance methylation enzyme DNMT1 remained unchanged in all those conditions, confirming that the differences in the methylation were mainly regulated by the *de novo* methylation of the genome. It is known that 2i media protects ESCs from *de novo* methylation through the activation of PRDM14, which represses DNMT3A and DNMT3B expression (Leitch et al., 2013, Grabole et al., 2013, Ma et al., 2011, Yamaji et al., 2013).

A negative association between 5meC and 5hmC was observed, and might be interpreted as consistent with conversion between these two forms of DNA modification according to the pluripotency of ESCs. However, these changes in 5hmC levels were not accompanied by

changes in the expression of putative hyroxymethylation enzyme TET1. This suggests that the changes in 5hmC levels are regulated by the different levels of *de novo* methylation enzymes rather than the levels of TET1. An earlier study found that the expression of TET1 was regulated by OCT4, and the expressions of OCT4 and TET1 were not reduced until 3 days after LIF removal (Koh et al., 2011). The findings are in agreement with the similar levels of OCT4 and TET1 in ESCs in all culture conditions found in the present study. Two other forms of TET, TET2 and TET3 have also been described and further analysis of their roles in regulating the pluripotency of ESCs is required.

The localisation of 5meC and 5hmC staining in plated ESCs was found to be heterogeneous; this may be the result of interactions with neighbouring cells. A general pattern of increased cell interactions being associated with lower levels of methylation was observed in each media type. The lower levels of heterogeneity in EBs may be accounted for by the high level of cell-cell interactions in these structures. During the morulae stage of embryo development, when the cells are exposed to different positional information for the first time, it is found that the cells exposed to the outside environment are generally more methylated than the cells located inside (Li and O'Neill, 2013b). EB formation may provide similar positional information, where some cells are exposed to the environment and some cells are surrounded by other cells; consistent with this hypothesis, cells internal to the EBs tended to have lower levels of methylation than those on the outside. Taken together, positional information may be one of the determinants of the methylation state of the cells that later determines the commitment of the cells into specific cell lineages by altering patterns of gene expression.

Culture of ESCs in 2i media also reduced the heterogeneity of 5meC, with an increased pattern of localised staining in the presumptive heterochromatic foci. The improved immunoassay methods used in this study found that the 5meC localisation pattern in 2i media is closer to the

5meC localisation in the inner cell mass (ICM) of embryos, where it is located in few heterochromatic foci (Li and O'Neill, 2013b). The results confirm that 2i media supports a pluripotent ground state of ESCs as published in the previous work (Silva et al., 2008), even though the methylation status is still far from the methylation status of embryos.

Several associated limitations are worth to be considered in interpreting the outcomes of this research. First, karyotype of the cells used in this study was not assessed. Therefore, the quality of the cells was assessed only by morphology assessment and alkaline phosphatase assay. For future studies, it is recommended to assess the quality of the cells by karyotyping. Second, there are inherent variabilities associated with analyses of EB cultures. Despite the extensive efforts to keep the EBs used in this study as identic as possible, the size and cell number would still vary per EB aggregate. This condition could affect the level of staining in the immunoassays performed for EB cultures, leading to false results in the analysis. However, several optimisations, including permeabilisation optimisation, adequate sample size, and random measurement, have been done to ensure that the variability in the EBs gave insignificant impact to the results. It was found in the study that all EBs in one experiment group had similar staining intensities irrelevant to their size. Moreover, the EBs cultured in 2i media were smaller by default which possibly contribute to the mechanism of 2i media to maintain the ground state pluripotency of ESCs. A considered alternative approach is to assess the staining intensity in conjunction with protein levels for high numbers of single cells to see the correlation between staining intensity and protein levels. Finally, there is also major reliance on alkaline phosphatase assay to determine the pluripotency of ESCs in this study. However, it is proven that the alkaline phosphatase assay is more sensitive compared to the OCT4 immunoassay in detecting changes in pluripotency in ESCs. Possible alternative is to examine further markers of pluripotency in addition to OCT4.

In conclusion, this thesis shows how global 5meC levels in ESCs change in response to culture conditions. Using an immunolocalisation assay with full epitope retrieval, it shows that hypomethylation is associated with the pluripotent state and that hypermethylation caused by increased DNMT3A and DNMT3B is a very early response to the loss of pluripotency. The cost-effectiveness of the immunoassay and its capacity to measure changes in individual cells and changes in sub-nuclear localisation make it a powerful tool for the detailed analysis of the control of methylation changes during cell ontogeny.

The next step of this research is to utilise this developed immunoassay method to analyse the global 5meC and 5hmC levels in multiple pluripotent cell lines such as pluripotent cells derived from different mouse strains, human pluripotent cells, or iPS cells. Recent major developments in reprogramming adult cells into pluripotent cells open new approaches in the field of regenerative therapy. While the potential is great, little is known regarding the safety of using these cells in patients. DNA methylation analyses showed that the DNA methylation status of iPS cells are not identical to ESCs, despite the similar characteristics shared by both cell types (Takahashi and Yamanaka, 2006, Takahashi et al., 2007). DNA methylation mapping of iPS cells shows increased deviation from the ESCs references in small number of genes, including the hypermethylation of several genes similar to the condition in several fibroblast cell lines (Bock et al., 2011). The results suggest partial reprogramming occurs in generating iPS cells, which leads to concerns regarding the effectiveness and safety of using iPS cells for therapy. Furthermore, a prolonged culture of ESCs *in vitro* showed aberrant hypermethylation of CpG islands associated with a specific set of developmentally regulated genes, in a similar pattern with some primary tumours (Meissner et al., 2008). This raises the general concerns regarding propagating pluripotent cells *in vitro*. Although, 2i media is proven to support the ground state pluripotency of ESCs *in vitro*, the methylation levels of ESCs in 2i media are still different compared to the methylation levels of embryos. The differences in pluripotency between

embryos and ESCs can be so subtle occurring in the epigenetic levels, even before the changes in the level of pluripotent transcription factors and other signs of loss of pluripotency. Those subtle differences tend to be overlooked by functional analyses such as chimaerism competencies. Using the current immunoassay method, the global 5meC and 5hmC levels of iPS cells, as well as the positional information associated with the DNA methylation and demethylation, can be retrieved for more thorough assessment of the cells.

For the fields of methylation analysis and immunoassay in general, the importance of a complete antigen retrieval in performing immunoassay for methylation analysis is worth to be considered. The antigen retrieval used in this study was also used in flow cytometry for methylation analysis in mouse embryonic fibroblasts (Çelik et al., 2014). Future possible approach is to study methylation in clinically relevant culture systems, for example live cells analysis using high-content screening. However, a different strategy for antigen retrieval would be needed for that purpose, as the current antigen retrieval method is optimised for fixed cells. DNA methylation in living embryos can be visualised by using methyl-CpG-binding domain (Kimura et al., 2010). Yet, the effectiveness of this method compared to the acid and trypsin antigen retrieval method for methylation analysis in ESCs has to be verified. Using these approaches for future studies, the culture conditions for pluripotent cells propagation can be developed more effectively. The aim is to generate a pluripotent cell line identical to the normal development embryos in a robust, reliable, and stable manner.

7. REFERENCES

AAPOLA, U., KAWASAKI, K., SCOTT, H. S., OLLILA, J., VIHINEN, M., HEINO, M., SHINTANI, A., KAWASAKI, K., MINOSHIMA, S., KROHN, K., ANTONARAKIS, S. E., SHIMIZU, N., KUDOH, J. & PETERSON, P. 2000. Isolation and initial characterization of a novel zinc finger gene, DNMT3L, on 21q22.3, related to the cytosine-5-methyltransferase 3 gene family. *Genomics,* 65**,** 293-8.

AAPOLA, U., LIIV, I. & PETERSON, P. 2002. Imprinting regulator DNMT3L is a transcriptional repressor associated with histone deacetylase activity. *Nucleic Acids Res,* 30**,** 3602-8.

AAPOLA, U., LYLE, R., KROHN, K., ANTONARAKIS, S. E. & PETERSON, P. 2001. Isolation and initial characterization of the mouse Dnmt3l gene. *Cytogenet Cell Genet,* 92**,** 122-6.

AASLAND, R., GIBSON, T. J. & STEWART, A. F. 1995. The PHD finger: implications for chromatin-mediated transcriptional regulation. *Trends Biochem Sci,* 20**,** 56-9.

ALTUN, G., LORING, J. F. & LAURENT, L. C. 2010. DNA methylation in embryonic stem cells. *J Cell Biochem,* 109**,** 1-6.

AOKI, A., SUETAKE, I., MIYAGAWA, J., FUJIO, T., CHIJIWA, T., SASAKI, H. & TAJIMA, S. 2001. Enzymatic properties of de novo-type mouse DNA (cytosine-5) methyltransferases. *Nucleic Acids Res,* 29**,** 3506-12.

ARIMA, T., HATA, K., TANAKA, S., KUSUMI, M., LI, E., KATO, K., SHIOTA, K., SASAKI, H. & WAKE, N. 2006. Loss of the maternal imprint in Dnmt3Lmat-/- mice leads to a differentiation defect in the extraembryonic tissue. *Dev Biol,* 297**,** 361-73.

AUCLAIR, G. & WEBER, M. 2012. Mechanisms of DNA methylation and demethylation in mammals. *Biochimie,* 94**,** 2202-11.

BACHMAN, K. E., ROUNTREE, M. R. & BAYLIN, S. B. 2001. Dnmt3a and Dnmt3b are transcriptional repressors that exhibit unique localization properties to heterochromatin. *J Biol Chem,* 276**,** 32282-7.

BALL, M. P., LI, J. B., GAO, Y., LEE, J. H., LEPROUST, E. M., PARK, I. H., XIE, B., DALEY, G. Q. & CHURCH, G. M. 2009. Targeted and genome-scale strategies reveal gene-body methylation signatures in human cells. *Nat Biotechnol,* 27**,** 361-8.

BEAUJEAN, N., HARTSHORNE, G., CAVILLA, J., TAYLOR, J., GARDNER, J., WILMUT, I., MEEHAN, R. & YOUNG, L. 2004. Non-conservation of mammalian preimplantation methylation dynamics. *Curr Biol,* 14**,** R266-7.

BERNSTEIN, B. E., MIKKELSEN, T. S., XIE, X., KAMAL, M., HUEBERT, D. J., CUFF, J., FRY, B., MEISSNER, A., WERNIG, M., PLATH, K., JAENISCH, R., WAGSCHAL, A., FEIL, R., SCHREIBER, S. L. & LANDER, E. S. 2006. A bivalent chromatin structure marks key developmental genes in embryonic stem cells. *Cell,* 125**,** 315-26.

BESTOR, T. H. 1992. Activation of mammalian DNA methyltransferase by cleavage of a Zn binding regulatory domain. *EMBO J,* 11**,** 2611-7.

BESTOR, T. H. & VERDINE, G. L. 1994. DNA methyltransferases. *Curr Opin Cell Biol,* 6**,** 380-9.

BHUTANI, N., BRADY, J. J., DAMIAN, M., SACCO, A., CORBEL, S. Y. & BLAU, H. M. 2010. Reprogramming towards pluripotency requires AID-dependent DNA demethylation. *Nature,* 463**,** 1042-7.

BIRD, A. 2002. DNA methylation patterns and epigenetic memory. *Genes Dev,* 16**,** 6-21.

BIRD, A. P. & SOUTHERN, E. M. 1978. Use of Restriction Enzymes to Study Eukaryotic DNA Methylation .1. Methylation Pattern in Ribosomal DNA from Xenopus-Laevis. *Journal of Molecular Biology,* 118**,** 27-47.

BOCK, C., KISKINIS, E., VERSTAPPEN, G., GU, H., BOULTING, G., SMITH, Z. D., ZILLER, M., CROFT, G. F., AMOROSO, M. W., OAKLEY, D. H., GNIRKE, A., EGGAN, K. & MEISSNER, A. 2011. Reference Maps of human ES and iPS cell variation enable high-throughput characterization of pluripotent cell lines. *Cell,* 144**,** 439-52.

BOOTH, M. J., BRANCO, M. R., FICZ, G., OXLEY, D., KRUEGER, F., REIK, W. & BALASUBRAMANIAN, S. 2012. Quantitative sequencing of 5-methylcytosine and 5-hydroxymethylcytosine at single-base resolution. *Science,* 336**,** 934-7.

BOOTH, M. J., MARSICO, G., BACHMAN, M., BERALDI, D. & BALASUBRAMANIAN, S. 2014. Quantitative sequencing of 5-formylcytosine in DNA at single-base resolution. *Nat Chem,* 6**,** 435-40.

BOOTH, M. J., OST, T. W., BERALDI, D., BELL, N. M., BRANCO, M. R., REIK, W. & BALASUBRAMANIAN, S. 2013. Oxidative bisulfite sequencing of 5-methylcytosine and 5-hydroxymethylcytosine. *Nat Protoc,* 8**,** 1841-51.

BORGEL, J., GUIBERT, S., LI, Y., CHIBA, H., SCHUBELER, D., SASAKI, H., FORNE, T. & WEBER, M. 2010. Targets and dynamics of promoter DNA methylation during early mouse development. *Nat Genet,* 42**,** 1093-100.

BOSTICK, M., KIM, J. K., ESTEVE, P. O., CLARK, A., PRADHAN, S. & JACOBSEN, S. E. 2007. UHRF1 plays a role in maintaining DNA methylation in mammalian cells. *Science,* 317**,** 1760-4.

BOURC'HIS, D. & BESTOR, T. H. 2004. Meiotic catastrophe and retrotransposon reactivation in male germ cells lacking Dnmt3L. *Nature,* 431**,** 96-9.

BOURC'HIS, D., XU, G. L., LIN, C. S., BOLLMAN, B. & BESTOR, T. H. 2001. Dnmt3L and the establishment of maternal genomic imprints. *Science,* 294**,** 2536-9.

BOYER, L. A., LEE, T. I., COLE, M. F., JOHNSTONE, S. E., LEVINE, S. S., ZUCKER, J. P., GUENTHER, M. G., KUMAR, R. M., MURRAY, H. L., JENNER, R. G., GIFFORD, D. K., MELTON, D. A., JAENISCH, R. & YOUNG, R. A. 2005. Core transcriptional regulatory circuitry in human embryonic stem cells. *Cell,* 122**,** 947-56.

BRAHIMI-HORN, M. C. & POUYSSEGUR, J. 2007. Oxygen, a source of life and stress. *FEBS Lett,* 581**,** 3582-91.

BRANCO, M. R., FICZ, G. & REIK, W. 2012. Uncovering the role of 5-hydroxymethylcytosine in the epigenome. *Nat Rev Genet,* 13**,** 7-13.

BURDON, T., SMITH, A. & SAVATIER, P. 2002. Signalling, cell cycle and pluripotency in embryonic stem cells. *Trends Cell Biol,* 12**,** 432-8.

BUTKUS, V., PETRAUSKIENE, L., MANELIENE, Z., KLIMASAUSKAS, S., LAUCYS, V. & JANULAITIS, A. 1987. Cleavage of methylated CCCGGG sequences containing either N4-methylcytosine or 5-methylcytosine with MspI, HpaII, SmaI, XmaI and Cfr9I restriction endonucleases. *Nucleic Acids Res,* 15**,** 7091-102.

CALLEBAUT, I., COURVALIN, J. C. & MORNON, J. P. 1999. The BAH (bromo-adjacent homology) domain: a link between DNA methylation, replication and transcriptional regulation. *FEBS Lett,* 446**,** 189-93.

CARTWRIGHT, P., MCLEAN, C., SHEPPARD, A., RIVETT, D., JONES, K. & DALTON, S. 2005. LIF/STAT3 controls ES cell self-renewal and pluripotency by a Myc-dependent mechanism. *Development,* 132**,** 885-896.

ÇELIK, S., LI, Y. & O'NEILL, C. 2014. The Exit of Mouse Embryonic Fibroblasts from the Cell-Cycle Changes the Nature of Solvent Exposure of the 5′-Methylcytosine Epitope within Chromatin. *PLoS ONE,* 9**,** e92523.

CHAMBERS, I., COLBY, D., ROBERTSON, M., NICHOLS, J., LEE, S., TWEEDIE, S. & SMITH, A. 2003. Functional expression cloning of Nanog, a pluripotency sustaining factor in embryonic stem cells. *Cell,* 113**,** 643-55.

CHAZAUD, C., YAMANAKA, Y., PAWSON, T. & ROSSANT, J. 2006. Early lineage segregation between epiblast and primitive endoderm in mouse blastocysts through the Grb2-MAPK pathway. *Dev Cell,* 10**,** 615-24.

CHEDIN, F. 2011. The DNMT3 family of mammalian de novo DNA methyltransferases. *Prog Mol Biol Transl Sci,* 101**,** 255-85.

CHEN, T., HEVI, S., GAY, F., TSUJIMOTO, N., HE, T., ZHANG, B., UEDA, Y. & LI, E. 2007. Complete inactivation of DNMT1 leads to mitotic catastrophe in human cancer cells. *Nat Genet,* 39**,** 391-6.

CHEN, T. & LI, E. 2004. Structure and function of eukaryotic DNA methyltransferases. *Curr Top Dev Biol,* 60**,** 55-89.

CHEN, T., UEDA, Y., DODGE, J. E., WANG, Z. & LI, E. 2003. Establishment and maintenance of genomic methylation patterns in mouse embryonic stem cells by Dnmt3a and Dnmt3b. *Mol Cell Biol,* 23**,** 5594-605.

CHEN, T., UEDA, Y., XIE, S. & LI, E. 2002. A novel Dnmt3a isoform produced from an alternative promoter localizes to euchromatin and its expression correlates with active de novo methylation. *J Biol Chem,* 277**,** 38746-54.

CHEN, Z. X. & RIGGS, A. D. 2011. DNA methylation and demethylation in mammals. *J Biol Chem,* 286**,** 18347-53.

CHENG, X. 1995a. DNA modification by methyltransferases. *Curr Opin Struct Biol,* 5**,** 4-10.

CHENG, X. 1995b. Structure and function of DNA methyltransferases. *Annu Rev Biophys Biomol Struct,* 24**,** 293-318.

CHEW, J. L., LOH, Y. H., ZHANG, W., CHEN, X., TAM, W. L., YEAP, L. S., LI, P., ANG, Y. S., LIM, B., ROBSON, P. & NG, H. H. 2005. Reciprocal transcriptional regulation of Pou5f1 and Sox2 via the Oct4/Sox2 complex in embryonic stem cells. *Mol Cell Biol,* 25**,** 6031-46.

CHOUDHRY, Z., RIKANI, A. A., CHOUDHRY, A. M., TARIQ, S., ZAKARIA, F., ASGHAR, M. W., SARFRAZ, M. K., HAIDER, K., SHAFIQ, A. A. & MOBASSARAH, N. J. 2014. Sonic hedgehog signalling pathway: a complex network. *Ann Neurosci,* 21**,** 28-31.

CHUANG, L. S., NG, H. H., CHIA, J. N. & LI, B. F. 1996. Characterisation of independent DNA and multiple Zn-binding domains at the N terminus of human DNA-(cytosine-5) methyltransferase: modulating the property of a DNA-binding domain by contiguous Zn-binding motifs. *J Mol Biol,* 257**,** 935-48.

CICCARONE, F., KLINGER, F. G., CATIZONE, A., CALABRESE, R., ZAMPIERI, M., BACALINI, M. G., DE FELICI, M. & CAIAFA, P. 2012. Poly(ADP-ribosyl)ation acts in the DNA demethylation of mouse primordial germ cells also with DNA damage-independent roles. *PLoS One,* 7**,** e46927.

CLARK, S. J., HARRISON, J., PAUL, C. L. & FROMMER, M. 1994. High sensitivity mapping of methylated cytosines. *Nucleic Acids Res,* 22**,** 2990-7.

CORTAZAR, D., KUNZ, C., SAITO, Y., STEINACHER, R. & SCHAR, P. 2007. The enigmatic thymine DNA glycosylase. *DNA Repair (Amst),* 6**,** 489-504.

CORTELLINO, S., XU, J., SANNAI, M., MOORE, R., CARETTI, E., CIGLIANO, A., LE COZ, M., DEVARAJAN, K., WESSELS, A., SOPRANO, D., ABRAMOWITZ, L. K., BARTOLOMEI, M. S., RAMBOW, F., BASSI, M. R., BRUNO, T., FANCIULLI, M., RENNER, C., KLEIN-SZANTO, A. J., MATSUMOTO, Y., KOBI, D., DAVIDSON, I., ALBERTI, C., LARUE, L. & BELLACOSA, A. 2011. Thymine DNA glycosylase

is essential for active DNA demethylation by linked deamination-base excision repair. *Cell,* 146**,** 67-79.

DANG, L. & TROPEPE, V. 2006. Neural induction and neural stem cell development. *Regen Med,* 1**,** 635-52.

DARWISH, I., EMARA, S., ASKAL, H., EL-RABBAT, N., OMURA, K., HIROSE, K., AKIZAWA, T. & YOSHIOKA, M. 2000. Competitive immunoassay method for 5-methyl-2 '-deoxycytidine. *Analytica Chimica Acta,* 413**,** 79-86.

DAWSON, E., MAPILI, G., ERICKSON, K., TAQVI, S. & ROY, K. 2008. Biomaterials for stem cell differentiation. *Adv Drug Deliv Rev,* 60**,** 215-28.

DEB-RINKER, P., LY, D., JEZIERSKI, A., SIKORSKA, M. & WALKER, P. R. 2005. Sequential DNA methylation of the Nanog and Oct-4 upstream regions in human NT2 cells during neuronal differentiation. *J Biol Chem,* 280**,** 6257-60.

DENG, J., SHOEMAKER, R., XIE, B., GORE, A., LEPROUST, E. M., ANTOSIEWICZ-BOURGET, J., EGLI, D., MAHERALI, N., PARK, I. H., YU, J., DALEY, G. Q., EGGAN, K., HOCHEDLINGER, K., THOMSON, J., WANG, W., GAO, Y. & ZHANG, K. 2009. Targeted bisulfite sequencing reveals changes in DNA methylation associated with nuclear reprogramming. *Nat Biotechnol,* 27**,** 353-60.

DEOBAGKAR, D. D., PANIKAR, C., RAJPATHAK, S. N., SHAIWALE, N. S. & MUKHERJEE, S. 2012. An immunochemical method for detection and analysis of changes in methylome. *Methods,* 56**,** 260-7.

DESBAILLETS, I., ZIEGLER, U., GROSCURTH, P. & GASSMANN, M. 2000. Embryoid bodies: an in vitro model of mouse embryogenesis. *Exp Physiol,* 85**,** 645-51.

DODGE, J. E., OKANO, M., DICK, F., TSUJIMOTO, N., CHEN, T., WANG, S., UEDA, Y., DYSON, N. & LI, E. 2005. Inactivation of Dnmt3b in mouse embryonic fibroblasts

results in DNA hypomethylation, chromosomal instability, and spontaneous immortalization. *J Biol Chem,* 280**,** 17986-91.

DOETSCHMAN, T. C., EISTETTER, H., KATZ, M., SCHMIDT, W. & KEMLER, R. 1985. The in vitro development of blastocyst-derived embryonic stem cell lines: formation of visceral yolk sac, blood islands and myocardium. *J Embryol Exp Morphol,* 87**,** 27-45.

DONG, A., YODER, J. A., ZHANG, X., ZHOU, L., BESTOR, T. H. & CHENG, X. 2001. Structure of human DNMT2, an enigmatic DNA methyltransferase homolog that displays denaturant-resistant binding to DNA. *Nucleic Acids Res,* 29**,** 439-48.

DOWN, T. A., RAKYAN, V. K., TURNER, D. J., FLICEK, P., LI, H., KULESHA, E., GRAF, S., JOHNSON, N., HERRERO, J., TOMAZOU, E. M., THORNE, N. P., BACKDAHL, L., HERBERTH, M., HOWE, K. L., JACKSON, D. K., MIRETTI, M. M., MARIONI, J. C., BIRNEY, E., HUBBARD, T. J., DURBIN, R., TAVARE, S. & BECK, S. 2008. A Bayesian deconvolution strategy for immunoprecipitation-based DNA methylome analysis. *Nat Biotechnol,* 26**,** 779-85.

EADS, C. A., DANENBERG, K. D., KAWAKAMI, K., SALTZ, L. B., BLAKE, C., SHIBATA, D., DANENBERG, P. V. & LAIRD, P. W. 2000. MethyLight: a high-throughput assay to measure DNA methylation. *Nucleic Acids Res,* 28**,** E32.

EDEN, A., GAUDET, F., WAGHMARE, A. & JAENISCH, R. 2003. Chromosomal instability and tumors promoted by DNA hypomethylation. *Science,* 300**,** 455.

EVANS, M. J. & KAUFMAN, M. H. 1981. Establishment in culture of pluripotential cells from mouse embryos. *Nature,* 292**,** 154-6.

EZASHI, T., DAS, P. & ROBERTS, R. M. 2005. Low O2 tensions and the prevention of differentiation of hES cells. *Proc Natl Acad Sci U S A,* 102**,** 4783-8.

FATEMI, M., HERMANN, A., PRADHAN, S. & JELTSCH, A. 2001. The activity of the murine DNA methyltransferase Dnmt1 is controlled by interaction of the catalytic

domain with the N-terminal part of the enzyme leading to an allosteric activation of the enzyme after binding to methylated DNA. *J Mol Biol,* 309**,** 1189-99.

FICZ, G., HORE, T. A., SANTOS, F., LEE, H. J., DEAN, W., ARAND, J., KRUEGER, F., OXLEY, D., PAUL, Y. L., WALTER, J., COOK, S. J., ANDREWS, S., BRANCO, M. R. & REIK, W. 2013. FGF signaling inhibition in ESCs drives rapid genome-wide demethylation to the epigenetic ground state of pluripotency. *Cell Stem Cell,* 13**,** 351-9.

FLEMING, T. P., SHETH, B. & FESENKO, I. 2001. Cell adhesion in the preimplantation mammalian embryo and its role in trophectoderm differentiation and blastocyst morphogenesis. *Front Biosci,* 6**,** D1000-7.

FOLKMAN, J., HAHNFELDT, P. & HLATKY, L. 2000. Cancer: looking outside the genome. *Nat Rev Mol Cell Biol,* 1**,** 76-9.

FOUSE, S. D., SHEN, Y., PELLEGRINI, M., COLE, S., MEISSNER, A., VAN NESTE, L., JAENISCH, R. & FAN, G. 2008. Promoter CpG methylation contributes to ES cell gene regulation in parallel with Oct4/Nanog, PcG complex, and histone H3 K4/K27 trimethylation. *Cell Stem Cell,* 2**,** 160-9.

FROMMER, M., MCDONALD, L. E., MILLAR, D. S., COLLIS, C. M., WATT, F., GRIGG, G. W., MOLLOY, P. L. & PAUL, C. L. 1992. A genomic sequencing protocol that yields a positive display of 5-methylcytosine residues in individual DNA strands. *Proc Natl Acad Sci U S A,* 89**,** 1827-31.

FUKS, F., BURGERS, W. A., BREHM, A., HUGHES-DAVIES, L. & KOUZARIDES, T. 2000. DNA methyltransferase Dnmt1 associates with histone deacetylase activity. *Nat Genet,* 24**,** 88-91.

FUKS, F., BURGERS, W. A., GODIN, N., KASAI, M. & KOUZARIDES, T. 2001. Dnmt3a binds deacetylases and is recruited by a sequence-specific repressor to silence transcription. *EMBO J,* 20**,** 2536-44.

GE, C., FANG, Z., CHEN, J., LIU, J., LU, X. & ZENG, L. 2012. A simple colorimetric detection of DNA methylation. *Analyst,* 137**,** 2032-5.

GIDEKEL, S. & BERGMAN, Y. 2002. A unique developmental pattern of Oct-3/4 DNA methylation is controlled by a cis-demodification element. *J Biol Chem,* 277**,** 34521-30.

GITAN, R. S., SHI, H., CHEN, C. M., YAN, P. S. & HUANG, T. H. 2002. Methylation-specific oligonucleotide microarray: a new potential for high-throughput methylation analysis. *Genome Res,* 12**,** 158-64.

GOLL, M. G., KIRPEKAR, F., MAGGERT, K. A., YODER, J. A., HSIEH, C. L., ZHANG, X., GOLIC, K. G., JACOBSEN, S. E. & BESTOR, T. H. 2006. Methylation of tRNAAsp by the DNA methyltransferase homolog Dnmt2. *Science,* 311**,** 395-8.

GONZALGO, M. L. & JONES, P. A. 1997. Rapid quantitation of methylation differences at specific sites using methylation-sensitive single nucleotide primer extension (Ms-SNuPE). *Nucleic Acids Res,* 25**,** 2529-31.

GOWHER, H., LIEBERT, K., HERMANN, A., XU, G. & JELTSCH, A. 2005. Mechanism of stimulation of catalytic activity of Dnmt3A and Dnmt3B DNA-(cytosine-C5)-methyltransferases by Dnmt3L. *J Biol Chem,* 280**,** 13341-8.

GRABOLE, N., TISCHLER, J., HACKETT, J. A., KIM, S., TANG, F., LEITCH, H. G., MAGNUSDOTTIR, E. & SURANI, M. A. 2013. Prdm14 promotes germline fate and naive pluripotency by repressing FGF signalling and DNA methylation. *EMBO Rep,* 14**,** 629-37.

GRANA, X., GARRIGA, J. & MAYOL, X. 1998. Role of the retinoblastoma protein family, pRB, p107 and p130 in the negative control of cell growth. *Oncogene,* 17**,** 3365-83.

GRUNSTEIN, M. 1998. Yeast heterochromatin: regulation of its assembly and inheritance by histones. *Cell,* 93**,** 325-8.

GU, T. P., GUO, F., YANG, H., WU, H. P., XU, G. F., LIU, W., XIE, Z. G., SHI, L., HE, X., JIN, S. G., IQBAL, K., SHI, Y. G., DENG, Z., SZABO, P. E., PFEIFER, G. P., LI, J. & XU, G. L. 2011. The role of Tet3 DNA dioxygenase in epigenetic reprogramming by oocytes. *Nature,* 477**,** 606-10.

GUO, G., WANG, W. & BRADLEY, A. 2004. Mismatch repair genes identified using genetic screens in Blm-deficient embryonic stem cells. *Nature,* 429**,** 891-5.

GUO, H., ZHU, P., WU, X., LI, X., WEN, L. & TANG, F. 2013. Single-cell methylome landscapes of mouse embryonic stem cells and early embryos analyzed using reduced representation bisulfite sequencing. *Genome Res,* 23**,** 2126-35.

GUO, J. U., SU, Y., ZHONG, C., MING, G. L. & SONG, H. 2011. Hydroxylation of 5-methylcytosine by TET1 promotes active DNA demethylation in the adult brain. *Cell,* 145**,** 423-34.

HABIBI, E., BRINKMAN, A. B., ARAND, J., KROEZE, L. I., KERSTENS, H. H., MATARESE, F., LEPIKHOV, K., GUT, M., BRUN-HEATH, I., HUBNER, N. C., BENEDETTI, R., ALTUCCI, L., JANSEN, J. H., WALTER, J., GUT, I. G., MARKS, H. & STUNNENBERG, H. G. 2013. Whole-genome bisulfite sequencing of two distinct interconvertible DNA methylomes of mouse embryonic stem cells. *Cell Stem Cell,* 13**,** 360-9.

HATA, K., OKANO, M., LEI, H. & LI, E. 2002. Dnmt3L cooperates with the Dnmt3 family of de novo DNA methyltransferases to establish maternal imprints in mice. *Development,* 129**,** 1983-93.

HAYATSU, H., WATAYA, Y., KAI, K. & IIDA, S. 1970a. Reaction of sodium bisulfite with uracil, cytosine, and their derivatives. *Biochemistry,* 9**,** 2858-65.

HAYATSU, H., WATAYA, Y. & KAZUSHIGE, K. 1970b. The addition of sodium bisulfite to uracil and to cytosine. *J Am Chem Soc,* 92**,** 724-6.

HE, Y. F., LI, B. Z., LI, Z., LIU, P., WANG, Y., TANG, Q., DING, J., JIA, Y., CHEN, Z., LI, L., SUN, Y., LI, X., DAI, Q., SONG, C. X., ZHANG, K., HE, C. & XU, G. L. 2011. Tet-mediated formation of 5-carboxylcytosine and its excision by TDG in mammalian DNA. *Science,* 333**,** 1303-7.

HERMAN, J. G., GRAFF, J. R., MYOHANEN, S., NELKIN, B. D. & BAYLIN, S. B. 1996. Methylation-specific PCR: a novel PCR assay for methylation status of CpG islands. *Proc Natl Acad Sci U S A,* 93**,** 9821-6.

HIRASAWA, R., CHIBA, H., KANEDA, M., TAJIMA, S., LI, E., JAENISCH, R. & SASAKI, H. 2008. Maternal and zygotic Dnmt1 are necessary and sufficient for the maintenance of DNA methylation imprints during preimplantation development. *Genes Dev,* 22**,** 1607-16.

HIRASAWA, R. & SASAKI, H. 2009. Dynamic transition of Dnmt3b expression in mouse pre- and early post-implantation embryos. *Gene Expr Patterns,* 9**,** 27-30.

HONG, Y. & STAMBROOK, P. J. 2004. Restoration of an absent G1 arrest and protection from apoptosis in embryonic stem cells after ionizing radiation. *Proc Natl Acad Sci U S A,* 101**,** 14443-8.

HOOKER, C. W. & HURLIN, P. J. 2006. Of Myc and Mnt. *J Cell Sci,* 119**,** 208-16.

HUANG, Y., PASTOR, W. A., SHEN, Y., TAHILIANI, M., LIU, D. R. & RAO, A. 2010. The behaviour of 5-hydroxymethylcytosine in bisulfite sequencing. *PLoS One,* 5**,** e8888.

HWANG, N. S., VARGHESE, S. & ELISSEEFF, J. 2008. Controlled differentiation of stem cells. *Adv Drug Deliv Rev,* 60**,** 199-214.

IIDA, T., SUETAKE, I., TAJIMA, S., MORIOKA, H., OHTA, S., OBUSE, C. & TSURIMOTO, T. 2002. PCNA clamp facilitates action of DNA cytosine methyltransferase 1 on hemimethylated DNA. *Genes Cells,* 7**,** 997-1007.

INOUE, A., SHEN, L., DAI, Q., HE, C. & ZHANG, Y. 2011. Generation and replication-dependent dilution of 5fC and 5caC during mouse preimplantation development. *Cell Res,* 21**,** 1670-6.

INOUE, A. & ZHANG, Y. 2011. Replication-dependent loss of 5-hydroxymethylcytosine in mouse preimplantation embryos. *Science,* 334**,** 194.

IQBAL, K., JIN, S. G., PFEIFER, G. P. & SZABO, P. E. 2011. Reprogramming of the paternal genome upon fertilization involves genome-wide oxidation of 5-methylcytosine. *Proc Natl Acad Sci U S A,* 108**,** 3642-7.

ITO, S., D'ALESSIO, A. C., TARANOVA, O. V., HONG, K., SOWERS, L. C. & ZHANG, Y. 2010. Role of Tet proteins in 5mC to 5hmC conversion, ES-cell self-renewal and inner cell mass specification. *Nature,* 466**,** 1129-33.

ITO, S., SHEN, L., DAI, Q., WU, S. C., COLLINS, L. B., SWENBERG, J. A., HE, C. & ZHANG, Y. 2011. Tet proteins can convert 5-methylcytosine to 5-formylcytosine and 5-carboxylcytosine. *Science,* 333**,** 1300-3.

IVANOVA, N., DOBRIN, R., LU, R., KOTENKO, I., LEVORSE, J., DECOSTE, C., SCHAFER, X., LUN, Y. & LEMISCHKA, I. R. 2006. Dissecting self-renewal in stem cells with RNA interference. *Nature,* 442**,** 533-8.

IWAI, N., KITAJIMA, K., SAKAI, K., KIMURA, T. & NAKANO, T. 2001. Alteration of cell adhesion and cell cycle properties of ES cells by an inducible dominant interfering Myb mutant. *Oncogene,* 20**,** 1425-34.

IYER, L. M., TAHILIANI, M., RAO, A. & ARAVIND, L. 2009. Prediction of novel families of enzymes involved in oxidative and other complex modifications of bases in nucleic acids. *Cell Cycle,* 8**,** 1698-710.

JACKSON-GRUSBY, L., BEARD, C., POSSEMATO, R., TUDOR, M., FAMBROUGH, D., CSANKOVSZKI, G., DAUSMAN, J., LEE, P., WILSON, C., LANDER, E. & JAENISCH, R. 2001. Loss of genomic methylation causes p53-dependent apoptosis and epigenetic deregulation. *Nat Genet,* 27**,** 31-9.

JACOBS, S. A. & KHORASANIZADEH, S. 2002. Structure of HP1 chromodomain bound to a lysine 9-methylated histone H3 tail. *Science,* 295**,** 2080-3.

JAENISCH, R. & BIRD, A. 2003. Epigenetic regulation of gene expression: how the genome integrates intrinsic and environmental signals. *Nat Genet,* 33 Suppl**,** 245-54.

JI, L., LIU, Y. X., YANG, C., YUE, W., SHI, S. S., BAI, C. X., XI, J. F., NAN, X. & PEI, X. T. 2009. Self-renewal and pluripotency is maintained in human embryonic stem cells by co-culture with human fetal liver stromal cells expressing hypoxia inducible factor 1alpha. *J Cell Physiol,* 221**,** 54-66.

JIA, D., JURKOWSKA, R. Z., ZHANG, X., JELTSCH, A. & CHENG, X. 2007. Structure of Dnmt3a bound to Dnmt3L suggests a model for de novo DNA methylation. *Nature,* 449**,** 248-51.

JIA, J., ZHENG, X., HU, G., CUI, K., ZHANG, J., ZHANG, A., JIANG, H., LU, B., YATES, J., 3RD, LIU, C., ZHAO, K. & ZHENG, Y. 2012. Regulation of pluripotency and self-renewal of ESCs through epigenetic-threshold modulation and mRNA pruning. *Cell,* 151**,** 576-89.

JIN, S. G., KADAM, S. & PFEIFER, G. P. 2010. Examination of the specificity of DNA methylation profiling techniques towards 5-methylcytosine and 5-hydroxymethylcytosine. *Nucleic Acids Res,* 38**,** e125.

JOAQUIN, M. & WATSON, R. J. 2003. Cell cycle regulation by the B-Myb transcription factor. *Cell Mol Life Sci,* 60**,** 2389-401.

JOHNSON, M. H. & MCCONNELL, J. M. 2004. Lineage allocation and cell polarity during mouse embryogenesis. *Semin Cell Dev Biol,* 15**,** 583-97.

JOHNSON, M. H. & ZIOMEK, C. A. 1981. The foundation of two distinct cell lineages within the mouse morula. *Cell,* 24**,** 71-80.

KANEDA, M., OKANO, M., HATA, K., SADO, T., TSUJIMOTO, N., LI, E. & SASAKI, H. 2004. Essential role for de novo DNA methyltransferase Dnmt3a in paternal and maternal imprinting. *Nature,* 429**,** 900-3.

KELKAR, A. & DEOBAGKAR, D. 2009. A novel method to assess the full genome methylation profile using monoclonal antibody combined with the high throughput based microarray approach. *Epigenetics,* 4**,** 415-20.

KIM, M. S., KONDO, T., TAKADA, I., YOUN, M. Y., YAMAMOTO, Y., TAKAHASHI, S., MATSUMOTO, T., FUJIYAMA, S., SHIRODE, Y., YAMAOKA, I., KITAGAWA, H., TAKEYAMA, K., SHIBUYA, H., OHTAKE, F. & KATO, S. 2009. DNA demethylation in hormone-induced transcriptional derepression. *Nature,* 461**,** 1007-12.

KIMURA, H., HAYASHI-TAKANAKA, Y. & YAMAGATA, K. 2010. Visualization of DNA methylation and histone modifications in living cells. *Curr Opin Cell Biol,* 22**,** 412-8.

KLIMASAUSKAS, S., KUMAR, S., ROBERTS, R. J. & CHENG, X. 1994. HhaI methyltransferase flips its target base out of the DNA helix. *Cell,* 76**,** 357-69.

KLOSE, R. J. & BIRD, A. P. 2006. Genomic DNA methylation: the mark and its mediators. *Trends Biochem Sci,* 31**,** 89-97.

KO, M., HUANG, Y., JANKOWSKA, A. M., PAPE, U. J., TAHILIANI, M., BANDUKWALA, H. S., AN, J., LAMPERTI, E. D., KOH, K. P., GANETZKY, R., LIU, X. S., ARAVIND, L., AGARWAL, S., MACIEJEWSKI, J. P. & RAO, A. 2010.

Impaired hydroxylation of 5-methylcytosine in myeloid cancers with mutant TET2. *Nature,* 468**,** 839-43.

KOH, K. P., YABUUCHI, A., RAO, S., HUANG, Y., CUNNIFF, K., NARDONE, J., LAIHO, A., TAHILIANI, M., SOMMER, C. A., MOSTOSLAVSKY, G., LAHESMAA, R., ORKIN, S. H., RODIG, S. J., DALEY, G. Q. & RAO, A. 2011. Tet1 and Tet2 regulate 5-hydroxymethylcytosine production and cell lineage specification in mouse embryonic stem cells. *Cell Stem Cell,* 8**,** 200-13.

KRIAUCIONIS, S. & HEINTZ, N. 2009. The nuclear DNA base 5-hydroxymethylcytosine is present in Purkinje neurons and the brain. *Science,* 324**,** 929-30.

KUMAR, S., CHENG, X., KLIMASAUSKAS, S., MI, S., POSFAI, J., ROBERTS, R. J. & WILSON, G. G. 1994. The DNA (cytosine-5) methyltransferases. *Nucleic Acids Res,* 22**,** 1-10.

KURITA, R. & NIWA, O. 2012. DNA methylation analysis triggered by bulge specific immuno-recognition. *Anal Chem,* 84**,** 7533-8.

KURODA, T., TADA, M., KUBOTA, H., KIMURA, H., HATANO, S. Y., SUEMORI, H., NAKATSUJI, N. & TADA, T. 2005. Octamer and Sox elements are required for transcriptional cis regulation of Nanog gene expression. *Mol Cell Biol,* 25**,** 2475-85.

LATHAM, T., GILBERT, N. & RAMSAHOYE, B. 2008. DNA methylation in mouse embryonic stem cells and development. *Cell and Tissue Research,* 331**,** 31-55.

LEE, J. H., VOO, K. S. & SKALNIK, D. G. 2001. Identification and characterization of the DNA binding domain of CpG-binding protein. *J Biol Chem,* 276**,** 44669-76.

LEES-MURDOCK, D. J., SHOVLIN, T. C., GARDINER, T., DE FELICI, M. & WALSH, C. P. 2005. DNA methyltransferase expression in the mouse germ line during periods of de novo methylation. *Dev Dyn,* 232**,** 992-1002.

LEITCH, H. G., MCEWEN, K. R., TURP, A., ENCHEVA, V., CARROLL, T., GRABOLE, N., MANSFIELD, W., NASHUN, B., KNEZOVICH, J. G., SMITH, A., SURANI, M. A. & HAJKOVA, P. 2013. Naive pluripotency is associated with global DNA hypomethylation. *Nat Struct Mol Biol,* 20**,** 311-6.

LEONHARDT, H., PAGE, A. W., WEIER, H. U. & BESTOR, T. H. 1992. A targeting sequence directs DNA methyltransferase to sites of DNA replication in mammalian nuclei. *Cell,* 71**,** 865-73.

LEPIKHOV, K., ZAKHARTCHENKO, V., HAO, R., YANG, F., WRENZYCKI, C., NIEMANN, H., WOLF, E. & WALTER, J. 2008. Evidence for conserved DNA and histone H3 methylation reprogramming in mouse, bovine and rabbit zygotes. *Epigenetics Chromatin,* 1**,** 8.

LI, A., YANG, Y., GAO, C., LU, J., JEONG, H. W., LIU, B. H., TANG, P., YAO, X., NEUBERG, D., HUANG, G., TENEN, D. G. & CHAI, L. 2013. A SALL4/MLL/HOXA9 pathway in murine and human myeloid leukemogenesis. *J Clin Invest,* 123**,** 4195-207.

LI, E. 2002. Chromatin modification and epigenetic reprogramming in mammalian development. *Nat Rev Genet,* 3**,** 662-73.

LI, Y. & O'NEILL, C. 2012. Persistence of cytosine methylation of DNA following fertilisation in the mouse. *PLoS One,* 7**,** e30687.

LI, Y. & O'NEILL, C. 2013a. 5'-Methylcytosine and 5'-hydroxymethylcytosine each provide epigenetic information to the mouse zygote. *PLoS One,* 8**,** e63689.

LI, Y. & O'NEILL, C. 2013b. Methylation and hydroxymethylation of CpG display dynamic landscapes in early embryo development and define differentiation into embryonic and placental lineages. *Epigenetics & Chomatin,* 6.

LISTER, R., O'MALLEY, R. C., TONTI-FILIPPINI, J., GREGORY, B. D., BERRY, C. C., MILLAR, A. H. & ECKER, J. R. 2008. Highly integrated single-base resolution maps of the epigenome in Arabidopsis. *Cell,* 133**,** 523-36.

LISTER, R., PELIZZOLA, M., DOWEN, R. H., HAWKINS, R. D., HON, G., TONTI-FILIPPINI, J., NERY, J. R., LEE, L., YE, Z., NGO, Q. M., EDSALL, L., ANTOSIEWICZ-BOURGET, J., STEWART, R., RUOTTI, V., MILLAR, A. H., THOMSON, J. A., REN, B. & ECKER, J. R. 2009. Human DNA methylomes at base resolution show widespread epigenomic differences. *Nature,* 462**,** 315-22.

LIU, Y., OAKELEY, E. J., SUN, L. & JOST, J. P. 1998. Multiple domains are involved in the targeting of the mouse DNA methyltransferase to the DNA replication foci. *Nucleic Acids Res,* 26**,** 1038-45.

LOH, Y. H., WU, Q., CHEW, J. L., VEGA, V. B., ZHANG, W., CHEN, X., BOURQUE, G., GEORGE, J., LEONG, B., LIU, J., WONG, K. Y., SUNG, K. W., LEE, C. W., ZHAO, X. D., CHIU, K. P., LIPOVICH, L., KUZNETSOV, V. A., ROBSON, P., STANTON, L. W., WEI, C. L., RUAN, Y., LIM, B. & NG, H. H. 2006. The Oct4 and Nanog transcription network regulates pluripotency in mouse embryonic stem cells. *Nat Genet,* 38**,** 431-40.

LU, X., SONG, C. X., SZULWACH, K., WANG, Z., WEIDENBACHER, P., JIN, P. & HE, C. 2013. Chemical modification-assisted bisulfite sequencing (CAB-Seq) for 5-carboxylcytosine detection in DNA. *J Am Chem Soc,* 135**,** 9315-7.

LUO, R. X., POSTIGO, A. A. & DEAN, D. C. 1998. Rb interacts with histone deacetylase to repress transcription. *Cell,* 92**,** 463-73.

MA, Y., CUI, W., YANG, J., QU, J., DI, C., AMIN, H. M., LAI, R., RITZ, J., KRAUSE, D. S. & CHAI, L. 2006. SALL4, a novel oncogene, is constitutively expressed in human

acute myeloid leukemia (AML) and induces AML in transgenic mice. *Blood,* 108**,** 2726-35.

MA, Z., SWIGUT, T., VALOUEV, A., RADA-IGLESIAS, A. & WYSOCKA, J. 2011. Sequence-specific regulator Prdm14 safeguards mouse ESCs from entering extraembryonic endoderm fates. *Nat Struct Mol Biol,* 18**,** 120-7.

MAITI, A. & DROHAT, A. C. 2011. Thymine DNA glycosylase can rapidly excise 5-formylcytosine and 5-carboxylcytosine: potential implications for active demethylation of CpG sites. *J Biol Chem,* 286**,** 35334-8.

MARKS, H., KALKAN, T., MENAFRA, R., DENISSOV, S., JONES, K., HOFEMEISTER, H., NICHOLS, J., KRANZ, A., STEWART, A. F., SMITH, A. & STUNNENBERG, H. G. 2012. The transcriptional and epigenomic foundations of ground state pluripotency. *Cell,* 149**,** 590-604.

MATOBA, R., NIWA, H., MASUI, S., OHTSUKA, S., CARTER, M. G., SHAROV, A. A. & KO, M. S. 2006. Dissecting Oct3/4-regulated gene networks in embryonic stem cells by expression profiling. *PLoS One,* 1**,** e26.

MAURER-STROH, S., DICKENS, N. J., HUGHES-DAVIES, L., KOUZARIDES, T., EISENHABER, F. & PONTING, C. P. 2003. The Tudor domain 'Royal Family': Tudor, plant Agenet, Chromo, PWWP and MBT domains. *Trends Biochem Sci,* 28**,** 69-74.

MAYER, W., NIVELEAU, A., WALTER, J., FUNDELE, R. & HAAF, T. 2000. Demethylation of the zygotic paternal genome. *Nature,* 403**,** 501-2.

MEISSNER, A., GNIRKE, A., BELL, G. W., RAMSAHOYE, B., LANDER, E. S. & JAENISCH, R. 2005. Reduced representation bisulfite sequencing for comparative high-resolution DNA methylation analysis. *Nucleic Acids Res,* 33**,** 5868-77.

MEISSNER, A., MIKKELSEN, T. S., GU, H., WERNIG, M., HANNA, J., SIVACHENKO, A., ZHANG, X., BERNSTEIN, B. E., NUSBAUM, C., JAFFE, D. B., GNIRKE, A.,

JAENISCH, R. & LANDER, E. S. 2008. Genome-scale DNA methylation maps of pluripotent and differentiated cells. *Nature,* 454**,** 766-70.

MILLAR, C. B., GUY, J., SANSOM, O. J., SELFRIDGE, J., MACDOUGALL, E., HENDRICH, B., KEIGHTLEY, P. D., BISHOP, S. M., CLARKE, A. R. & BIRD, A. 2002. Enhanced CpG mutability and tumorigenesis in MBD4-deficient mice. *Science,* 297**,** 403-5.

MITJAVILA-GARCIA, M. T., SIMONIN, C. & PESCHANSKI, M. 2005. Embryonic stem cells: meeting the needs for cell therapy. *Adv Drug Deliv Rev,* 57**,** 1935-43.

MITSUI, K., TOKUZAWA, Y., ITOH, H., SEGAWA, K., MURAKAMI, M., TAKAHASHI, K., MARUYAMA, M., MAEDA, M. & YAMANAKA, S. 2003. The homeoprotein Nanog is required for maintenance of pluripotency in mouse epiblast and ES cells. *Cell,* 113**,** 631-42.

MOHYELDIN, A., GARZON-MUVDI, T. & QUINONES-HINOJOSA, A. 2010. Oxygen in stem cell biology: a critical component of the stem cell niche. *Cell Stem Cell,* 7**,** 150-61.

MORGAN, H. D., DEAN, W., COKER, H. A., REIK, W. & PETERSEN-MAHRT, S. K. 2004. Activation-induced cytidine deaminase deaminates 5-methylcytosine in DNA and is expressed in pluripotent tissues: implications for epigenetic reprogramming. *J Biol Chem,* 279**,** 52353-60.

MORGAN, H. D., SANTOS, F., GREEN, K., DEAN, W. & REIK, W. 2005. Epigenetic reprogramming in mammals. *Hum Mol Genet,* 14 Spec No 1**,** R47-58.

NEIDIGH, J. W., DARWANTO, A., WILLIAMS, A. A., WALL, N. R. & SOWERS, L. C. 2009. Cloning and characterization of Rhodotorula glutinis thymine hydroxylase. *Chem Res Toxicol,* 22**,** 885-93.

NELSON, P. S., PAPAS, T. S. & SCHWEINFEST, C. W. 1993. Restriction endonuclease cleavage of 5-methyl-deoxycytosine hemimethylated DNA at high enzyme-to-substrate ratios. *Nucleic Acids Res,* 21**,** 681-6.

NESTOR, C., RUZOV, A., MEEHAN, R. & DUNICAN, D. 2010. Enzymatic approaches and bisulfite sequencing cannot distinguish between 5-methylcytosine and 5-hydroxymethylcytosine in DNA. *Biotechniques,* 48**,** 317-9.

NG, H. H. & BIRD, A. 2000. Histone deacetylases: silencers for hire. *Trends Biochem Sci,* 25**,** 121-6.

NICHOLS, J., SILVA, J., ROODE, M. & SMITH, A. 2009. Suppression of Erk signalling promotes ground state pluripotency in the mouse embryo. *Development,* 136**,** 3215-22.

NICHOLS, J. & SMITH, A. 2011. The origin and identity of embryonic stem cells. *Development,* 138**,** 3-8.

NICHOLS, J., ZEVNIK, B., ANASTASSIADIS, K., NIWA, H., KLEWE-NEBENIUS, D., CHAMBERS, I., SCHOLER, H. & SMITH, A. 1998. Formation of pluripotent stem cells in the mammalian embryo depends on the POU transcription factor Oct4. *Cell,* 95**,** 379-91.

NIELSEN, P. R., NIETLISPACH, D., MOTT, H. R., CALLAGHAN, J., BANNISTER, A., KOUZARIDES, T., MURZIN, A. G., MURZINA, N. V. & LAUE, E. D. 2002. Structure of the HP1 chromodomain bound to histone H3 methylated at lysine 9. *Nature,* 416**,** 103-7.

NISHIMOTO, M., FUKUSHIMA, A., OKUDA, A. & MURAMATSU, M. 1999. The gene for the embryonic stem cell coactivator UTF1 carries a regulatory element which selectively interacts with a complex composed of Oct-3/4 and Sox-2. *Mol Cell Biol,* 19**,** 5453-65.

NISHIMOTO, M., MIYAGI, S., YAMAGISHI, T., SAKAGUCHI, T., NIWA, H., MURAMATSU, M. & OKUDA, A. 2005. Oct-3/4 maintains the proliferative embryonic stem cell state via specific binding to a variant octamer sequence in the regulatory region of the UTF1 locus. *Mol Cell Biol,* 25**,** 5084-94.

NIWA, H. 2001. Molecular mechanism to maintain stem cell renewal of ES cells. *Cell Struct Funct,* 26**,** 137-48.

NIWA, H. 2007. How is pluripotency determined and maintained? *Development,* 134**,** 635-646.

NIWA, H., BURDON, T., CHAMBERS, I. & SMITH, A. 1998. Self-renewal of pluripotent embryonic stem cells is mediated via activation of STAT3. *Genes Dev,* 12**,** 2048-60.

NIWA, H., MIYAZAKI, J. & SMITH, A. G. 2000. Quantitative expression of Oct-3/4 defines differentiation, dedifferentiation or self-renewal of ES cells. *Nat Genet,* 24**,** 372-6.

NIWA, H., TOYOOKA, Y., SHIMOSATO, D., STRUMPF, D., TAKAHASHI, K., YAGI, R. & ROSSANT, J. 2005. Interaction between Oct3/4 and Cdx2 determines trophectoderm differentiation. *Cell,* 123**,** 917-29.

OKAMOTO, A. 2009. Chemical approach toward efficient DNA methylation analysis. *Org Biomol Chem,* 7**,** 21-6.

OKAMOTO, A., TANABE, K. & SAITO, I. 2002. Site-specific discrimination of Cytosine and 5-methylcytosine in duplex DNA by Peptide nucleic acids. *J Am Chem Soc,* 124**,** 10262-3.

OKANO, M., BELL, D. W., HABER, D. A. & LI, E. 1999. DNA methyltransferases Dnmt3a and Dnmt3b are essential for de novo methylation and mammalian development. *Cell,* 99**,** 247-57.

OKANO, M., XIE, S. & LI, E. 1998. Dnmt2 is not required for de novo and maintenance methylation of viral DNA in embryonic stem cells. *Nucleic Acids Res,* 26**,** 2536-40.

OOI, S. K., O'DONNELL, A. H. & BESTOR, T. H. 2009. Mammalian cytosine methylation at a glance. *J Cell Sci,* 122**,** 2787-91.

OOI, S. K., QIU, C., BERNSTEIN, E., LI, K., JIA, D., YANG, Z., ERDJUMENT-BROMAGE, H., TEMPST, P., LIN, S. P., ALLIS, C. D., CHENG, X. & BESTOR, T. H. 2007. DNMT3L connects unmethylated lysine 4 of histone H3 to de novo methylation of DNA. *Nature,* 448**,** 714-7.

OSWALD, J., ENGEMANN, S., LANE, N., MAYER, W., OLEK, A., FUNDELE, R., DEAN, W., REIK, W. & WALTER, J. 2000. Active demethylation of the paternal genome in the mouse zygote. *Curr Biol,* 10**,** 475-8.

PARK, J. S., JEONG, Y. S., SHIN, S. T., LEE, K. K. & KANG, Y. K. 2007. Dynamic DNA methylation reprogramming: active demethylation and immediate remethylation in the male pronucleus of bovine zygotes. *Dev Dyn,* 236**,** 2523-33.

PASTOR, W. A., ARAVIND, L. & RAO, A. 2013. TETonic shift: biological roles of TET proteins in DNA demethylation and transcription. *Nat Rev Mol Cell Biol,* 14**,** 341-56.

PEASE, S., BRAGHETTA, P., GEARING, D., GRAIL, D. & WILLIAMS, R. L. 1990. Isolation of embryonic stem (ES) cells in media supplemented with recombinant leukemia inhibitory factor (LIF). *Dev Biol,* 141**,** 344-52.

PICKETTS, D. J., HIGGS, D. R., BACHOO, S., BLAKE, D. J., QUARRELL, O. W. & GIBBONS, R. J. 1996. ATRX encodes a novel member of the SNF2 family of proteins: mutations point to a common mechanism underlying the ATR-X syndrome. *Hum Mol Genet,* 5**,** 1899-907.

PLUSA, B., FRANKENBERG, S., CHALMERS, A., HADJANTONAKIS, A. K., MOORE, C. A., PAPALOPULU, N., PAPAIOANNOU, V. E., GLOVER, D. M. & ZERNICKA-GOETZ, M. 2005. Downregulation of Par3 and aPKC function directs cells towards the ICM in the preimplantation mouse embryo. *J Cell Sci,* 118**,** 505-15.

POLLARD, K. J., SAMUELS, M. L., CROWLEY, K. A., HANSEN, J. C. & PETERSON, C. L. 1999. Functional interaction between GCN5 and polyamines: a new role for core histone acetylation. *EMBO J,* 18**,** 5622-33.

POPP, C., DEAN, W., FENG, S., COKUS, S. J., ANDREWS, S., PELLEGRINI, M., JACOBSEN, S. E. & REIK, W. 2010. Genome-wide erasure of DNA methylation in mouse primordial germ cells is affected by AID deficiency. *Nature,* 463**,** 1101-5.

POSFAI, J., BHAGWAT, A. S., POSFAI, G. & ROBERTS, R. J. 1989. Predictive motifs derived from cytosine methyltransferases. *Nucleic Acids Res,* 17**,** 2421-35.

PRADHAN, M., ESTEVE, P. O., CHIN, H. G., SAMARANAYKE, M., KIM, G. D. & PRADHAN, S. 2008. CXXC domain of human DNMT1 is essential for enzymatic activity. *Biochemistry,* 47**,** 10000-9.

QIAO, Y., WANG, R., YANG, X., TANG, K. & JING, N. 2015. Dual roles of histone H3 lysine 9 acetylation in human embryonic stem cell pluripotency and neural differentiation. *J Biol Chem,* 290**,** 9949.

QIU, C., SAWADA, K., ZHANG, X. & CHENG, X. 2002. The PWWP domain of mammalian DNA methyltransferase Dnmt3b defines a new family of DNA-binding folds. *Nat Struct Biol,* 9**,** 217-24.

RAI, K., CHIDESTER, S., ZAVALA, C. V., MANOS, E. J., JAMES, S. R., KARPF, A. R., JONES, D. A. & CAIRNS, B. R. 2007. Dnmt2 functions in the cytoplasm to promote liver, brain, and retina development in zebrafish. *Genes Dev,* 21**,** 261-6.

RAI, K., HUGGINS, I. J., JAMES, S. R., KARPF, A. R., JONES, D. A. & CAIRNS, B. R. 2008. DNA demethylation in zebrafish involves the coupling of a deaminase, a glycosylase, and gadd45. *Cell,* 135**,** 1201-12.

REIS SILVA, A. R., ADENOT, P., DANIEL, N., ARCHILLA, C., PEYNOT, N., LUCCI, C. M., BEAUJEAN, N. & DURANTHON, V. 2011. Dynamics of DNA methylation levels in maternal and paternal rabbit genomes after fertilization. *Epigenetics,* 6**,** 987-93.

REYNAUD, C., BRUNO, C., BOULLANGER, P., GRANGE, J., BARBESTI, S. & NIVELEAU, A. 1992. Monitoring of urinary excretion of modified nucleosides in cancer patients using a set of six monoclonal antibodies. *Cancer Lett,* 61**,** 255-62.

ROBERTSON, K. D., AIT-SI-ALI, S., YOKOCHI, T., WADE, P. A., JONES, P. L. & WOLFFE, A. P. 2000. DNMT1 forms a complex with Rb, E2F1 and HDAC1 and represses transcription from E2F-responsive promoters. *Nat Genet,* 25**,** 338-42.

ROBERTSON, K. D., UZVOLGYI, E., LIANG, G., TALMADGE, C., SUMEGI, J., GONZALES, F. A. & JONES, P. A. 1999. The human DNA methyltransferases (DNMTs) 1, 3a and 3b: coordinate mRNA expression in normal tissues and overexpression in tumors. *Nucleic Acids Res,* 27**,** 2291-8.

RODDA, D. J., CHEW, J. L., LIM, L. H., LOH, Y. H., WANG, B., NG, H. H. & ROBSON, P. 2005. Transcriptional regulation of nanog by OCT4 and SOX2. *J Biol Chem,* 280**,** 24731-7.

ROUGIER, N., BOURC'HIS, D., GOMES, D. M., NIVELEAU, A., PLACHOT, M., PALDI, A. & VIEGAS-PEQUIGNOT, E. 1998. Chromosome methylation patterns during mammalian preimplantation development. *Genes Dev,* 12**,** 2108-13.

ROUNTREE, M. R., BACHMAN, K. E. & BAYLIN, S. B. 2000. DNMT1 binds HDAC2 and a new co-repressor, DMAP1, to form a complex at replication foci. *Nat Genet,* 25**,** 269-77.

RUSSO, V. E. A., MARTIENSSEN, R. A. & RIGGS, A. D. 1996. *Epigenetic mechanisms of gene regulation,* Plainview, N.Y., Cold Spring Harbor Laboratory Press.

RUZOV, A., TSENKINA, Y., SERIO, A., DUDNAKOVA, T., FLETCHER, J., BAI, Y., CHEBOTAREVA, T., PELLS, S., HANNOUN, Z., SULLIVAN, G., CHANDRAN, S., HAY, D. C., BRADLEY, M., WILMUT, I. & DE SOUSA, P. 2011. Lineage-specific distribution of high levels of genomic 5-hydroxymethylcytosine in mammalian development. *Cell Res,* 21**,** 1332-42.

SAKAI, Y., SUETAKE, I., SHINOZAKI, F., YAMASHINA, S. & TAJIMA, S. 2004. Co-expression of de novo DNA methyltransferases Dnmt3a2 and Dnmt3L in gonocytes of mouse embryos. *Gene Expr Patterns,* 5**,** 231-7.

SAKAKI-YUMOTO, M., KOBAYASHI, C., SATO, A., FUJIMURA, S., MATSUMOTO, Y., TAKASATO, M., KODAMA, T., ABURATANI, H., ASASHIMA, M., YOSHIDA, N. & NISHINAKAMURA, R. 2006. The murine homolog of SALL4, a causative gene in Okihiro syndrome, is essential for embryonic stem cell proliferation, and cooperates with Sall1 in anorectal, heart, brain and kidney development. *Development,* 133**,** 3005-13.

SAKAUE, M., OHTA, H., KUMAKI, Y., ODA, M., SAKAIDE, Y., MATSUOKA, C., YAMAGIWA, A., NIWA, H., WAKAYAMA, T. & OKANO, M. 2010. DNA methylation is dispensable for the growth and survival of the extraembryonic lineages. *Curr Biol,* 20**,** 1452-7.

SALVAING, J., AGUIRRE-LAVIN, T., BOULESTEIX, C., LEHMANN, G., DEBEY, P. & BEAUJEAN, N. 2012. 5-Methylcytosine and 5-hydroxymethylcytosine spatiotemporal profiles in the mouse zygote. *PLoS One,* 7**,** e38156.

SALVAING, J., LI, Y., BEAUJEAN, N. & O'NEILL, C. 2014. Determinants of valid measurements of global changes in 5'-methylcytosine and 5'-hydroxymethylcytosine by immunolocalisation in the early embryo. *Reprod Fertil Dev*.

SANTOS, F., HENDRICH, B., REIK, W. & DEAN, W. 2002. Dynamic reprogramming of DNA methylation in the early mouse embryo. *Dev Biol,* 241**,** 172-82.

SATO, N., MEIJER, L., SKALTSOUNIS, L., GREENGARD, P. & BRIVANLOU, A. H. 2004. Maintenance of pluripotency in human and mouse embryonic stem cells through activation of Wnt signaling by a pharmacological GSK-3-specific inhibitor. *Nat Med,* 10**,** 55-63.

SCADDEN, D. T. 2006. The stem-cell niche as an entity of action. *Nature,* 441**,** 1075-9.

SEISENBERGER, S., PEAT, J. R. & REIK, W. 2013. Conceptual links between DNA methylation reprogramming in the early embryo and primordial germ cells. *Curr Opin Cell Biol,* 25**,** 281-8.

SELENKO, P., SPRANGERS, R., STIER, G., BUHLER, D., FISCHER, U. & SATTLER, M. 2001. SMN tudor domain structure and its interaction with the Sm proteins. *Nat Struct Biol,* 8**,** 27-31.

SHAO, X., ZHANG, C., SUN, M. A., LU, X. & XIE, H. 2014. Deciphering the heterogeneity in DNA methylation patterns during stem cell differentiation and reprogramming. *BMC Genomics,* 15**,** 978.

SHAPIRO, R., SERVIS, R. E. & WELCHER, M. 1970. Reactions of Uracil and Cytosine Derivatives with Sodium Bisulfite . A Specific Deamination Method. *Journal of the American Chemical Society,* 92**,** 422-&.

SHARIF, J., MUTO, M., TAKEBAYASHI, S., SUETAKE, I., IWAMATSU, A., ENDO, T. A., SHINGA, J., MIZUTANI-KOSEKI, Y., TOYODA, T., OKAMURA, K., TAJIMA, S., MITSUYA, K., OKANO, M. & KOSEKI, H. 2007. The SRA protein Np95 mediates epigenetic inheritance by recruiting Dnmt1 to methylated DNA. *Nature,* 450**,** 908-12.

SHEN, L., WU, H., DIEP, D., YAMAGUCHI, S., D'ALESSIO, A. C., FUNG, H. L., ZHANG, K. & ZHANG, Y. 2013. Genome-wide analysis reveals TET- and TDG-dependent 5-methylcytosine oxidation dynamics. *Cell,* 153**,** 692-706.

SILVA, J., BARRANDON, O., NICHOLS, J., KAWAGUCHI, J., THEUNISSEN, T. W. & SMITH, A. 2008. Promotion of reprogramming to ground state pluripotency by signal inhibition. *PLoS Biol,* 6**,** e253.

SINGER, Z. S., YONG, J., TISCHLER, J., HACKETT, J. A., ALTINOK, A., SURANI, M. A., CAI, L. & ELOWITZ, M. B. 2014. Dynamic heterogeneity and DNA methylation in embryonic stem cells. *Mol Cell,* 55**,** 319-31.

SLATER, L. M., ALLEN, M. D. & BYCROFT, M. 2003. Structural variation in PWWP domains. *J Mol Biol,* 330**,** 571-6.

SMALLWOOD, S. A., TOMIZAWA, S., KRUEGER, F., RUF, N., CARLI, N., SEGONDS-PICHON, A., SATO, S., HATA, K., ANDREWS, S. R. & KELSEY, G. 2011. Dynamic CpG island methylation landscape in oocytes and preimplantation embryos. *Nat Genet,* 43**,** 811-4.

SMILEY, J. A., KUNDRACIK, M., LANDFRIED, D. A., BARNES, V. R., SR. & AXHEMI, A. A. 2005. Genes of the thymidine salvage pathway: thymine-7-hydroxylase from a Rhodotorula glutinis cDNA library and iso-orotate decarboxylase from Neurospora crassa. *Biochim Biophys Acta,* 1723**,** 256-64.

SMITH, Z. D., CHAN, M. M., MIKKELSEN, T. S., GU, H., GNIRKE, A., REGEV, A. & MEISSNER, A. 2012. A unique regulatory phase of DNA methylation in the early mammalian embryo. *Nature,* 484**,** 339-44.

SONG, C. X., SZULWACH, K. E., DAI, Q., FU, Y., MAO, S. Q., LIN, L., STREET, C., LI, Y., POIDEVIN, M., WU, H., GAO, J., LIU, P., LI, L., XU, G. L., JIN, P. & HE, C.

2013. Genome-wide profiling of 5-formylcytosine reveals its roles in epigenetic priming. *Cell,* 153**,** 678-91.

SONG, J., RECHKOBLIT, O., BESTOR, T. H. & PATEL, D. J. 2011. Structure of DNMT1-DNA complex reveals a role for autoinhibition in maintenance DNA methylation. *Science,* 331**,** 1036-40.

SONG, J., TEPLOVA, M., ISHIBE-MURAKAMI, S. & PATEL, D. J. 2012. Structure-based mechanistic insights into DNMT1-mediated maintenance DNA methylation. *Science,* 335**,** 709-12.

STEC, I., NAGL, S. B., VAN OMMEN, G. J. & DEN DUNNEN, J. T. 2000. The PWWP domain: a potential protein-protein interaction domain in nuclear proteins influencing differentiation? *FEBS Lett,* 473**,** 1-5.

TAHILIANI, M., KOH, K. P., SHEN, Y., PASTOR, W. A., BANDUKWALA, H., BRUDNO, Y., AGARWAL, S., IYER, L. M., LIU, D. R., ARAVIND, L. & RAO, A. 2009. Conversion of 5-methylcytosine to 5-hydroxymethylcytosine in mammalian DNA by MLL partner TET1. *Science,* 324**,** 930-5.

TAJBAKHSH, J., STEFANOVSKI, D., TANG, G., WAWROWSKY, K., LIU, N. & FAIR, J. H. 2015. Dynamic heterogeneity of DNA methylation and hydroxymethylation in embryonic stem cell populations captured by single-cell 3D high-content analysis. *Exp Cell Res,* 332**,** 190-201.

TAKAHASHI, K., MITSUI, K. & YAMANAKA, S. 2003. Role of ERas in promoting tumour-like properties in mouse embryonic stem cells. *Nature,* 423**,** 541-5.

TAKAHASHI, K., MURAKAMI, M. & YAMANAKA, S. 2005. Role of the phosphoinositide 3-kinase pathway in mouse embryonic stem (ES) cells. *Biochem Soc Trans,* 33**,** 1522-5.

TAKAHASHI, K., TANABE, K., OHNUKI, M., NARITA, M., ICHISAKA, T., TOMODA, K. & YAMANAKA, S. 2007. Induction of pluripotent stem cells from adult human fibroblasts by defined factors. *Cell,* 131**,** 861-72.

TAKAHASHI, K. & YAMANAKA, S. 2006. Induction of pluripotent stem cells from mouse embryonic and adult fibroblast cultures by defined factors. *Cell,* 126**,** 663-76.

TANAKA, K. & OKAMOTO, A. 2007. Degradation of DNA by bisulfite treatment. *Bioorg Med Chem Lett,* 17**,** 1912-5.

TANG, F., BARBACIORU, C., BAO, S., LEE, C., NORDMAN, E., WANG, X., LAO, K. & SURANI, M. A. 2010. Tracing the derivation of embryonic stem cells from the inner cell mass by single-cell RNA-Seq analysis. *Cell Stem Cell,* 6**,** 468-78.

TANIMURA, N., SAITO, M., EBISUYA, M., NISHIDA, E. & ISHIKAWA, F. 2013. Stemness-related factor Sall4 interacts with transcription factors Oct-3/4 and Sox2 and occupies Oct-Sox elements in mouse embryonic stem cells. *J Biol Chem,* 288**,** 5027-38.

TASSERON-DE JONG, J. G., AKER, J. & GIPHART-GASSLER, M. 1988. The ability of the restriction endonuclease EcoRI to digest hemi-methylated versus fully cytosine-methylated DNA of the herpes tk promoter region. *Gene,* 74**,** 147-9.

TEITELL, M. A. 2005. The TCL1 family of oncoproteins: co-activators of transformation. *Nat Rev Cancer,* 5**,** 640-8.

TSAI, A. G., CHEN, D. M., LIN, M., HSIEH, J. C., OKITSU, C. Y., TAGHVA, A., SHIBATA, D. & HSIEH, C. L. 2012. Heterogeneity and randomness of DNA methylation patterns in human embryonic stem cells. *DNA Cell Biol,* 31**,** 893-907.

TSUMURA, A., HAYAKAWA, T., KUMAKI, Y., TAKEBAYASHI, S., SAKAUE, M., MATSUOKA, C., SHIMOTOHNO, K., ISHIKAWA, F., LI, E., UEDA, H. R., NAKAYAMA, J. & OKANO, M. 2006. Maintenance of self-renewal ability of mouse

embryonic stem cells in the absence of DNA methyltransferases Dnmt1, Dnmt3a and Dnmt3b. *Genes Cells,* 11**,** 805-14.

UEDA, Y., OKANO, M., WILLIAMS, C., CHEN, T., GEORGOPOULOS, K. & LI, E. 2006. Roles for Dnmt3b in mammalian development: a mouse model for the ICF syndrome. *Development,* 133**,** 1183-92.

VAN DEN WYNGAERT, I., SPRENGEL, J., KASS, S. U. & LUYTEN, W. H. 1998. Cloning and analysis of a novel human putative DNA methyltransferase. *FEBS Lett,* 426**,** 283-9.

VILKAITIS, G., SUETAKE, I., KLIMASAUSKAS, S. & TAJIMA, S. 2005. Processive methylation of hemimethylated CpG sites by mouse Dnmt1 DNA methyltransferase. *J Biol Chem,* 280**,** 64-72.

WANG, L., ZHANG, J., DUAN, J., GAO, X., ZHU, W., LU, X., YANG, L., ZHANG, J., LI, G., CI, W., LI, W., ZHOU, Q., ALURU, N., TANG, F., HE, C., HUANG, X. & LIU, J. 2014. Programming and inheritance of parental DNA methylomes in mammals. *Cell,* 157**,** 979-91.

WANG, X., SONG, Y., SONG, M., WANG, Z., LI, T. & WANG, H. 2009. Fluorescence polarization combined capillary electrophoresis immunoassay for the sensitive detection of genomic DNA methylation. *Anal Chem,* 81**,** 7885-91.

WANG, Z. X., WANG, X. L., LIU, S. Q., YIN, J. F. & WANG, H. L. 2010. Fluorescently Imaged Particle Counting Immunoassay for Sensitive Detection of DNA Modifications. *Analytical Chemistry,* 82**,** 9901-9908.

WARNECKE, P. M., STIRZAKER, C., SONG, J., GRUNAU, C., MELKI, J. R. & CLARK, S. J. 2002. Identification and resolution of artifacts in bisulfite sequencing. *Methods,* 27**,** 101-7.

WATANABE, D., SUETAKE, I., TADA, T. & TAJIMA, S. 2002. Stage- and cell-specific expression of Dnmt3a and Dnmt3b during embryogenesis. *Mech Dev,* 118**,** 187-90.

WATANABE, M., YANAGI, Y., MASUHIRO, Y., YANO, T., YOSHIKAWA, H., YANAGISAWA, J. & KATO, S. 1998. A putative tumor suppressor, TSG101, acts as a transcriptional suppressor through its coiled-coil domain. *Biochem Biophys Res Commun,* 245**,** 900-5.

WATANABE, S., UMEHARA, H., MURAYAMA, K., OKABE, M., KIMURA, T. & NAKANO, T. 2006. Activation of Akt signaling is sufficient to maintain pluripotency in mouse and primate embryonic stem cells. *Oncogene,* 25**,** 2697-707.

WEBSTER, K. E., O'BRYAN, M. K., FLETCHER, S., CREWTHER, P. E., AAPOLA, U., CRAIG, J., HARRISON, D. K., AUNG, H., PHUTIKANIT, N., LYLE, R., MEACHEM, S. J., ANTONARAKIS, S. E., DE KRETSER, D. M., HEDGER, M. P., PETERSON, P., CARROLL, B. J. & SCOTT, H. S. 2005. Meiotic and epigenetic defects in Dnmt3L-knockout mouse spermatogenesis. *Proc Natl Acad Sci U S A,* 102**,** 4068-73.

WILSON, G. G. 1992. Amino acid sequence arrangements of DNA-methyltransferases. *Methods Enzymol,* 216**,** 259-79.

WINSTON, F. & ALLIS, C. D. 1999. The bromodomain: a chromatin-targeting module? *Nat Struct Biol,* 6**,** 601-4.

WOSSIDLO, M., ARAND, J., SEBASTIANO, V., LEPIKHOV, K., BOIANI, M., REINHARDT, R., SCHOLER, H. & WALTER, J. 2010. Dynamic link of DNA demethylation, DNA strand breaks and repair in mouse zygotes. *EMBO J,* 29**,** 1877-88.

WOSSIDLO, M., NAKAMURA, T., LEPIKHOV, K., MARQUES, C. J., ZAKHARTCHENKO, V., BOIANI, M., ARAND, J., NAKANO, T., REIK, W. &

WALTER, J. 2011. 5-Hydroxymethylcytosine in the mammalian zygote is linked with epigenetic reprogramming. *Nature Communications,* 2**,** 241.

WRAY, J., KALKAN, T. & SMITH, A. G. 2010. The ground state of pluripotency. *Biochem Soc Trans,* 38**,** 1027-32.

WU, H., ZENG, H., LAM, R., TEMPEL, W., AMAYA, M. F., XU, C., DOMBROVSKI, L., QIU, W., WANG, Y. & MIN, J. 2011. Structural and histone binding ability characterizations of human PWWP domains. *PLoS One,* 6**,** e18919.

WU, H. & ZHANG, Y. 2011. Mechanisms and functions of Tet protein-mediated 5-methylcytosine oxidation. *Genes Dev,* 25**,** 2436-52.

WU, H. & ZHANG, Y. 2014. Reversing DNA methylation: mechanisms, genomics, and biological functions. *Cell,* 156**,** 45-68.

WU, J. C. & SANTI, D. V. 1987. Kinetic and catalytic mechanism of HhaI methyltransferase. *J Biol Chem,* 262**,** 4778-86.

WU, Q., CHEN, X., ZHANG, J., LOH, Y. H., LOW, T. Y., ZHANG, W., ZHANG, W., SZE, S. K., LIM, B. & NG, H. H. 2006. Sall4 interacts with Nanog and co-occupies Nanog genomic sites in embryonic stem cells. *J Biol Chem,* 281**,** 24090-4.

XIE, S., WANG, Z., OKANO, M., NOGAMI, M., LI, Y., HE, W. W., OKUMURA, K. & LI, E. 1999. Cloning, expression and chromosome locations of the human DNMT3 gene family. *Gene,* 236**,** 87-95.

XU, Y., WU, F., TAN, L., KONG, L., XIONG, L., DENG, J., BARBERA, A. J., ZHENG, L., ZHANG, H., HUANG, S., MIN, J., NICHOLSON, T., CHEN, T., XU, G., SHI, Y., ZHANG, K. & SHI, Y. G. 2011. Genome-wide regulation of 5hmC, 5mC, and gene expression by Tet1 hydroxylase in mouse embryonic stem cells. *Mol Cell,* 42**,** 451-64.

YAMAJI, M., UEDA, J., HAYASHI, K., OHTA, H., YABUTA, Y., KURIMOTO, K., NAKATO, R., YAMADA, Y., SHIRAHIGE, K. & SAITOU, M. 2013. PRDM14

ensures naive pluripotency through dual regulation of signaling and epigenetic pathways in mouse embryonic stem cells. *Cell Stem Cell,* 12**,** 368-82.

YANG, J., CHAI, L., FOWLES, T. C., ALIPIO, Z., XU, D., FINK, L. M., WARD, D. C. & MA, Y. 2008. Genome-wide analysis reveals Sall4 to be a major regulator of pluripotency in murine-embryonic stem cells. *Proc Natl Acad Sci U S A,* 105**,** 19756-61.

YANG, J., CHAI, L., LIU, F., FINK, L. M., LIN, P., SILBERSTEIN, L. E., AMIN, H. M., WARD, D. C. & MA, Y. 2007. Bmi-1 is a target gene for SALL4 in hematopoietic and leukemic cells. *Proc Natl Acad Sci U S A,* 104**,** 10494-9.

YANG, J., GAO, C., CHAI, L. & MA, Y. 2010. A novel SALL4/OCT4 transcriptional feedback network for pluripotency of embryonic stem cells. *PLoS One,* 5**,** e10766.

YING, Q. L., WRAY, J., NICHOLS, J., BATLLE-MORERA, L., DOBLE, B., WOODGETT, J., COHEN, P. & SMITH, A. 2008. The ground state of embryonic stem cell self-renewal. *Nature,* 453**,** 519-23.

ZERNICKA-GOETZ, M., MORRIS, S. A. & BRUCE, A. W. 2009. Making a firm decision: multifaceted regulation of cell fate in the early mouse embryo. *Nat Rev Genet,* 10**,** 467-77.

ZHANG, X., YAZAKI, J., SUNDARESAN, A., COKUS, S., CHAN, S. W., CHEN, H., HENDERSON, I. R., SHINN, P., PELLEGRINI, M., JACOBSEN, S. E. & ECKER, J. R. 2006. Genome-wide high-resolution mapping and functional analysis of DNA methylation in arabidopsis. *Cell,* 126**,** 1189-201.

ZHANG, X., YUAN, X., ZHU, W., QIAN, H. & XU, W. 2015. SALL4: an emerging cancer biomarker and target. *Cancer Lett,* 357**,** 55-62.

ZHANG, Y., SUN, Z. W., IRATNI, R., ERDJUMENT-BROMAGE, H., TEMPST, P., HAMPSEY, M. & REINBERG, D. 1998. SAP30, a novel protein conserved between

human and yeast, is a component of a histone deacetylase complex. *Mol Cell,* 1**,** 1021-31.

ZHU, B., ZHENG, Y., ANGLIKER, H., SCHWARZ, S., THIRY, S., SIEGMANN, M. & JOST, J. P. 2000a. 5-Methylcytosine DNA glycosylase activity is also present in the human MBD4 (G/T mismatch glycosylase) and in a related avian sequence. *Nucleic Acids Res,* 28**,** 4157-65.

ZHU, B., ZHENG, Y., HESS, D., ANGLIKER, H., SCHWARZ, S., SIEGMANN, M., THIRY, S. & JOST, J. P. 2000b. 5-methylcytosine-DNA glycosylase activity is present in a cloned G/T mismatch DNA glycosylase associated with the chicken embryo DNA demethylation complex. *Proc Natl Acad Sci U S A,* 97**,** 5135-9.

ZHU, J. K. 2009. Active DNA demethylation mediated by DNA glycosylases. *Annu Rev Genet,* 43**,** 143-66.

ZILLER, M. J., GU, H., MULLER, F., DONAGHEY, J., TSAI, L. T., KOHLBACHER, O., DE JAGER, P. L., ROSEN, E. D., BENNETT, D. A., BERNSTEIN, B. E., GNIRKE, A. & MEISSNER, A. 2013. Charting a dynamic DNA methylation landscape of the human genome. *Nature,* 500**,** 477-81.

8. APPENDIX: GENERAL EQUIPMENT USED

- Autoclave (S-B Autoclaves by I.L.A.T. Pty. Ltd.)
- Centrifuges (Beckman GPR and Sorvall MC-12V)
- Class II Biological Safety Cabinet (Gelaire Pty. Ltd.)
- CO_2 incubator (Thermo Scientific, Steri-Cycle CO_2 Incubator and Forma Series II Water Jacket)
- Freezer (-20 °C) (Westinghouse Silhouette Series II and Freestyle)
- Freezer (-80 °C) (Sanyo VIP Series)
- Fridges (Westinghouse and Kelvinator Opal)
- Fume cupboard (Conditionaire International Pty. Ltd.)
- Hotplate/stirrer (Townson)
- Light microscopes (Nikon TMS)
- Liquid nitrogen tank (Taylor-Wharton ABS-20K, Australia Pty. Ltd.)
- Microbalance (Cahn C-33 Series)
- Milli-Q Water (Merck Millipore)
- pH meter (PHM61 Laboratory pH meter)
- Rocker (BioSan Mini Rocker MR-1)
- Stereo microscope (Olympus SZ Stereo Zoom Microscope)
- Water Bath (Ratek)
- Weighers (Mettler AE166 / Delta Range and Shimadzu AUW220D)